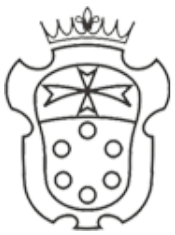

SCUOLA
NORMALE
SUPERIORE

Classe di Scienze

PhD Thesis in Condensed Matter Physics

Quantum Engineering in Open Quantum Systems

Candidate:

Stefano Cusumano

Supervisor:

Prof. Vittorio Giovannetti

"Sei un grande!"
"No, tu sei un grande!"

Anonymous chatters

"And when he came back to, he was flat on his back on the beach in the freezing sand, and it was raining out of a low sky, and the tide was way out"

David Foster Wallace, *Infinite Jest*

Abstract

The huge technological advancement achieved in the last years has allowed for the emergence of a new field of physics dubbed "quantum engineering": with this term people refer to a wide range of topics, from planning and building physical systems for specific tasks to developing algorithms to control those systems, from ways to create specific quantum states to new theoretical tools to describe and plan new physical systems.

As the field of quantum engineering covers many topics in physics, this is reflected in the community interested in it, ranging from quantum optics theorists to solid state experimentalists. This also includes the possibility, and sometimes the necessity, for a scientist willing to enter the field to study very different problems, as it happened for the material in this thesis, where at least two main topics are covered.

One of them is the study of open quantum systems, more specifically in the context of collisional model and cascade networks. The latter are networks of quantum systems interacting through the interaction with a common environment with unidirectional, i.e. *chiral*, propagation of the signal. Thanks to the chirality of the environment it is possible to obtain non symmetrical couplings between the quantum systems composing the network, opening the way to engineer the steady state of the system.

The tool used to derive master equation describing dynamics and properties of such systems is the one of collisional models: these models are nowadays extensively used in a wide range of topics concerning open quantum systems, from the description of both Markovian and non Markovian dynamics, to quantum optics and quantum thermodynamics.

In collisional models the environment is depicted as a collection of smaller systems,

dubbed ancillas, which interact in a collisional fashion with the quantum system under examination. This way of describing open systems dynamics leads to a discrete master equation on which it is then possible to enforce a continuous time limit. Among the advantages provided by such an approach there is the simplicity with which is possible to switch from a Markovian to a non-Markovian dynamics and the possibility of keeping track of the environmental degrees of freedom.

The last feature cited is the one exploited in this thesis when studying a quantum system thermalizing through the interaction with a thermal bath: having at disposal the environmental state at each discrete step of the thermalization process, it is possible to compute the thermodynamic functionals relative to the environment. Specifically, by computing the quantum mutual information between the system and the environment, it is possible to show that the final joint state reached by the system and the environment is a factorized state.

The other part of this thesis focuses instead on quantum state engineering by potential engineering. By appropriately engineering a potential profile, it is possible to obtain a class of quantum states, dubbed *stretchable*, which have the property of having a flat wave function in some regions, somehow analogously to what happens in photonic metamaterials: in this materials, where either the permittivity or the permeability is zero, the temporal and spatial variation of the electric field are decoupled, leading to the possibility of having a stretched wave with both large frequency and large wavelength.

Finally, in this thesis it is shown how, by properly engineering a spatially varying potential landscape, it is possible to attach a geometric phase to the quantum state of a traveling wave. More specifically, as the confining potential of a traveling wave varies along a closed loop in parameters space, it is possible to implement an operation, usually called *holonomy*, which attaches a geometric phase to the state, analogously to what happens in the Berry phase phenomenon for a time dependent Hamiltonian.

Acknowledgements

The first people I would like to thank are the ones I will not mention here, either because I will forget, but most importantly because to list all the wonderful people I met during these four years would be an impossible task. This being said, let me start with this titanic challenge!

First I like to thank my supervisor Prof. Vittorio Giovannetti for all his work and help during these five years of mentoring.

I also like to thank Dr. Andrea Mari and Dr. Antonella De Pasquale, without whom this PhD would have been far more difficult and stressful, for their constant supervision and precious suggestions.

It would be unforgivable not to thank all the past and present people in the Condensed Matter and Quantum Information group at Scuola Normale, both for the fruitful discussions over physics and the awesome experiences shared over the years. In particular Vasco Cavina and Marcello Andolina deserve a special mention as constant travel buddies in most conferences I attended during these years: even when you will not see me, you will know where to find me[1].

Besides my colleagues from the Condensed Matter and Quantum Information group, I wish to thank all the PhD and undergraduates I met at Scuola Normale with whom I had the pleasure to share something, from scientific thoughts to awesome parties and (mis)adventures, during my PhD experience.

Concerning Scuola Normale Superiore, I also need to thank all the people I had the pleasure to collaborate with during my experience as member of the Academic Board:

[1]No, it won't be deep in your heart. You will just find me outside, smoking.

from the other member of the board to all the students and staff I collaborated with in making proposal and trying to get a better Scuola for everybody.

The completion of this PhD would not have been possible without the help of many other people.

Among them I first like to thank all my friends from Palermo, especially the ones that have always been there, for years, since the very start of everything.

A special mention goes to all my former colleagues from Università di Palermo, the so-called "Giampaoli", with whom I shared an entire, though still short, academic career.

During these years in Pisa I had the pleasure to share many political adventures with many different people, and thus I wish to thank all the wonderful comrades I met here in Pisa. Nonetheless I feel the urge to cite among them all the people form "Idee Follette", with whom I shared much more than politics.

Last, but definitely not least, I want to thank my parents for their constant support over the years, both moral and material, without which even thinking of doing a PhD would have been very hard, if not impossible: thank you!

Contents

List of Figures

CHAPTER 1

Introduction

Ever since in history physics has had a double goal: on one hand it aims at discovering the principles of Nature, but on the other hand it is interested in exploiting the laws of Nature in order to get some advantage in practical purposes.

These two goals are not independent, but rather intertwined: as new theoretical discoveries and predictions are made, they allows for better technology which indeed allows for new results and data that need to be understood, pushing for new discoveries and "closing" the loop.

It was along this line that, for instance, the field of thermodynamics first arose: scientists at that time were first interested in discovering the relations between heat, work, temperature and the other thermodynamical quantities, but as their researches allowed for the construction of new machines and engines, the new data and experimental evidences allowed them to push even further their knowledge.

Every time there has been a change of paradigm in physics, after a first settlement period where the new principles discovered were understood and "new" physical laws and effects were discovered, it always followed a period where those discoveries were exploited for new technologies [Kuhn 1970]: think for instance of the relativity theory, which was later used to better telecommunications and build spaceships able to reach the borders of our stellar system.

Quantum mechanics in this regard was no exception: after a first period where the new paradigms had to be interiorized by physicists and first predictions of quantum

mechanics were verified, people started looking for applications of these new effects.

A huge development of physics in all of its fields started after World War II, with a continuous interplay between new discoveries and new applications: from WWII to the present days physicists have been able to almost complete their understanding of the standard model, new discoveries in the field of material science and electronics have allowed to revolution electronics, building new devices such as smaller and more efficient transistors, new sources of light like LED and ultra precise atomic clocks, just to cite some examples.

We could say that the last big paradigm change in physics has happened in the 80s', as the field of quantum information science started arising: this new paradigm put together the fields of information science, which has played a main role in the development of modern computers, and quantum mechanics, fostering for the creation of the quantum computer, a calculator able to solve certain problems exponentially faster than its classical counterparts thanks to its ability to use quantum mechanical properties of information.

It was Richard Feynman one of the first who recognized the importance of exploiting quantum mechanics principles in order to achieve new research results: he noted that while it is computationally very hard to simulate a quantum system with classical resources, the same is not true when one has quantum resources at his disposal. He used as example a system made out of N interacting spins: while the computational complexity grows exponentially with N using classical computation, thus making it impossible to solve numerically the problem, with quantum computation complexity would grow only linearly with N, thus allowing for an efficient simulation of the system.

This paradigm shift is somehow the successful completion of a path started long ago: since its first formulation in the 20', quantum mechanics has led scientists to face new and controversial results [Schrödinger 1926]. The Heisenberg uncertainty principle [Heisenberg 1927] and the wave particle duality [Broglie 1924] put a serious challenge to physicists, who spent years trying to understand the implications of the new born quantum theory, finally accepting the Copenhagen interpretation as the most convenient paradigm to interpret the new theory [N. Bohr 1928]. From that time on, physicist had continuously improved their knowledge and understanding of quantum mechanics, obtaining astonishing results both from a fundamental and a practical point of view.

It was in the 40's, fostered by war necessities, that the field of information theory was first established by Shannon in his groundbreaking work [Shannon 1948], where he first defined the concept of information. The concept of information was then extended to

the quantum realm thanks to the work of Von Neumann [von Neumann 1932]. As people started studying the possibilities offered by the exploitation of quantum mechanics in the field of information theory, soon new discoveries were made: it was already in the 80s' that the first quantum algorithms for quantum communication were conceived, the most famous instances being the quantum teleportation protocol [Bennett and Brassard 2014; Bennett, Brassard, et al. 1993], the Deutsch algorithm [Deutsch 1985], the Deutsch-Jozsa algorithmm [Deutsch and Jozsa 1992], the Grover search algorithm [Grover 1996, 1997] and the Shor algorithm [Shor 1994, 1997] for prime factorization.

All these algorithms can provide an example of how quantum information differs from classical one: in the quantum teleportation protocol a quantum state is faithfully transmitted between two parties thanks to an entangled pair of qubits and two bits of classical information, while the same task would require an infinite amount of information to be transmitted if one were to use only classical bits. On the same line the Shor's algorithm is able to compute the prime factors of a number with a number of operations that grows linearly with the number of ciphers, while in the classical case the complexity grows exponentially with the dimension of the number: thus a task that would take centuries with a classical computers (a fact that is daily used to guarantee security in digital payments), it would take a few months with a quantum computer.

On the other hand, physicists soon realized that *information is physical*, by this meaning that while Shannon theory allows for a general treatment of information [Cover and Thomas 2006], independently from the way it is stored and transmitted, one actually has to deal with the necessity of a material support for information processing, storage and transmission: just as classical computers have been possible thanks to proper technological supports able to implement the gates necessary to perform logical operations, the possibility of creating a quantum computer also relies on the ability to build a proper physical support able to implement all the gates necessary for quantum algorithms to run. This implies both the ability to create very sharp quantum systems and also the ability to externally control such systems with a very high degree of precision.

This compelling necessity for controlling quantum systems has been a main driving for physical research in the last decades: during these years physicists have tried to create new platforms for implementing quantum algorithms, like ion traps, optical lattices and the most promising superconducting quantum circuits and new techniques for quantum control, like adiabatic driving and reservoir engineering.

The huge technological advancement achieved in the last years has allowed for the emergence of a new field of physics dubbed "quantum engineering": with this term people

refer to a wide range of topics, from planning and building physical systems for specific tasks to developing algorithms to control those systems, from ways to create specific quantum states to new theoretical tools to describe and plan new physical systems.

As the field of quantum engineering covers many topics in physics, this is reflected in the community interested in it, ranging from quantum optics theorists to solid state experimentalists. This also includes the possibility, and sometimes the necessity, for a scientist willing to enter the field to study very different problems, as it happened to me during my PhD: in this thesis at least two main topics are covered.

On one side the study of open quantum systems has led me to look at quantum cascade systems, which are networks of quantum systems often called *nodes* driven by an external signal propagating unidirectionally, i.e. *chirally*. While studying such systems and deriving expressions for the master equation describing their dynamics can be ascribed to the field of dissipation engineering, their study has introduced me to the concept of collisional models, a method for studying open quantum systems that has gained more and more attention in the last years.

Studying such models has led me also into the field of quantum thermodynamics, which also gained much attention in recent times: the progressive demand for miniaturization of electrical components has pushed scientists to start ask themselves how and if the usual laws of classical thermodynamics apply in the quantum realm. Moreover, the extension of the thermodynamics law to the quantum realm allowed for the discovery of new problems and issue, both from the practical and the theoretical point of view, renewing the interest towards fundamental topics such as the validity of standard master equation and their ability to give correct and coherent thermodynamic results. Also, just as in the classical case, there is a strong and deep relationship between thermodynamics and information theory, exemplified by the interpretation of entropy both as a thermodynamic state function and as average missing information on a system.

Conversely, I also found myself dealing with more practical problems, such as the connection between solid state system and quantum optics: thanks to the technological possibilities implied by band engineering and to mature platform such as superconducting circuits, it is nowadays possible to recreate physical phenomena belonging to the field of quantum optics in the solid state context. With this in mind, I studied a class of potentials which we dubbed "stretching potentials", giving rise to stretched wave functions of the particle inside the potential, in analogy with what happens optically in photonic metamaterials.

Finally I studied also the geometric phase, also known as holonomy, imprinted on a

particle moving in a varying potential: while for time-dependent potentials this phenomenon received first attention by Berry, we studied the problem for space-dependent potentials in more than one dimension. This phenomenon allows for the manipulation of the state of a moving particle without worrying of its velocity, as the phase imprinted by the varying potential is a geometric invariant.

This thesis proceeds as follows: in Chap. 2 we will review some standard properties of open quantum systems, focusing in particular on the Markovian generator, its properties and its derivation, both within the standard microscopic approach and within the collisional model approach. In Chap. 3 we will examine cascade networks, seeing how to derive a Markovian master equation for the nodes with a properly defined collisional model and how cascade networks can be exploited to obtain interesting interference effects. Subsequently in Chap. 4, we will talk about qubit thermalization, showing how, thanks to a collisional model, it is possible to demonstrate the factorization of the thermalizing qubit state from the state of the thermal bath, thus showing the absence of correlations between a system and its thermal bath after thermalization took on. In Chap. 5 we will introduce the second part of the thesis, briefly reviewing some basic concepts of condensed matter physics, such as the band structure of solids, the effective mass approximation and band engineering. After this, in Chap. 6 we will look at stretching potentials, defining first the properties characterizing this class of potentials and then showing how these properties are reflected in the wave functions and eigenenergies associated to such potentials. Then in Chap. 7 we will show how a geometric phase can be attached to a particle moving in a 2D potential landscape by properly inserting a spatial dependence on the potential itself. Finally in Chap. 8 we will draw the conclusions and try to give an outlook for the future.

CHAPTER 2

Open quantum systems

Every physicist in the world was once a student, and all students, when dealing with quantum mechanics for the first time, are introduced to the subject starting from the study of closed systems, i.e. systems that can be described through an operator $\hat{H}$, possibly time-dependent, called the *Hamiltonian* of the system. The Hamiltonian operator is nothing but the energy of the system, and just as in classical mechanics, its knowledge is sufficient to describe the dynamics of a closed system.

But, just as grown up children find out that Santa Claus does not exist, so physicists soon have to understand that most of the systems they actually deal with are not closed, but rather open: a quantum system is always interacting with its surroundings, which is also known as *environment*.

The unavoidable presence of the environment is a crucial feature of quantum mechanics: it is something one must account for in the equations, in order to both give correct forecasts on experiments and to foresee interesting quantum mechanical effects. The first attempts in this direction usually lead to a phenomenological approach, with the inclusion of effective terms describing the effects of noise and dissipation, as in the case of the Bloch equations for the nuclear magnetic spin [Bloch 1946; Bloch, Hansen, and Packard 1946] or the optical Bloch equation for a two levels system [Arecchi and Bonifacio 1965].

The presence of the environment is also crucial to explain very fundamental questions, such as the emergence of classicality from the quantum world [Zurek 1993, 2003, 2018]:

in the quantum realm we observe superposition and interference phenomena between quantum states, giving rise to probabilistic phenomena, while the world we are used to observe and live in is deterministic, i.e. governed by classical physics laws.

The presence of the environment is naturally crucial not only when dealing with fundamental aspects of the theory, but also in more practical issues, such as the thermodynamic description of a system [Kosloff 2013], where the system is usually interacting with a thermal bath, or in the field of quantum optics, where, just to cite the most famous effect, the environment is responsible for the phenomenon of spontaneous emission and the shift of the energy levels of an atom [Dirac and N. H. D. Bohr 1927; Scully and Zubairy 1997].

A turning point in the context of open quantum systems dynamics is for sure represented by the works of Gorini, Kossakowski, Sudarshan and Lindblad [Gorini, Kossakowski, and Sudarshan 1976; Lindblad 1976], where for the first time an equation describing the Markovian dynamics of an open quantum system was derived. These works fostered a huge amount of work in the field of open quantum systems which still goes on today: from the study of the time-locality of the generators [Chruściński 2014; Filippov and Chruściński 2018; Reimer et al. 2019] to the spectral properties of such generators [V. V. Albert and Jiang 2014; Hatano and Ordonez 2019; Janßen 2017], from numerical simulation of open systems [Daley 2014; Dalibard, Castin, and Mølmer 1992; Mascherpa et al. 2019; Torres 2014; Zanardi, Marshall, and Campos Venuti 2016] to the extension of the GKSL equation beyond its original assumptions, for instance allowing for a time dependence of the generator [Dann, Levy, and Kosloff 2018] or for ultrastrong coupling of system and environment [H. P. Breuer, Dietz, and Holthaus 1988; H.-P. Breuer and Petruccione 1997].

The field of open quantum systems is also of paramount importance in the context of mathematical physics, where the concept of CPT maps can be studied under a mathematical perspective, leading to the concepts of quantum channels and operations [Caruso et al. 2014; Holevo and Giovannetti 2012; Kretschmann and Werner 2004] for which bounds on their entropic and informational properties [Giovannetti, García-Patrón, et al. 2014; Giovannetti, Holevo, and Mari 2015; Mari, Giovannetti, and Holevo 2014] can be derived, leading to important technological implication in the context of information processing and transmission [Chiribella and Adesso 2014; Macchiavello and Palma 2002; Pirandola and Lloyd 2008].

Given the importance and the broad range of topics covered by the field of open quantum systems, we find it necessary to give a brief review of some important concepts

before proceeding with the rest of the thesis. In this chapter we are going to briefly review the mathematical description of a closed quantum system in Sec. 2.1, which will also allow us to set the notation. Then we will review open quantum systems and their properties in Sec. 2.2, illustrating two ways of deriving a Markovian master equation, namely the dynamical semigroup approach and the microscopic derivation. Finally in Sec. 2.3 we will describe the collisional model and how it can be used to depict the dynamics of an open quantum system.

2.1. Closed systems

Mathematically speaking the physical properties of the state of a quantum system S are encoded in a *state vector* $|\psi\rangle_S$ living on the Hilbert space $\mathcal{H}_S$. Observable quantities are described by Hermitian operators belonging to the set $\Sigma(\mathcal{H}_S)$ of operators acting on Hilbert space $\mathcal{H}_S$. The time evolution of the state vector is given by the Schrödinger equation:

$$i\hbar\frac{d}{dt}|\psi(t)\rangle_S = \hat{H}_S|\psi(t)\rangle_S\,, \tag{2.1}$$

where $\hat{H}_S$ is the Hamiltonian operator of system S. Analogously to the classical case the Hamiltonian operator is nothing but the energy of the system, and thus is an Hermitian operator. Eq. (2.1) can be formally solved as:

$$|\psi(t)\rangle_S = \hat{U}_S(t,t_0)|\psi(t_0)\rangle_S\,, \tag{2.2}$$

where $\hat{U}_S(t,t_0)$ is the *time evolution operator*, a unitary operator describing the temporal evolution of $|\psi(t)\rangle_S$ from the initial time t_0 up to time t. The most general form of $\hat{U}_S(t,t_0)$, from Eq. (2.1) results:

$$\hat{U}_S(t,t_0) = \mathcal{T}\exp\left[-\frac{i}{\hbar}\int_{t_0}^{t}\hat{H}_S(t')dt'\right], \tag{2.3}$$

where $\mathcal{T}$ indicates the *time-ordered product*. Eq. (2.3) express the temporal evolution operator for the most generic case of a time-dependent Hamiltonian $\hat{H}_S(t)$ that does not commute with itself at different times, i.e.:

$$\left[\hat{H}_S(t_1),\hat{H}_S(t_2)\right] \neq 0 \quad \text{for } t_1 \neq t_2. \tag{2.4}$$

In the following of this chapter we will assume $\hat{H}_S(t) = \hat{H}_S$, that is, a time-independent Hamiltonian, unless differently specified. Here we limit ourselves to remember that the formal expression of a time-ordered product is given by the Dyson series:

$$\hat{U}_S(t, t_0) = 1 + \sum_{n=1}^{\infty} \left(-\frac{i}{\hbar}\right)^n \int_{t_0}^{t} dt_1 \int_{t_0}^{t_1} dt_2 \cdots \int_{t_0}^{t_{n-1}} dt_n \hat{H}_S(t_1)\hat{H}_S(t_2)\cdots\hat{H}_S(t_n). \quad (2.5)$$

For the case of a time-independent Hamiltonian the temporal evolution operator in Eq. (2.3) has the very simple form:

$$\hat{U}_S(t, t_0) = \exp\left[-\frac{i}{\hbar}\hat{H}_S(t - t_0)\right]. \quad (2.6)$$

When written as in Eq. (2.6) it is immediate to see that $\hat{U}_S(t, t_0)$ has the property:

$$\hat{U}_S(t_0, t) = \exp\left[-\frac{i}{\hbar}\hat{H}_S(t_0 - t)\right] = \exp\left[\frac{i}{\hbar}\hat{H}_S(t - t_0)\right] = \hat{U}_S^\dagger(t, t_0), \quad (2.7)$$

which means that the inverse operator of $\hat{U}_S(t, t_0)$ is its *adjoint* $\hat{U}_S^\dagger(t, t_0)$:

$$\hat{U}_S(t, t_0)\hat{U}_S^\dagger(t, t_0) = \hat{\mathbb{I}}_S, \quad (2.8)$$

where $\hat{\mathbb{I}}_S$ is the identity operator on S.

As for any other self-adjoint operator, it is possible to diagonalize $\hat{H}_S$: by diagonalizing an operator we mean finding a set of state vectors $\{|\phi_i\rangle_S\}$ such that:

$$\hat{H}_S |\phi_i\rangle_S = E_i |\phi_i\rangle_S . \quad (2.9)$$

The $|\phi_i\rangle_S$ are called *eigenvectors* of $\hat{H}_S$ and E_i is the energy eigenvalue corresponding to state $|\phi_i\rangle_S$. The set of all eigenvectors $\{|\phi_i\rangle_S\}$ forms an orthonormal basis of the Hilbert space $\mathcal{H}_S$, and thus any state $|\psi\rangle_S$ can be expressed as a linear combination of such base vectors:

$$|\psi\rangle_S = \sum_i |\phi_i\rangle_S \langle\phi_i|\psi\rangle_S = \sum_i c_i |\phi_i\rangle_S , \quad (2.10)$$

where we have defined $c_i = \langle\phi_i|\psi\rangle_S$ and inserted the identity in the $\{|\phi_i\rangle_S\}$ basis.

From Eq. (2.1) and Eq. (2.9) we can write the temporal evolution of an eigenvector

of the Hamiltonian as:

$$i\hbar\frac{\partial}{\partial t}\left|\phi_i\right\rangle_S = E_i\left|\phi_i\right\rangle_S \Rightarrow \left|\phi_i(t)\right\rangle_S = e^{-\frac{i}{\hbar}E_i(t-t_0)}\left|\phi_i\right\rangle_S . \tag{2.11}$$

The eigenstates of $\hat{H}_S$ are stationary states with respect to temporal evolution. From Eq. (2.11) it is then straightforward to see that expressing the state $\left|\psi(t)\right\rangle_S$ as in Eq. (2.10) the solution to the Schrödinger equation is:

$$\left|\psi(t)\right\rangle_S = \sum_i c_i e^{-\frac{i}{\hbar}E_i(t-t_0)}\left|\phi_i\right\rangle_S = \sum_i c_i(t)\left|\phi_i\right\rangle . \tag{2.12}$$

Knowing the state $\left|\psi(t)\right\rangle_S$ allows one to compute the expectation value (ensemble average) of any operator $\hat{A}_S$ as:

$$\left\langle \hat{A}_S(t)\right\rangle = {}_S\langle\psi(t)|\hat{A}_S\left|\psi(t)\right\rangle_S . \tag{2.13}$$

All of this is valid for a *pure ensemble*, that is, we are sure that the quantum system is indeed in the state $\left|\psi(t)\right\rangle$. In most scenarios however we do not have this certainty: this is why one needs to introduce the *density matrix* $\hat{\rho}_S(t)$. Consider for instance the case where system S can be in either of two states $\left|\psi_1(t)\right\rangle_S(t)$ or $\left|\psi_2(t)\right\rangle_S$ with probability w_1 and w_2 respectively. Then if we were to compute the expectation value of an observable for this state we would get:

$$\begin{aligned}\left\langle \hat{A}_S(t)\right\rangle &= w_1\,{}_S\langle\psi_1(t)|\hat{A}_S\left|\psi_1(t)\right\rangle_S + w_2\,{}_S\langle\psi_2(t)|\hat{A}_S\left|\psi_2(t)\right\rangle_S \\ &= \sum_i w_i\left\langle\psi_i(t)|\hat{A}_S|\psi_i(t)\right\rangle .\end{aligned} \tag{2.14}$$

If we now insert twice the identity operator for a base set $\{\left|\phi_i\right\rangle_S\}$ into Eq. (2.14) we get:

$$\left\langle \hat{A}(t)\right\rangle = \sum_i\sum_{\ell,\ell'} w_i\left\langle\phi_\ell|\psi_i(t)\right\rangle_S\left\langle\psi_i(t)|\phi_{\ell'}\right\rangle_S\left\langle\phi_{\ell'}|\hat{A}_S|\phi_\ell\right\rangle . \tag{2.15}$$

Since the properties of the ensemble shall not depend on the specific base chosen, we define the density matrix $\hat{\rho}_S(t)$ as:

$$\hat{\rho}_S(t) = \sum_i w_i\left|\psi_i(t)\right\rangle\!\left\langle\psi_i(t)\right| . \tag{2.16}$$

With this definition it is possible to write the expectation value of $\hat{A}_S$ as:

$$\left\langle \hat{A}_S(t) \right\rangle = \sum_{\ell,\ell'} \langle \phi_{\ell'} | \hat{\rho}_S(t) | \phi_\ell \rangle \ \langle \phi_\ell | \hat{A}_S(t) | \phi_{\ell'} \rangle = \mathrm{Tr}\Big\{ \hat{A}_S \hat{\rho}_S(t) \Big\}. \tag{2.17}$$

From Eq. (2.16) some important properties of the density matrix can be immediately derived. As the weights w_i are just classical probabilities they must sum up to 1, and thus:

$$\mathrm{Tr}\{\hat{\rho}_S(t)\} = 1, \quad \mathrm{Tr}\Big\{ \hat{\rho^2(t)}_S \Big\} \leq 1, \quad \hat{\rho}_{\ell\ell'} = \hat{\rho}^*_{\ell'\ell}, \tag{2.18}$$

where the inequality is saturated only for pure states.

Finally it is clear from the definition that the density matrix $\hat{\rho}_S(t)$ evolves in time as:

$$\frac{d}{dt}\hat{\rho}_S(t) = -\frac{i}{\hbar}\Big[\hat{H}_S, \hat{\rho}_S(t) \Big]. \tag{2.19}$$

This representation of quantum dynamics is known as the *Schrödinger picture*: in this picture one assumes the observable quantities to be time-independent while only the states are affected by time evolution. There are infinite possible pictures to represent quantum dynamics, but only two are commonly used and of importance for our purposes, namely the *Heisenberg picture* and the *interaction picture* which we are going to see in the next two sections.

2.1.1. The Heisenberg picture

The main goal of any physical theory is to provide expectation values for some quantities to be measured in experiments. As we have seen observable quantities in quantum mechanics are described by Hermitean operators belonging to $\Sigma(\mathcal{H}_S)$. Specifically the expectation value of any Hermitean operator $\hat{A}_S$ for a system in the state $|\psi(t)\rangle_S$ is given by Eq. (2.13).

In the previous section we treated time-evolution in such a way that only the state vectors evolve, while the operators corresponding to observable quantities were assumed constant. Starting from Eq. (2.13) and inserting Eq. (2.2) we get:

$$\langle \hat{A}(t) \rangle = {}_S\langle \psi(t_0) | \hat{U}^\dagger_S(t,t_0) \hat{A}_S \hat{U}_S(t,t_0) \, |\psi(t_0)\rangle_S = {}_S\langle \psi(t_0) | \hat{A}_S(t) \, |\psi(t_0)\rangle_S \,, \tag{2.20}$$

where now

$$\hat{A}_S(t) = \hat{U}_S^\dagger(t, t_0)\hat{A}_S\hat{U}_S(t, t_0). \tag{2.21}$$

In the last passage we have moved the effect of the temporal evolution operator from the state vector to the operator $\hat{A}_S$: in this way one has time-independent state vectors and time-dependent operators. Deriving $\hat{A}_S(t)$ with respect to t and remembering Eq. (2.6) one gets:

$$\frac{d}{dt}\hat{A}_S(t) = \frac{\partial}{\partial t}\hat{A}_S(t) - \frac{i}{\hbar}\Big[\hat{A}_S(t), \hat{H}_S\Big] \tag{2.22}$$

Eq. (2.22) is known as the *Heisenberg equation of motion*: it is the differential equation describing the evolution of time-dependent operators while all state vectors are time-independent.

2.1.2. The Interaction picture

We consider then the *interaction picture*, which is widely used in the study of open quantum systems. The interaction picture can be considered somehow in between the Schrödinger and the Heisenberg ones. In order to define the interaction picture for a system S one has to divide the Hamiltonian in two parts $\hat{H}_S = \hat{H}_{0,S} + \hat{H}_{I,S}$, where usually $\hat{H}_{0,S}$ is called the *free Hamiltonian* and $\hat{H}_{I,S}$ the *interaction Hamiltonian*. We define:

$$\big|\psi^{(I)}(t)\big\rangle_S = e^{\frac{i}{\hbar}\hat{H}_{0,S}(t-t_0)}\,|\psi(t_0)\rangle_S \tag{2.23}$$

$$\hat{A}_S^{(I)}(t) = e^{\frac{i}{\hbar}\hat{H}_{0,S}(t-t_0)}\hat{A}_S(t_0)e^{-\frac{i}{\hbar}\hat{H}_{0,S}(t-t_0)} \tag{2.24}$$

The symbol (I) here signals the object to be meant in the interaction representation, but throughout this thesis it will be often omitted when no confusion can arise, in order not to burden the notation. One can directly compute the time evolution of both states and operators in this picture. As for states one has:

$$\begin{aligned} &i\hbar\frac{d}{dt}\big|\psi^{(I)}(t)\big\rangle_S = -\hat{H}_{0,S}\big|\psi^{(I)}(t)\big\rangle_S + e^{\frac{i}{\hbar}\hat{H}_{0,S}(t-t_0)}\hat{H}_S e^{-\frac{i}{\hbar}\hat{H}_{0,S}(t-t_0)}\big|\psi^{(I)}(t)\big\rangle_S \\ &= e^{\frac{i}{\hbar}\hat{H}_{0,S}(t-t_0)}\hat{H}_{I,S}e^{-\frac{i}{\hbar}\hat{H}_{0,S}(t-t_0)}\big|\psi^{(I)}(t)\big\rangle_S = \hat{H}_{I,S}^{(I)}\big|\psi^{(I)}(t)\big\rangle_S\,, \end{aligned} \tag{2.25}$$

which implies for the density matrix:

$$\frac{d}{dt}\hat{\rho}_S^{(I)}(t) = -\frac{i}{\hbar}\Big[\hat{H}_S^{(I)}(t), \hat{\rho}_S^{(I)}(t)\Big]. \tag{2.26}$$

The evolution of an operator is instead given by:

$$\begin{aligned}\frac{d}{dt}\hat{A}_S^{(I)}(t) &= \frac{\partial}{\partial t}\hat{A}_S^{(I)}(t) - \frac{i}{\hbar}\Big[\hat{A}_S^{(I)}(t), \hat{H}_{0,S}\Big] \\ &= \frac{\partial}{\partial t}\hat{A}_S^{(I)}(t) - \frac{i}{\hbar}\Big[\hat{A}_S^{(I)}(t), \hat{H}_{0,S}^{(I)}\Big].\end{aligned} \tag{2.27}$$

From Eq. (2.25) and Eq. (2.27) we see that in the interaction picture the states evolve only through the interaction Hamiltonian, while the operators evolve only through the free Hamiltonian, both the free and the interaction Hamiltonian being meant in the interaction picture. This representation is particularly useful in scenarios where the interaction Hamiltonian represents a perturbation on the system, since the operators have their unperturbed forms and the states can be treated through perturbation theory.

2.1.3. Composite systems

Before moving to the study of open quantum systems, we need to deal with composite quantum systems. As it is often the case in physics, the distinction between a single quantum system and a composite quantum system is just a matter of perspective: if one is interested in a global property of a system it might be convenient to treat the system as a unique block, while if one were interested, for instance, in the correlations among the single components of the system, then it might be more convenient to treat the system as a composite one.

To treat the latter case in quantum mechanics the concept of *tensor product* is introduced. Consider two independent quantum systems S_1, S_2, each described by a Schrödinger picture state vector $|\psi(t)\rangle_{S_i}$ living in the Hilbert space $\mathcal{H}_{S_i}$ spanned by the orthonormal basis $\{|\phi_i\rangle_{S_i}\}$. The joint state of sytems S_1 and S_2 can then be described through the state vector

$$|\psi(t)\rangle_{S_1S_2} = |\psi(t)\rangle_{S_1} \otimes |\psi(t)\rangle_{S_2}\,, \tag{2.28}$$

which is the tensor product of the state vectors describing S_1 and S_2 separately. The state vector $|\psi(t)\rangle_{S_1S_2}$ lives in the Hilbert space $\mathcal{H}_{S_1S_2} = \mathcal{H}_{S_1} \otimes \mathcal{H}_{S_2}$ spanned by the orthonormal basis $\{|\phi_{ij}\rangle_{S_1S_2} = |\phi_i\rangle_{S_1} \otimes |\phi_j\rangle_{S_2}\}$. As we are assuming the two systems to

be independent of each other, this means that each has its own Hamiltonian $\hat{H}_{S_i}$, and that the evolution of the joint state vector is given by:

$$i\hbar\frac{d}{dt}\left|\psi(t)\right\rangle_{S_1S_2} = \left(\hat{H}_{S_1}\otimes\hat{I}_{S_2} + \hat{I}_{S_1}\otimes\hat{H}_{S_2}\right)\left|\psi(t)\right\rangle_{S_1S_2}, \tag{2.29}$$

where $\hat{I}_{S_i}$ is the identity operator in the Hilbert space $\mathcal{H}_{S_i}$. Things become more complicated when S_1 and S_2 are no longer independent, as in most of the cases, but there is instead an interaction between the two systems. In this case $\{|\phi_{ij}\rangle_{S_1S_2}\}$ is still an orthonormal basis spanning $\mathcal{H}_{S_1S_2}$, but the basis vectors won't be also energy eigenstates anymore: though this might seem a minor fact, it is actually this feature that renders the study of composite quantum system computationally hard as the size of the system (i.e. the number of components) increases [Feynman 1982], and that eventually lead to the development of new computational techniques [Schollwöck 2011; Verstraete, Garcia-Ripoll, and Cirac 2004; Verstraete and Cirac 2004; Vidal 2004].

Dealing with composite systems, one is almost compelled to speak about quantum entanglement: this phenomenon is one of the iconic features of quantum mechanics that lead to several discussions over the interpretation of quantum mechanics, for instance prompting Einstein, Podolski and Rosen to elaborate the paradox that still brings their name [Einstein, Podolsky, and Rosen 1935]. Their work stimulated the elaboration of the hidden variable framework by Bell [Bell 1964] and the discovery of the so called CHSH inequality [Clauser et al. 1969], which was finally seen to be violated experimentally by the group of Alain Aspects [Aspect, Dalibard, and Roger 1982; Aspect, Grangier, and Roger 1982].

Entanglement is now considered to be a fundamental resource in the context of quantum information, since many of the protocol introduced in this field, such as quantum key distribution [A. K. Ekert 1991], quantum dense coding [Barenco and A. K. Ekert 1995] and quantum teleportation [Bennett, Brassard, et al. 1993] are based on the exploitation of entangled states of bipartite systems.

From a mathematical perspective one observes that it is not always possible to write a pure state of a composite system as in Eq. (2.28). When this is not possible, i.e. when

$$\left|\psi\right\rangle_{S_1S_2} = \sum_i c_i \left|\psi_i\right\rangle_{S_1}\otimes\left|\psi_i\right\rangle_{S_2}, \tag{2.30}$$

the the state $|\psi\rangle_{S_1S_2}$ is entangled. As for mixed states, one is said to be entangled when

it cannot be written as a convex combination of product states, that is:

$$\hat{\rho}_{S_1S_2} \neq \sum_i p_i \hat{\rho}^{(i)}_{S_1} \otimes \hat{\sigma}^{(i)}_{S_2}. \tag{2.31}$$

From the definitions in Eqs.(2.30, 2.31) it is quite evident that determining whether a state is entangled or not is not an easy task. Actually some criterions exist for certain categories of states and systems [M. Horodecki, P. Horodecki, and R. Horodecki 1996; Peres 1996; Terhal 2000; Werner 1989], but no general criterion has yet been found, especially for multipartite systems. All in all the study of entanglement, including its determination and quantification, is a field still full of open questions in spite of the great attention that has been given to the subject [R. Horodecki et al. 2009].

A natural question coming to mind is how we can recover the state of one part of the composite system, for instance the state of S_1, knowing the joint state $\hat{\rho}_{S_1S_2}$. The answer is given by the *partial trace* operation: this operation consists in tracing away the degrees of freedom relative to the part of the composite system we are not interested in. Applying the partial trace operation to a joint state of a composite system, it is possible to recover the *reduced state* of the system

$$\mathrm{Tr}_{S_2}\{\hat{\rho}_{S_1S_2}\} = \hat{\rho}_{S_1} \quad \mathrm{Tr}_{S_1}\{\hat{\rho}_{S_1S_2}\} = \hat{\rho}_{S_2}, \tag{2.32}$$

where now $\hat{\rho}_{S_1}$ (respectively $\hat{\rho}_{S_2}$) contains information on the state of S_1 only (resp. S_2). Another important operation in quantum mechanics is the *purification* of a state: from Eq. (2.32) it is clear that any state of a system S can be seen as the reduced state of a larger system made out by S itself and an auxiliary system S'. The important point is that given a mixed state $\hat{\rho}_S$ it is always possible to choose the state of the enlarged system to be a pure one, i.e. it exists a state $|\psi_{SS'}\rangle$ such that:

$$\mathrm{Tr}_{S'}\{|\psi_{SS'}\rangle\langle\psi_{SS'}|\} = \hat{\rho}_S. \tag{2.33}$$

This concept will turn out to be useful when dealing with CPT maps, as we are going to see in the following sections: in facts Eq. (2.33) implies that the action of a CPT map acting on $\hat{\rho}_S$ can be seen as the action of a unitary operator $\hat{U}_{SS'}$ acting on the pure state $|\psi_{SS'}\rangle$.

After reviewing the various pictures used in quantum mechanics and the way we describe composite systems, we have all the ingredients to treat the dynamics of an open quantum system.

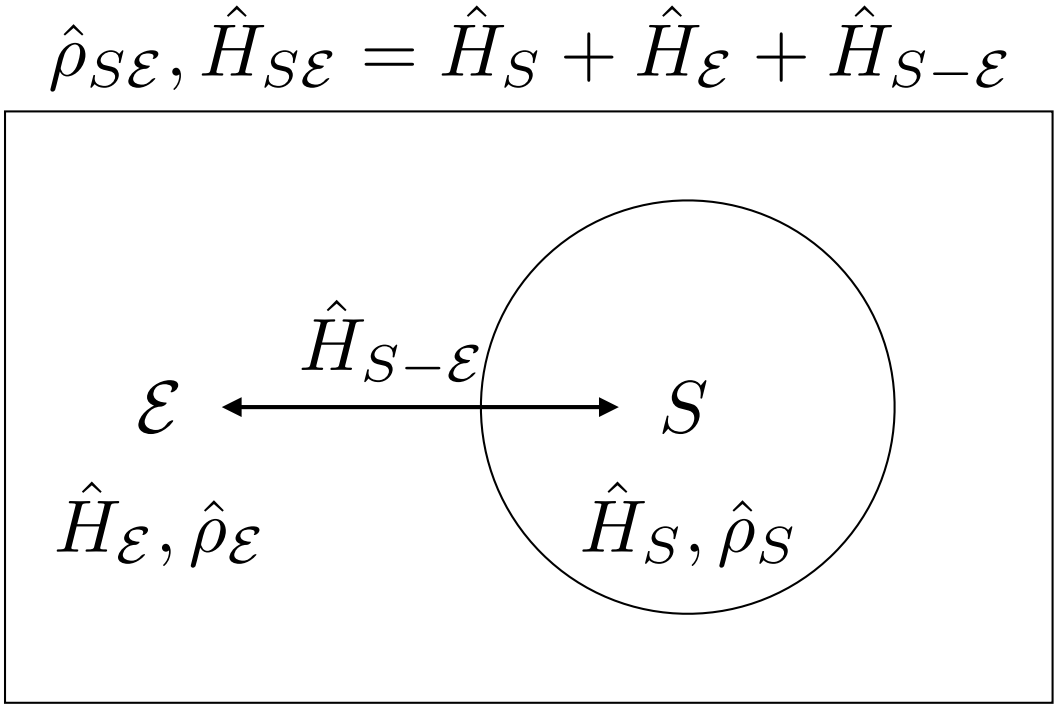

Figure 2.1.: A sketch of an open quantum system: the composite $S + \mathcal{E}$ system is considered closed, and thus it is described by the density matrix $\hat{\rho}_{S\mathcal{E}}$ whose closed dynamics is dictated by $\hat{H}_{S\mathcal{E}}$. $\hat{H}_{S\mathcal{E}}$ is the sum of the free hamiltonians of system and environment, $\hat{H}_S$ and $\hat{H}_\mathcal{E}$ respectively, plus $\hat{H}_{S-\mathcal{E}}$ describing the interaction between S and $\mathcal{E}$.

2.2. Open quantum systems dynamics

2.2.1. CPT maps and dynamical semigroups

All the formalism exposed in the previous section is valid for any closed system. Thus we still have to answer the question of how to describe the dynamics of a quantum system S interacting with an external environment $\mathcal{E}$.

First of all it must be noted that, as in the case of composite systems, the distinction between the system S and the environment $\mathcal{E}$ is more a matter of definition than a physical matter: the distinction only comes from our way of modeling the dynamics of a physical system. What we usually mean when we talk of an open system interacting with the environment instead of two interacting quantum systems is that that the environment has a somehow special role [Davies 1976]: in most scenarios the environment $\mathcal{E}$ is far larger than the system S and, moreover, it is usually through the environment that we are able to perform measurements to gain information on S itself.

All of this being said, we can start to depict the dynamics of an open quantum system. The starting point is to represent the joint $S + \mathcal{E}$ system as a closed system, as shown pictorially in Fig. 2.1. The state of the joint system is encoded into the density matrix $\hat{\rho}_{S\mathcal{E}}$. This density matrix evolves according to the Hamiltonian $\hat{H}_{S\mathcal{E}}$ which is the sum of the Hamiltonians of S and $\mathcal{E}$ if they were isolated plus a contribution $\mathcal{H}_{S-\mathcal{E}}$ describing the interaction between the system and the environment.

As already shown in the previous section, the density matrix of either S or $\mathcal{E}$ can be found by partially tracing away the degrees of freedom of the system we want to discard:

$$\hat{\rho}_S = \mathrm{Tr}_{\mathcal{E}} \left\{ \hat{\rho}_{S\mathcal{E}} \right\} \quad \hat{\rho}_{\mathcal{E}} = \mathrm{Tr}_S \left\{ \hat{\rho}_{S\mathcal{E}} \right\}. \tag{2.34}$$

As the joint $S - \mathcal{E}$ system is closed, its density matrix evolves according to:

$$\frac{d}{dt}\hat{\rho}_{S\mathcal{E}}(t) = -\frac{i}{\hbar}[H_{S\mathcal{E}}, \hat{\rho}_{S\mathcal{E}}(t)] \Rightarrow \hat{\rho}_{S\mathcal{E}}(t) = \hat{U}_{S\mathcal{E}}(t, t_0)\hat{\rho}_{S\mathcal{E}}(t_0)\hat{U}^{\dagger}_{S\mathcal{E}}(t, t_0) \tag{2.35}$$

Further assuming the initial state of S and $\mathcal{E}$ to be a factorized one

$$\hat{\rho}_{S\mathcal{E}}(0) = \hat{\rho}_S(t_0) \otimes \hat{\rho}_{\mathcal{E}}(t_0), \tag{2.36}$$

in order to ensure positivity [Modi 2012; Pollock et al. 2018; Ringbauer et al. 2015; Rodríguez-Rosario, Modi, and Aspuru-Guzik 2010; Štelmachovič and Bužek 2001], from Eq. (2.35) it is then possible to compute the reduced density matrix of S through:

$$\hat{\rho}_S(t) = \mathrm{Tr}_{\mathcal{E}} \left\{ \hat{U}_{S\mathcal{E}}(t, t_0)\hat{\rho}_{S\mathcal{E}}(t_0)\hat{U}^{\dagger}_{S\mathcal{E}}(t, t_0) \right\} = \mathcal{V}_S(t, t_0)\hat{\rho}_S(t_0), \tag{2.37}$$

where we have introduced the *dynamical map* $\mathcal{V}(t, t_0)$, a super-operator [Alicki 2002; Alicki and Lendi 1987; Kraus 1971] (i.e. an operator acting on other operators) describing the evolution of $\hat{\rho}_S$ from time t_0 to time t. The dynamical map $\mathcal{V}(t, t_0)$ can be a very complicated and involuted object in general, as the interaction of S with the environment might include effects, such as information back-flow, which are difficult to describe. The action of $\mathcal{V}_S(t, t_0)$ is resumed in Fig. 2.2.

2.2.2. The Markovian master equation

From a physical point of view Markovianity is usually associated with the absence of memory effects on the interaction between S and $\mathcal{E}$. In facts the distinction between Markovian and non-Markovian dynamics [H.-P. Breuer 2012; Li, Hall, and Wiseman

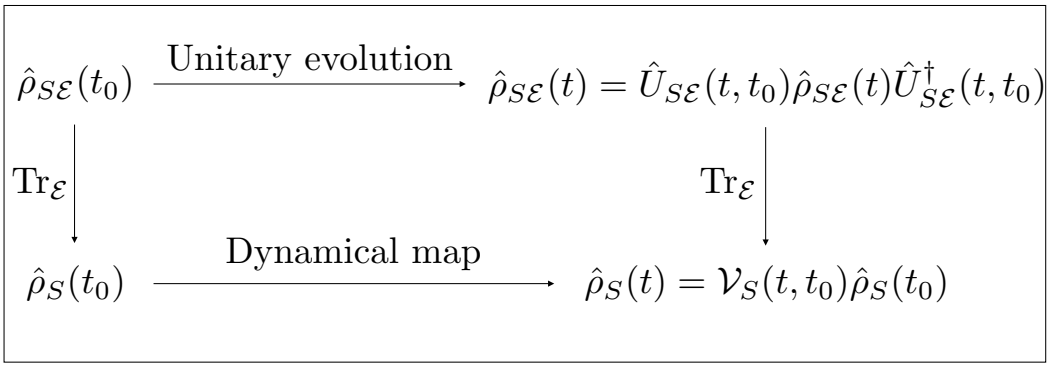

Figure 2.2.: Diagram showing the action of the dynamical map $\mathcal{V}_S(t,t_0)$.

2018] has been the object of great attention in the last 20 years, leading to the definition of different measures of the non-Markovianity of a process [H.-P. Breuer, Laine, and Piilo 2009; H.-P. Breuer, Laine, Piilo, and Vacchini 2016; Rivas, Huelga, and Plenio 2014; Smirne et al. 2013] and to the individuation of several methods to treat such systems [Cangemi et al. 2018; Ferialdi 2016; Strunz, Diósi, and Gisin 1999; Vega and Alonso 2017], among which the Nakajima-Zwanzig projection operator technique is probably the most known [Nakajima 1958; Prigogine 1962; Zwanzig 1960]. Non-Markovianity is involved also in more fundamental issues, like its relation with time-divisibility [Chruściński and Kossakowski 2010] and causality [Budini 2018]. Though non-Markovianity can be also exploited in technological applications, in this work we will focus on Markovian systems.

A much simpler distinction between Markovian and non-Markovian dynamics can be obtained from a mathematical perspective, as a stochastic process is said to be Markovian if the probability distribution describing its future evolution depends only on the present and not on the past [Cover and Thomas 2006]. Conversely the dynamics is said to be non-Markovian when this property does not hold.

In what follows we are going to see how the Markovian master equation can be derived either via dynamical semigroups theory and via microscopic derivation, so that when discussing the collisional model we will be able to highlight and discuss the main differences between these approaches.

As we saw in the previous pages tracing away the degrees of freedom of the environment after letting the whole $S+\mathcal{E}$ system evolve defines a dynamical map $\mathcal{V}_S(t,t_0)$: since after its action we must still have a density matrix, $\mathcal{V}_S(t,t_0)$ has to be a Completely Positive

Trace preserving map (CPT). A map is said to be trace preserving if:

$$\mathrm{Tr}\left\{\mathcal{V}_S(t,t_0)\hat{A}_S\right\} = \mathrm{Tr}\left\{\hat{A}_S\right\} \quad \forall\, \hat{A}_S, t. \tag{2.38}$$

Positivity is the property of a map of mapping positive semidefinite operators into positive semidefinite operators. An operator $\hat{A}_S$ is positive semidefinite if:

$$\langle\phi_i|\, \hat{A}_S\, |\phi_i\rangle \geq 0 \quad \forall\, |\phi_i\rangle \tag{2.39}$$

Complete positivity is a stronger property than positivity: it requires not only that any positive semidefinite operator is mapped into a positive semidefinite operator, but also that any extension of a positive semidefinite operator is mapped into a positive semidefinite operator. By an extension of an operator we mean an operator whose action is extended to another Hilbert space. Consider an auxiliary Hilbert space $\mathcal{H}_{S'}$ and the identity operator on this space $\mathcal{I}_{S'}$. The map $\mathcal{V}_S(t,t_0)$ is said to be completely positive if its tensor product with the identity map $\mathcal{I}_{S'}$ maps any positive operator acting on the Hilbert space $\mathcal{H}_S \otimes \mathcal{H}_{S'}$ into positive operators:

$$(\mathcal{V}_S(t,t_0) \otimes \mathcal{I}_{S'})(\hat{A}_{SS'}) \geq 0 \quad \forall \hat{A}_{SS'} \geq 0. \tag{2.40}$$

Physically this amounts to the requirement that the local action of $\mathcal{V}_S(t,t_0)$ on S should map states into states, even in presence of quantum correlations, like entanglement, between S and S'.

The axiomatic approach to the derivation of the Markovian master equation assumes that the maps $\mathcal{V}_S(t,t_0)$ form a dynamical semigroup as t varies. That is, in the time-homogeneous case, the maps fulfill the property:

$$\mathcal{V}_S(t_2,t_1)\mathcal{V}_S(t_1,t_0) = \mathcal{V}_S(t_2,t_0) \tag{2.41}$$

It is also required that the one parameter family of maps $\mathcal{V}_S(t,t_0)$ is ultraweak continuous, that is:

$$\lim_{\epsilon\to 0} \mathrm{Tr}_S\left\{(\mathcal{V}_S^\dagger(t_0+\epsilon,t_0)\hat{A}_S - \hat{A}_S)\hat{\rho}_S(t_0)\right\} = 0 \tag{2.42}$$

This property allows for the introduction of the *generator* $\mathcal{L}$ of the dynamical semi-

group, thank to which we can write:

$$\mathcal{V}_S(t) = \exp\{\mathcal{L}t\} \Rightarrow \frac{d}{dt}\hat{\rho}_S(t) = \mathcal{L}\hat{\rho}_S(t) \tag{2.43}$$

This is the Markovian master equation: we can now proceed in deriving the standard form of the generator $\mathcal{L}$.

The map $\mathcal{V}_S(t)$, and thus the generator $\mathcal{L}$, can be characterized in terms of operators acting on S only. To show this we write the density matrix $\hat{\rho}_\mathcal{E}$ through its spectral decomposition:

$$\hat{\rho}_\mathcal{E} = \sum_\alpha \lambda_\alpha \left|\phi_\alpha\right\rangle\!\left\langle\phi_\alpha\right| . \tag{2.44}$$

Accordingly we can write the dynamical map as:

$$\mathcal{V}_S(t)\hat{\rho}_S(0) = \sum_{\alpha,\beta} \hat{W}_{S\alpha\beta}(t)\hat{\rho}_S(0)\hat{W}^\dagger_{S\alpha\beta}(t), \tag{2.45}$$

where the operators $\hat{W}_{S\alpha\beta}(t)$ are defined as:

$$\hat{W}_{S\alpha\beta}(t) = \sqrt{\lambda_\beta}\left\langle\phi_\alpha\right| \hat{U}_{S\mathcal{E}}(t,0)\left|\phi_\beta\right\rangle , \tag{2.46}$$

and have the property:

$$\sum_{\alpha,\beta} \hat{W}^\dagger_{S\alpha\beta}(t)\hat{W}_{S\alpha\beta}(t) = \hat{\mathbb{I}}_S, \tag{2.47}$$

which guarantees that $\mathcal{V}_S(t)$ is trace preserving.

For the sake of simplicity let us focus on the case where $dim(\mathcal{H}_S) = d < \infty$. We can then define an orthonormal base of operators acting on $\mathcal{H}_S$ made out of d^2 elements $\left\{\hat{F}_{Si}\right\}$ fulfilling:

$$\left(\hat{F}_{Si}, \hat{F}_{Sj}\right) = \mathrm{Tr}_S\left\{\hat{F}^\dagger_{Si}\hat{F}_{Sj}\right\} = \delta_{ij}. \tag{2.48}$$

We also choose the operator $\hat{F}_{Sd^2}$ to be proportional to the identity operator, so that all

the other $\hat{F}_{Si}$ are traceless. Decomposing the operators $\mathcal{W}_{S\alpha\beta}(t)$ in this basis, we get:

$$\hat{W}_{S\alpha\beta}(t) = \sum_{i=1}^{d^2} \hat{F}_{Si} \left(\hat{F}_{Si}, \hat{W}_{S\alpha\beta} \right) \Rightarrow \mathcal{V}_S(t)\hat{\rho}_S(0) = \sum_{ij} c_{ij}(t) \hat{F}_{Si} \hat{\rho}_S(0) \hat{F}_{Sj}^\dagger, \tag{2.49}$$

where the c_{ij} are defined as:

$$c_{ij}(t) = \sum_{\alpha,\beta} \left(\hat{F}_{Si}, \hat{W}_{S\alpha\beta}(t) \right) \left(\hat{F}_{Sj}, \hat{W}_{S\alpha\beta}(t) \right)^*, \tag{2.50}$$

and form an Hermitian positive definite matrix. At this point we can go back to Eq. (2.43) and get from the definition:

$$\begin{aligned} \mathcal{L}\hat{\rho}_S &= \lim_{\epsilon \to 0} \frac{1}{\epsilon} \left[\mathcal{V}_S(\epsilon)\hat{\rho}_S(0) - \hat{\rho}_S(0) \right] \\ &= \lim_{\epsilon \to 0} \left[\frac{1}{d} \frac{c_{d^2 d^2}(\epsilon) - d}{\epsilon} \hat{\rho}_S(t) + \frac{1}{\sqrt{d}} \sum_{i=1}^{d^2-1} \left(\frac{c_{id^2}(\epsilon)}{\epsilon} \hat{F}_{Si} \hat{\rho}_S(t) + \frac{c_{d^2 i}(\epsilon)}{\epsilon} \hat{\rho}_S(t) \hat{F}_{Si}^\dagger \right) \right. \\ &+ \left. \sum_{i,j=1}^{d^2-1} \frac{c_{ij}(\epsilon)}{\epsilon} \hat{F}_{Si} \hat{\rho}_S(0) \hat{F}_{Sj}^\dagger \right]. \end{aligned} \tag{2.51}$$

In order to find the standard form of the Markovian generator $\mathcal{L}$ we define the coefficients:

$$a_{d^2 d^2} = \lim_{\epsilon \to 0} \frac{c_{d^2 d^2}(\epsilon) - d}{\epsilon} \tag{2.52}$$

$$a_{id^2} = \lim_{\epsilon \to 0} \frac{c_{id^2}(\epsilon)}{\epsilon} \tag{2.53}$$

$$a_{ij} = \lim_{\epsilon \to 0} \frac{c_{ij}(\epsilon)}{\epsilon}, \tag{2.54}$$

where the matrix formed by the a_{ij} is Hermitian and positive definite, since the c_{ij} are. The coefficients a_{ij} allow us to define the three operators:

$$\hat{F}_S = \frac{1}{\sqrt{d}} \sum_{i=1}^{d^2-1} a_{id^2} \hat{F}_{Si} \tag{2.55}$$

$$\hat{G}_S = \frac{1}{2d} a_{d^2 d^2} \hat{\mathbb{I}}_S + \frac{1}{2} \left(\hat{F}_S^\dagger + \hat{F}_S \right) \tag{2.56}$$

$$\hat{H} = \frac{1}{2i} \left(\hat{F}_S^\dagger - \hat{F}_S \right) \tag{2.57}$$

Thank to these operators we can write the Markovian generator as:

$$\mathcal{L}\hat{\rho}_S(t) = -i\Big[\hat{H}, \hat{\rho}_S(t)\Big] + \Big\{\hat{G}_S, \hat{\rho}_S(t)\Big\} + \sum_{i,j=1}^{d^2-1} a_{ij}\hat{F}_{Si}\hat{\rho}_S(t)\hat{F}_j^\dagger. \tag{2.58}$$

This equation can be further simplified by exploiting the fact that the dynamical semigroup elements are trace preserving:

$$\mathrm{Tr}_S\left\{\mathcal{L}\hat{\rho}_S(t)\right\} = 0 \Rightarrow \hat{G}_S = -\frac{1}{2}\sum_{i,j=1}^{d^2-1} a_{ij}\hat{F}_{sj}^\dagger\hat{F}_{Si}, \tag{2.59}$$

so that substituting we can write the *first standard form* of the Markovian generator:

$$\mathcal{L}\hat{\rho}_S(t) = -i\Big[\hat{H}, \hat{\rho}_S(t)\Big] + \sum_{i,j=1}^{d^2-1} a_{ij}\left(\hat{F}_{Si}\hat{\rho}_S(t)\hat{F}_{Sj}^\dagger - \frac{1}{2}\Big\{\hat{F}_{Sj}^\dagger\hat{F}_{Si}, \hat{\rho}_S(t)\Big\}\right). \tag{2.60}$$

Because of its positivity, the matrix formed by the coefficients a_{ij} can be diagonalized with the help of an appropriate unitary transformation $\hat{u}$ with matrix elements u_{ij} such that:

$$\hat{u}^\dagger\hat{a}\hat{u} = \mathrm{Diag}\left\{\gamma_1, \gamma_2, \cdots, \gamma_{d^2-1}\right\} \quad \text{with } \gamma_i \geq 0, \tag{2.61}$$

so that defining the operators $\hat{A}_{Sk}$ through:

$$\hat{F}_{Si} = \sum_{k=1}^{d^2-1} u_{ki}\hat{A}_{Sk} \tag{2.62}$$

it is possible to write the generator $\mathcal{L}$ in its diagonal form:

$$\mathcal{L}\hat{\rho}_S(t) = -i\Big[\hat{H}, \hat{\rho}_S(t)\Big] + \sum_{k=1}^{d^2-1} \gamma_k\left(\hat{A}_{Sk}\hat{\rho}_S(t)\hat{A}_{Sk}^\dagger - \frac{1}{2}\Big\{\hat{A}_{Sk}^\dagger\hat{A}_{Sk}, \hat{\rho}_S(t)\Big\}\right). \tag{2.63}$$

Equation (2.63) is known as the Gorini-Kossakowski-Sudarshan-Lindblad (GKSL) equation, as it was first derived independently by Gorini, Kossakowski and Sudarshan [Gorini, Kossakowski, and Sudarshan 1976] and Lindblad [Lindblad 1976]. The operators $\hat{A}_{Sk}$ are usually dubbed *Lindblad operators*.

The generator $\mathcal{L}$ does not fix univocally the form of $\mathcal{H}$ or the Lindblad operators $\hat{A}_{Sk}$: in fact there a two kinds of "gauge transformation" that leaves unchanged the generator:

- unitary transformations of the set of Lindblad operators such:

$$\sqrt{\gamma_k}\hat{A}_{Sk} \to \sqrt{\gamma'_k}\hat{A}'_{sk} = \sum_{ki} u_{ki}\sqrt{\gamma_i}\hat{A}_{Si} \tag{2.64}$$

  with u_{ki} the elements of a unitary matrix.

- inhomogeneous transformations of the form:

$$\hat{A}_{Sk} \to \hat{A}'_{sk} = \hat{A}_{Sk} + a_k \tag{2.65}$$

$$\hat{H} \to \hat{H}' = \hat{H} + \frac{1}{2i}\sum_j \gamma_j \left(a_j^* \hat{A}_{Sj} - a_j \hat{A}_{Sj}^\dagger\right) + b, \tag{2.66}$$

  with $a_j \in \mathbb{C}$ and $b \in \mathbb{R}$. This property allows one to choose traceless Lindblad operators.

Though perfectly legitimate, the axiomatic derivation of the GKSL equation leaves the physics "under the rug": just for instance, it is not clear what is the meaning of the coefficients γ_k, nor the origin and the role of $\hat{H}$, which though being Hermitian cannot be identified with the free Hamiltonian of the system.

Thus in the next section we are going to write down the GKSL equation using the so called *microscopic derivation*.

2.2.3. Microscopic derivation

The microscopic derivation of the Markovian generator [H. P. Breuer and Petruccione 2002] is an *ab initio* procedure that, starting from the interaction picture equation of motion of the joint density matrix $\hat{\rho}_{S\mathcal{E}}$ of the system, allows one to write down Eq. (2.63) through a series of approximations that highlight the physical conditions needed to derive a Markovian master equation.

The microscopic derivation is most easily performed in the interaction picture, which we shall adopt here. To start the derivation we assume the joint $S + \mathcal{E}$ system to be described by the Hamiltonian:

$$\hat{H}_{S\mathcal{E}} = \hat{H}_S + \hat{H}_\mathcal{E} + \hat{H}_{S-\mathcal{E}} \tag{2.67}$$

and we assume the interaction Hamiltonian $\hat{H}_{S-\mathcal{E}}$ to represent a small perturbation.

In the interaction picture we have:

$$\frac{d}{dt}\hat{\rho}_{S\mathcal{E}}(t) = -i\Big[\hat{H}_{S-\mathcal{E}}(t), \hat{\rho}_{S\mathcal{E}}(t)\Big] \Rightarrow \tag{2.68}$$

$$\hat{\rho}_{S\mathcal{E}}(t) = \hat{\rho}_{S\mathcal{E}}(0) - i\int_0^t ds\Big[\hat{H}_{S-\mathcal{E}}(d), \hat{\rho}_{S\mathcal{E}}(s)\Big]. \tag{2.69}$$

As usual we assume that the initial state of the joint system is a factorized state, i.e.:

$$\hat{\rho}_{S\mathcal{E}}(0) = \hat{\rho}_S(0) \otimes \hat{\rho}_{\mathcal{E}}. \tag{2.70}$$

This assumption is crucial in order to get a Markovian evolution, as the presence of initial correlations between system and environment leads to non-Markovian dynamics and is still the object of several studies [Hayashi, Kimura, and Ota 2003; Modi 2012; Pollock et al. 2018; Ringbauer et al. 2015; Štelmachovič and Bužek 2001; Usha Devi, Rajagopal, and Sudha 2011].

We will also assume that the *stability condition* holds:

$$\mathrm{Tr}_{\mathcal{E}}\left\{\Big[\hat{H}_{S-\mathcal{E}}, \hat{\rho}_{S\mathcal{E}}(0)\Big]\right\} = 0. \tag{2.71}$$

For the stability condition to hold the environmental average of the interaction Hamiltonian must be null. With these assumptions, inserting Eq. (2.69) into Eq. (2.68) and tracing over the environmental degrees of freedom we get:

$$\frac{d}{dt}\hat{\rho}_S(t) = -\int_0^t ds\,\mathrm{Tr}_{\mathcal{E}}\left\{\Big[\hat{H}_{S-\mathcal{E}}(t), \Big[\hat{H}_{S-\mathcal{E}}(s), \hat{\rho}_{S\mathcal{E}}(s)\Big]\Big]\right\}. \tag{2.72}$$

Equation (2.72) still contains the joint $S+\mathcal{E}$ density matrix $\hat{\rho}_{S\mathcal{E}}$: in order to solve this we perform the so called *Born approximation*. Within this approximation one assumes that, because of the weak-coupling assumption, the environment is only slightly affected by the interaction with the system S, and so is its density matrix, such that one can approximate the joint state of S and $\mathcal{E}$ with a tensor product for all times t:

$$\hat{\rho}_{S\mathcal{E}} \simeq \hat{\rho}_S(t) \otimes \hat{\rho}_{\mathcal{E}}. \tag{2.73}$$

It is important to note that this assumption by no means states that there are no excitations in the environment: as it will be clearer with the Markovian approximation to be performed in a few passages and in the collisional derivation, we just assume

that the environmental excitations decay over a timescale which is far smaller than the coarse-grained timescale at which we look at system's dynamics.

Thanks to the Born approximation we can write:

$$\frac{d}{dt}\hat{\rho}_S(t) = -\int_0^t ds\, \mathrm{Tr}_{\mathcal{E}}\left[\hat{H}_{S-\mathcal{E}}(t), [H_{S-\mathcal{E}}(s), \hat{\rho}_S(s)\otimes\hat{\rho}_{\mathcal{E}}]\right]. \tag{2.74}$$

Equation (2.74) is manifestly non-Markovian, since it depends on $\hat{\rho}_S(s)$: the Markov approximation consist exactly in substituting $\hat{\rho}_S(s)$ with $\hat{\rho}_S(t)$, so that one can write the *Redfield equation* [Redfield 1957; Schmidt 1981]:

$$\frac{d}{dt}\hat{\rho}_S(t) = -\int_0^t ds\, \mathrm{Tr}_{\mathcal{E}}\left[\hat{H}_{S-\mathcal{E}}(t), [H_{S-\mathcal{E}}(s), \hat{\rho}_S(t)\otimes\hat{\rho}_{\mathcal{E}}]\right]. \tag{2.75}$$

The Redfield equation is local in time, but still depends on the initial preparation time, and thus may fail positivity in general, though this issue can be solved under appropriate hypothesis [Farina and Giovannetti 2019]. In order to solve this we want to substitute s with $t-s$ and let the upper limit of the integral go to infinity: this is allowed as long as the timescale $\tau_{\mathcal{E}}$ at which the environmental correlations decay is much smaller than the relaxation time τ_R. If this condition justifying the Markov approximation is fulfilled, then the integral decays sufficiently fast for $s >> \tau_{\mathcal{E}}$ and we can let the upper limit of the integral to infinity. It is this we meant when we said that the Markovian description represents a coarse-grained description of the system. Performing the substitution into Eq. (2.75) we get:

$$\frac{d}{dt}\hat{\rho}_S(t) = -\int_0^\infty ds\, \mathrm{Tr}_{\mathcal{E}}\left[\hat{H}_{S-\mathcal{E}}(t), [H_{S-\mathcal{E}}(t-s), \hat{\rho}_S(t)\otimes\hat{\rho}_{\mathcal{E}}]\right]. \tag{2.76}$$

The approximations performed up to now are usually dubbed *Born-Markov approximation*, but still they do not guarantee that $\mathcal{L}$ is the generator of a dynamical semigroup. In order to attain this we must further approximate, introducing the *secular approximation*. In order to do so we write the interaction Hamiltonian as:

$$\hat{H}_{S-\mathcal{E}} = \sum_\alpha \hat{A}_{S\alpha}\otimes\hat{B}_{\mathcal{E}\alpha}, \tag{2.77}$$

where the operators $\hat{A}_{S\alpha}$ and $\hat{B}_{\mathcal{E}\alpha}$ are Hermitian. We then define the eigenoperators of the Hamiltonian $\hat{H}_S$: this is readily done by considering the projectors $\hat{\Pi}_S(\epsilon)$ onto the

eigenspace with energy ϵ. Then we can define:

$$\hat{A}_{S\alpha}(\omega) = \sum_{\epsilon-\epsilon'=\omega} \hat{\Pi}_S(\epsilon')\hat{A}_{S\alpha}\hat{\Pi}_S(\epsilon). \tag{2.78}$$

The operators $\hat{A}_{S\alpha}(\omega)$ are eigenoperators of $\hat{H}_S$ since it can be verified that:

$$\left[\hat{H}_S, \hat{A}_{S\alpha}(\omega)\right] = -\omega\hat{A}_{S\alpha}(\omega) \quad \left[\hat{H}_S, \hat{A}^\dagger_{S\alpha}(\omega)\right] = \omega\hat{A}^\dagger_{S\alpha}(\omega). \tag{2.79}$$

The eigenoperators $\hat{A}_{S\alpha}(\omega)$ have the properties:

$$\hat{A}_{S\alpha}(\omega) = \hat{A}^\dagger_{S\alpha}(-\omega) \tag{2.80}$$

$$\hat{A}_{S\alpha} = \sum_\omega \hat{A}_{S\alpha}(\omega) = \sum_\omega \hat{A}^\dagger_{S\alpha}(\omega) \Rightarrow \tag{2.81}$$

$$\hat{H}_{S-\mathcal{E}} = \sum_{\alpha,\omega} \hat{A}_{S\alpha}(\omega) \otimes \hat{B}_{\mathcal{E}\alpha} = \sum_{\alpha,\omega} \hat{A}^\dagger_{S\alpha}(\omega) \otimes \hat{B}^\dagger_{\mathcal{E}\alpha}. \tag{2.82}$$

where the first property comes directly from the definition and the second from the completeness relation. The advantage of working in the basis of the eigenoperators of $\hat{H}_S$ is that in the interaction picture they evolve in athe very simple fashion:

$$\hat{H}_{S-\mathcal{E}}(t) = \sum_{\alpha,\omega} e^{-i\omega t}\hat{A}_{S\alpha}(\omega) \otimes \hat{B}_{\mathcal{E}\alpha}(t) = \sum_{\alpha,\omega} e^{i\omega t}\hat{A}^\dagger_{S\alpha}(\omega) \otimes \hat{B}^\dagger_{\mathcal{E}\alpha}(t), \tag{2.83}$$

where $\hat{B}_{\mathcal{E}\alpha}$ are the bath operators in the interaction picture. Note also that the stability condition in Eq. (2.71) now becomes:

$$\langle \hat{B}_{\mathcal{E}\alpha}(t)\rangle = \mathrm{Tr}\left\{\hat{B}_{\mathcal{E}\alpha}(t)\hat{\rho}_\mathcal{E}\right\} = 0. \tag{2.84}$$

We can now develop the commutators in Eq. (2.76) and get:

$$\begin{aligned}
\frac{d}{dt}\hat{\rho}_S(t) &= \int_0^\infty ds \Bigg\{ \Big[\hat{H}_{S-\mathcal{E}}(t-s)\left(\hat{\rho}_S(t)\otimes\hat{\rho}_\mathcal{E}\right)\hat{H}_{S-\mathcal{E}}(t) \\
&- \left(\hat{\rho}_S(t)\otimes\hat{\rho}_\mathcal{E}\right)\hat{H}_{S-\mathcal{E}}(t-s)\hat{H}_{S-\mathcal{E}}(t)\Big] + h.c.\Bigg\} \qquad (2.85) \\
&= \sum_{\omega,\omega'}\sum_{\alpha,\beta} e^{i(\omega'-\omega)t}\Gamma_{\alpha\beta}(\omega)\Big(\hat{A}_{S\beta}(\omega)\hat{\rho}_S(t)\hat{A}^\dagger_{S\alpha}(\omega') \\
&- \hat{A}^\dagger_{S\alpha}(\omega')\hat{A}_{S\beta}(\omega)\hat{\rho}_S(t)\Big) + h.c. \qquad (2.86)
\end{aligned}$$

where the quantities

$$\Gamma_{\alpha\beta}(\omega) = \int_0^\infty ds\, e^{i\omega s} \left\langle \hat{B}^\dagger_{\mathcal{E}\alpha}(t)\hat{B}_{\mathcal{E}\beta}(t-s)\right\rangle, \tag{2.87}$$

are the one-sided Fourier transforms of the *environmental correlation functions*:

$$\left\langle \hat{B}^\dagger_{\mathcal{E}\alpha}(t)\hat{B}_{\mathcal{E}\beta}(t-s)\right\rangle = \mathrm{Tr}_{\mathcal{E}}\left\{\hat{B}^\dagger_{\mathcal{E}\alpha}(t)\hat{B}_{\mathcal{E}\beta}(t-s)\hat{\rho}_{\mathcal{E}}\right\}. \tag{2.88}$$

Moreover, if $\hat{\rho}_{\mathcal{E}}$ is a stationary state of the environment, that is $\left[\hat{H}_{\mathcal{E}}, \hat{\rho}_{\mathcal{E}}\right] = 0$, than the correlation functions are homogeneous in time, so that their Fourier transform is time-independent. This is the case, for instance, when the environmental state is a thermal state, while it is not true if the environmental state is, say, a squeezed vacuum.

It is in Eq. (2.86) that the secular approximation comes into play: system S is characterized by a timescale $\tau_S \simeq |\omega - \omega'|^{-1}$ over which the state of S changes appreciably. When τ_S is small compared with the relaxation time τ_R of the joint system, than the non-secular terms in Eq. (2.86) can be neglected, as they average out on timescale τ_R. We can thus eliminate all the terms for which $\omega \neq \omega'$ getting:

$$\frac{d}{dt}\hat{\rho}_S(t) = \sum_\omega \sum_{\alpha,\beta} \left[\Gamma_{\alpha\beta}(\omega)\left(\hat{A}_{S\beta}(\omega)\hat{\rho}_S(t)\hat{A}^\dagger_{S\alpha}(\omega) - \hat{A}^\dagger_{S\alpha}(\omega)\hat{A}_{S\beta}(\omega)\hat{\rho}_S(t)\right) + h.c.\right]. \tag{2.89}$$

The last step to do to write the Markovian generator in its first form is to divide the $\Gamma_{\alpha\beta}(\omega)$ as follows:

$$\Gamma_{\alpha\beta}(\omega) = \frac{1}{2}\gamma_{\alpha\beta}(\omega) + i\Sigma_{\alpha\beta}(\omega), \tag{2.90}$$

where the coefficients $\Sigma_{\alpha\beta}(\omega)$ are defined as:

$$\Sigma_{\alpha\beta}(\omega) = -\frac{i}{2}\left(\Gamma_{\alpha\beta}(\omega) - \Gamma^*_{\beta\alpha}(\omega)\right), \tag{2.91}$$

and at fixed ω form an Hermitian matrix, while the coefficients

$$\gamma_{\alpha\beta}(\omega) = \Gamma_{\alpha\beta}(\omega) + \Gamma^*_{\beta\alpha}(\omega) = \int_{-\infty}^{+\infty} ds e^{i\omega s}\left\langle \hat{B}_{\mathcal{E}\alpha}(s)\hat{B}_{\mathcal{E}\beta}(0)\right\rangle \tag{2.92}$$

form a positive matrix. We can then write the Markovian master equation in the inter-

action picture as:

$$\begin{aligned}\frac{d}{dt}\hat{\rho}_S(t) &= -i\Big[\hat{H}_{LS}, \hat{\rho}_S(t)\Big] \\ &+ \sum_{\omega}\sum_{\alpha,\beta}\gamma_{\alpha\beta}(\omega)\left(\hat{A}_{S\beta}(\omega)\hat{\rho}_S(t)\hat{A}^{\dagger}_{S\alpha}(\omega) - \frac{1}{2}\Big\{\hat{A}^{\dagger}_{S\alpha}(\omega)\hat{A}_{S\beta}(\omega), \hat{\rho}_S(t)\Big\}\right),\end{aligned} \tag{2.93}$$

where the Hermitian operator $\hat{H}_{LS}$ is defined as:

$$\hat{H}_{LS} = \sum_{\omega}\sum_{\alpha\beta}\Sigma_{\alpha\beta}(\omega)\hat{A}^{\dagger}_{S\alpha}(\omega)\hat{A}_{S\beta}(\omega), \tag{2.94}$$

and represents a renormalization contribution to the Hamiltonian, usually called *Lamb shift* Hamiltonian. The other part of the generator, usually dubbed the *dissipator*, can be brought in the GKSL form by diagonalizing the matrix $\gamma_{\alpha\beta}(\omega)$ through an appropriate unitary $u(\omega)$ and introducing the operators

$$\hat{A}'_{\alpha}(\omega) = \sum_{\beta} u_{\alpha\beta}(\omega)\hat{A}_{S\beta}(\omega), \tag{2.95}$$

so that we can write

$$\begin{aligned}\frac{d}{dt}\hat{\rho}_S(t) &= -i\Big[\hat{H}_{LS}, \hat{\rho}_S(t)\Big] \\ &+ \sum_{\omega,\alpha}\gamma_{\alpha}(\omega)\left(\hat{A}'_{S\alpha}(\omega)\hat{\rho}_S(t)\hat{A}'^{\dagger}_{S\alpha}(\omega) - \frac{1}{2}\Big\{\hat{A}'^{\dagger}_{S\alpha}(\omega)\hat{A}'_{S\alpha}(\omega), \hat{\rho}_S(t)\Big\}\right).\end{aligned} \tag{2.96}$$

We have finally derived the Markovian generator in the GKSL form through a microscopic derivation: during the procedure we invoked several approximations, the most important being:

- the weak coupling approximation: the coupling between S and $\mathcal{E}$ is small, so that it affects only slightly the environment and we are able to work at the second order of perturbation theory;

- the Born approximation: because of the weak coupling we assume that it is possible to write the joint state of $S + \mathcal{E}$ as a tensor product at any time;

- the Markov approximation: thank to the fast decay of environmental correlation functions we can write an equation which is time local;

- the secular approximation: when the timescale τ_S over which the state of system S varies appreciably is small compared to the relaxation time of the joint $S + \mathcal{E}$ system, then it is possible to neglect the counter rotating terms in Eq. (2.86).

The microscopic derivation, at glance with the axiomatic one, makes clear which are the physical assumptions entailing the possibility of writing a Markovian generator of the dynamics: nonetheless if only one of these assumptions is false, then the derivation is not valid anymore, and one would have to rely to other methods and approximations in order to write a master equation. This is completely different with what happens with collisional models, as we are going to see in the next section.

2.3. Collisional model

Collisional models were introduced long ago as a tool to describe open quantum systems [Rau 1963], but it was only until recently that they gained much attention from the community. This interest stems from the great flexibility in depicting the dynamics of an open quantum systems given by collisional models: just by changing a few parameters one can describe very different situation, from Markovian dynamics [Amato, H.-P. Breuer, and Vacchini 2019] to non-Markovian dynamics [Campbell et al. 2018; Kretschmer, Luoma, and Strunz 2016; Lorenzo, Ciccarello, Palma, and Vacchini 2017; McCloskey and Paternostro 2014; Pellegrini and Petruccione 2009], from feedback processes [Altamirano et al. 2017; Grimsmo 2015] to measurement processes [Seah et al. 2019]. Moreover, as we are going to see in Chap. 4, collisional models also entails the possibility of keeping track of the environmental degrees of freedom, a very important feature in the study of open quantum systems.

In collisional models one describes the environment $\mathcal{E}$ as a collection $\{E_i\}$ of quantum subsystems usually called *ancillas*. These ancillas interact in a collisional fashion with system S for a short but finite time interval δt according to some interaction Hamiltonian. The sequence of this collisions gives rise to a time discrete evolution of S, the continuous limit being recovered sending to zero the collision time δt and to infinity the number n of collisions.

Already from this simple description of collisional model we can observe that there are many knobs on which to intervene to modify the dynamics: one could change the state of the ancillas to describe different environments, introduce intra-ancilla collisions to introduce non-Markovian effects [Ciccarello, Palma, and Giovannetti 2013; Lorenzo,

Ciccarello, and Palma 2016] or change the order with which the ancillas interact with S in order to obtain feedback dynamics and more.

Before seeing in Chap. 3 how a collisional model can be used to describe cascade systems dynamics, let us show how to derive the Markovian master equation through a collisional model.

We consider once again a system S characterized by the Hamiltonian $\hat{H}_S$, while we describe the environment $\mathcal{E}$ as a collection of ancillas $\{E_\ell\}$ all in the same reference state $\hat{\eta}_\ell = \hat{\eta}$, characterized by the Hamiltonian $\hat{H}_\mathcal{E} = \sum_\ell \hat{H}_{E_\ell}$. The interaction between S and $\mathcal{E}$ is described by the Hamiltonian $\hat{H}_{S-\mathcal{E}} = \sum_\ell \hat{H}_{S-E_\ell}$, which is the sum of the interaction Hamiltonians of S and the ancillas E_ℓ. We further assume the initial state to be factorized:

$$\hat{\rho}_{S\mathcal{E}}(0) = \hat{\rho}_S(0) \bigotimes_\ell \hat{\eta}_\ell \tag{2.97}$$

Furthermore we assume, without loss of generality, the interaction picture interaction Hamiltonian between S and an ancilla E_ℓ to be of the generic form:

$$\hat{H}_{S-E_\ell} = g \sum_{\alpha,\omega} \hat{A}_{S\alpha}(\omega) \otimes \hat{B}_{E_\ell\alpha}(\omega) \tag{2.98}$$

with $\hat{A}_{S\alpha}$, $\hat{B}_{E_i\alpha}$ Hermitian and g being a coefficient measuring the strength of the interaction. Assuming the $\hat{A}_{S\alpha}(\omega)$ to be eigenoperators of $\hat{H}_S$ one can write the evolution of the interaction Hamiltonian as:

$$\hat{H}_{S-E_\ell} = \sum_{\alpha,\omega} e^{-i\omega\ell\delta t} \hat{A}_{S\alpha}(\omega) \otimes \hat{B}_{E_\ell}(\ell\delta t, \omega) \tag{2.99}$$

where the time evolution of the environmental operators is given by:

$$\hat{B}_{E_\ell\alpha}(\ell\delta t) = \hat{B}_{E_\ell\alpha}((\ell-1)\delta t, \omega) - i\Big[\hat{H}_{E_\ell}, \hat{B}_{E_\ell\alpha}((\ell-1)\delta t, \omega)\Big]\delta t \tag{2.100}$$

Fig. 2.3 shows how the collisional model proceeds: the reduced density matrix $\hat{\rho}_S$ evolves in discrete steps. At the first step S interacts with the first ancilla E_1 according to:

$$\hat{\rho}_S(0) \otimes \hat{\eta}_1 \to \mathcal{U}_{SE_1}(\hat{\rho}_S(0) \otimes \hat{\eta}_1) = \hat{U}_{SE_1}(\hat{\rho}_S(0) \otimes \hat{\eta}_1)\hat{U}^\dagger_{SE_1}, \tag{2.101}$$

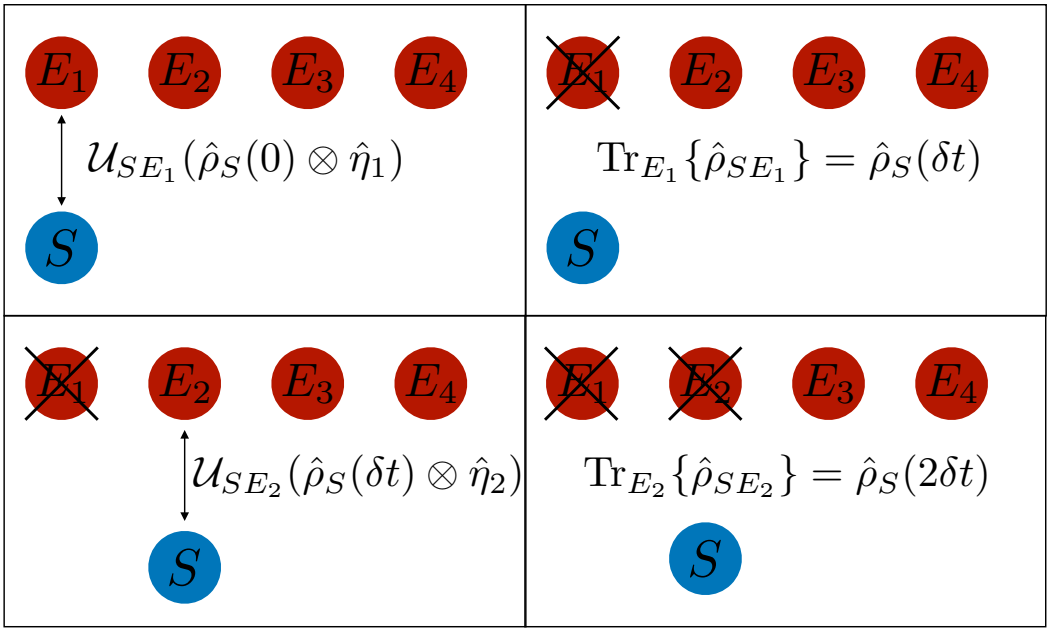

Figure 2.3.: A sketch resuming the dynamics as described by a collisional model. First S interacts with the ancilla E_1 through $\mathcal{U}_{SE_1}$, as shown in panel (a). Then, as in panel (b), one traces away the degrees of freedom belonging to E_1 in order to get the state $\hat{\rho}_S(\delta t)$ of S after the first collision. After it is traced away, the ancilla E_1 will partecipate to the dynamics no more. Then S interacts with the second ancilla as in panel (c), which is then traced away in panel (d) in order to get the state $\hat{\rho}_S(2\delta t)$ of S after the second collision.

with

$$\hat{U}_{SE_\ell} = \exp\left[-i\hat{H}_{SE_\ell}\delta t\right]. \tag{2.102}$$

At this point one traces away the ancilla E_1, which will not partecipate to the dynamics anymore, getting the reduced state after the first step of length δt:

$$\hat{\rho}_S(\delta t) = \mathrm{Tr}_{E_1}\left\{\mathcal{U}_{SE_1}(\hat{\rho}_S(0) \otimes \hat{\eta}_1)\right\} \tag{2.103}$$

Consider next the state $\hat{\rho}_S(\delta t) \otimes \hat{\eta}_2$ and iterates the procedure, so that we can write the recursive relation:

$$\hat{\rho}_S((\ell+1)\delta t) = \mathrm{Tr}_{E_\ell}\left\{\hat{U}_{SE_\ell}\left(\hat{\rho}_S(\ell\delta t) \otimes \hat{\eta}_\ell\right)\hat{U}_{SE_\ell}\right\}, \tag{2.104}$$

which, as we shall see, allows us to derive the master equation. First we expand the

unitary operator $\hat{U}_{SE_\ell}$ in powers of $g\delta t$:

$$\hat{U}_{SE_\ell} = \hat{\mathbb{I}}_{SE_\ell} - i\delta t\hat{H}_{SE_\ell} - \frac{\delta t^2}{2}\hat{H}^2_{SE_\ell} + \mathcal{O}\Big((g\delta t)^3\Big). \tag{2.105}$$

Inserting this expression in Eq. (2.104) and retaining terms up to second order in $g\delta t$ we can write:

$$\begin{aligned}\hat{\rho}_S((\ell+1)\delta t) &= \mathrm{Tr}_{E_\ell}\Bigg\{\hat{\rho}_S(\ell\delta t)\otimes\hat{\eta}_\ell - i\delta t\Big[\hat{H}_{SE_\ell}, \hat{\rho}_S(\ell\delta t)\otimes\hat{\eta}_\ell\Big] \\ &- \frac{\delta t^2}{2}\Big\{\hat{H}_{SE_\ell}, \hat{\rho}_S(\ell\delta t)\otimes\hat{\eta}_\ell\Big\} + \delta t^2\hat{H}_{SE_\ell}(\hat{\rho}_S(\ell\delta t)\otimes\hat{\eta}_\ell)\hat{H}_{SE_\ell}\Bigg\}.\end{aligned} \tag{2.106}$$

As in the previous section, we now invoke a stability condition, which in the collisional model takes the form:

$$\mathrm{Tr}_{E_\ell}\Big\{\hat{B}_{E_\ell\alpha}\hat{\eta}_\ell\Big\} = 0 \quad \forall\ell,\alpha. \tag{2.107}$$

Thank to Eq. (2.107) the first order term in Eq. (2.106) vanishes, leading to:

$$\begin{aligned}&\hat{\rho}_S((\ell+1)\delta t) = \hat{\rho}_S(\ell\delta t) + \delta t^2 g^2\sum_{\substack{\alpha,\beta\\ \omega\omega'}}\mathrm{Tr}_{E_\ell}\Big\{\hat{B}^\dagger_{E_\ell\beta}(\ell\delta t,\omega')\hat{B}_{E_\ell\alpha}(\ell\delta t,\omega)\hat{\eta}_\ell\Big\}\cdot \\ &e^{-i(\omega-\omega')\ell\delta t}\left(\hat{A}_{S\alpha}(\omega)\hat{\rho}_S(\ell\delta t)\hat{A}^\dagger_{S\beta}(\omega') - \frac{1}{2}\Big\{\hat{A}^\dagger_{S\beta}(\omega')\hat{A}_{S\alpha}(\omega), \hat{\rho}_S(\ell\delta t)\Big\}\right).\end{aligned}$$

This is the discrete form of the Markovian master equation, where we still did not invoke the secular approximation. If we enforce this approximation, i.e. we discard all the term with $\omega \neq \omega'$ we get:

$$\begin{aligned}&\hat{\rho}_S((\ell+1)\delta t) = \hat{\rho}_S(\ell\delta t) \\ &+\delta t^2 g^2\sum_{\substack{\alpha,\beta\\ \omega}}\mathrm{Tr}_{E_\ell}\Big\{\hat{B}^\dagger_{E_\ell\beta}(\ell\delta t,\omega)\hat{B}_{E_\ell\alpha}(\ell\delta t,\omega)\hat{\eta}_\ell\Big\} \\ &\left(\hat{A}_{S\alpha}(\omega)\hat{\rho}_S(\ell\delta t)\hat{A}^\dagger_{S\beta}(\omega) - \frac{1}{2}\Big\{\hat{A}^\dagger_{S\beta}(\omega)\hat{A}_{S\alpha}(\omega), \hat{\rho}_S(\ell\delta t)\Big\}\right).\end{aligned} \tag{2.108}$$

As in the microscopic derivation, if $\hat{\eta}_{E_\ell}$ is a stationary state of $\hat{H}_{E_\ell}$ then the environ-

mental correlation functions do not depend on time, and we can write:

$$\frac{\hat{\rho}_S((\ell+1)\delta t) - \hat{\rho}_S(\ell\delta t)}{\delta t} = \\ \delta t g^2 \sum_{\substack{\alpha,\beta \\ \omega}} \gamma_{\alpha\beta}(\omega) \left(\hat{A}_{S\alpha}(\omega)\hat{\rho}_S(\ell\delta t)\hat{A}^\dagger_{S\beta}(\omega) - \frac{1}{2}\left\{ \hat{A}^\dagger_{S\beta}(\omega)\hat{A}_{S\alpha}(\omega), \hat{\rho}_S(\ell\delta t) \right\} \right) \tag{2.109}$$

where we have defined

$$\gamma_{\alpha\beta}(\omega) = \mathrm{Tr}_{E_\ell} \left\{ \hat{B}^\dagger_{E_\ell\beta}(\omega)\hat{B}_{E_\ell\alpha}(\omega)\hat{\eta}_\ell \right\}. \tag{2.110}$$

One can then diagonalize the matrix of coefficients $\gamma_{\alpha\beta}(\omega)$ through a unitary u such that:

$$\hat{u}\gamma_{\alpha\beta}(\omega)\hat{u}^\dagger = \mathrm{Diag}\left(\gamma_1, \gamma_2 \cdots \gamma_{d^2-1}\right). \tag{2.111}$$

After this operation we can write:

$$\frac{\hat{\rho}_S((\ell+1)\delta t) - \hat{\rho}_S(\ell\delta t)}{\delta t} = \\ \delta t g^2 \sum_{\alpha,\omega} \gamma_{\alpha}(\omega) \left(\hat{A}_{S\alpha}(\omega)\hat{\rho}_S(\ell\delta t)\hat{A}^\dagger_{S\alpha}(\omega) - \frac{1}{2}\left\{ \hat{A}^\dagger_{S\alpha}(\omega)\hat{A}_{S\alpha}(\omega), \hat{\rho}_S(\ell\delta t) \right\} \right). \tag{2.112}$$

Equation (2.112) is the discrete form of the Markovian generator in the GKSL form: it is identical to the standard Markovian generator, with the only difference that in this case the evolution of the reduced density matrix proceeds in discrete time steps of length δt. Any master equation derived via a collisional model will have this discrete feature before taking the continuous time limit.

To get a continuous time equation in a collision model, one has to consider the limit in which the finite time interval δt becomes a differential. In order to get meaningful results one must, at the same time, consider the limit of an infinite number of collisions, so that:

$$\lim_{\delta t \to 0} \delta t = dt \tag{2.113}$$

$$\lim_{\substack{\delta t \to 0 \\ \ell \to \infty}} \ell \delta t = t \tag{2.114}$$

$$\lim_{\substack{\delta t \to 0 \\ \ell \to \infty}} \delta t g^2 = \gamma \tag{2.115}$$

Applying these limits to Eq. (2.112) we retrieve the continuous time Marokovian generator:

$$\frac{d}{dt}\hat{\rho}_S(t) = \sum_{\alpha,\omega} \tilde{\gamma}_\alpha(\omega) \left(\hat{A}_{S\alpha}(\omega)\hat{\rho}_S(t)\hat{A}^\dagger_{S\alpha}(\omega) - \frac{1}{2}\Big\{ \hat{A}^\dagger_{S\alpha}(\omega)\hat{A}_{S\alpha}(\omega), \hat{\rho}_S(t) \Big\} \right) \tag{2.116}$$

where $\tilde{\gamma}_\alpha(\omega) = \gamma\gamma_\alpha(\omega)$.

Now that we have completed the derivation of the Markovian master equation through a collisional model, we can comment on similarities and differences between this derivation and the microscopic one we saw in the previous section.

In the microscopic derivation we first invoked the Born approximation, which allowed us to assume the reduced state and the environmental state to be in a product state for all time t due to the weakness of the interaction. In the collision model one does not need such an approximation, because the environment is modeled as a collection of degrees of freedom, the ancillas, that are independent from each other and interact piecewise with the reduced system. In the collisional setting the markovianity of the reduced dynamics is dictated by the intra-ancilla interactions: in absence of such interactions, as we assumed, the dynamics is automatically Markovian. This also implies that in the collisional setting one does not need the Markov approximation, the one that in the microscopic derivation allows for a time-local generator: dynamics in the collisional model we used in this section is time local *per se*.

Then in both derivations we called in our help the stability condition in order to eliminate first order terms from the generator: it must however be noted that this condition is not restricting us, as the stability condition can always be enforced by moving to an appropriate rotating reference frame.

Finally in both derivations we invoked the secular approximation: though this approximation allows to simplify a lot the equations, it is actually not crucial in order to get a Markovian dynamics: as it can be found in literature [H. P. Breuer, Dietz, and Holthaus 1988; H. P. Breuer and Petruccione 2002; H.-P. Breuer and Petruccione 1997; Kohler, Dittrich, and Hänggi 1997], the strong coupling regime can be dealt with via Floquet theory. The approximations used in the two models are resumed in table 2.1.

The important point to note is that collisional models allow for greater elasticity in depicting the dynamics: as it can be seen from the literature, and as we are going to see in Chap. 3, by changing the order in which the ancilla interact with the reduced system S, or introducing intra-ancilla interactions, one can easily adapt the collisional model to many situations, ranging from cascade systems to non-Markovian dynamics.

Approximation	Microscopic derivation	Collisional model
Born Approximation	$\hat{\rho}_{S\mathcal{E}}(t) = \hat{\rho}_S(t) \otimes \hat{\rho}_{\mathcal{E}}$	Not needed
Stability condition	$\mathrm{Tr}_{\mathcal{E}} \left\{ \left[\hat{H}_{S-\mathcal{E}}, \hat{\rho}_{S\mathcal{E}}(0) \right] \right\} = 0$	$\mathrm{Tr}_{E_\ell} \left\{ \hat{B}_{E_\ell \alpha} \hat{\eta}_\ell \right\} = 0$
Markov approximation	$\hat{\rho}_S(s) \to \hat{\rho}_S(t)$	Not needed, Markovianity is provided by the absence of intra-ancilla interactions
Secular approximation	$\tau_S \simeq \lvert\omega - \omega'\rvert^{-1} << \tau_R$	$\tau_S \simeq \lvert\omega - \omega'\rvert^{-1} << \tau_R$

Table 2.1.: Table resuming the approximations performed in both the microscopic and collisional derivation of the Markovian generator.

Moreover, as we will see in Chap. 4, while in the microscopic derivation it is hard to keep track of the environmental degrees of freedom, in collisional models we have the freedom of not tracing away the ancilla after each interaction, but rather keep the joint system-ancilla state and proceed with the next collision. This allows one to monitor the correlations that are created between the system and the environment, a very precious feature when, for instance, one is interested in the transient dynamics and not only in the steady state.

In the following two chapters we will thus see some of the power of collisional models.

CHAPTER 3

Cascade systems

Cascade systems are multipartite quantum systems were two or more subsystems $S_1, S_2, \ldots$ are linked via their interaction with a common environment in a *chiral* fashion. By chiral we mean that there is a hierarchy between the subsystems $S_1, S_2, \ldots$, often called *nodes*: the simplest example of such hierarchy is given by the case of only two subsystems S_1, S_2 where the output from S_1 is fed as input to S_2, but not *viceversa*. This directional interaction can happen only thanks to the presence of the environment mediating the interaction, as a simple Hamiltonian coupling is inherently symmetric, and thus unable to induce a controller-idler dualism between the nodes.

It was just with this simple case that the study of cascade systems started: the input-output (IO) formalism was developed by Gardiner and collaborators [Carmichael 1993; C. W. Gardiner 1993; C. W. Gardiner and Collett 1985; C. W. Gardiner and Parkins 1994] in order to analyze situations where the output from a quantum system is used as an input for another quantum system, and was then extended to account for fermion statistics of the driving [C. Gardiner 2004; Grimsmo et al. 2016] and other situation such as ultra-strong coupling [Ciuti and Carusotto 2006] and pulsed driving [Kiilerich and Mølmer 2019].

With the development of 1D waveguides [Das et al. 2018; Fischer et al. 2018; Mahmoodian et al. 2018], the IO formalism has found a natural application in this scenario, where various quantum nodes interact in a circuit-like fashion, eventually leading to the development of the LSH formalism [Combes, Kerckhoff, and Sarovar 2017; J. E. Gough,

Gohm, and Yanagisawa 2008; J. Gough and James 2009], which can be used to describe and conceive a wide range of networks.

Though the IO formalism fits perfectly the goal of describing the signals propagating in such networks, in order to derive master equations for the dynamics of the nodes one has to deal with stochastic calculus, passing through both the Ito and Stratonovich definitions of the increment [C. Gardiner 2009; C. Gardiner, C. Gardiner, and Zoller 2000]. While this procedure leads to correct results, it is possible to use a collisional model to describe the dynamics of the network, which simplifies a lot the derivation of a master equation, especially for complicated networks.

Thus in this chapter we will show how a collisional model can be used to describe cascade networks, which are networks where the signals propagate unidirectionally between some quantum nodes, possibly passing through optical elements, such as beam splitters and phase shifters. We will then see how it is possible to use this formalism to study a network able to simulate various many-body dynamics by simply changing a few parameters of the optical elements.

3.1. A minimal example

The simplest, and widely studied [Giovannetti and Palma 2012a,b; Lorenzo, Farace, et al. 2015], setting of a cascade system consists in having two quantum systems S_1 and S_2 interacting with the same environment $\mathcal{E}$ in a chiral fashion: by this we mean that there is a hierarchy between S_1 and S_2, in the sense that the environment first interact with S_1 and only then with S_2, and there is no backscattering. Thus S_2 is influenced by S_1, but *viceversa* is not true, see Fig. 3.1.

Let us show how to model this situation in a collisional model setting. The Hamiltonian of the two systems S_1 and S_2 is:

$$\hat{H}_S = \hat{H}_{S_1} + \hat{H}_{S_2}. \tag{3.1}$$

Note that there is no direct interaction between S_1 and S_2. In the spirit of collisional models we depict the environment $\mathcal{E}$ as a collection of independent ancillas $\{E_1, E_2, \cdots E_n, \cdots\}$, all in the same reference state $\hat{\eta}_{E_n}$, whose free Hamiltonian reads:

$$\hat{H}_{\mathcal{E}} = \sum_n \hat{H}_{E_n} \tag{3.2}$$

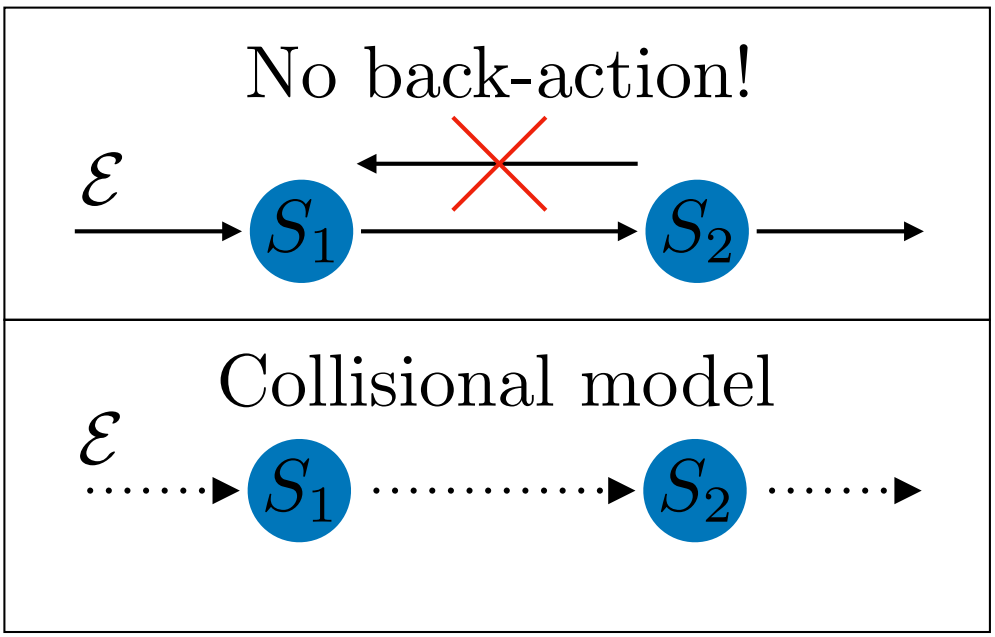

Figure 3.1.: A minimal example of cascade system: a cascade system's characteristic feature is the unidirectionality of the signal propagation, thus excluding backscattering and feedback effects. This feature is reflected in the collisional model thrugh the causal structure under which the ancillas collide with the nodes, i.e. all the ancillas interact first with S_1 and only then with S_2.

Finally, as both systems interact with the environment, we write the interaction Hamiltonian:

$$\hat{H}_{S-\mathcal{E}} = \hat{H}_{S_1-\mathcal{E}} + \hat{H}_{S_2-\mathcal{E}}, \tag{3.3}$$

where we have treated the environment as a unique block. Considering that the environment is made out of a collection of ancillas we rewrite the interaction with each S_m as:

$$\hat{H}_{S_m-\mathcal{E}} = \sum_n \hat{H}_{S_m-E_n}, \tag{3.4}$$

where the Hamiltonian describing the interaction between S_m and a single ancilla can be written as:

$$\hat{H}_{S_m-E_n} = \sum_\ell \hat{A}^{(\ell)}_{S_m} \otimes \hat{B}^{(\ell,m)}_{E_n} \tag{3.5}$$

where the $\hat{A}^{(\ell)}_{S_m}$ act on S_m and the $\hat{B}^{(\ell,m)}_{E_n}$ act on the ancilla E_n. A subsystem S_m and an ancilla E_n interact collisionally for a short time interval δt, so that the unitary interaction between them is described by the superoperator $\mathcal{U}_{S_m,E_n}$:

$$\mathcal{U}_{S_m,E_n}(\cdots) = \hat{U}_{S_m,E_n}(\cdots)\hat{U}^{\dagger}_{S_m,E_n} \tag{3.6}$$

where

$$\hat{U}_{S_m,E_n} = \exp\left[-ig\delta t \sum_{\ell} \hat{A}^{(\ell)}_{S_m} \otimes \hat{B}^{(\ell,m)}_{E_n}\right]. \tag{3.7}$$

where g is a coupling constant gauging the strength of the interaction.

After each collision between the nodes and the ancillas we introduce the possibility of acting on the ancillas through the CPT maps $\mathcal{M}_{E_n}$: these maps might represent, for instance, the action of noise on the ancillas or the action of some optical elements as beam splitters and phase shifters, as we will see in the next sections.

To represent the cascade nature of the interaction we further impose that the ancillas interact with the subsystems in an ordered way: at each step of the evolution, each ancilla interacts first with S_1, and only after with S_2. This reflects practically in the fact that the evolution of the whole system during a step of the evolution is given by:

$$\mathcal{C}_{S,E_n} = \mathcal{U}_{S_2,E_n} \circ \mathcal{M}_{E_n} \circ \mathcal{U}_{S_1,E_n}, \tag{3.8}$$

where $\mathcal{C}_{S,E_n}$ is the superoperator defined by the ordered composition of the maps describing the interaction between the nodes and the ancilla: first the ancilla E_n interacts with S_1, then it undergoes an evolution dictated by the map $\mathcal{M}_{E_n}$, and finally it interacts with S_2. This interaction scheme can be represented in a circuit like fashion, as shown in Fig. 3.2.

Thus, for the joint state of the nodes and the environment $\hat{\rho}_{S\mathcal{E}}(n)$, we have the recursive relation:

$$\hat{\rho}_{S\mathcal{E}}(n+1) = \mathcal{C}_{S,E_{n+1}}(\hat{\rho}_{S\mathcal{E}}(n) \otimes \eta_{E_{n+1}}) \tag{3.9}$$

In order to derive a master equation for the nodes we want to expand the superoperator $\mathcal{C}_{S,E_n}$ in power series of $g\,\delta t$. In order to do so we first expand the superoperator $\mathcal{U}_{S_m,E_n}$:

$$\mathcal{U}_{S_m,E_n} = \mathcal{I}_{S_m,E_n} + (g\,\delta t)\,\mathcal{U}'_{S_m,E_n} + (g\,\delta t)^2\,\mathcal{U}''_{S_m,E_n} + \mathcal{O}\big((g\delta t)^3\big) \tag{3.10}$$

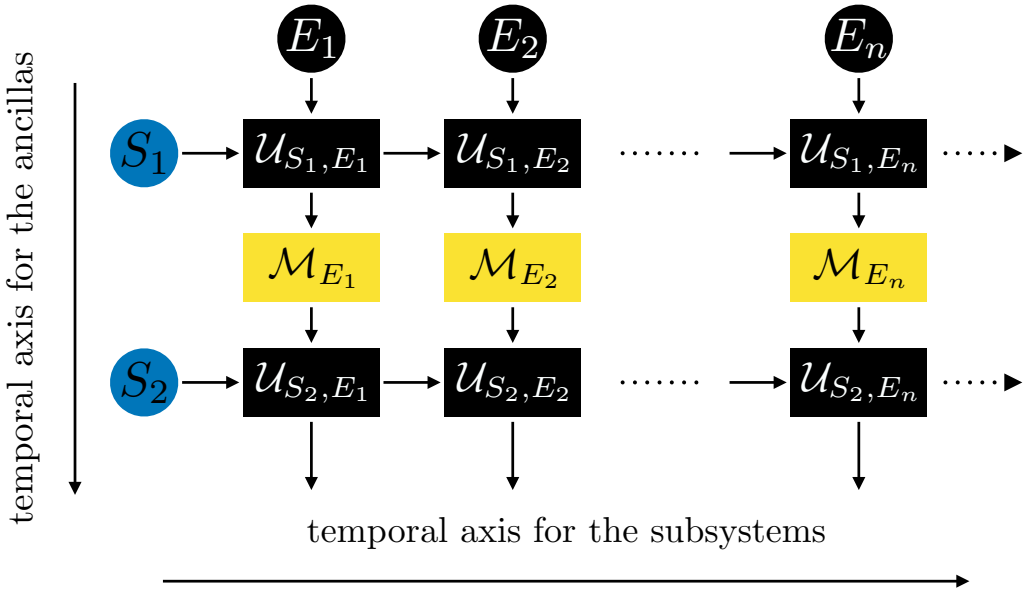

Figure 3.2.: A circuit-like representation of the dynamics: the nodes S_1 and S_2 sequentially interact with the ancillas $E_1, E_2, \ldots$, with the difference that the ancillas interact with S_2 only after they interacted with S_1, so that when an ancilla collides with S_2 it contains information about S_1, in this way inducing an interaction between the two nodes. In between the collisions with the nodes, each ancilla is subject to an evolution described by the CPT map $\mathcal{M}_{E_n}$.

where $\mathcal{I}_{S_m,E_n}$ is the identity superoperator and the superoperators in the expansion are defined as:

$$\mathcal{U}'_{S_m,E_n}(\cdots) = -i\Big[\hat{H}_{S_m,E_n}, \cdots\Big] \tag{3.11}$$

$$\mathcal{U}''_{S_m,E_n}(\cdots) = \hat{H}_{S_m,E_n}(\cdots)\hat{H}_{S_m,E_n} - \frac{1}{2}\Big\{\hat{H}^2_{S_m,E_n}, \cdots\Big\}. \tag{3.12}$$

With the expansion in Eq. (3.10) it is possible to write the superoperator $\mathcal{C}_{S,E_n}$ as:

$$\mathcal{C}_{S,E_n} = \mathcal{C}^{(0)}_{S,E_n} + (g\,\delta t)\,\mathcal{C}'_{S,E_n} + (g\,\delta t)^2\,\mathcal{C}''_{S,E_n} + \mathcal{O}\big((g\delta t)^3\big) \tag{3.13}$$

with

$$\mathcal{C}^{(0)}_{S,E_n} = \mathcal{M}_{E_n} \tag{3.14}$$

$$\mathcal{C}'_{S,E_n} = \mathcal{U}'_{S_2,E_n} \circ \mathcal{M}_{E_n} + \mathcal{U}'_{S_1,E_n} \tag{3.15}$$

$$\mathcal{C}''_{S,E_n} = \mathcal{U}''_{S_2,E_n} \circ \mathcal{M}_{E_n} + \mathcal{U}''_{S_1,E_n} + \mathcal{U}'_{S_2,E_n} \circ \mathcal{M}_{E_n} \circ \mathcal{U}'_{S_1,E_n} \tag{3.16}$$

Now, in order to derive the master equation for the nodes we have to trace out the ancillas' degrees of freedom. Let us show this procedure term by term. From the zeroth order term we get:

$$\mathrm{Tr}_{E_n}\left\{\mathcal{C}^{(0)}_{S,E_n}\left(\hat{\rho}_S(n-1)\otimes\hat{\eta}_{E_n}\right)\right\}=\hat{\rho}_S(n-1), \tag{3.17}$$

since $\mathcal{M}_{E_n}$ is a CPT map acting on E_n only.

From the first order term we get:

$$\begin{aligned}\mathrm{Tr}_{E_n}\left\{\mathcal{C}'_{S,E_n}\left(\hat{\rho}_S(n-1)\otimes\hat{\eta}_{E_n}\right)\right\} &= \sum_{\ell}\mathrm{Tr}_{E_n}\left\{\hat{B}^{(\ell,2)}_{E_n}\mathcal{M}_{E_n}\hat{\eta}_n\right\}\left[\hat{A}^{(\ell)}_{S_2},\hat{\rho}_S(n-1)\right]\\ &+ \mathrm{Tr}_{E_n}\left\{\hat{B}^{(\ell,1)}_{E_n}\hat{\eta}_{E_n}\right\}\left[\hat{A}^{(\ell)}_{S_1},\hat{\rho}_S(n-1)\right]\end{aligned} \tag{3.18}$$

This term nullifies if we impose the stability condition, which in this setting has the form:

$$\mathrm{Tr}_{E_n}\left\{\hat{B}^{(\ell,1)}_{E_n}\hat{\eta}_{E_n}\right\}=0 \tag{3.19}$$

$$\mathrm{Tr}_{E_n}\left\{\hat{B}^{(\ell,2)}_{E_n}\mathcal{M}_{E_n}\hat{\eta}_{E_n}\right\}=0 \tag{3.20}$$

We are then left with the second order term $\mathcal{C}''_{S,E_n}$, in which two different contributions can be individuated: one has two local terms given by $\mathcal{U}''_{S_m,E_n}$, where by local we mean that only one node S_m is involved; the other second order contribution is instead given by the combination of the two first order terms $\mathcal{U}'_{S_m,E_n}$, and thus is non-local, by this meaning that this term introduces an indirect interaction between the nodes provided by the cascade nature of the environment.

In facts, tracing away the environmental degrees of freedom in the local contributions leads to:

$$\begin{aligned}&\mathrm{Tr}_{E_n}\left\{\mathcal{U}''_{S_1,E_n}(\hat{\rho}_S(n-1)\otimes\hat{\eta}_{E_n})\right\}= \\ &\sum_{\ell,\ell'}\frac{\gamma_1^{(\ell,\ell')}}{2}\left\{2\hat{A}^{(\ell)}_{S_1}\hat{\rho}_S(n-1)\hat{A}^{(\ell')}_{S_1}-\left\{\hat{A}^{(\ell')}_{S_1}\hat{A}^{(\ell)}_{S_1},\hat{\rho}_S(n-1)\right\}\right\}\end{aligned} \tag{3.21}$$

$$\begin{aligned}&\mathrm{Tr}_{E_n}\left\{\mathcal{U}''_{S_2,E_n}\circ\mathcal{M}_{E_n}(\hat{\rho}_S(n-1)\otimes\hat{\eta}_{E_n})\right\}= \\ &\sum_{\ell,\ell'}\frac{\gamma_2^{(\ell,\ell')}}{2}\left\{2\hat{A}^{(\ell)}_{S_2}\hat{\rho}_S(n-1)\hat{A}^{(\ell')}_{S_2}-\left\{\hat{A}^{(\ell')}_{S_2}\hat{A}^{(\ell)}_{S_2},\hat{\rho}_S(n-1)\right\}\right\},\end{aligned} \tag{3.22}$$

where we have defined:

$$\gamma_1^{(\ell,\ell')} = \mathrm{Tr}_{E_n}\left\{\hat{B}_{E_n}^{(\ell',1)}\hat{B}_{E_n}^{(\ell,1)}\hat{\eta}_{E_n}\right\} \tag{3.23}$$

$$\gamma_2^{(\ell,\ell')} = \mathrm{Tr}_{E_n}\left\{\hat{B}_{E_n}^{(\ell',2)}\hat{B}_{E_n}^{(\ell,2)}\mathcal{M}_{E_n}(\hat{\eta}_{E_n})\right\}. \tag{3.24}$$

One can immediately see that both contributions in Eqs.(3.21, 3.22) involve only local operators, so that the first term only affects S_1 and the other only S_2. The same is not true when tracing away the environment from the remaining contribution:

$$\begin{aligned}&\mathrm{Tr}_{E_n}\left\{\mathcal{U}'_{S_2,E_n}\circ\mathcal{M}_{E_n}\circ\mathcal{U}_{S_1,E_n}(\hat{\rho}_S(n-1)\otimes\hat{\eta}_n)\right\} = \\ &\sum_{\ell,\ell'}\left\{\zeta_{12}^{(\ell,\ell')}\hat{A}_{S_1}^{(\ell)}\left[\hat{\rho}_S(n-1),\hat{A}_{S_2}^{(\ell')}\right] - \xi_{12}^{(\ell,\ell')}\left[\hat{A}_{S_2}^{(\ell')},\hat{\rho}_S(n-1)\right]\hat{A}_{S_1}^{(\ell)}\right\},\end{aligned} \tag{3.25}$$

where

$$\zeta_{12}^{(\ell,\ell')} = \mathrm{Tr}\left\{\hat{B}_{E_n}^{(\ell',2)}\mathcal{M}_{E_n}\left(\hat{B}_{E_n}^{(\ell,1)}\hat{\eta}_{E_n}\right)\right\} \tag{3.26}$$

$$\xi_{12}^{(\ell,\ell')} = \mathrm{Tr}\left\{\hat{B}_{E_n}^{(\ell',2)}\mathcal{M}_{E_n}\left(\hat{\eta}_{E_n}\hat{B}_{E_n}^{(\ell,1)}\right)\right\}. \tag{3.27}$$

At glance with the previous terms, the contribution in Eq. (3.25) contains operators acting on both S_1 and S_2, thus introducing an interaction between the two nodes which is induced by the common interaction with the environment. We will see later that upon diagonalizing the master equation in order to put it in Lindblad form, cross terms like the one in Eq. (3.25) give rise to a unitary contribution to the dynamics which is chiral, by this meaning that the induced Hamiltonian changes sign upon exchange of S_1 and S_2.

In the end, substituting the terms we have just computed in Eq. (3.9), we are left with a discrete master equation of the form:

$$\frac{\hat{\rho}_S(n+1)-\hat{\rho}_S(n)}{\delta t} = g^2\,\delta t\left[\mathcal{L}_1+\mathcal{L}_2+\mathcal{D}_{12}\right](\hat{\rho}_S(n)) \tag{3.28}$$

where we have defined

$$\mathcal{L}_1(\cdots) = \sum_{\ell,\ell'} \frac{\gamma_1^{(\ell,\ell')}}{2} \left\{ 2\hat{A}_{S_1}^{(\ell)}(\cdots)\hat{A}_{S_1}^{(\ell')} - \left\{ \hat{A}_{S_1}^{(\ell')}\hat{A}_{S_1}^{(\ell)}, \cdots \right\} \right\} \tag{3.29}$$

$$\mathcal{L}_2(\cdots) = \sum_{\ell,\ell'} \frac{\gamma_2^{(\ell,\ell')}}{2} \left\{ 2\hat{A}_{S_2}^{(\ell)}(\cdots)\hat{A}_{S_2}^{(\ell')} - \left\{ \hat{A}_{S_2}^{(\ell')}\hat{A}_{S_2}^{(\ell)}, \cdots \right\} \right\} \tag{3.30}$$

$$\mathcal{D}_{12}(\cdots) = \sum_{\ell,\ell'} \left\{ \zeta_{12}^{(\ell,\ell')} \hat{A}_{S_1}^{(\ell)} \left[\cdots, \hat{A}_{S_2}^{(\ell')} \right] - \xi_{12}^{(\ell,\ell')} \left[\hat{A}_{S_2}^{(\ell')}, \cdots \right] \hat{A}_{S_1}^{(\ell)} \right\} \tag{3.31}$$

Rearranging the terms in Eq. (3.28) and performing the continuous time limit the same way we did in Sec. 2.3 we can finally write the master equation for a two nodes cascade system:

$$\frac{d}{dt}\hat{\rho}_S(t) = \gamma \left[\mathcal{L}_1 + \mathcal{L}_2 + \mathcal{D}_{12} \right] (\hat{\rho}_S(t)) = \gamma \mathcal{C}_S(\hat{\rho}_S(t)). \tag{3.32}$$

It can be seen that this master equation contains three terms: the two terms $\mathcal{L}_{1,2}$ describe the local dissipation due to the interaction of the nodes with the environment, while the term $\mathcal{D}_{12}$ is characteristic of cascade systems, and describe the interaction between the two nodes due to their common interaction with the environment. This is even more evident if one tries to trace away one node from the master equation: if one tries to trace away the second node, he finds that the dynamics of the first node is fully contained in the term $\mathcal{L}_1$. Conversely, tracing away the second node does not nullify the term $\mathcal{D}_{12}$, and as a result one would obtain a master equation containing the local term $\mathcal{L}_2$ and another term, obtained from the trace over $\mathcal{D}_{12}$, describing the influence of S_1 on S_2.

Once we have analyzed this very simple cascade system and highlighted its main features, we are ready to make a step further and complicate things, moving to the analisys of a cascade network.

3.2. Cascade networks

As already said in the introduction to this chapter, a cascade network consists in an ensemble of M quantum systems $\{S_1, S_2, \cdots, S_M\}$, often called the nodes, connected by one or more transmission lines, each described as a distinct environment $\{\mathcal{E}^{(1)}, \mathcal{E}^{(2)}, \cdots, \mathcal{E}^{(K)}\}$. These environments can moreover interact between themselves through optical elements, such as beam splitters and phase shifters, which introduce in-

terference effects in the signal propagation, thus influencing the dynamics of the nodes. A very simple sketch of this kind of systems is shown in Fig. 3.3. In analogy with the example exposed in the previous section, we expect to find a master equation made out of local terms, describing the local dissipative dynamics of the nodes, and non-local terms describing the cascade interaction between the nodes and containing the information over the hierarchy between the nodes. Furthermore, we expect these non-local terms to be influenced by the optical elements and the interference effects induced by their presence. In this section we are first going to expose our model to derive the Markovian master equation, highlighting some features of the master equation, before finally recasting it in the GKSL form.

3.2.1. The model

In this section we are going to see how it is possible, through a collisional model, to describe the presence of more than one environment and the interference effects given by their interaction through optical elements.

In the spirit of collisional models, we divide each of the environments in an ensemble of ancillas, $\mathcal{E}^{(k)} = \{E_n^{(k)},\, n = 1, 2, \cdots\}$. It will also turn out to be useful to regroup the ancillas according to the index n, i.e. defining the sets $\mathcal{E}_n = \{E_n^{(1)}, E_n^{(2)}, \cdots, E_n^{(K)}\}$: this amounts to dividing the ancillas in "temporal slices", that is, grouping the ancillas according to the time they enter the dynamics. Associating the index n with a temporal label can however be done only under the assumption that the traveling time between one node and another, i.e. the time it takes for an ancilla to move from a node S_m to a node $S_{m'}$, is negligible. This is a necessary assumption in order to keep the dynamics Markovian, as time delays unavoidably introduce non-Markovian features due to feedback effects. We also note that this assumption is necessary only when dealing with a network where more transmission lines are present: for the case of a series of nodes connected through a linear chain, like the minimal one we examined in the previous section, one can redefine the operators acting on the nodes such that the phase shift gained during the traveling time is absorbed into the new definition, leaving the expectation values of any Hermitian operator unchanged [C. W. Gardiner 1993].

Once the time-delays have been assumed to be negligible, it is then possible to enforce a causal structure on the network by simply imposing that the superoperator $\mathcal{U}_{S_m,\mathcal{E}_n}$ describing the collisional event involving the node S_m and the ancillas belonging to the set $\mathcal{E}_n$ should precede both $\mathcal{U}_{S_{m+1},\mathcal{E}_n}$ and $\mathcal{U}_{S_m,\mathcal{E}_{n+1}}$, as the ancillas from $\mathcal{E}_n$ see S_{m+1} only

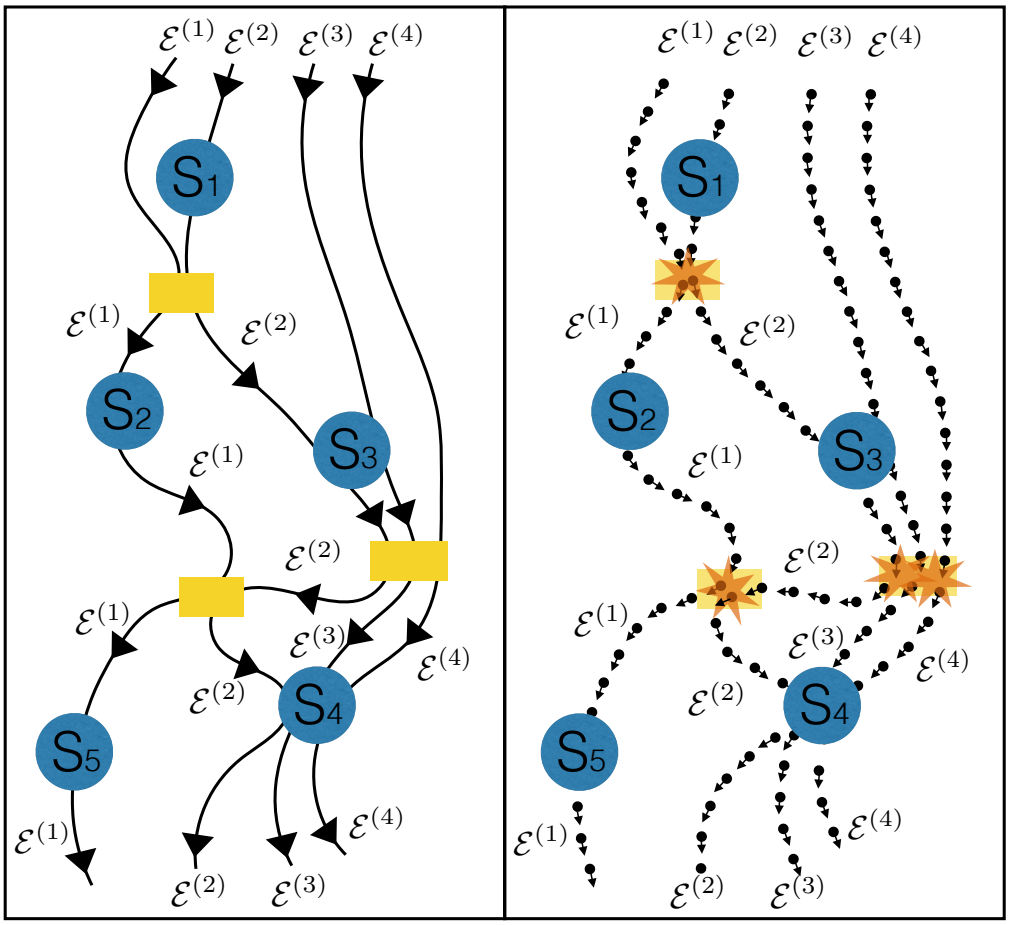

Figure 3.3.: A very simple representation of a cascade network: in the left panel we sketch the typical structure of a cascade network, namely an ensemble of nodes (blue dots) connected by various transmission lines (i.e. environmental channels) that can interact through optical elements such as beam splitters and phase shifters (yellow boxes). On the right panel we sketch the same network in a collisional model setting: each environmental channel is depicted as a collection of ancillas that interact collisionally with the nodes, but also interact with each other through the optical elements. This collisions between ancillas are the ones giving rise to interference effects.

after they interacted with S_m, and the elements of $\mathcal{E}_n$ enter the network before the ones from $\mathcal{E}_{n+1}$. No ordering is instead required between $\mathcal{U}_{S_{m+1},\mathcal{E}_n}$ and $\mathcal{U}_{S_m,\mathcal{E}_{n+1}}$, as they act on different systems and thus commute with each other.

In analogy with the previous section we assume S to have free Hamiltonian $\hat{H}_S = \sum_m \hat{H}_{S_m}$, while the Hamiltonian of the environment is $\hat{H}_{\mathcal{E}} = \sum_{k,n} \hat{H}_{E_n^{(k)}}$. We also assume once again the interaction Hamiltonian between a node and an ancilla to be of

the form:

$$\hat{H}_{S_m-E_n^{(k)}} = \sum_{\ell} \hat{A}_{S_m}^{(\ell,k)} \otimes \hat{B}_{E_n^{(k)}}^{(\ell,m)}, \tag{3.33}$$

with $\hat{A}_{S_m}^{(\ell,k)}$ and $\hat{B}_{E_n^{(k)}}^{(\ell,m)}$ Hermitian. This assumption however is only imposed in order to simplify the derivation, but it could be relaxed leading to equivalent expressions that render less explicit the mathematical and physical features of the model.

Once the interaction Hamiltonian has been defined we can write the superoperator $\mathcal{U}_{S_m,\mathcal{E}_n}$ as:

$$\mathcal{U}_{S_m,\mathcal{E}_n}(\cdots) = \hat{U}_{S_m,\mathcal{E}_n}(\cdots)\hat{U}^{\dagger}_{S_m,\mathcal{E}_n}, \tag{3.34}$$

$$\hat{U}_{S_m,\mathcal{E}_n} = \exp\left[-ig\,\delta t \sum_{k=1}^{K} \hat{H}_{S_m,E_n^{(k)}}\right], \tag{3.35}$$

where as usual g is a coupling constant gauging the strength of the interaction and δt is the time interval over which the collisions take place.

At this point we want to write the superoperator $\mathcal{C}_{S,\mathcal{E}_n}$ describing the n-th step of the dynamics:

$$\hat{\rho}_{S\mathcal{E}}(n) = \mathcal{C}_{S,\mathcal{E}_n}\left(\hat{\rho}_S(n-1) \otimes \hat{\eta}_{\mathcal{E}_n}\right). \tag{3.36}$$

At glance with the previous case, here with the symbol $\hat{\eta}_{\mathcal{E}_n}$ we mean the joint state of the ancillas belonging to the set $\mathcal{E}_n$. It is important to note at this point that in the following we will assume the state $\hat{\eta}_{\mathcal{E}_n}$ to be independent of n, that is, we will assume the environments $\mathcal{E}^{(k)}$ to form a stationary medium. On the same footing we will assume also the couplings $\mathcal{U}_{S_m,\mathcal{E}_n}$ and the maps $\mathcal{M}_{\mathcal{E}_n^{(m)}}$ to be independet from n. These hypothesis can however be relaxed, given the condition that the changes are slow compared with the characteristic time scale of the node S_m.

Within the above scenario, we can write the superoperator $\mathcal{C}_{S,\mathcal{E}_n}$ by looking at the circuit-like representation of the dynamics shown in Fig. 3.4: The ancillas belonging to the set $\mathcal{E}_n$ enter the network and interact first with S_1, then they undergo some evolution dictated by the CPT map $\mathcal{M}_{\mathcal{E}_n}^{(1)}$ before interacting with S_2 and so forth. Thus, using the symbol $\overleftarrow{\prod}$ to indicate the ordered product of superoperators from left to right, we can

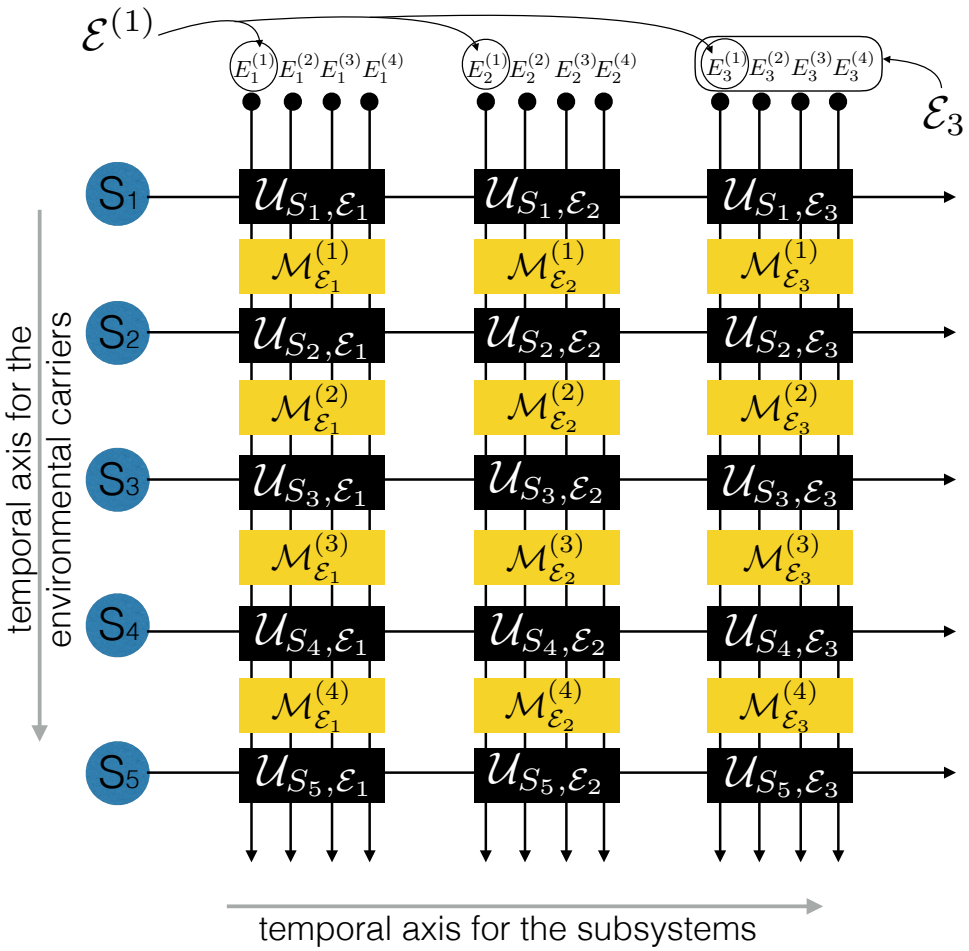

Figure 3.4.: A circuit-like representation of the cascade network model under examination: the ancillas belonging to the set $\mathcal{E}_n$ enter the network first interacting with S_1, then undergo an evolution dictated by the CPT map $\mathcal{M}_{\mathcal{E}_n}^{(1)}$ before interacting with S_2 and so forth. On the other hand the node S_m interact with the ensemble $\mathcal{E}_n$ only after the latter has interacted with the previous nodes $S_{m'}$ with $m' < m$. This feature, together with the inclusion of interaction between the ancillas belonging to the same $\mathcal{E}_n$ described by the maps $\mathcal{M}_{\mathcal{E}_n}^{(m)}$, give rise to interference effects, at glance with the example from the previous section.

write:

$$\mathcal{C}_{S,\mathcal{E}_n} = \overleftarrow{\Pi}_{m=1}^{M} \left[\mathcal{M}_{\mathcal{E}_n}^{(m)} \circ \mathcal{U}_{S_m,\mathcal{E}_n} \right]. \tag{3.37}$$

When writing Eq. (3.37) we are implicitly assuming that there is no temporal correlation between the ancillas, i.e. the input state of the ancillas is factorized with respect to the grouping $\mathcal{E}_1, \mathcal{E}_2, \cdots$. In fact admitting temporal correlations between the ancillas

would lead to non-Markovian effects: this kind of situations actually still represents an open problem in the field of open quantum system dynamics, and a rich literature on the topic exists [H.-P. Breuer 2012; Li, Hall, and Wiseman 2018], but for the scope of this work we will keep the assumption of no temporal correlations among ancillas.

As in the previous section we want to expand the superoperator $\mathcal{C}_{S,\mathcal{E}_n}$ in power series of $g\,\delta t$ up to second order and then perform the continuous time limit. In order to be able to power expand $\mathcal{C}_{S,\mathcal{E}_n}$ we must first compute the power expansion of $\mathcal{U}_{S_m,\mathcal{E}_n}$, which is similar to the one in Eq. (3.10):

$$\mathcal{U}_{S_m,\mathcal{E}_n} = \mathcal{I}_{S_m,\mathcal{E}_n} + (g\,\delta t)\,\mathcal{U}'_{S_m,\mathcal{E}_n} + (g\,\delta t)^2\,\mathcal{U}''_{S_m,\mathcal{E}_n} + \mathcal{O}\big((g\,\delta t)^3\big), \tag{3.38}$$

where $\mathcal{I}_{S,\mathcal{E}_n}$ is once again the identity superoperator and now we have:

$$\mathcal{U}'_{S,\mathcal{E}_n}(\cdots) = -i\sum_{k=1}^{K}\Big[\hat{H}_{S_m,E_n^{(k)}},(\cdots)\Big], \tag{3.39}$$

$$\mathcal{U}''_{S,\mathcal{E}_n}(\cdots) = \sum_{k,k'=1}^{K}\left\{\hat{H}_{S_m,E_n^{(k)}}(\cdots)\,\hat{H}_{S_m,E_n^{(k')}} - \frac{1}{2}\Big\{\hat{H}_{S_m,E_n^{(k')}}\hat{H}_{S_m,E_n^{(k)}},(\cdots)\Big\}\right\}. \tag{3.40}$$

These two terms of the power expansion of $\mathcal{U}_{S_m,\mathcal{E}_n}$ have the same form of the ones in Eq. (3.11) and Eq. (3.12) respectively, with the only difference that in this case we need to sum up the Hamiltonians of all the environmental channels with which the node S_m interacts.

Given the expansion of $\mathcal{U}_{S_m,\mathcal{E}_n}$ we can perform the series expansion of $\mathcal{C}_{S,\mathcal{E}_n}$, which leads to:

$$\mathcal{C}_{S,\mathcal{E}_n} = \mathcal{C}^{(0)}_{S,\mathcal{E}_n} + (g\,\delta t)\,\mathcal{C}'_{S,\mathcal{E}_n} + (g\,\delta t)^2\,\mathcal{C}''_{S,\mathcal{E}_n} + \mathcal{O}\big((g\,\delta t)^3\big), \tag{3.41}$$

where now:

$$\mathcal{C}^{(0)}_{S,\mathcal{E}_n} = \mathcal{M}^{(M\leftarrow 1)}_{\mathcal{E}_n}, \tag{3.42}$$

$$\mathcal{C}'_{S,\mathcal{E}_n} = \sum_{m=1}^{M}\mathcal{M}^{(M\leftarrow m)}_{\mathcal{E}_n}\circ\mathcal{U}'_{S_m,\mathcal{E}_n}\circ\mathcal{M}^{(m\leftarrow 1)}_{\mathcal{E}_n}, \tag{3.43}$$

$$\mathcal{C}''_{S,\mathcal{E}_n} = \mathcal{C}''^{(a)}_{S,\mathcal{E}_n} + \mathcal{C}''^{(b)}_{S,\mathcal{E}_n}, \tag{3.44}$$

with

$$\mathcal{C}''^{(a)}_{S,\mathcal{E}_n} = \sum_{m=1}^{M} \mathcal{M}^{(M\leftarrow m)}_{\mathcal{E}_n} \circ \mathcal{U}''_{S_m\mathcal{E}_n} \circ \mathcal{M}^{m-1\leftarrow 1}_{\mathcal{E}_n}, \tag{3.45}$$

$$\mathcal{C}''^{(b)}_{S,\mathcal{E}_n} = \sum_{m'=m+1}^{M} \sum_{m=1}^{M-1} \mathcal{M}^{(M\leftarrow m')}_{\mathcal{E}_n} \circ \mathcal{U}'_{S'_m,\mathcal{E}_n} \circ \mathcal{M}^{(m'-1\leftarrow m)}_{\mathcal{E}_n} \circ \mathcal{U}'_{S_m,\mathcal{E}_n} \circ \mathcal{M}^{(m-1\leftarrow 1)}_{\mathcal{E}_n}. \tag{3.46}$$

In writing the above equations we have defined

$$\mathcal{M}^{(m_2\leftarrow m_1)}_{\mathcal{E}_n} = \begin{cases} \overleftarrow{\prod}^{m_2}_{m=m_1} \mathcal{M}^{(m)}_{\mathcal{E}_n} & \text{for } m_2 \geq m_1, \\ \mathcal{I} & \text{for } m_2 < m_1. \end{cases} \tag{3.47}$$

In order to derive the master equation for the reduced density matrix, just as we did for the case of only two nodes, we must insert the expansion of Eq. (3.41) into Eq. (3.36) and trace away the environmental degrees of freedom.

The zeroth order term in Eq. (3.42), being a composition of CPT maps acting only on the ancillas, gives the very simple contribution:

$$\mathrm{Tr}\left\{\mathcal{C}^{(0)}_{S,\mathcal{E}_n}\left(\hat{\rho}_S(n-1)\otimes\hat{\eta}_{\mathcal{E}_n}\right)\right\} = \hat{\rho}_S(n-1). \tag{3.48}$$

We then turn to the first order term: from Eq. (3.43) it is immediately seen that the CPT maps acting after the evolution superoperator $\mathcal{U}'_{S_m,\mathcal{E}_{n+1}}$ have no effects. Then, after the trace operations, we are left with:

$$\mathrm{Tr}_{\mathcal{E}_n}\left\{\mathcal{C}'_{S,\mathcal{E}_n}\left(\hat{\rho}_S(n-1)\otimes\hat{\eta}_{\mathcal{E}_n}\right)\right\} = -i\sum_{m,k,\ell}\gamma^{(\ell)}_{m(k)}\left[\hat{A}^{(\ell,k)}_{S_m},\hat{\rho}_S(n-1)\right], \tag{3.49}$$

$$\tag{3.50}$$

where we have defined:

$$\gamma^{(\ell)}_{m(k)} = \mathrm{Tr}_{\mathcal{E}_n}\left\{\hat{B}^{(m,\ell)}_{E^{(k)}_n}\mathcal{M}^{(m-1\leftarrow 1)}_{\mathcal{E}_n}\left(\hat{\eta}_{\mathcal{E}_n}\right)\right\}. \tag{3.51}$$

As explained in Chap. 2, in order to avoid the explosion of this first order contribution in the final expression, we want to impose a stability condition on the environmental degrees of freedom, which in this case amounts to nullify the coefficients of the first order

contributions, i.e.:

$$\gamma^{\ell}_{m(k)} = 0 \quad \forall\, m, k, \ell. \tag{3.52}$$

Thus, in the final expression we want to derive, we will not insert the first order term, having already assumed this condition.

At this point we are left with the second order contribution, which we have divided in two parts: the first contribution, $\mathcal{C}^{''(a)}_{S,\mathcal{E}_n}$ contains all the local contributions to the dissipative dynamics, while the second contribution $\mathcal{C}^{''(b)}_{S,\mathcal{E}_n}$ gives rise to the cross terms like the one in Eq. (3.31).

Let us start from $\mathcal{C}^{''(a)}_{S,\mathcal{E}_n}$. Just as for the first order contribution, the CPT maps acting on the left of $\mathcal{U}''_{S_m,\mathcal{E}_n}$ give in facts no contribution after the trace operation. After some straightforward algebra it is possible to write:

$$\begin{aligned}&\mathrm{Tr}_{\mathcal{E}_n}\left\{\mathcal{C}^{''(a)}_{S,\mathcal{E}_n}\left(\hat{\rho}_S(n-1)\otimes\hat{\eta}_{\mathcal{E}_n}\right)\right\} = \\ &\frac{1}{2}\sum_{m=1}^{M}\sum_{k,k'}\sum_{\ell,\ell'}\gamma^{(\ell,\ell')}_{m(kk')}\left\{2\hat{A}^{(\ell,k)}_{S_m}\hat{\rho}_S(n-1)\hat{A}^{(\ell',k')}_{S_m} - \left\{\hat{A}^{(\ell',k')}_{S_m}\hat{A}^{(\ell,k)}_{S_m},\hat{\rho}_S(n-1)\right\}\right\},\end{aligned} \tag{3.53}$$

where the coefficients $\gamma^{(\ell,\ell')}_{m(k,k')}$ are worth:

$$\gamma^{(\ell,\ell')}_{m(kk')} = \mathrm{Tr}_{\mathcal{E}_n}\left\{\hat{B}^{(\ell',m)}_{E^{(k')}_n}\hat{B}^{(\ell,m)}_{E^{(k)}_n}\mathcal{M}^{(m-1\leftarrow 1)}_{\mathcal{E}_n}\left(\hat{\eta}_{\mathcal{E}_n}\right)\right\}. \tag{3.54}$$

On a similar footing one can compute the non-local contributions stemming from the term $\mathcal{C}^{''(b)}_{S,\mathcal{E}_n}$: once again the CPT maps acting after $\mathcal{U}'_{S_{m'},\mathcal{E}_n}$ give no contribution after the trace operation, so that we can write:

$$\begin{aligned}&\mathrm{Tr}\left\{\mathcal{C}^{''(b)}_{S,\mathcal{E}_n}\left(\hat{\rho}_S(n-1)\otimes\hat{\eta}_{\mathcal{E}_n}\right)\right\} = \\ &\sum_{m'=m+1}^{M}\sum_{m=1}^{M-1}\sum_{\substack{k,k'\\ \ell,\ell'}}\left\{\zeta^{(\ell,\ell')}_{mm'(kk')}\hat{A}^{(\ell,k)}_{S_m}\left[\hat{\rho}_S(n-1),\hat{A}^{(\ell',k')}_{S_{m'}}\right] - \xi^{(\ell,\ell')}_{mm'(kk')}\left[\hat{\rho}_S(n-1),\hat{A}^{(\ell',k')}_{S_{m'}}\right]\hat{A}^{(\ell,k)}_{S_m}\right\},\end{aligned} \tag{3.55}$$

where we have defined:

$$\zeta^{(\ell,\ell')}_{mm'(kk')} = \mathrm{Tr}\left\{\hat{B}^{(\ell',m')}_{E^{(k')}_n}\mathcal{M}^{(m'-1\leftarrow m)}_{\mathcal{E}_n}\hat{B}^{(\ell,m)}_{E^{(k)}_n}\mathcal{M}^{(m-1\leftarrow 1)}_{\mathcal{E}_n}\left(\hat{\eta}_{\mathcal{E}_n}\right)\right\}, \tag{3.56}$$

$$\xi^{(\ell,\ell')}_{mm'(kk')} = \mathrm{Tr}\left\{\hat{B}^{(\ell',m')}_{E^{(k')}_n}\mathcal{M}^{(m'-1\leftarrow m)}_{\mathcal{E}_n}\left(\mathcal{M}^{(m-1\leftarrow 1)}_{\mathcal{E}_n}\left(\hat{\eta}_{\mathcal{E}_n}\right)\hat{B}^{(\ell,m)}_{E^{(k)}_n}\right)\right\}. \tag{3.57}$$

Once all the contributions have been computed, and taking the continuous time limit as in Chap. 2, we can write the master equation for S as:

$$\frac{d\hat{\rho}_S(t)}{dt} = \gamma\mathcal{C}(\hat{\rho}_S(t)) = \gamma\left[\sum_m \mathcal{L}_m + \sum_{m'=m+1}^{M}\sum_m \mathcal{D}_{mm'}\right](\hat{\rho}_S(t)). \tag{3.58}$$

This is a Markovian master equation describing the dissipative dynamics of an ensemble of nodes connected through chiral environments in a cascade fashion. Being a Markovian master equation it can be recast in GKSL form by properly rearranging the various terms on the right hand side of Eq. (3.58): before doing this, it is worth to look at the various terms in the master equation and understand their meaning.

The local terms $\mathcal{L}_m$ describe a local dissipative dynamics due to the interaction of the nodes S with the environments $\mathcal{E}^{(k)}$. As each $\mathcal{L}_m$ contains operators acting on the node S_m only, these terms do not create correlations among the various nodes, they only account for dissipative behaviours.

On the other hand, as we anticipated in Sec. 3.1, the terms $\mathcal{D}_{mm'}$ are characteristic of cascade systems: in facts they describe an interaction between node S_m and node $S_{m'}$ which is due to a common interaction of the nodes with the same environment. Thus, at glance with what would happen in presence of an Hamiltonian coupling between S_m and $S_{m'}$, the $\mathcal{D}_{mm'}$ terms are intrinsically asymmetric, in accordance with the cascade nature of the network. This can be seen by looking at the structure of these non local terms: first of all only terms with $m' > m$ are present, due to the fact that the ancillas interact with $S_{m'}$ after they have interacted with S_m, but note viceversa. To see the fact that $S_{m'}$ has no influence over S_m, one can simply trace away $S_{m'}$ from $\mathcal{D}_{mm'}$ getting:

$$\mathrm{Tr}\left\{\mathcal{D}_{mm'}(\hat{\rho}_S(t))\right\} = 0. \tag{3.59}$$

The opposite, as already anticipated, is not true: if we were to trace away S_m, we would get a term describing the effects of S_m on $S_{m'}$, in accordance with the causal structure described.

Another thing to be noted is that the information about interactions between ancillas belonging to different environmental channels $\mathcal{E}^{(k)}$ is stored into the coefficients $\gamma^{(\ell,\ell')}_{m(kk')}$, $\zeta^{(\ell,\ell')}_{mm'(kk')}$ and $\zeta^{(\ell,\ell')}_{mm'(kk')}$, as these are the result of the trace over the ancillary degrees of freedom.

3.2.2. GKSL form of the master equation

After these considerations, it is time to see how the rhs of Eq. (3.58) can be recast in order to get a Markovian generator in the GKSL form and understand another feature of cascade systems by looking at the Hamiltonian terms induced by the open dynamics.

We start this operation by noticing that, as we assumed both the $\hat{A}_{S_m}^{(\ell,k)}$ and the $\hat{B}_{E_n^{(k)}}^{(\ell,m)}$ to be Hermitean, it holds:

$$\gamma_{m(kk')}^{(\ell,\ell')} = \left[\gamma_{m(k'k)}^{(\ell',\ell)}\right]^*, \tag{3.60}$$

$$\xi_{mm'(kk')}^{(\ell,\ell')} = \left[\zeta_{mm'(kk')}^{(\ell,\ell')}\right]^*. \tag{3.61}$$

Both these relations will turn out to be useful in the derivation of the GKSL form of the Markovian generator. Our goal is to write the $\mathcal{C}(\cdots)$ superoperator in Eq. (3.58) in the form:

$$\mathcal{C}(\cdots) = -i\Big[\hat{H}, (\cdots)\Big] + \sum_i 2\hat{L}^{(i)}(\cdots)\hat{L}^{(i)\dagger} - \Big\{\hat{L}^{(i)\dagger}\hat{L}(i), (\cdots)\Big\}, \tag{3.62}$$

with $\hat{H}$ being a self-adjoint operator and the $\hat{L}^{(i)}$'s being a collection of operators acting on S. We start from the local terms $\mathcal{L}_m$: from Eq. (3.60) we note that, dubbing j the joint index (ℓ, k), the matrix $\theta_{jj'}$ whose elements are the $\gamma_{m(kk')}^{(\ell,\ell')}/2$ is Hermitian. Moreover, since the $\hat{B}_{E_n^{(k)}}^{(\ell,m)}$ are Hermitian and the definition of the $\gamma_{m(kk')}^{(\ell,\ell')}$ in Eq. (3.54), $\Theta_{jj'}$ is also semi-positive definite. As a consequence of this, it follows immediately that we can rewrite the local terms $\mathcal{L}_m$ as purely dissipative terms:

$$\mathcal{L}_m(\cdots) = \sum_s \lambda_s \left\{2\hat{\Lambda}_{S_m}^{(s)}(\cdots)\hat{\Lambda}_{S_m}^{(s)\dagger} - \left\{\hat{\Lambda}_{S_m}^{(s)\dagger}\hat{\Lambda}_{S_m}^{(s)}, (\cdots)\right\}\right\}, \tag{3.63}$$

where the λ_s are the eigenvalues of $\Theta_{jj'}$ and the operators $\hat{\Lambda}_{S_m}^{(s)}$ are defined as:

$$\hat{\Lambda}_{S_m}^{(s)} = \sum_{k,\ell} v_{(\ell,k),s}\hat{A}_{S_m}^{(\ell,k)}, \tag{3.64}$$

$v_{j,s}$ being the unitary matrix that allows to diagonalize $\Theta_{jj'}$, that is $\Theta_{jj'} = \sum_s v_{j,s}\lambda_s v_{s,j'}^*$. In the end, the $\hat{\Lambda}_{S_m}^{(s)}$ are linear combinations of the $\hat{A}_{S_m}^{(\ell,k)}$, and if it were not for the non local terms $\mathcal{D}_{mm'}$, the procedure would have already been completed, identifying the Lindblad operators $\hat{L}^{(i)}$ in Eq. (3.62) with $\sqrt{\lambda_s}\hat{\Lambda}_{S_m}^{(s)}$ and $\hat{H} = 0$.

We then need to analyze the non local contributions. Looking at these terms it would

seem that they cannot directly produce terms in the Lindblad form. However, with little algebra, it is possible to derive the identities

$$\begin{aligned}\hat{A}^{(\ell,k)}_{S_m}\Big[(\cdots),\hat{A}^{(\ell',k')}_{S_{m'}}\Big] &= -\frac{1}{2}\Big[\hat{A}^{(\ell,k)}_{S_m}\hat{A}^{(\ell',k')}_{S_{m'}},(\cdots)\Big] \\ &+ \hat{A}^{(\ell,k)}_{S_m}(\cdots)\hat{A}^{(\ell',k')}_{S_{m'}} - \frac{1}{2}\Big\{\hat{A}^{(\ell,k)}_{S_m}\hat{A}^{(\ell',k')}_{S_{m'}},(\cdots)\Big\}, \end{aligned} \tag{3.65}$$

$$\begin{aligned}\Big[(\cdots),\hat{A}^{(\ell',k')}_{S_{m'}}\Big]\hat{A}^{(\ell,k)}_{S_m} &= -\frac{1}{2}\Big[\hat{A}^{(\ell',k')}_{S_{m'}}\hat{A}^{(\ell,k)}_{S_m},(\cdots)\Big] \\ &- \hat{A}^{(\ell',k')}_{S_{m'}}(\cdots)\hat{A}^{(\ell,k)}_{S_m} + \frac{1}{2}\Big\{\hat{A}^{(\ell',k')}_{S_{m'}}\hat{A}^{(\ell,k)}_{S_m},(\cdots)\Big\}. \end{aligned} \tag{3.66}$$

Thanks to these expressions it is now possible to rearrange the non local contributions into two pieces:

$$\mathcal{D}_{mm'}(\cdots) = -i\Big[\hat{H}_{mm'},(\cdots)\Big] + \Delta\mathcal{L}_{mm'}(\cdots). \tag{3.67}$$

The first contribution on the rhs of Eq. (3.67) has the form of an effective Hamiltonian and is worth:

$$\begin{aligned}\hat{H}_{mm'} &= \sum_{k,k'=1}^{K}\sum_{\ell,\ell'}\frac{\xi^{(\ell,\ell')}_{mm'(kk')} - \zeta^{(\ell,\ell')}_{mm'(kk')}}{2i}\hat{A}^{(\ell,k)}_{S_m}\hat{A}^{(\ell',k')}_{S_{m'}} \\ &= \sum_{k,k'=1}^{K}\sum_{\ell,\ell'}\mathrm{Im}[\xi^{(\ell,\ell')}_{mm'(kk')}]\hat{A}^{(\ell,k)}_{S_m}\hat{A}^{(\ell',k')}_{S_{m'}}, \end{aligned} \tag{3.68}$$

where in passing from the first to the second line we made use of Eq. (3.61).

We then turn our attention to the second contribution on the rhs of Eq. (3.67), which reads:

$$\Delta\mathcal{L}_{mm'} = \sum_{m,m'}\sum_{k,k'=1}^{K}\sum_{\ell,\ell'}\Delta D^{(\ell,\ell')}_{mm'(kk')}\left\{2\hat{A}^{(\ell,k)}_{S_m}(\cdots)\hat{A}_{S^{(\ell',k')}_{m'}} - \left\{\hat{A}^{(\ell',k')}_{S_{m'}}\hat{A}^{(\ell,k)}_{S_m},(\cdots)\right\}\right\}, \tag{3.69}$$

where we have defined:

$$\Delta D^{(\ell,\ell')}_{mm'(kk')} = \frac{1}{2}\begin{cases}\zeta^{(\ell,\ell')}_{mm'(kk')} & \text{for } m<m', \\ 0 & \text{for } m=m', \\ \xi^{(\ell'\ell)}_{m'm(k'k)} & \text{for } m>m'. \end{cases} \tag{3.70}$$

Exploiting once again Eq. (3.61) one can immediately see that the matrix $\Delta\Omega_{jj'}$ of elements $\Delta D^{(\ell,\ell')}_{mm'(kk')}$, this time j being the joint index (ℓ,k,m), is Hermitian. Still, there is no guarantee that $\Delta\Omega_{jj'}$ is semi-positive definite, and this prevents us from directly diagonalizing $\Delta\Omega_{jj'}$ and expressing directly the $\Delta\mathcal{L}_{mm'}$ contributions as dissipative contributions as we did for the local terms. Nonetheless, inserting Eq. (3.67) into Eq. (3.58) we are able to write:

$$\begin{aligned}\mathcal{C}(\cdots) &= -i\Big[\hat{H},(\cdots)\Big] \\ &+\sum_{m,m'}\sum_{k,k'=1}^{K}\sum_{\ell,\ell'} D^{(\ell,\ell')}_{mm'(kk')}\left\{2\hat{A}^{(\ell,k)}_{S_m}(\cdots)\hat{A}^{(\ell',k')}_{S_{m'}} - \left\{\hat{A}^{(\ell',k')}_{S_{m'}}\hat{A}^{(\ell,k)}_{S_m},\cdots\right\}\right\},\end{aligned} \tag{3.71}$$

where now the effective Hamiltonian $\hat{H}$ is worth

$$\hat{H} = \sum_{m'>m}\sum_{m=1}^{M}\hat{H}_{mm'}, \tag{3.72}$$

and the coefficients $D^{(\ell,\ell')}_{mm'(kk')}$ have been defined as:

$$D^{(\ell,\ell')}_{mm'(kk')} = \begin{cases} \Delta D^{(\ell,\ell')}_{mm'(kk')} & \text{for } m\neq m', \\ \gamma^{(\ell,\ell')}_{m(kk')} & \text{for } m = m'. \end{cases} \tag{3.73}$$

In order to cast the master equation in GKSL form we are only left to demonstrate that the matrix $\Omega_{jj'}$ of elements $D^{(\ell,\ell')}_{mm'(kk')}$, j being still the joint index (ℓ,k,m), is semi-positive definite. As the demonstration is quite long and gives no particular insight on the problem, we report it in App. A.1.

Given the semi-positive definiteness of $\Omega_{jj'}$ we can compute its eigenvalues κ_i and the matrix $w_{j,i}$ that diagonalizes it, finally identifying the Lindblad operators for the generator of the master equation (3.58) with:

$$\hat{L}^{(i)} = \sqrt{k_i}\sum_{\ell,k,m} w_{(\ell,k,m),i}\hat{A}^{(\ell,k)}_{S_m}. \tag{3.74}$$

In this section we have derived the master equation for a network of cascade systems, highlighting its main feature and showing its main mathematical properties. We are now ready to move to the next section, where we will see two simple but yet illuminating examples of cascade network with non trivial topology, i.e. where the nodes are not simply ordered in a linear chain, but instead more than one transmission line is present

together with interference effects. In particular we will first see a cascade network made out of two nodes and two transmission lines that behaves like a Mach-Zehnder interferometer, then we will focus on a three nodes network where the relative strengths of the interactions among the nodes can be tuned thanks to interference effects.

3.3. Simple non-trivial cascade networks

In this section we are going to show two simple applications of the formalism presented in the previous section. These two examples allow us to show how, thanks to the presence of only passive elements, interference effects can arise in cascade systems, what is their effect and how it is manifested in the master equation.

3.3.1. A cascade Mach-Zehner interferometer

The first example we are going to analyze is the network shown in Fig. 3.5. In this network we have $M = 2$ nodes S_1 and S_2 that interact via $K = 2$ unidirectional channels $\mathcal{E}^{(1)}$ and $\mathcal{E}^{(2)}$ that are interweaved to form a Mach-Zehnder interferometer. The two nodes can be thought either as monochromatic quantum electrodynamical cavities (QED) of frequency ω or as two levels systems (TLS) of energy gap $\hbar\omega$.

In this model the first node S_1 interacts with $\mathcal{E}^{(1)}$, which is assumed to be in a thermal state at temperature T_1, through a standard excitation hopping interaction Hamiltonian. The output from S_1 is then mixed via a first beam splitter BS_1 with the channel $\mathcal{E}^{(2)}$ which we also assume to be in a thermal state at temperature T_2. The two signals then propagate in the interferometer along paths of different length, accumulating a phase shift PS. Then the two states are mixed once again in the second beam splitter BS_2 before the output from one of the two ports is fed into S_2.

In order to apply the formalism of Sec. 3.2 we model the two environmental channels as a collection of quantum ancillas $\{E_n^{(1)}; n = 1, 2, \cdots\}$ ($E_n^{(2)}; n = 1, 2, \cdots$ respectively) described by bosonic annihilation operators $\{\hat{b}_{E_n^{(1)}}; n = 1, 2, \cdots\}$ ($\{\hat{b}_{E_n^{(2)}}; n = 1, 2, \cdots\}$). Each ancilla is initialized in the Gibbs state of temperature T_1 (T_2):

$$\hat{\eta}_{E_n^{(1)}} = \frac{\exp\left[-\beta_1 \hat{b}^\dagger_{E_n^{(1)}} \hat{b}_{E_n^{(1)}}\right]}{\mathrm{Tr}\left\{\exp\left[-\beta_1 \hat{b}^\dagger_{E_n^{(1)}} \hat{b}_{E_n^{(1)}}\right]\right\}}, \tag{3.75}$$

where $\beta_1 = \hbar\omega/k_B T_1$ ($\beta_2 = \hbar\omega/k_B T_2$ for $\hat{\eta}_{E_n^{(2)}}$). Accordingly, the input states $\hat{\eta}_{\mathcal{E}_n}$ at each

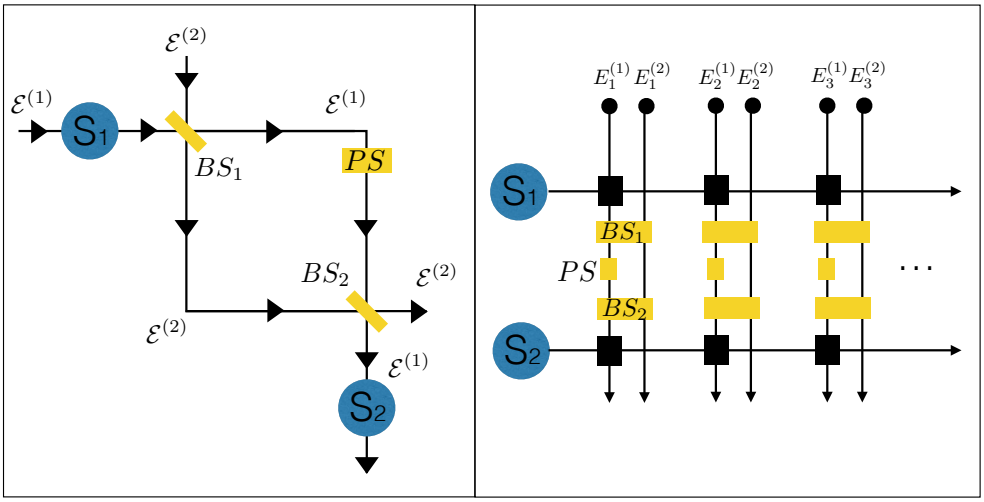

Figure 3.5.: Left panel: a sketch of the system under examination. The signal propagates along two different environmental channels that interact through passive optical elements, in particular two beam splitters and a phase shifter. The node S_1 interact with the channel $\mathcal{E}^{(1)}$, then the output from S_1 interferes first with the signal propagating along $\mathcal{E}^{(2)}$ through the first beam splitter (BS_1 in figure), then the signal along $\mathcal{E}^{(1)}$ is phase shifted (PS) before interfering once again with $\mathcal{E}^{(2)}$ via another beam splitter (BS_2). Then the signal along $\mathcal{E}_1$ interacts with the node S_2. Right panel: circuit-like representation of the dynamics under the collisional model approach.

step n are expressed as:

$$\hat{\eta}_{\mathcal{E}_n} = \hat{\eta}_{E_n^{(1)}} \otimes \hat{\eta}_{E_n^{(2)}}. \tag{3.76}$$

We want to describe the dynamics following the scheme shown in the right panel of Fig. 3.5. According to this we set to zero the interaction Hamiltonian between the nodes and $\mathcal{E}^{(2)}$, $\hat{H}_{S_m,E_n^{(2)}} = 0$. On the other hand, as already anticipated, we assume an excitation hopping coupling between the nodes and $\mathcal{E}^{(1)}$, which takes the form:

$$\hat{H}_{S_m,E_n^{(1)}} = \hat{a}_m^\dagger \hat{b}_{E_n^{(1)}} + \hat{a}_m \hat{b}^\dagger_{E_n^{(1)}}, \tag{3.77}$$

where the operators $\hat{a}_m$, $\hat{a}_m^\dagger$ are bosonic annihilation and creation operators for the cavity S_m, or the corresponding raising and lowering Pauli operators in case we are dealing with TLS. The last thing to do is to define the action of the CPT map $\mathcal{M}_{\mathcal{E}_n}^{(1)}$ acting on the ancillas between their collisions with S_1 and S_2. This map describes the action of the beam splitters and the phase shift: more specifically it is given by

the concatenation of three unitary terms $\hat{V}_{BS_2}\hat{V}_{PS}\hat{V}_{BS_1}$, where the first and the third operator describe the action of the two beam splitters, while the second describes the phase shift. The map $\mathcal{M}^{(1)}_{\mathcal{E}_n}$ acts on states as:

$$\mathcal{M}^{(1)}_{\mathcal{E}_n}(\cdots) = \hat{V}_{BS_2}\hat{V}_{PS}\hat{V}_{BS_1}(\cdots)\hat{V}^\dagger_{BS_1}\hat{V}^\dagger_{PS}\hat{V}^\dagger_{BS_2}. \tag{3.78}$$

Thanks to the cyclicity properties of the trace operation, we can move the effects of $\mathcal{M}^{(1)}_{\mathcal{E}_n}$ on the environmental operators, i.e.:

$$\tilde{\mathcal{M}}^{(1)}_{\mathcal{E}_n}(\hat{B}) = \hat{V}^\dagger_{BS_1}\hat{V}^\dagger_{PS}\hat{V}^\dagger_{BS_2}(\hat{B})\hat{V}_{BS_2}\hat{V}_{PS}\hat{V}_{BS_1}, \tag{3.79}$$

where we have indicated with $\tilde{\mathcal{M}}^{(1)}_{\mathcal{E}_n}$ the complementary to $\mathcal{M}^{(1)}_{\mathcal{E}_n}$, which acts on operators instead of density matrices.

The action of a beam splitter, indicating with ϵ_j the transmissivity of BS_j, can be described using the identities:

$$\hat{V}^\dagger_{BS_j}\hat{b}_{E^{(1)}_n}\hat{V}_{BS_j} = \sqrt{\epsilon_j}\hat{b}_{E^{(1)}_n} - i\sqrt{1-\epsilon_j}\hat{b}_{E^{(2)}_n}, \tag{3.80}$$

$$\hat{V}^\dagger_{BS_j}\hat{b}_{E^{(2)}_n}\hat{V}_{BS_j} = -i\sqrt{1-\epsilon_j}\hat{b}_{E^{(1)}_n} + \sqrt{\epsilon_j}\hat{b}_{E^{(2)}_n}. \tag{3.81}$$

Similarly, the action of the phase shift is described via:

$$\hat{V}^\dagger_{PS}\hat{b}_{E^{(1)}_n}\hat{V}_{PS} = e^{-i\varphi}\hat{b}_{E^{(1)}_n}, \tag{3.82}$$

$$\hat{V}^\dagger_{PS}\hat{b}_{E^{(2)}_n}\hat{V}_{PS} = \hat{b}_{E^{(2)}_n}. \tag{3.83}$$

Before proceeding and compute the master equation for the nodes, it is worth noticing that in the limit $\epsilon_1 = \epsilon_2 = 1$, corresponding to beam splitters with unit transmissivity, the model reduces to the one shown in Sec. 3.1.

We then observe that with the input choice in Eq. (3.75) the stability condition is automatically fulfilled, as both the annihilation and creation operators have zero expectation value on a Gibbs state. In facts, has the interaction Hamiltonian with $\mathcal{E}^{(2)}$ is zero, we have automatically that $\gamma^{(\ell)}_{m(2)} = 0$. Moreover, from the expression of the interaction

Hamiltonian in Eq. (3.77), we can make the following identifications:

$$\hat{A}^{(\ell,k)}_{S_m} = \delta_{k,1} \begin{cases} \hat{a}^\dagger_m & \text{for } \ell = 1, \\ \hat{a}_m & \text{for } \ell = 2, \end{cases} \tag{3.84}$$

$$\hat{B}^{(\ell,m)}_{E^{(k)}_n} = \delta_{k,1} \begin{cases} \hat{b}_{E^{(k)}_n} & \text{for } \ell = 1, \\ \hat{b}_{E^{(k)}_n} & \text{for } \ell = 2, \end{cases} \tag{3.85}$$

from which we have that:

$$\gamma^{(1)}_{1(1)} = \left[\gamma^{(2)}_{1(1)}\right]^* = \mathrm{Tr}_{\mathcal{E}_n}\left\{\hat{b}_{E^{(1)}_n}\hat{\eta}_{\mathcal{E}_n}\right\} = \mathrm{Tr}_{\mathcal{E}_n}\left\{\hat{b}_{E^{(1)}_n}\hat{\eta}_{E^{(1)}_n}\right\} = 0. \tag{3.86}$$

We can also compute $\gamma^{(\ell)}_{2(1)}$ as:

$$\begin{aligned} \gamma^{(1)}_{2(1)} &= \left[\gamma^{(2)}_{2(1)}\right]^* = \mathrm{Tr}_{\mathcal{E}_n}\left\{\hat{b}_{E^{(1)}_n}\mathcal{M}^{(1)}_{\mathcal{E}_n}\left(\hat{\eta}_{\mathcal{E}_n}\right)\right\} = \mathrm{Tr}_{\mathcal{E}_n}\left\{\tilde{\mathcal{M}}^{(1)}_{\mathcal{E}_n}\left(\hat{b}_{E^{(1)}_n}\right)\hat{\eta}_{\mathcal{E}_n}\right\} \\ &= c(\varphi)\,\mathrm{Tr}_{\mathcal{E}_n}\left\{\hat{b}_{E^{(1)}_n}\hat{\eta}_{E^{(1)}_n}\right\} + s(\varphi)\,\mathrm{Tr}_{\mathcal{E}_n}\left\{\hat{b}_{E^{(2)}_n}\hat{\eta}_{E^{(2)}_n}\right\} = 0, \end{aligned} \tag{3.87}$$

where we have defined:

$$c(\varphi) = e^{-i\varphi}\sqrt{\epsilon_1\epsilon_2} - \sqrt{(1-\epsilon_1)(1-\epsilon_2)}, \tag{3.88}$$

$$s(\varphi) = -ie^{-i\varphi}\sqrt{(1-\epsilon_1)\epsilon_2} - i\sqrt{\epsilon_1(1-\epsilon_2)}. \tag{3.89}$$

In an analogous way we can compute the remaining coefficients $\gamma^{(\ell,\ell')}_{m(kk')}$, $\zeta^{(\ell,\ell')}_{mm'(kk')}$, $\xi^{(\ell,\ell')}_{mm'(kk')}$. In order to achieve this goal we first note that, as $\hat{H}_{S_m,E^{(2)}_n} = 0$, then only those terms for which $k = k' = 1$ will be non null.

Then, indicating the mean photon numbers in the environments with:

$$N_k = \mathrm{Tr}\left\{b^\dagger_{E^{(k)}_n}\hat{b}_{E^{(k)}_n}\hat{\eta}_{E^{(k)}_n}\right\} = \left(e^{\beta_k} - 1\right)^{-1}, \tag{3.90}$$

we can compute the local coefficients for S_1 as:

$$\gamma^{(kk')}_{1(11)} = \left[\gamma^{(2,2)}_{1(kk')}\right]^* = \delta_{k,1}\delta_{k',1}\,\mathrm{Tr}_{\mathcal{E}_n}\left\{b^2_{E^{(1)}_n}\hat{\eta}_{E^{(}_n1)}\right\} = 0 \tag{3.91}$$

$$\gamma^{(2,1)}_{1(kk')} = \delta_{k,1}\delta_{k',1}\,\mathrm{Tr}_{\mathcal{E}_n}\left\{b^\dagger_{E^{(1)}_n}\hat{b}_{E^{(1)}_n}\hat{\eta}_{E^{(}_n1)}\right\} = \delta_{k,1}\delta_{k',1}N_1 \tag{3.92}$$

$$\gamma^{(1,2)}_{1(kk')} = \delta_{k,1}\delta_{k',1}\,\mathrm{Tr}_{\mathcal{E}_n}\left\{b_{E^{(1)}_n}\hat{b}^\dagger_{E^{(1)}_n}\hat{\eta}_{E^{(}_n1)}\right\} = \delta_{k,1}\delta_{k',1}(N_1+1). \tag{3.93}$$

From this expression we can write the local dissipative term for S_1 as:

$$\begin{aligned}\mathcal{L}_1(\cdots) &= (N_1+1)\left\{\hat{a}_1(\cdots)\hat{a}_1^\dagger - \frac{1}{2}\left\{\hat{a}_1^\dagger\hat{a}_1,(\cdots)\right\}\right\} \\ &+ N_1\left\{\hat{a}_1^\dagger(\cdots)\hat{a}_1 - \frac{1}{2}\left\{\hat{a}_1\hat{a}_1^\dagger,(\cdots)\right\}\right\}. \end{aligned} \tag{3.94}$$

The form of this local term is quite standard, it is already in GKSL form, and it describes a thermalization process with a thermal bath at temperature T_1.

The local coefficients for S_2 can be computed in a similar way as:

$$\gamma^{(1,1)}_{2(kk')} = \left[\gamma^{(2,2)}_{2(kk')}\right]^* = \delta_{k,1}\delta_{k',1}\,\mathrm{Tr}_{\mathcal{E}_n}\left\{b^2_{E_n^{(}1)}\mathcal{M}^{(1)}_{\mathcal{E}_n}(\hat{\eta}_{\mathcal{E}_n})\right\} \tag{3.95}$$

$$= \delta_{k,1}\delta k', 1\,\mathrm{Tr}_{\mathcal{E}_n}\left\{\left(c(\varphi)\hat{b}_{E_n^{(1)}} + s(\varphi)\hat{b}_{E_n^{(2)}}\right)^2\hat{\eta}_{\mathcal{E}_n}\right\} = 0$$

$$\gamma^{(2,1)}_{2(kk')} = \mathrm{Tr}_{\mathcal{E}_n}\left\{\hat{b}^\dagger_{E_n^{(1)}}\hat{b}_{E_n^{(1)}}\mathcal{M}^{(1)}_{\mathcal{E}_n}(\hat{\eta}_{\mathcal{E}_n})\right\} \tag{3.96}$$

$$= \mathrm{Tr}_{\mathcal{E}_n}\left\{\left(c^*(\varphi)\hat{b}^\dagger_{E_n^{(1)}} + s^*(\varphi)\hat{b}^\dagger_{E_n^{(2)}}\right)\left(c(\varphi)\hat{b}_{E_n^{(1)}} + s(\varphi)\hat{b}_{E_n^{(2)}}\right)\hat{\eta}_{\mathcal{E}_n}\right\} = \delta_{k,1}\delta_{k',1}N_{12}(\varphi)$$

$$\gamma^{(1,2)}_{2(kk')} = \mathrm{Tr}_{\mathcal{E}_n}\left\{\hat{b}_{E_n^{(1)}}\hat{b}^\dagger_{E_n^{(1)}}\mathcal{M}^{(1)}_{\mathcal{E}_n}(\hat{\eta}_{\mathcal{E}_n})\right\} = \tag{3.97}$$

$$\mathrm{Tr}_{\mathcal{E}_n}\left\{\left(c(\varphi)\hat{b}_{E_n^{(1)}} + s(\varphi)\hat{b}_{E_n^{(2)}}\right)\left(c^*(\varphi)\hat{b}^\dagger_{E_n^{(1)}} + s^*(\varphi)\hat{b}^\dagger_{E_n^{(2)}}\right)\hat{\eta}_{\mathcal{E}_n}\right\} = \delta_{k,1}\delta_{k',1}\left(N_{12}(\varphi)+1\right),$$

where it has been defined:

$$N_{12}(\varphi) = |c(\varphi)|^2N_1 + |s(\varphi)|^2N_2 = N_2 + (N_1 - N_2)|c(\varphi)|^2 \tag{3.98}$$

and in the second equality we exploited $|c(\varphi)|^2 + |s(\varphi)|^2 = 1$. At this point we can write the local dissipator for S_2 as:

$$\begin{aligned}\mathcal{L}_2(\cdots) &= (N_{12}(\varphi)+1)\left\{\hat{a}_2(\cdots)\hat{a}_2^\dagger - \frac{1}{2}\left\{\hat{a}_2^\dagger\hat{a}_2,(\cdots)\right\}\right\} \\ &+ N_{12}(\varphi)\left\{\hat{a}_2^\dagger(\cdots)\hat{a}_2 - \frac{1}{2}\left\{\hat{a}_2\hat{a}_2^\dagger,(\cdots)\right\}\right\} \end{aligned} \tag{3.99}$$

This term, similarly to $\mathcal{L}_1$, is already in GKSL form, and describes a thermalization process with a thermal bath at an intermidiate temperature between T_1 and T_2, depending on the transmissivity of the two beam splitters and on the phase shift through $N_{12}(\varphi)$.

We are thus left with evaluating the non-local term $\mathcal{D}_{12}$. Computing the coefficients

leads to:

$$\begin{aligned}\zeta^{(1,1)}_{12(kk')} &= \left[\xi^{(2,2)}_{12(kk')}\right]^* = \delta_{k,1}\delta_{k',1}\,\mathrm{Tr}_{\mathcal{E}_n}\left\{\hat{b}_{E_n^{(1)}}\mathcal{M}^{(1)}_{\mathcal{E}_n}(\hat{b}_{E_n^{(1)}}\hat{\eta}_{\mathcal{E}_n})\right\} \qquad (3.100)\\ &= \delta_{k,1}\delta_{k',1}\,\mathrm{Tr}_{\mathcal{E}_n}\left\{\left(c(\varphi)\hat{b}_{E_n^{(1)}} + s(\varphi)\hat{b}_{E_n^{(2)}}\right)\hat{b}_{E_n^{(1)}}\hat{\eta}_{\mathcal{E}_n}\right\} = 0,\\ \zeta^{(2,2)}_{12(kk')} &= \left[\xi^{(1,1)}_{12(kk')}\right]^* = \delta_{k,1}\delta_{k',1}\,\mathrm{Tr}_{\mathcal{E}_n}\left\{\hat{b}^\dagger_{E_n^{(1)}}\mathcal{M}^{(1)}_{\mathcal{E}_n}(\hat{b}^\dagger_{E_n^{(1)}}\hat{\eta}_{\mathcal{E}_n})\right\} \qquad (3.101)\\ &= \delta_{k,1}\delta_{k',1}\,\mathrm{Tr}_{\mathcal{E}_n}\left\{\left(c^*(\varphi)\hat{b}^\dagger_{E_n^{(1)}} + s^*(\varphi)\hat{b}^\dagger_{E_n^{(2)}}\right)\hat{b}^\dagger_{E_n^{(1)}}\hat{\eta}_{\mathcal{E}_n}\right\} = 0,\end{aligned}$$

for the terms with $\ell = \ell'$, while for $\ell \neq \ell'$ we get:

$$\begin{aligned}\zeta^{(1,2)}_{12(kk')} &= \left[\xi^{(2,1)}_{12(kk')}\right]^* = \delta_{k,1}\delta_{k',1}\,\mathrm{Tr}_{\mathcal{E}_n}\left\{\hat{b}^\dagger_{E_n^{(1)}}\mathcal{M}^{(1)}_{\mathcal{E}_n}(\hat{b}_{E_n^{(1)}}\hat{\eta}_{\mathcal{E}_n})\right\} \qquad (3.102)\\ &= \delta_{k,1}\delta_{k',1}\,\mathrm{Tr}_{\mathcal{E}_n}\left\{\left(c^*(\varphi)\hat{b}^\dagger_{E_n^{(1)}} + s^*(\varphi)\hat{b}^\dagger_{E_n^{(2)}}\right)\hat{b}_{E_n^{(1)}}\hat{\eta}_{\mathcal{E}_n}\right\} = \delta_{k,1}\delta_{k',1}c^*(\varphi)N_1,\\ \zeta^{(2,1)}_{12(kk')} &= \left[\xi^{(1,2)}_{12(kk')}\right]^* = \delta_{k,1}\delta_{k',1}\,\mathrm{Tr}_{\mathcal{E}_n}\left\{\hat{b}_{E_n^{(1)}}\mathcal{M}^{(1)}_{\mathcal{E}_n}(\hat{b}^\dagger_{E_n^{(1)}}\hat{\eta}_{\mathcal{E}_n})\right\} \qquad (3.103)\\ &= \delta_{k,1}\delta_{k',1}\,\mathrm{Tr}_{\mathcal{E}_n}\left\{\left(c(\varphi)\hat{b}_{E_n^{(1)}} + s(\varphi)\hat{b}_{E_n^{(2)}}\right)\hat{b}^\dagger_{E_n^{(1)}}\hat{\eta}_{\mathcal{E}_n}\right\} = \delta_{k,1}\delta_{k',1}c(\varphi)(N_1+1).\end{aligned}$$

Once we computed these expressions, we can write the non-local term as:

$$\begin{aligned}\mathcal{D}_{12}(\cdots) &= N_1\left\{c^*(\varphi)\hat{a}_1^\dagger[(\cdots),\hat{a}_2] - c(\varphi)\left[(\cdots),\hat{a}_2^\dagger\right]\hat{a}_1\right\} \qquad (3.104)\\ &+ (N_1+1)\left\{c(\varphi)\hat{a}_1\left[(\cdots),\hat{a}_2^\dagger\right] - c^*(\varphi)[(\cdots),\hat{a}_2]\hat{a}_1^\dagger\right\}.\end{aligned}$$

Now, it must be noted that, at glance with the local term for S_1 in Eq. (3.94), both the local term $\mathcal{L}_2$ and the non-local term $\mathcal{D}_{12}$ depend on the phase φ, i.e. the dissipative dynamics of the second node is tunable. More specifically, setting $\epsilon_1 = \epsilon_2 = 1/2$, $c(\varphi)$ acquires an oscillating behavior, since:

$$c(\varphi) = -ie^{-i\frac{\varphi}{2}}\sin(\varphi/2) \quad \text{for } \epsilon_1 = \epsilon_2 = \tfrac{1}{2}. \qquad (3.105)$$

It must be stressed however that the local term $\mathcal{L}_2$ never nullifies, in accordance with the fact that a system is always interacting with the vacuum. On the contrary, the non-local term can nullify, since if the outputs from S_1 interfere destructively before being fed to S_2, then no interaction between the two systems is allowed.

Following the model, we can finally write the superoperator $\mathcal{L}_1+\mathcal{L}_2+\mathcal{D}_{12}$ in the GKSL form. Following the receipt of Sec. 3.2, we can compute the Hamiltonian contribution

to the dynamics in Eq. (3.68) as:

$$\begin{aligned}\hat{H}_{12} &= -\frac{i}{2}\left(c(\varphi)\hat{a}_1\hat{a}_2^\dagger - c^*(\varphi)\hat{a}_1^\dagger\hat{a}_2\right)\\ &= -\frac{i}{2}|c(\varphi)|\left(e^{i\arg[c(\varphi)]}\hat{a}_1\hat{a}_2^\dagger - e^{-i\arg[c(\varphi)]}\hat{a}_1^\dagger\hat{a}_2\right),\end{aligned} \tag{3.106}$$

while the $\Delta\mathcal{L}_{12}$ contribution of Eq. (3.69) can be written as:

$$\begin{aligned}\Delta\mathcal{L}_{12}(\cdots) &= N_1 c^*(\varphi)\left\{\hat{a}_1^\dagger(\cdots)\hat{a}_2 - \frac{1}{2}\left\{\hat{a}_1^\dagger\hat{a}_2,(\cdots)\right\}\right\}\\ &+ (N_1+1)c(\varphi)\left\{a_1(\cdots)\hat{a}_2^\dagger - \frac{1}{2}\left\{\hat{a}_1\hat{a}_2^\dagger,(\cdots)\right\}\right\}.\end{aligned} \tag{3.107}$$

In order to find the GKSL expression of the master equation, we note that in this case the matrix $\Delta D^{(\ell,\ell')}_{mm'(kk')}$ reduces to $\Delta D^{(\ell,\ell')}_{mm'(1,1)}$, so that we can write:

$$\Delta D^{(\ell,\ell')}_{mm'(1,1)} = \left[\begin{array}{cc|cc} 0 & 0 & N_1c^*(\varphi) & 0\\ 0 & 0 & 0 & (N_1+1)c(\varphi)\\ \hline N_1c(\varphi) & 0 & 0 & 0\\ 0 & (N_1+1)c^*(\varphi) & 0 & 0\end{array}\right] \tag{3.108}$$

where the top left and bottom right 2×2 blocks refer to $m = m' = 1,2$ respectively. As already said in the previous section, this matrix is Hermitean but not in principle positive semi-definite. On the other hand, adding the coefficients $\gamma^{(\ell,\ell')}_{m(1,1)}$ along the diagonal, we can write the matrix $D^{(\ell,\ell')}_{mm'(1,1)}$, which is positive semi-definite:

$$D^{(\ell,\ell')}_{mm'(1,1)} = \left[\begin{array}{cc|cc} N_1 & 0 & N_1c^*(\varphi) & 0\\ 0 & N_1+1 & 0 & (N_1+1)c(\varphi)\\ \hline N_1c(\varphi) & 0 & N_{12}(\varphi) & 0\\ 0 & (N_1+1)c^*(\varphi) & 0 & N_{12}(\varphi)+1\end{array}\right]. \tag{3.109}$$

The eigenvalues of $D^{(\ell,\ell')}_{mm'(1,1)}$ can be easily found:

$$\begin{aligned}\kappa_{1,\pm} &= \frac{1}{2}\left(N_1 + N_{12}(\varphi) + 2 \pm \sqrt{(N_1 - N_1 2(\varphi))^2 + 4(N_1+1)^2|c(\varphi)|^2}\right)\\ \kappa_{2,\pm} &= \frac{1}{2}\left(N_1 + N_{12}(\varphi) \pm \sqrt{(N_1 - N_1 2(\varphi))^2 + 4N_1^2|c(\varphi)|^2}\right),\end{aligned} \tag{3.110}$$

and can be easily seen to be non-negative for any choice of N_1, N_2, φ. Then, exploiting Eq. (3.74), we can write the Lindblad operators for the system under examination as:

$$\hat{L}^{(1,+)} = \sqrt{\kappa_{1,+}}\frac{w_{1,+}\hat{a}_1 + \hat{a}_2}{\sqrt{1+|w_{1,+}|^2}}, \quad \hat{L}^{(1,-)} = \sqrt{\kappa_{1,-}}\frac{w_{1,-}\hat{a}_1^\dagger + \hat{a}_2^\dagger}{\sqrt{1+|w_{1,-}|^2}},$$
$$\hat{L}^{(2,+)} = \sqrt{\kappa_{2,+}}\frac{w_{2,+}\hat{a}_1 + \hat{a}_2}{\sqrt{1+|w_{2,+}|^2}}, \quad \hat{L}^{(2,-)} = \sqrt{\kappa_{2,-}}\frac{w_{2,-}\hat{a}_1^\dagger + \hat{a}_2^\dagger}{\sqrt{1+|w_{2,-}|^2}},$$

where:

$$w_{1,\pm} = \frac{N_1 - N_{12}(\varphi) \pm \sqrt{(N_1 - N_{12}(\varphi))^2 + 4(N_1+1)^2|c(\varphi)|^2}}{2(N_1+1)c^*(\varphi)}, \tag{3.111}$$

$$w_{2,\pm} = \frac{N_1 - N_{12}(\varphi) \pm \sqrt{(N_1 - N_{12}(\varphi))^2 + 4N_1^2|c(\varphi)|^2}}{2N_1 c(\varphi)}. \tag{3.112}$$

We stress once again that setting $\epsilon_1 = \epsilon_2 = 1$ leads to the same model studied in Sec. 3.1. More specifically, setting also $T_1 = 0$, one would find that only $\kappa_{1,+} = 2$ would be different from zero, leading to a unique collective operator $L^{(\hat{1},+)} = \hat{a}_1 + \hat{a}_2$, which is a signature of super radiance effects.

With this very simple system we were able to expose practically the features of the model shown in Sec. 3.2, seeing how the presence of interactions among ancillas from different environments can lead to interference effects, and how they manifest themselves in the master equation and the expressions of the Lindblad operators.

3.3.2. Interference controlled topology

In this section we will move further with respect to the previous example, examining the system with three nodes illustrated in Fig. 3.6. This system is somehow similar to the Mach-Zehnder interferometer analyzed before, but the presence of the third node implies the appearance of three new terms in the master equation, namely $\mathcal{L}_3$, $\mathcal{D}_{13}$ and $\mathcal{D}_{23}$.

Since we will need to make comparison with the previous section, in this case we dub the nodes Q_1, Q_2 and Q_3: as it can be seen from the figure, the nodes Q_1 and Q_3 occupies the positions of S_1 and S_2 of the previous section respectively. The node Q_2 lays instead inside the interferometer, and thus in this network there will be two first-neighbor terms, the $\mathcal{D}_{12}$ and $\mathcal{D}_{23}$ terms, plus a non-local term describing the second-neighbor interaction $\mathcal{D}_{13}$ between Q_1 and Q_3.

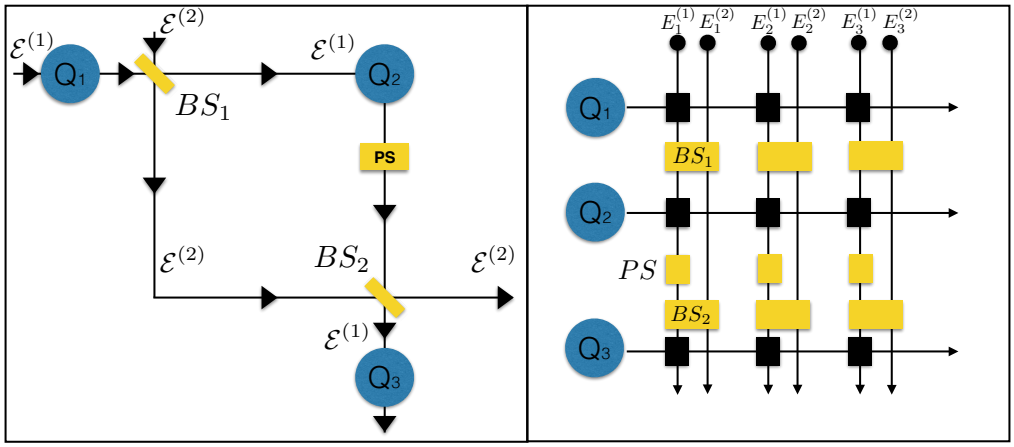

Figure 3.6.: Left panel: a sketch of the system under examination: once again there are two environmental channels $\mathcal{E}^{(1)}$,$\mathcal{E}^{(2)}$, two beam splitters and a phase shifter. The only difference with the Mach-Zehnder interferometer analyzed in the previous section is the presence of a third node in the circuit. Right panel: circuit-like representation of the dynamics in the collisional model approach.

Just as in the previous example we assume the nodes to be interacting only with channel $\mathcal{E}^{(1)}$, so that we write the interaction Hamiltonian between the nodes and the environments as:

$$\hat{H}_{Q_i,E_n^{(1)}} = \hat{a}_i^\dagger \hat{b}_{E_n^{(1)}} + \hat{a}_i \hat{b}^\dagger_{E_n^{(1)}} , \quad \hat{H}_{Q_i,E_n^{(2)}} = 0. \tag{3.113}$$

We also assume once again the environmental states $\hat{\eta}_{E_n^{(1)}}$ and $\hat{\eta}_{E_n^{(2)}}$ to be Gibbs states at temperature T_1 and T_2 respectively. As the computation of the various terms of the master equation is all in all similar to the one performed in Sec. 3.3.1, we report the explicit calculations for the various coefficients in App. A.2.

We start our analysis of this network from the local terms $\mathcal{L}_i$, which can be written

explicitly as:

$$\begin{aligned}
\mathcal{L}_1(\cdots) &= (N_1+1)\left\{\hat{a}_1(\cdots)\hat{a}_1^\dagger - \frac{1}{2}\left\{\hat{a}_1^\dagger\hat{a}_1,(\cdots)\right\}\right\} \\
&+ N_1\left\{\hat{a}_1^\dagger(\cdots)\hat{a}_1 - \frac{1}{2}\left\{\hat{a}_1\hat{a}_1^\dagger,(\cdots)\right\}\right\}, \qquad (3.114)\\
\mathcal{L}_2(\cdots) &= (\bar{N}_{12}+1)\left\{\hat{a}_2(\cdots)\hat{a}_2^\dagger - \frac{1}{2}\left\{\hat{a}_2^\dagger\hat{a}_2,(\cdots)\right\}\right\} \\
&+ \bar{N}_{12}\left\{\hat{a}_2^\dagger(\cdots)\hat{a}_2 - \frac{1}{2}\left\{\hat{a}_2\hat{a}_2^\dagger,(\cdots)\right\}\right\}, \qquad (3.115)\\
\mathcal{L}_3(\cdots) &= (N_{12}(\varphi)+1)\left\{\hat{a}_3(\cdots)\hat{a}_3^\dagger - \frac{1}{2}\left\{\hat{a}_3^\dagger\hat{a}_3,(\cdots)\right\}\right\} \\
&+ N_{12}(\varphi)\left\{\hat{a}_3^\dagger(\cdots)\hat{a}_3 - \frac{1}{2}\left\{\hat{a}_3\hat{a}_3^\dagger,(\cdots)\right\}\right\}, \qquad (3.116)
\end{aligned}$$

where $N_{12}(\varphi)$ is the same of Eq. (3.98) and we have defined:

$$\bar{N}_{12} = \epsilon_1 N_1 + (1-\epsilon_1)N_2 = N_2 + \epsilon_1(N_1 - N_2), \qquad (3.117)$$

as the mean photon number of the environment perceived by node Q_2.

We note immediately that Eq. (3.114) is identical to Eq. (3.94), and this come as no surprise as S_1 and Q_1 occupy the same position in the network. For the same reason the local term $\mathcal{L}_3$ in Eq. (3.116) is formally identical to Eq. (3.99). On the other hand the local term $\mathcal{L}_2$ does not depend upon φ, but only on the transmissivity of the first beam splitter BS_1, as the node Q_2 is placed before the phase shift.

We can then turn our focus on the non-local terms, starting from the first-neighbors couplings between nodes Q_1 and Q_2 and between Q_2 and Q_3, which can be written as:

$$\begin{aligned}
\mathcal{D}_{12}(\cdots) &= \sqrt{\epsilon_1}N_1\left\{\hat{a}_1^\dagger[(\cdots),\hat{a}_2] + \left[\hat{a}_2^\dagger,(\cdots)\right]\hat{a}_1\right\} \qquad (3.118)\\
&+ \sqrt{\epsilon_1}(N_1+1)\left\{\hat{a}_1\left[(\cdots),\hat{a}_2^\dagger\right] + [\hat{a}_2,(\cdots)]\hat{a}_1^\dagger\right\},\\
\mathcal{D}_{23}(\cdots) &= M_{12}^*(\varphi)\hat{a}_2^\dagger[(\cdots),\hat{a}_3] + M_{12}(\varphi)\left[\hat{a}_3^\dagger,(\cdots)\right]\hat{a}_2 \qquad (3.119)\\
&+ \left(M_{12}(\varphi)+\lambda(\varphi)\right)\hat{a}_2\left[(\cdots),\hat{a_3^\dagger}\right] + \left(M_{12}^*(\varphi)+\lambda^*(\varphi)\right)[\hat{a_3},(\cdots)]\hat{a}_2^\dagger,
\end{aligned}$$

where we have introduced:

$$M_{12}(\varphi) = \sqrt{\epsilon_1}c(\varphi)N_1 + i\sqrt{1-\epsilon_1}s(\varphi)N_2, \tag{3.120}$$

$$\lambda(\varphi) = \sqrt{\epsilon_1}c(\varphi) + i\sqrt{1-\epsilon_1}s(\varphi), \tag{3.121}$$

and $c(\varphi)$, $s(\varphi)$ as in Eq. (3.88) and (3.89) respectively.

Finally we can write the second-neighbor term describing the interaction between Q_1 and Q_3:

$$\begin{aligned}\mathcal{D}_{13}(\cdots) &= N_1\left\{c^*(\varphi)\hat{a}_1^\dagger[(\cdots),\hat{a}_3] + c(\varphi)\left[\hat{a}_3^\dagger,(\cdots)\right]\hat{a}_1\right\} \\ &+ (N_1+1)\left\{c(\varphi)\hat{a}_1\left[(\cdots),\hat{a}_3^\dagger\right] + c^*(\varphi)[\hat{a}_3,(\cdots)]\hat{a}_1^\dagger\right\},\end{aligned} \tag{3.122}$$

which formally coincides with the $\mathcal{D}_{12}$ of Sec. 3.3.1.

From Eqs. (3.118, 3.119, 3.122) it is evident that the coupling terms connecting the various nodes have all a different functional dependence on the phase φ. To better highlight the properties of this network, we find it useful to focus on the zero temperature regime (i.e. $T_1 = T_2 = 0$) and set the transmissivity of both beam splitters to 50% (i.e. $\epsilon_1 = \epsilon_2 = 1/2$). In this case the local contributions describe a purely dissipative process, acquiring the very simple form:

$$\mathcal{L}_m(\cdots) = \hat{a}_m(\cdots)\hat{a}_m^\dagger - \frac{1}{2}\{\hat{a}_m^\dagger\hat{a}_m,(\cdots)\}. \tag{3.123}$$

Conversely, the non-local terms become:

$$\mathcal{D}_{12}(\cdots) = \frac{1}{\sqrt{2}}\left\{\hat{a}_1\left[(\cdots),\hat{a}_2^\dagger\right] + [\hat{a}_2,(\cdots)]\hat{a}_1^\dagger\right\}, \tag{3.124}$$

$$\mathcal{D}_{23}(\cdots) = \frac{1}{\sqrt{2}}\left\{e^{-i\varphi}\hat{a}_2\left[(\cdots),\hat{a}_3^\dagger\right] + e^{i\varphi}[\hat{a}_3,(\cdots)]\hat{a}_2^\dagger\right\}, \tag{3.125}$$

$$\mathcal{D}_{13}(\cdots) = -i\sin\frac{\varphi}{2}\left\{e^{-i\frac{\varphi}{2}}\hat{a}_1\left[(\cdots),\hat{a}_3^\dagger\right] + e^{i\frac{\varphi}{2}}[\hat{a}_3,(\cdots)]\hat{a}_1^\dagger\right\}. \tag{3.126}$$

From the expressions of the non-local terms one can infer that the phase φ gives two kinds of contributions to the dynamics: first it introduces a relative phase between the three nodes that cannot be eliminated by simply absorbing it into a redefinition of the annihilation and creation operators. Second, it allows for a selective modulation of the strength of the interactions between the nodes. This can be seen easier by looking at the expression of the induced Hamiltonian one finds after recasting the master equation

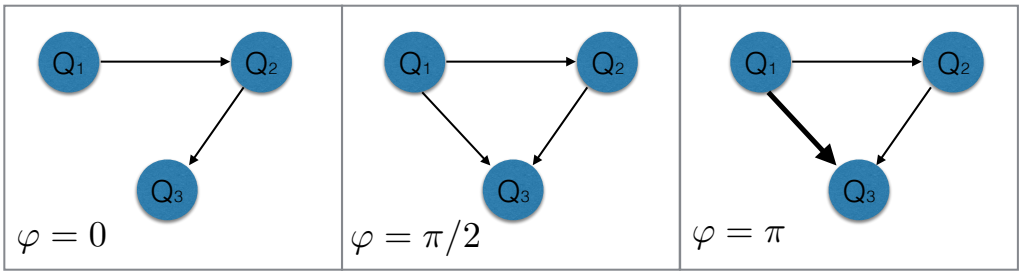

Figure 3.7.: A scheme resuming the phase dependence of the relative strengths of the interactions among the nodes Q_1, Q_2 and Q_3. In the left panel we can see the situation for $\varphi = 0$: as the sine function nullifies, there are only first-neighbor interactions among the nodes. The central panel shows instead the situation for $\varphi = \pi/2$: in this case the second-neighbor interaction is present and it has the same weight of the first-neighbor interactions. Finally, the right panel shows the situation as $\varphi = \pi$: not only the second-neighbor interaction is present, but it is also stronger than the first-neighbor interactions.

into the GKSL form (see App. A.2):

$$\hat{H}_{12} = -\frac{i}{2\sqrt{2}}\left(\hat{a}_1\hat{a}_2^\dagger - \hat{a}_1^\dagger\hat{a}_2\right), \tag{3.127}$$

$$\hat{H}_{23} = -\frac{i}{2\sqrt{2}}\left(e^{i\frac{\varphi}{2}}\hat{a}_2\hat{a}_3^\dagger - e^{-i\frac{\varphi}{2}}\hat{a}_2^\dagger\hat{a}_2\right), \tag{3.128}$$

$$\hat{H}_{13} = -\frac{i}{2}\sin\frac{\varphi}{2}\left(e^{i\frac{\varphi+\pi}{2}}\hat{a}_1\hat{a}_3^\dagger - e^{-i\frac{\varphi+\pi}{2}}\hat{a}_1^\dagger\hat{a}_3\right). \tag{3.129}$$

By looking at this expressions, we realize that tuning φ it is possible to modify the topology of the interactions between the nodes, as resumed schematically in Fig. 3.7: for instance, by setting $\varphi = 0$ we can shut down the interaction between Q_1 and Q_3, while setting $\varphi = \pi$ we move to a situation where the second-neighbor interaction is stronger than the first neighbor interactions. We can move continuously from both extreme into intermediate situations, like $\varphi = \pi/2$ where the first and second neighbor interactions have the same strength.

This example allowed us to show more features of cascade networks and the formalism we developed: as we are going to see in the next section, the network we studied in this section can be scaled up, giving rise to a complex-many-body network where all the interactions are in principle completely tunable.

3.4. A complex cascade network

It is time now to explore the last issue of cascade network we will meet in this work: in Sec. 3.3.2 we saw how it is possible, via interference effects, to tailor the interactions between the nodes of a quantum cascade network. Specifically we saw how, with the aid of beam splitters and phase shifts only, it is possible to obtain very different topologies of the intra nodes interactions, from suppressing second neighbor interactions to situations where second neighbor interactions were stronger than the first neighbor ones.

3.4.1. Path-dependent coupling constants

We want to show now that it is possible to scale up such network to an arbitrary number of sites, obtaining a network like the one shown in Fig. 3.8: we consider a set of M nodes $\{S_1, S_2, \cdots, S_m\}$ connected through a set of M multimode unidirectional environmental channels $\{\mathcal{E}^{(1)}, \mathcal{E}^{(2)}, \cdots, \mathcal{E}^{(M)}\}$, each one being described by the set of annihilation operators $\{\hat{b}_{\mathcal{E}_n^{(m)}}\}$ fulfilling the following commutation relations:

$$\left[\hat{b}_{\mathcal{E}_n^{(m)}}, \hat{b}^\dagger_{\mathcal{E}_{n'}^{(m')}}\right] = \delta_{mm'}\delta_{nn'}, \quad \left[\hat{b}_{\mathcal{E}_n^{(m)}}, \hat{b}_{\mathcal{E}_{n'}^{(m')}}\right] = 0, \tag{3.130}$$

where the index n accounts for the mode degeneracy of each channel. At variance with the previous section, all throughout this section we will assume all the environmental modes to be in the vacuum state.

As shown in Fig. 3.8 the environmental channels $\mathcal{E}^{(m)}$ and $\mathcal{E}^{(m')}$ intercept at the beam splitter $BS_{mm'}$, whose effects are described by the unitary transformation $\hat{U}_{mm'}$ acting on the environmental operators as:

$$\hat{b}_{\mathcal{E}_n^{(m)}} \to \hat{U}^\dagger_{mm'}\hat{b}_{\mathcal{E}_n^{(m)}}\hat{U}_{mm'} = \sqrt{t_{mm'}}\hat{b}_{\mathcal{E}_n^{(m)}} - i\sqrt{1-t_{mm'}}\hat{b}_{\mathcal{E}_n^{(m')}}, \tag{3.131}$$

$$\hat{b}_{\mathcal{E}_n^{(m')}} \to \hat{U}^\dagger_{mm'}\hat{b}_{\mathcal{E}_n^{(m')}}\hat{U}_{mm'} = e^{-i\varphi_{mm'}}\left(\sqrt{t_{mm'}}\hat{b}_{\mathcal{E}_n^{(m')}} - i\sqrt{1-t_{mm'}}\hat{b}_{\mathcal{E}_n^{(m)}}\right), \tag{3.132}$$

where $t_{mm'} \in [0,1]$ is the transmissivity of $BS_{mm'}$ and we have included a phase difference between the two ports of $BS_{mm'}$ described by $\varphi_{mm'} \in [0, 2\pi]$, as resumed in Fig. 3.9 on page 71.

In analogy with the choice of the previous sections, we assume the interaction between

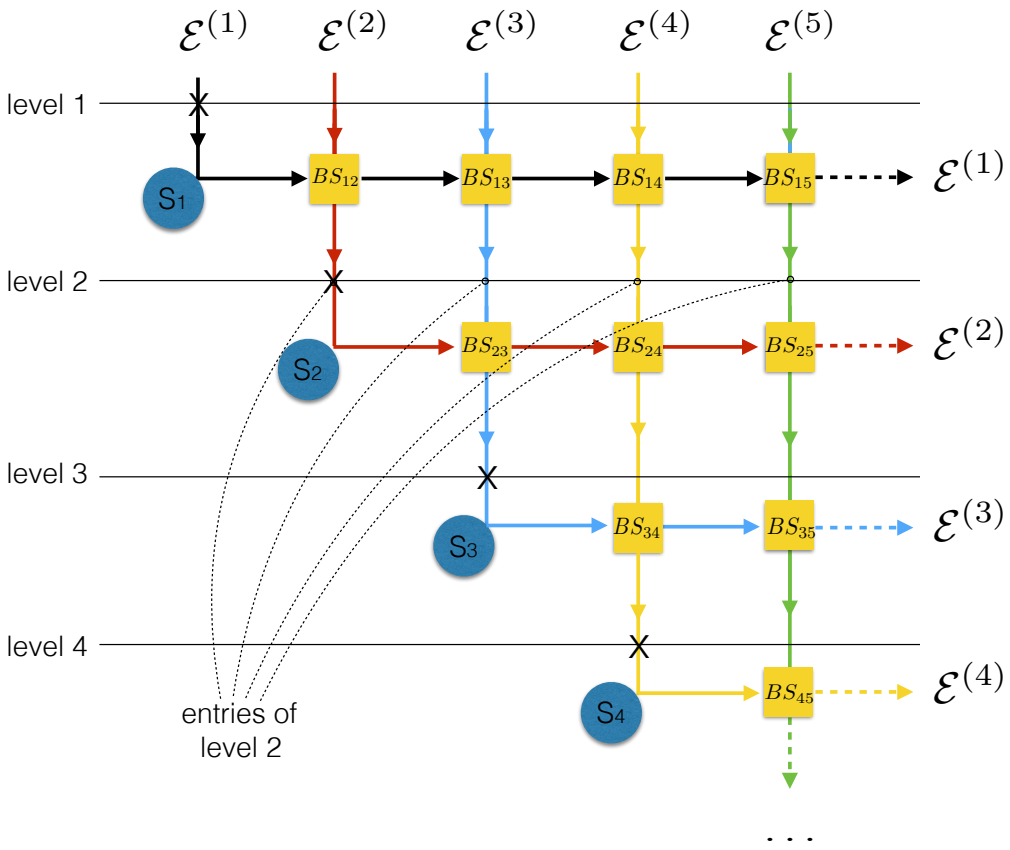

Figure 3.8.: A schematic representation of the network under examination: the interactions between the nodes $\{S_1, S_2, \cdots\}$ (blue dots) are mediated by a network of multimode environmental channels $\{\mathcal{E}^{(1)}, \mathcal{E}^{(2)}, \cdots\}$ (colored arrows) interfering via a series of beam splitters BS_{ij} (yellow squares) while moving unidirectionally along the network, from top to bottom, crossing the various levels of the network (horizontal solid lines).

the nodes and the environments to be described by the exchange Hamiltonian:

$$\hat{H}_{S_m,\mathcal{E}^{(m')}} = \delta_{mm'} \sum_n g_n \left(\hat{a}_m^\dagger \hat{b}_{\mathcal{E}_n^{(m')}} + \hat{a}_m \hat{b}^\dagger_{\mathcal{E}_n^{(m')}} \right), \tag{3.133}$$

where the g_n are the coupling constants between node S_m and the mode described by $\hat{b}_{\mathcal{E}_n^{(m)}}$, and $\hat{a}_m$ is the annihilation operator for the node S_m.

Within the assumptions made, the master equation of the system can be written as:

$$\frac{d\hat{\rho}_S(t)}{dt} = \sum_m \mathcal{L}_m(\hat{\rho}_S(t)) + \sum_{m'>m} \mathcal{D}_{mm'}(\hat{\rho}_S(t)), \tag{3.134}$$

where the $\mathcal{L}_m$ terms as usual describe local dissipation processes:

$$\mathcal{L}_m(\cdots) = \frac{\gamma}{2}\left\{2\hat{a}_m(\cdots)\hat{a}_m^\dagger - \left\{\hat{a}_m^\dagger\hat{a}_m, ,\right\}(\cdots)\right\}, \tag{3.135}$$

while the $\mathcal{D}_{mm'}$ are worth:

$$\mathcal{D}_{mm'}(\cdots) = \gamma\left\{\zeta_{mm'}\hat{a}_m\left[(\cdots), \hat{a}_{m'}^\dagger\right] + \zeta_{mm'}^*[\hat{a}_{m'}, (\cdots)]\hat{a}_m^\dagger\right\}. \tag{3.136}$$

Here it must be noted that the local terms are not tunable, i.e. they do not depend upon the transmissivities and the phases of the beam splitters $BS_{mm'}$. On the contrary the coefficients $\zeta_{mm'}$ do depend on the transmissivities and the phases: this fact entails the possibility of tuning the interactions among the nodes induced by the presence of the environmental channel. As we are going to see in a while, the coefficients $\zeta_{mm'}$ depend strictly on the paths connecting node S_m and node $S_{m'}$.

Even if this will not be the focus of this section, we note that the master equation in Eq. (3.134) could be recast in GKSL form. Following the method exposed in Sec. 3.2, we would find that the matrix $\Omega_{mm'}$ is worth:

$$\Omega_{mm'} = \begin{cases} \gamma & \text{for } m = m', \\ \gamma\,\zeta_{mm'} & \text{for } m' > m, \\ \gamma\,\zeta_{mm'}^* & \text{for } m' > m, \end{cases} \tag{3.137}$$

so that upon diagonalization it would yield the Lindblad operators:

$$\hat{L}_i = \sqrt{\kappa_i}\sum_m w_{m,i}^*\hat{a}_m, \tag{3.138}$$

where κ_i are the eigenvalues of $\Omega_{mm'}$ and the $w_{m,i}$ are the elements of the matrix diagonalizing $\Omega_{mm'}$, i.e. it holds:

$$\kappa_i = \sum_{m,m'} w_{mi}^*\Omega_{mm'}w_{m'i}. \tag{3.139}$$

While we are going to see in the following some cases where an explicit expression for the $\hat{L}_i$ can be written, this is in general not true for arbitrary choices of the network parameters, i.e. arbitrary choices of the transmissivities and phases of the beam splitters $BS_{mm'}$. However, in general the $\hat{L}_i$ will be non-local, giving rise to cooperative emission processes like Dicke superradiance. An explicit computation of the operators

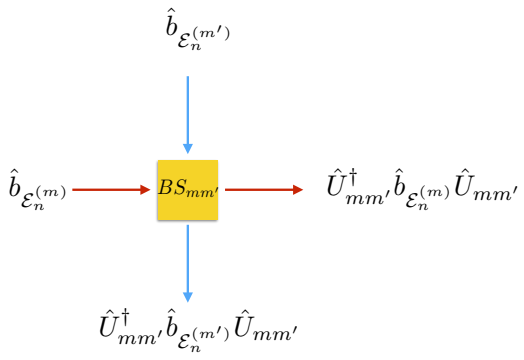

Figure 3.9.: A scheme resuming the input-output relations induced by the beam splitter $BS_{mm'}$ that couples channels $\mathcal{E}^{(m)}$ and $\mathcal{E}^{(m')}$. As one can see the two outputs are combinations of the inputs weighted according to the transmissivity of the beam splitter. Moreover the two outputs gain a relative phase φ.

in Eq. (3.138) is given in App. A.3.

3.4.2. Computing the coefficients $\zeta_{mm'}$

As we anticipated in the previous section, the coefficients $\zeta_{mm'}$ dictating the interaction between the nodes depend on the paths connecting the two nodes, and thus on the parameters of the beam splitters, namely the transmissivities $t_{mm'}$ and their induced relative phases $\varphi_{mm'}$.

In fact, according to our model, these coefficients can be written as:

$$\zeta_{mm'} = \mathrm{Tr}\left\{\hat{b}_{\mathcal{E}_n^{(m')}}\mathcal{M}_{\mathcal{E}}^{(m'-1\leftarrow m)}\left(\hat{b}_{\mathcal{E}_n^{(m)}}\mathcal{M}_{\mathcal{E}}^{(m-1\leftarrow 1)}(\hat{\eta}_{\mathcal{E}})\right)\right\}, \tag{3.140}$$

where $\hat{\eta}_{\mathcal{E}}$ is the joint initial state of the environmental channels (which we assumed to be the vacuum), and $\mathcal{M}_{\mathcal{E}}^{(m'\leftarrow m)}$ is the CPT map describing the evolution of the environmental state, in the absence of the nodes S, from level m to level m' of the network, see Fig. 3.8. This map can be described via the unitary transformations $\hat{U}_{mm'}$ induced by the beam splitters $BS_{mm'}$. In order to do this we use:

$$\hat{V}_m = \cdots \hat{U}_{m+3,m}\hat{U}_{m+2,m}\hat{U}_{m+1,m}, \tag{3.141}$$

to indicate the product of the beam splitter unitary operators coupling channel $\mathcal{E}^{(m)}$

with the following ones, so that we define

$$\hat{V}_{m'\leftarrow m} = \hat{V}_{m'} \cdots \hat{V}_{m+1}\hat{V}_m, \tag{3.142}$$

the ordered product of the $\hat{V}$ operators from level m to level $m' > m$, so that the CPT map $\mathcal{M}_{\mathcal{E}}^{m'\leftarrow m}$ can be expressed as:

$$\mathcal{M}_{\mathcal{E}}^{m'\leftarrow m}(\cdots) = \hat{V}_{m'\leftarrow m}(\cdots)\hat{V}_{m'\leftarrow m}^{\dagger}. \tag{3.143}$$

Since, as it can be verified directly, the composition rule:

$$\hat{V}_{m''\leftarrow m'}\hat{V}_{m'\leftarrow m} = \hat{V}_{m''\leftarrow m}, \tag{3.144}$$

holds for any $m'' > m' > m$, then Eq. (3.140) can be rewritten as:

$$\zeta_{mm'} = \mathrm{Tr}_{\mathcal{E}}\left\{\hat{c}_{\mathcal{E}_n^{(m')}}\hat{c}^{\dagger}_{\mathcal{E}_n^{(m)}}\hat{\eta}_{\mathcal{E}}\right\}, \tag{3.145}$$

where the operator $\hat{c}_{\mathcal{E}_n^{(m)}}$ is the operator $\hat{b}_{\mathcal{E}_n^{(m)}}$ evolved from level 1 to level m of the network in the Heisenberg picture:

$$\hat{c}_{\mathcal{E}_n^{(m)}} = \hat{V}_{m\leftarrow 1}^{\dagger}\hat{b}_{\mathcal{E}_n^{(m)}}\hat{V}_{m\leftarrow 1}, \tag{3.146}$$

where we included the case $m = 1$ by identifying $\hat{V}_{0\leftarrow 1}$ with the identity operator, so that $\hat{c}_{\mathcal{E}_n^{(1)}} = \hat{b}_{\mathcal{E}_n^{(1)}}$. To understand the meaning of Eq. (3.146), consider for instance the case $m = 2$:

$$\hat{c}_{\mathcal{E}_n^{(2)}} = \hat{U}_{12}^{\dagger}\hat{b}_{\mathcal{E}_n^{(2)}}\hat{U}_{12} = e^{-i\varphi_{12}}\left(\sqrt{t_{12}}\hat{b}_{\mathcal{E}_n^{(2)}} - i\sqrt{1-t_{12}}\hat{b}_{\mathcal{E}_n^{(1)}}\right), \tag{3.147}$$

where the fact that for $m > 3$ the operator $\hat{U}_{1m}$ commutes with $\hat{b}_{\mathcal{E}_n^{(2)}}$ has been used. Analogously for $m = 3$ we get:

$$\begin{aligned}\hat{c}_{\mathcal{E}_n^{(3)}} &= \hat{U}_{12}^{\dagger}\hat{U}_{13}^{\dagger}\hat{U}_{23}^{\dagger}\hat{b}_{\mathcal{E}_n^{(3)}}\hat{U}_{23}\hat{U}_{13}\hat{U}_{12} = e^{-i\varphi_{23}}\Big\{e^{-i\varphi_{13}}\sqrt{t_{13}t_{23}}\hat{b}_{\mathcal{E}_n^{(3)}} \\ &+ \left[-ie^{-i\varphi_{12}}\sqrt{t_{12}(1-t_{23})} - e^{-i\varphi_{13}}\sqrt{(1-t_{12})(1-t_{13})t_{23}}\right]\hat{b}_{\mathcal{E}_n^{(2)}} \\ &+ \left[e^{-i\varphi_{12}}\sqrt{(1-t_{12})(1-t_{23})} - ie^{-i\varphi_{13}}\sqrt{t_{12}(1-t_{13})t_{23}}\right]\hat{b}_{\mathcal{E}_n^{(1)}}\Big\}.\end{aligned} \tag{3.148}$$

As one can verify by direct inspection of the above expressions, the operator $\hat{c}_{\mathcal{E}_n^{(m)}}$ can

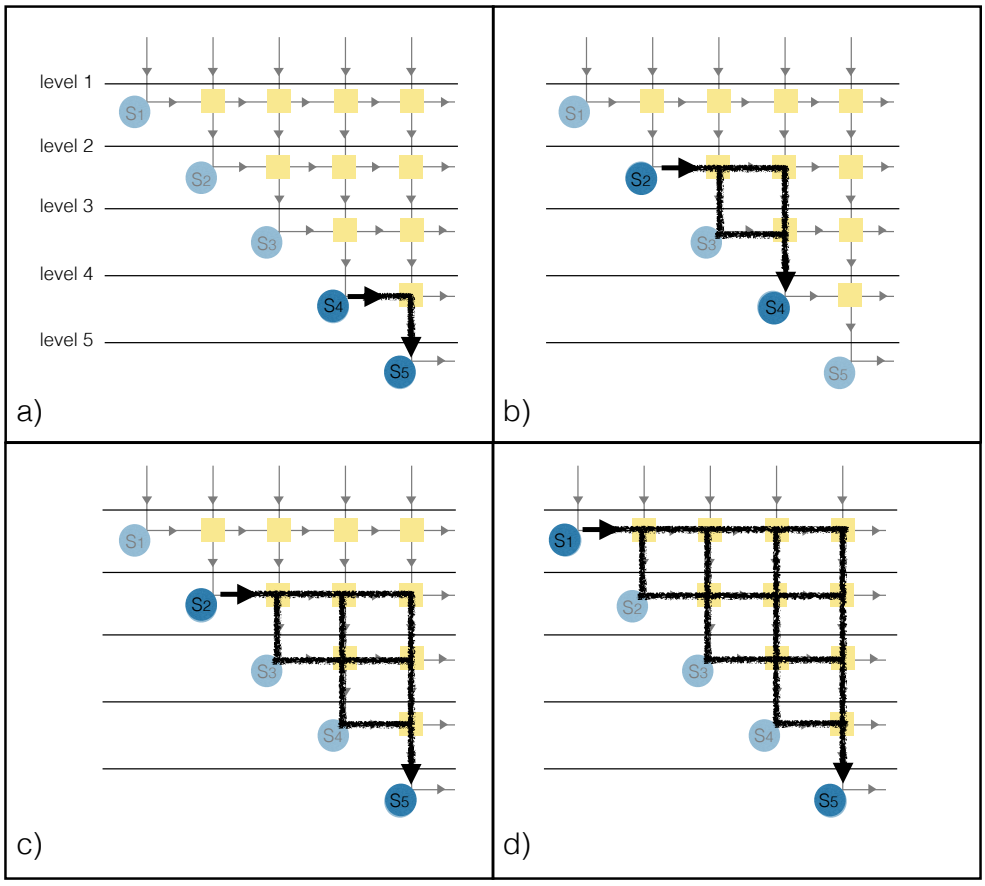

Figure 3.10.: Illustration of the paths (bold curves) contributing to the coupling constants $\zeta_{mm'}$. In panel (a) we see that for a first neighbor coupling there is only one path contributing to the coupling, while already for second-neighbor interactions there are two different paths connecting the nodes, as shown in panel (b). The number of paths contributing to the coupling clearly increases exponentially with the distance between the nodes, as exemplified in the other two panels (c) and (d), which show the paths connecting third-neighboring and fourth-neighboring sites respectively.

be written as:

$$\hat{c}_{\mathcal{E}_n^{(m)}} = \sum_{k=1}^{m} A^{(k)}_{m\leftarrow 1} \hat{b}_{\mathcal{E}_n^{(k)}}, \tag{3.149}$$

where with $\hat{A}^{(k)}_{m\leftarrow 1}$ we indicate the probability amplitudes obtained by coherently summing all the paths that bring the input mode $\hat{b}_{\mathcal{E}_n^{(k)}}$ from level 1 to level m of the network

(see Fig. 3.8). Inserting expression (3.149) in Eq. (3.140) we get:

$$\zeta_{mm'} = \sum_{k'=1}^{m'} \sum_{k=1}^{m} A^{(k')}_{m'\leftarrow 1} \left[A^{(k)}_{m\leftarrow 1}\right]^* \mathrm{Tr}\left\{\hat{b}_{\mathcal{E}_n^{(k')}} \hat{b}_{\mathcal{E}_n^{(k)}} \hat{\eta}_{\mathcal{E}}\right\}. \tag{3.150}$$

For the special case where the input modes state is a zero-mean factorized one, Eq. (3.150) can be further simplified. Specifically, under our assumption of having the input modes in the vacuum state $|\emptyset\rangle$, we have:

$$\langle\emptyset| \hat{b}_{\mathcal{E}_n^{(k')}} \hat{b}^\dagger_{\mathcal{E}_n^{(k)}} |\emptyset\rangle = \delta_{kk'}, \tag{3.151}$$

so that Eq. (3.150) becomes:

$$\zeta_{mm'} = \sum_{k=1}^{m} A^{(k)}_{m'\leftarrow 1} \left[A^{(k)}_{m\leftarrow 1}\right]^*. \tag{3.152}$$

Indeed the expression can be simplified further, thanks to the properties of the amplitudes $A_{m\leftarrow 1}$. As a matter of fact we can write the compact form:

$$\zeta_{mm'} = A^{(m)}_{m'\leftarrow m}. \tag{3.153}$$

This expression shows that for the case of vacuum input modes, the coupling between sites S_m, $S_{m'}$ is identical to the probability amplitudes associated with the propagation of signals from S_m to $S_{m'}$, as exemplified in Fig. 3.10.

To derive Eq. (3.153) we go back to Eq. 3.145 and note that the vacuum states are invariant under the action of the beam splitter operators $\hat{U}_{mm'}$, so that we are allowed to write:

$$\begin{aligned} \zeta_{mm'} &= \langle\emptyset| \left(\hat{V}_{m'-1\leftarrow m} \hat{b}_{\mathcal{E}_n^{(m')}} \hat{V}^\dagger_{m'-1\leftarrow m}\right) \hat{b}^\dagger_{\mathcal{E}_n^{(m)}} |\emptyset\rangle \\ &= \sum_{k=m}^{m'} A^{(k)}_{m'\leftarrow k} \langle\emptyset| \hat{b}_{\mathcal{E}_n^{(k)}} \hat{b}_{\mathcal{E}_n^{(m)}} |\emptyset\rangle = A^{(m)}_{m'\leftarrow m}. \end{aligned} \tag{3.154}$$

To derive Eq. (3.154) we used the identity:

$$\hat{V}^\dagger_{m'-1\leftarrow m} \hat{b}_{\mathcal{E}_n^{(m')}} \hat{V}_{m'-1\leftarrow m} = \sum_{k=m}^{m'} A^{(k)}_{m'\leftarrow k} \hat{b}_{\mathcal{E}_n^{(k)}}, \tag{3.155}$$

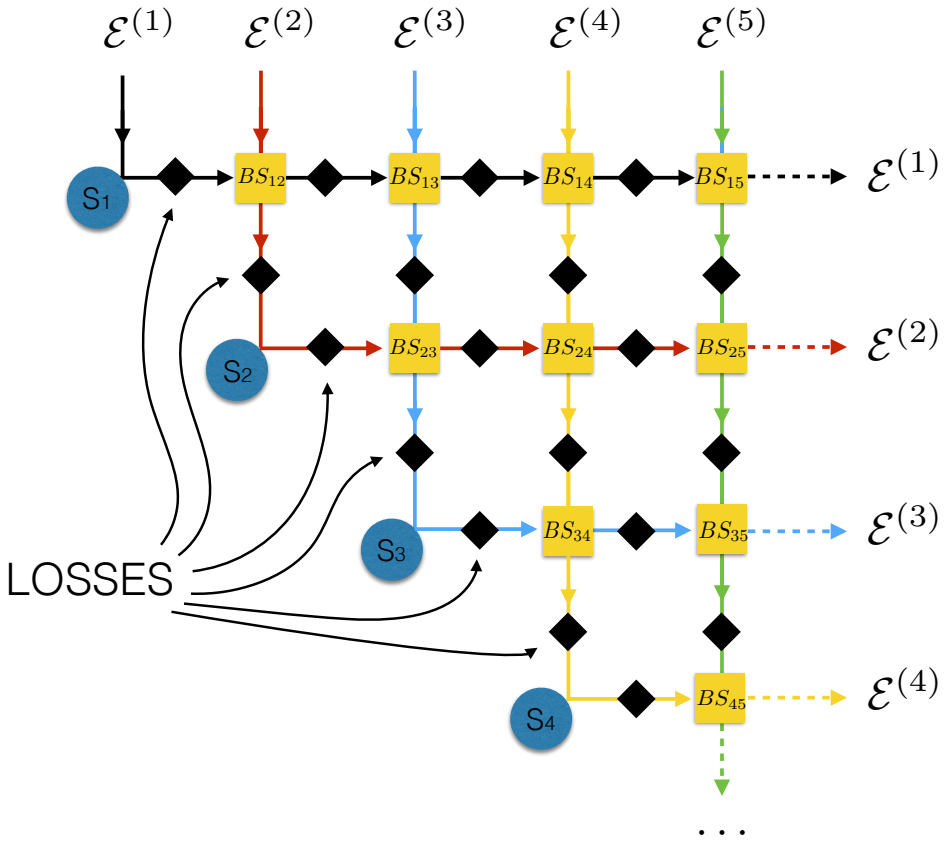

Figure 3.11.: Illustration of the network in the presence of losses: these can be modeled by adding auxiliary beam splitters interacting with auxiliary environments initialized in the vacuum state in the place indicated by black elements in figure. This induces a $(1-\nu)^{m'-m}$ damping factor on the coupling coefficients $\zeta^{(\mathrm{loss})}_{m,m'}$.

which is a straightforward generalization of Eq. (3.149).

We conclude this section by asserting that noise phenomena in the signal transmission, which have been ignored up to know, can be easily included in this formalism. Any form of disturbance can in fact be included by properly including it in the definition of the map $\mathcal{M}_{\mathcal{E}_n^{(m'\leftarrow m)}}$. Consider for instance the case, illustrated in Fig. 3.11, where each path composing the network is characterized by a probability $\nu \in [0,1]$ of losing the signal transmitting through it. We can then easily account for this effect in the expression of the coefficients $\zeta_{mm'}$, where an extra factor exponentially decreasing with the sites distance appears:

$$\zeta^{(\mathrm{loss})}_{mm'} = (1-\nu)^{m'-m} A^{(m)}_{m'\leftarrow m}. \tag{3.156}$$

This expression can be easily verified by representing the losses via the action of extra beam splitters placed along the network in correspondence of the black elements of Fig. 3.11 that mix the signal with an auxiliary environments initialized in the vacuum state.

3.4.3. Regular Network

In Sec. 3.4.1 we have seen how the couplings between the nodes of the network shown in Fig. 3.8 depend on the coherent sum of the paths connecting them. We have also seen that for generic parameters $t_{mm'}$ and $\varphi_{mm'}$, the computation of the coefficients $\zeta_{mm'}$ quickly becomes extremely hostile.

In order to see some practical instances, we want to focus in this section on the case of a regular network, like the one shown in Fig. 3.12, where the beam splitters dictating the n-th neighbor interaction are assumed to be identical, i.e. the beam splitters are grouped according to their index difference, so that for instance $\{BS_{12}, BS_{23}, \dots, BS_{m,m+1}\}$ have all the same transmissivity t_1 and the same relative phase φ_1, so that in general we set:

$$t_{m,m+k} = \tau_k \quad \varphi_{m,m+k} = \varphi_k \quad \forall m, k. \tag{3.157}$$

Under these assumptions the coefficients $\zeta_{mm'}$ become invariant under translation of the indexes:

$$\zeta_{mm'} = \zeta_{1,m'-m+1} \quad \forall m' > m, \tag{3.158}$$

so that we are allowed to write the master equation as:

$$\frac{d\hat{\rho}_S(t)}{dt} = \sum_m \mathcal{L}_m(\hat{\rho}_S(t)) + \sum_k \mathcal{D}_k(\hat{\rho}_S(t)), \tag{3.159}$$

where now the superoperators $\mathcal{D}_k$ are translationally invariant:

$$\mathcal{D}_k(\cdots) = \gamma \sum_m \xi_k \, \hat{a}_m \Big[(\cdots), \hat{a}^\dagger_{m+k}\Big] + \xi_k^* \, [\hat{a}_{m+k}, (\cdots)]\hat{a}^\dagger_m, \tag{3.160}$$

and we have defined

$$\xi_k = \zeta_{1,k+1} = A^{(1)}_{k+1\leftarrow 1}, \tag{3.161}$$

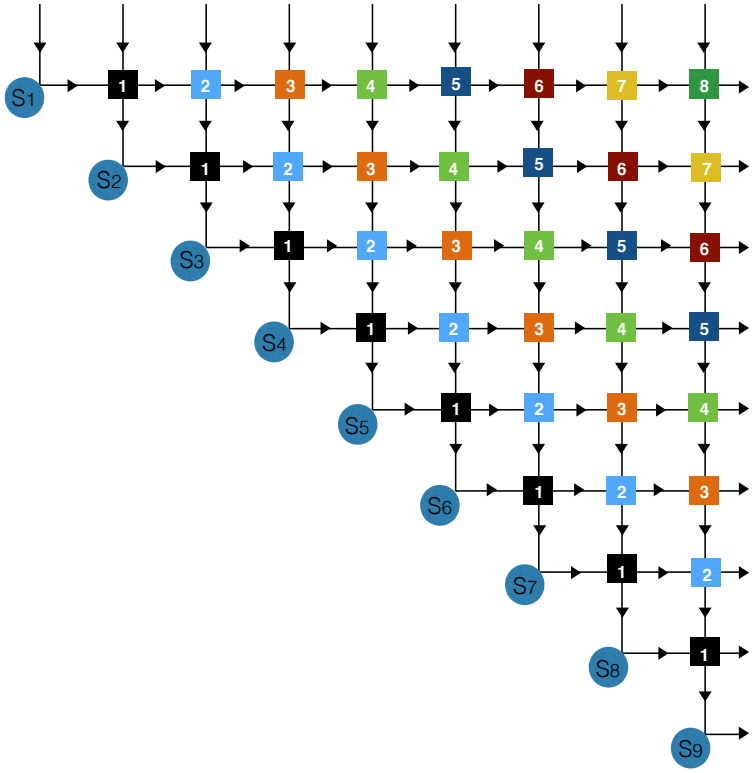

Figure 3.12.: Illustration of the regular network under examination: the beam splitters laying on the same diagonal, as the labels suggest, have the same properties, i.e. they have the same transmissivity t_k and they induce the same relative phase φ_k. This implies, for instance, that beam splitters $BS_{12}, BS_{23}, \ldots, BS_{m,m+1}$ all have the same transmissivity $\tau_{k=1}$ and relative phase $\varphi_{k=1}$, as well as the elements $BS_{13}, BS_{24}, \ldots, BS_{m,m+2}$ are characterized by transmissivity $\tau_{k=2}$ and relative phase $\varphi_{k=2}$.

which become

$$\xi_k^{(\text{loss})} = (1-\nu)^k A^{(k)}_{k+1\leftarrow 1} \tag{3.162}$$

in presence of losses (see Eq. (3.156)). The translational invariance of the $\mathcal{D}_k$ manifests itself also in the expression of the induced effective Hamiltonian, which is worth:

$$\hat{H} = \sum_k \hat{H}_k \,, \quad \hat{H}_k = -\frac{i\gamma}{2} \sum_m \left(\xi_k \hat{a}_m \hat{a}^\dagger_{m+k} - \xi_k^* \hat{a}^\dagger_m \hat{a}_{m+k} \right). \tag{3.163}$$

It is also clear by construction that ξ_k will depend upon the $\tau_{k'}$ and $\varphi_{k'}$ with $k' < k$, so that tuning appropriately these parameters one is able to tailor the dynamics of the

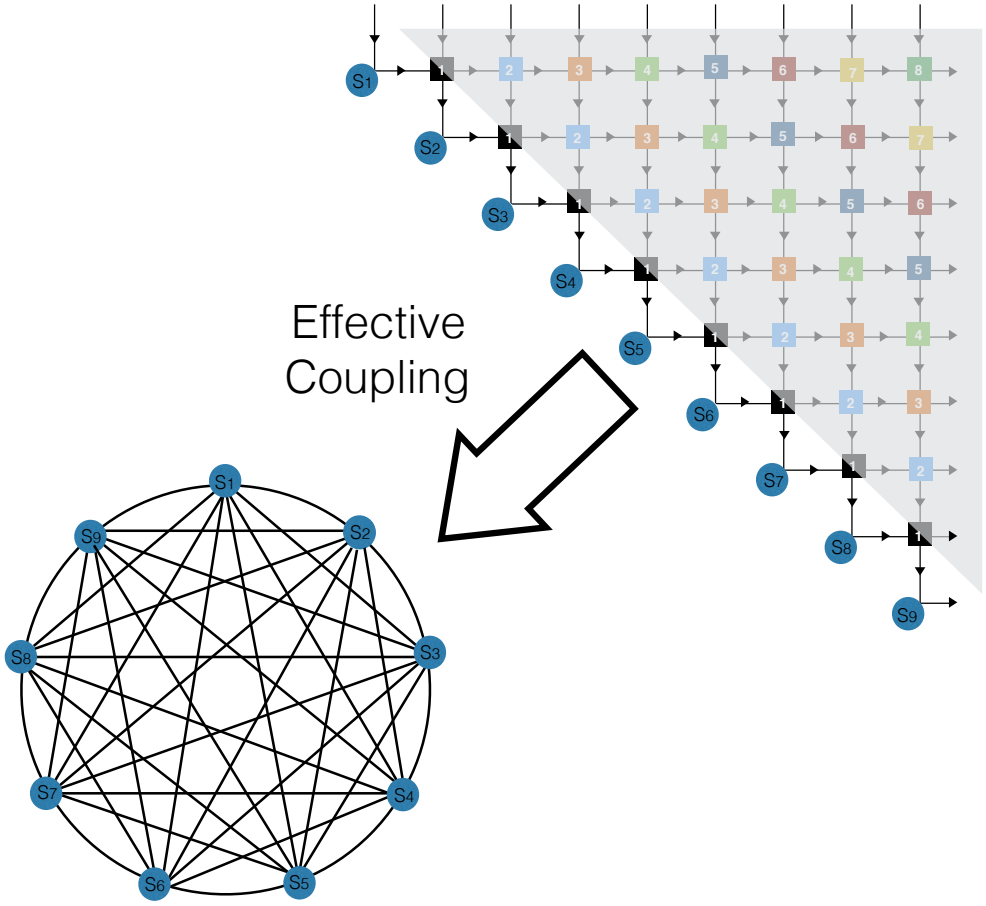

Figure 3.13.: Finite size network where $t_1 = 0$ has been set. This choice gives rise to a uniform chain of nodes connected through the one chiral channel $\mathcal{E}^{(1)}$. As a consequence any node interacts with all the other, giving rise to the interaction topology shown in figure.

network. Still, writing explicitly the functional dependence of the ξ_k is quite difficult, due to the complexity of this dependence. However, for some special cases we are going to analyze it is possible to find manageable analytic expressions. We thus consider two special instances of the regular network we have just shown: the case of a finite size network, and the case where we want to retain only one kind of interaction, i.e. only first-neighbor interactions or only second.neighbor and so on and so forth.

Finite size networks

Consider the case where the transmissivity of the beam splitters $BS_{m,m+1}$ coupling first neighboring sites is set to zero, $\tau_1 = 0$, as illustrated in Fig. 3.13. With this choice the

network splits up in two: one part is made out of the nodes S communicating through the chiral channel $\mathcal{E}^{(1)}$, the other part being the composed by the remaining environmental channels that do not interact with the nodes.

Under this hypothesis the couplings ξ_k are easily computed. As a metter of fact we have:

$$\xi_k = (-ie^{-i\varphi_1})^k = e^{-ik(\varphi_1+\pi/2)}, \tag{3.164}$$

showing that the nodes interact all with the same strenght independently of the distance between them. This comes as no surprise, since with the choice made we just recovered the many-body generalization of the model in Sec. 3.1, where M sites are coupled to a single chiral channel. This can be seen even better by looking at the effective Hamiltonian, which looks:

$$\hat{H}_k = -\frac{i\gamma}{2}\sum_m \left(e^{-ik(\varphi_1+\pi/2)}\hat{a}_m\hat{a}^\dagger_{m+k} - h.c.\right) = -\frac{i\gamma}{2}\sum_m \left(\hat{d}_m\hat{d}^\dagger_{m+k} - h.c.\right), \tag{3.165}$$

where in the second equality we show explicitly how the relative phase φ_1 is in this case irrelevant, as it can be reabsorbed into the system operators through the transformation:

$$\hat{a}_m \to \hat{d}_m = \hat{a}_m e^{-im(\varphi_1+\pi/2)}, \tag{3.166}$$

which leaves the other contributions to the master equation unchanged. A similar behavior is observed when we leave τ_1 arbitrary but we still assume all the other beam splitters of the network to have unitary transmissivity, i.e. $\tau_k = 1$ for $k > 1$. This choice implies that a signal which gets transmitted through $BS_{m,m+1}$ will never have the opportunity to interact with a node, so that the overall effect of this choice of parameters implies an exponential depression of the couplings,

$$\xi_k = e^{-ik(\varphi_1+\pi/2)}(1-\tau_1)^{k/2}, \tag{3.167}$$

which is the same expression one would get considering the case $\tau_1 = 0$ in presence of losses, upon the identification of $\sqrt{1-\tau_1}$ with the factor $(1-\nu)$.

Actually, this is not the end of the story: Eq. (3.164) can be generalized to the case where, for a given integer $K \geq 2$, the transmissivity of beam splitters $BS_{m,m+K}$ is set equal to zero, i.e. $\tau_K = 0$. As in the previous case, the network splits up in two parts,

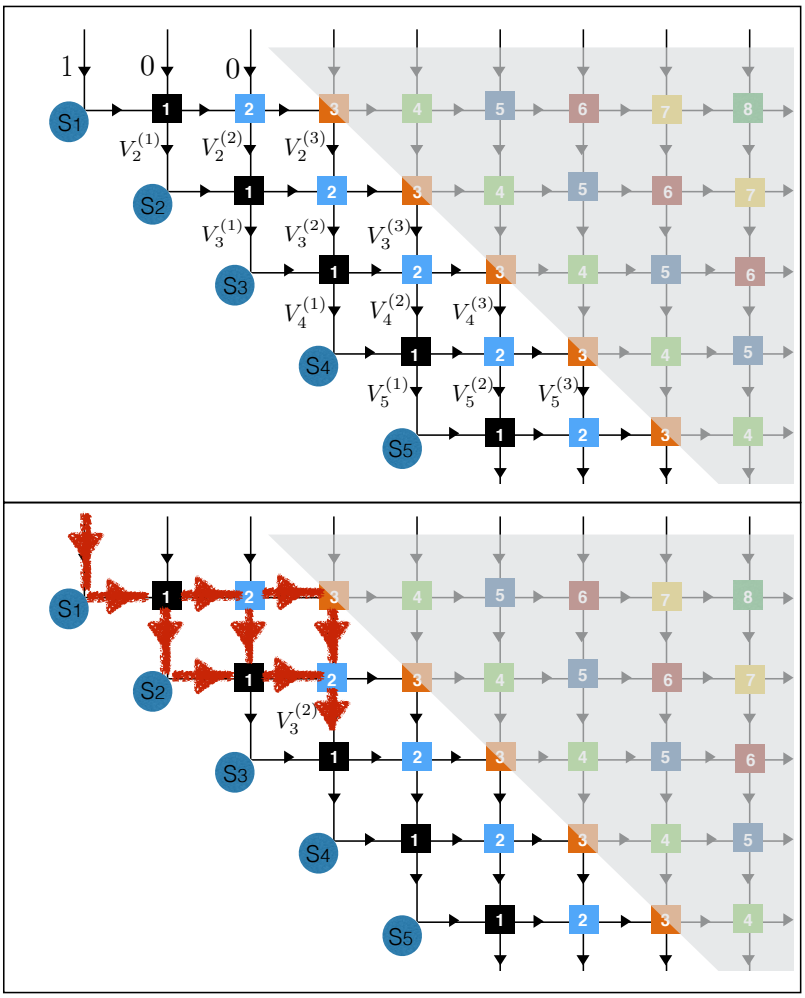

Figure 3.14.: Schematic illustration of the components of the vectors $\vec{V}_\ell$ for the case $K = 3$. For ℓ and k integer, the component $V_\ell^{(k)}$ describes the probability amplitude associated to the path connecting the first entry of level 1 and the k-th entry of level ℓ (upper panel). In the lower panel we highlight the paths contributing to $V_3^{(2)}$.

the first on containing the nodes and the first K chiral channels, the other containing all the rest of the network, which does not contribute to the dynamics.

To show this we introduce a K dimensional vector $\vec{V}_\ell$ having as components the probability amplitudes associated with the propagation of $\mathcal{E}^{(1)}$ from level 1 of the network up to the first K entries of level ℓ (see Fig. 3.14):

$$\vec{V}_\ell^T = \left(V_\ell^{(1)}, V_\ell^{(2)}, \ldots, V_\ell^{(K)}\right) \quad \text{for } \ell \geq 2, \tag{3.168}$$

$$\vec{V}_1^T = (1, 0, \ldots, 0)\,. \tag{3.169}$$

To better understand this notation we highlight that the amplitude $A^{(1)}_{k+1\leftarrow -1}$, which basically determines the coupling ξ_k, corresponds to the first entry of $\vec{V}_{k+1}$, so that we have:

$$A^{(1)}_{k+1\leftarrow -1} = V^{(1)}_{k+1} = \vec{V}_1^T \cdot \vec{V}_{k+1}. \tag{3.170}$$

Moreover the vectors $\vec{V}_\ell$ and $\vec{V}_{\ell+1}$ are clearly not independent, but instead they are related via:

$$\vec{V}_{\ell+1} = T\,\vec{V}_\ell, \tag{3.171}$$

where T is a $K \times K$ matrix describing the propagation of a signal from one level of the network to the next whose elements are worth:

$$T_{ij} = \begin{cases} e^{-i\varphi_i}\sqrt{\tau_i} & \text{for } j = i+1, \\ e^{-i\varphi_i}(-i\sqrt{1-\tau_i})(-i\sqrt{1-\tau_{i-1}}) & \text{for } i = j, \\ e^{-i\varphi_i}(-i\sqrt{1-\tau_{j-1}})(\prod_{\ell=j}^{i-1}\sqrt{\tau_\ell})(-i\sqrt{1-\tau_i}) & \text{for } j < i, \\ 0 & \text{otherwise.} \end{cases} \tag{3.172}$$

where we adopted the convention $-i\sqrt{1-\tau_0} \to 1$ for ease of notation. Writing the matrix $T = UDU^\dagger$, where D is the diagonal matrix formed by the eigenvalues of T and U the unitary operator diagonalizing T, whose rows are the corresponding eigenvectors, we can write from Eq. (3.171):

$$\vec{V}_{\ell+1} = T^\ell \vec{V}_1 = UD^\ell U^\dagger \vec{V}_1. \tag{3.173}$$

Inserting this into Eq. (3.170) we get the expression for the ξ_k:

$$\xi_k = A^{(1)}_{k+1\leftarrow -1} = \vec{V}_1^T \cdots \vec{V}_{k+1} = \vec{V}_1^T U D^k U^\dagger \vec{V}_1. \tag{3.174}$$

This is a general formula allowing one to compute the coupling ξ_k for the general case where the transmissivities of beam splitters $BS_{m,m+K}$ have been set to zero. Consider for instance the case $K = 2$. In this case T is a 2×2 matrix which is worth:

$$T = \begin{pmatrix} -i\sqrt{1-\tau_1}e^{-i\varphi_1} & \sqrt{\tau_1}e^{-i\varphi_1} \\ -i\sqrt{\tau_2}e^{-i\varphi_2} & -\sqrt{1-\tau_1}e^{-i\varphi_2} \end{pmatrix} = UDU^\dagger, \tag{3.175}$$

where the matrices D and U can be expressed as:

$$D = \begin{pmatrix} e^{i\theta_+} & 0 \\ 0 & e^{i\theta_-} \end{pmatrix}, \quad U = \begin{pmatrix} \frac{u_+}{\sqrt{\tau_1+|u_+|^2}} & \frac{u_-}{\sqrt{\tau_1+|u_-|^2}} \\ \frac{\sqrt{\tau_1}}{\sqrt{\tau_1+|u_+|^2}} & \frac{\sqrt{\tau_1}}{\sqrt{\tau_1+|u_-|^2}} \end{pmatrix}, \tag{3.176}$$

with:

$$\begin{aligned} e^{i\theta_\pm} &= \frac{1}{2}\Big[-\sqrt{1-\tau_1}(ie^{-i\varphi_1} + e^{-i\varphi_2}) \\ &\pm \sqrt{(e^{-i\varphi_2} - ie^{-i\varphi_1})^2 - \tau_1(ie^{-i\varphi_1} + e^{-i\varphi_2})^2}\Big], \qquad (3.177) \\ u_\pm &= \sqrt{1-\tau_1}(e^{-i(\varphi_1-\varphi_2)} + i) \\ &\pm i\sqrt{(1-\tau_1)(1-e^{-i2(\varphi_1-\varphi_2)}) - 2ie^{-i(\varphi_1-\varphi_2)}(1+\tau_1)}. \qquad (3.178) \end{aligned}$$

From Eq. (3.174) it then follows:

$$\xi_k = \frac{u_+ e^{ik\theta_+} - u_- e^{ik\theta_-}}{u_+ - u_-}, \tag{3.179}$$

from which we deduce an oscillatory behavior of the ξ_k and a complex functional dependence on the beam splitter characteristics. To better illustrate the functional dependence of the ξ_k upon the beam splitter parameters, in Fig. 3.15 we plot the modulus of the couplings $|\xi_1|$, $|\xi_2|$, $|\xi_3|$ and $|\xi_4|$ as a function of τ_1 and φ_2, assuming $\varphi_1 = 0$. As one can see from the plots, there is a rich variety of behaviors depending on the choice of τ_1, φ_1 and φ_2.

For instance it suffices to set $\tau_1 = 0$ to find $u_- = 0$ and recover the case in Eq. (3.164). On the other hand, setting $\tau_1 = 1$ we have $u_+ = u_-$ and $e^{i\theta_\pm} = \pm e^{-i\left(\frac{2\varphi_1+2\varphi_2+\pi}{4}\right)}$, so that:

$$\xi_k = e^{-ik\left(\frac{2\varphi_1+2\varphi_2+\pi}{4}\right)} \times \begin{cases} 0 & \text{for } k \text{ odd} \\ 1 & \text{for } k \text{ even} \end{cases} \tag{3.180}$$

which implies that odd (even) sites interact with odd (even) sites only. Another interesting feature of Eq. (3.179) is that, by setting $\varphi_2 = \varphi_1 + \pi/2$, it becomes:

$$\xi_k = e^{-ik(\varphi_1+\pi/2)} \times \begin{cases} \sqrt{1-\tau_1} & \text{for } k \text{ odd}, \\ 1 & \text{for } k \text{ even}, \end{cases} \tag{3.181}$$

so that under this parameters choice two nodes belonging to the same set (even or odd sites) interact with strength 1, while the interactions among nodes of different species

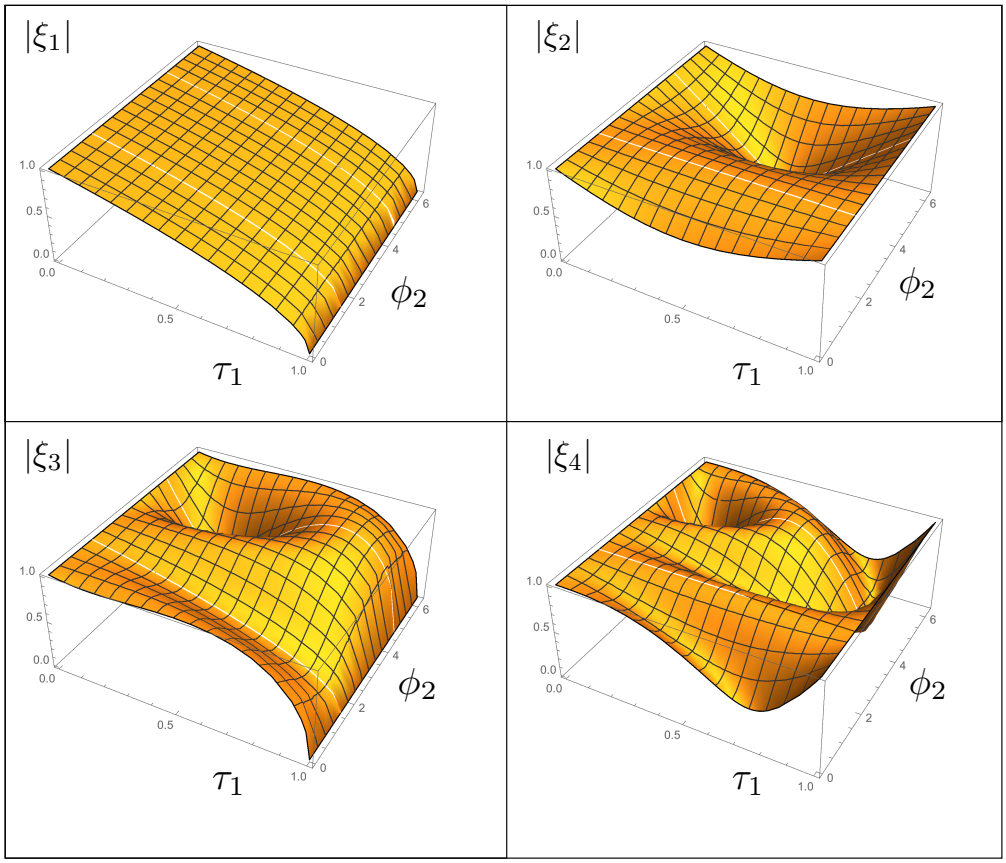

Figure 3.15.: Plots of the modulus of the first four couplings ξ_k for the case $\tau_2 = 0$ and $\varphi_1 = 0$, as a function of τ_1 and φ_2. As one can notice, for $\tau_1 = 0$ all the couplings have unitary modulus, in agreement with Eq. (3.164). On the other hand, for $\tau_1 = 1$ the odd terms ξ_1 and ξ_3 nullify, the even ones getting their maximum value.

are suppressed by a factor $\sqrt{1-\tau_1}$. Under these hypotheses the master equation for the nodes becomes:

$$\begin{aligned}\frac{d\hat{\rho}_S(t)}{dt} &= \sum_m \frac{\gamma}{2}\left\{2\hat{a}_m\hat{\rho}_S\hat{a}_m^\dagger - \left\{\hat{a}_m^\dagger\hat{a}_m, \hat{\rho}_S\right\}\right\} + \sum_{k\,\text{even}} \gamma\left\{\hat{a}_m\left[\hat{\rho}_S, \hat{a}_{m+k}^\dagger\right] + [\hat{a}_{m+k}, \hat{\rho}_S]\hat{a}_m^\dagger\right\} \\ &+ \sum_{k\,\text{odd}} \gamma\sqrt{1-\tau_1}\left\{\hat{a}_m\left[\hat{\rho}_S, \hat{a}_{m+k}^\dagger\right] + [\hat{a}_{m+k}, \hat{\rho}_S]\hat{a}_m^\dagger\right\}. \end{aligned} \tag{3.182}$$

It is possible to diagonalize this master equation obtaining analytical expressions for

both the effective Hamiltonian and the Lindblad operators. The former reads:

$$\begin{aligned}\hat{H} = & - \frac{i\gamma}{2}\sum_{k,\text{even}}\sum_{m}\left(\hat{a}_m\hat{a}^\dagger_{m+k} - h.c.\right) \\ & - \frac{i\gamma}{2}\sqrt{1-\tau_1}\sum_{k\,\text{odd}}\sum_{m}\left(\hat{a}_m\hat{a}^\dagger_{m+k} - h.c.\right),\end{aligned} \tag{3.183}$$

illustrating once more the fact that the nodes interact among them differently according to the set they belong to. As for the Lindblad operators $\hat{L}_i$ and their associated eigenvalues κ_i, it turns out that, independently of the number of nodes M, only two of them are non-null. More specifically, the expressions of these Lindblad operators change depending on the parity of M itself. For M even we have in fact:

$$\hat{L}_j = \frac{1}{\sqrt{M}}\sum_{m=1}^{M}(-1)^{mj}\hat{a}_m, \tag{3.184}$$

$$\kappa_j = M\gamma\frac{1+(-1)^j\sqrt{1-\tau_1}}{2}, \tag{3.185}$$

which for the particular choice $\tau_1 = 1$ become:

$$\hat{L}_1 = \sqrt{\frac{2}{M}}\sum_{j=0}^{M/2-1}\hat{a}_{2j+1}, \quad \hat{L}_2 = \sqrt{\frac{2}{M}}\sum_{j=1}^{M/2}\hat{a}_{2j}, \tag{3.186}$$

$$\kappa_1 = \kappa_2 = \frac{M\gamma}{2}, \tag{3.187}$$

which is in agreement with the fact that for this value of τ_1 the even nodes decouple from the odd ones. If instead we have an odd number of sites the previous expressions become:

$$\hat{L}_j = \frac{1}{\sqrt{A}}\left[\sum_{m=0}^{(M-1)/2}\hat{a}_{2m+1} + \frac{-1+(-1)^j\sqrt{M^2-(M^2-1)\tau_1}}{(M-1)\sqrt{1-\tau_1}}\sum_{m=1}^{(M-1)/2}\hat{a}_{2m}\right], \tag{3.188}$$

$$A = \frac{M+1}{2} + \frac{1}{2(M-1)}\left|\frac{1+\sqrt{M^2-(M^2-1)\tau_1}}{\sqrt{1-\tau_1}}\right|, \tag{3.189}$$

$$\kappa_j = \gamma M\frac{1+(-1)^j\sqrt{1-(1-1/M^2)\tau_1}}{2}, \tag{3.190}$$

which simplify further setting $\tau_1 = 1$:

$$\hat{L}_1 = \sqrt{\frac{2}{M+1}} \sum_{j=0}^{(M-1)/2} \hat{a}_{2j+1}, \tag{3.191}$$

$$\hat{L}_2 = \sqrt{\frac{2}{M-1}} \sum_{j=1}^{(M-1)/2} \hat{a}_{2j}, \tag{3.192}$$

$$\kappa_1 = \frac{M-1}{2}\gamma \quad \kappa_2 = \frac{M+1}{2}\gamma. \tag{3.193}$$

3.4.4. Retaining only one interaction

Another interesting case to analyze is the one where we can eliminate long range interactions between the nodes. In fact in all the example we saw up to know all the ξ_k were different from zero, while here we want to check whether it is possible to have one kind of interaction, for instance retaining only first-neighbor interactions while suppressing all the others. To tackle this problem we proceed in a reverse manner, i.e. we require that the transmissivities and the relative phases of the beam splitters are such that:

$$\xi_k = 0 \quad \forall\, k \geq 2. \tag{3.194}$$

As shown in detailed manner in App. A.4, it is possible to obtain such result given the transmissivity τ_1 is above the threshold value of $3/4$. Specifically, for $\tau_1 \in [3/4, 1]$ we have:

$$\xi_1 = -ie^{-i\varphi_1}\sqrt{1-\tau_1}, \tag{3.195}$$

while the condition in Eq. (3.194) can be enforced by properly tuning the relative phases φ_k and choosing the transmissivities according to the recursive formula:

$$\tau_k = 1 - \left(\frac{1 - \tau_{k-1}\tau_{k-2}\cdots\tau_1}{\tau_{k-1}\tau_{k-2}\cdots\tau_1}\right)\left(\frac{1-\tau_{k-1}}{\tau_{k-1}}\right). \tag{3.196}$$

We immediately note that also in this case the relative phase appearing in the expression for ξ_1 can be eliminated by proper absorbing it into a redefinition of the system operators, so that it is irrelevant to the dynamics. Another thing to be noted is that Eq. (3.196) can be adapted in order to retain only n-th neighbor interactions: to do this it suffices to set $\tau_k = 1$ for all $k < n$ and then use Eq. (3.196) with the index shift

$k \to k+n$.

When Eqs.(3.194, 3.195) are fulfilled, the master equation for the network becomes:

$$\begin{aligned}\frac{\hat{\rho}_S(t)}{dt} &= \sum_m \frac{\gamma}{2}\left\{2\hat{a}_m\hat{\rho}_S\hat{a}_m^\dagger - \left\{\hat{a}_m^\dagger\hat{a}_m, \hat{\rho}_S\right\}\right\} \\ &+ \sum_m \gamma\sqrt{1-\tau_1}\left\{\hat{a}_m\left[\hat{\rho}_S, \hat{a}_{m+1}^\dagger\right] + [\hat{a}_{m+1}, \hat{\rho}_S]\hat{a}_m^\dagger\right\}, \end{aligned} \tag{3.197}$$

where we set $\varphi = \pi/2$ in order to simplify the expression, as it is irrelevant. Upon recasting the master equation in GKSL form, one would find the Hamiltonian contribution:

$$\hat{H} = \hat{H}_1 = -\frac{i\gamma\sqrt{1-\tau_1}}{2}\sum_m\left(\hat{a}_m\hat{a}_{m+1}^\dagger - h.c.\right). \tag{3.198}$$

This Hamiltonian contains only first-neighboring sites exchange terms and presents a chiral symmetry which causes the Hamiltonian to change sign when reversing the ordering of the sites. As for the Lindblad operators, they can be computed and an analytical expression obtained, but the latter is not very informative, as we have M collective jump operators which are combinations of the original nodes operators $\hat{a}_m$.

With this we conclude our treatment of quantum cascade networks: throughout this chapter we first saw how to derive the master equation for an arbitrary network, highlighting its features and properly highlighting the conditions upon which the model is valid. Then we turned our attention to some examples, first studying systems with a limited number of sites, to get acquainted with the interference effects that can arise, moving then to the analysis of more complex networks, with a high number of nodes and environmental channels. In this last context we saw how, exploiting interference effects, it is possible, by only changing the parameters of the optical elements in the network, to obtain a rich variety of different dynamics, some of which can be described by analytical formulas.

CHAPTER 4

Thermodynamics

In this chapter we will still talk about collisional models, moving away from cascade systems towards the realm of thermodynamics. It is a well known fact that thermodynamics has subdued a revival of interest in recent years [Alicki and Kosloff 2018; Kosloff and Levy 2014; Vinjanampathy and Anders 2016],which lead to new discoveries as well as to new questions, ranging from the energetic balance of nanoscale devices [Campisi and Fazio 2016; Gelbwaser-Klimovsky and Kurizki 2015; M. Horodecki and Oppenheim 2013; Lena, Palma, and De Chiara 2016; Linden, Popescu, and Skrzypczyk 2010] and the storageof energy in quantum batteries [Andolina, Farina, et al. 2018; Andolina, Keck, et al. 2019; Binder et al. 2015; Campaioli et al. 2017; D. Ferraro et al. 2018], to more fundamental questions, such as the generalization to the quantum realm of the fluctuation-dissipation relations [Elouard et al. 2017; Manzano, Horowitz, and Parrondo 2018], the ability of master equations of describing correctly heat exchange phenomena [Chiara et al. 2018; Hofer et al. 2017; Rodrigues et al. 2019], the quantification of irreversibility [Benenti and Palma 2007] and the relation between thermodynamics and information theory [Campisi and Goold 2017; Deffner and Jarzynski 2013; Goold et al. 2016].

It is just on irreversibility that the following chapter focus: the irreversibility of a process is well-known to be related with the entropy balance of a given thermodynamical transformation, or, in other terms, to the second principle of thermodynamics. The latter, in the quantum realm, can be formulated either via a Clausius-like formulation

or via a relation accounting for the presence of correlations [Alipour et al. 2016; Bera et al. 2017; Hewgill, A. Ferraro, and De Chiara 2018; Manzano, Galve, et al. 2016; Manzano, Plastina, and Zambrini 2018; Tacchino et al. 2018] between the system and the environment, which in this context is usually called a thermal bath.

It is thanks to the comparison between these two formulations and the aid of a collisional model [Barra 2015; Lorenzo, McCloskey, et al. 2015; Man, Xia, and Lo Franco 2018, 2019; Manatuly et al. 2019; Strasberg et al. 2017] that we are able to get a better insight into the final state of the joint system+bath system after the thermalization process is completed. In facts in Chap. 2 we anticipated that one interesting feature of collisional model is the possibility of keeping track of the environmental degrees of freedom: it is just this feature that allows our analysis, leading to a very interesting result, namely the factorization of the system and the environmental state after the thermalization.

We start by reviewing in Sec. 4.1 some of the thermodynamic functionals used in thermodynamics and their mutual relations. In Sec. 4.2 we are instead going to see how these thermodynamic functionals can be used to quantify the irreversibility of a thermodynamic process. Then in Sec. 4.3 we describe the collisional model used to describe the thermalization process, while finally in Sec. 4.4 we demonstrate, via analytical and numerical results, the decay of correlations between the system and the thermal bath.

4.1. Thermodynamic functionals

As in the next section we are going to use them, here we want to briefly review some of the thermodynamic functionals commonly used and some of their basic properties [Nielsen and Chuang 2010].

The main quantity we will be dealing with in the following is the Von Neumann entropy:

$$S(\hat{\rho}) = -\operatorname{Tr}\{\hat{\rho}\ln\hat{\rho}\}, \tag{4.1}$$

where $\hat{\rho}$ is the density matrix of a quantum state. The Von Neumann entropy is a non-negative quantity that nullifies only if $\hat{\rho}$ is a pure state, reaching its maximum value $\ln d$ for the completely mixed state $\hat{\rho} = \hat{\mathbb{I}}/d$, d being the dimension of the Hilbert space. When dealing with composite systems, the entropy of a state which is the tensor product

of states belonging to the subsystems is the sum of the entropies of the states:

$$S(\hat{\rho}_A \otimes \hat{\rho}_B) = S(\hat{\rho}_A) + S(\hat{\rho}_B). \tag{4.2}$$

When instead the joint state of A and B is not a tensor product, the entropy S is subadditive, that is:

$$S(\hat{\rho}_{AB}) \geq S(\hat{\rho}_A) + S(\hat{\rho}_B). \tag{4.3}$$

Finally, the entropy of a state is invariant under the action of unitary operations: this is readily seen considering that by definition the entropy of a state depend on the eigenvalues of density matrix, which are left unchanged by the action of unitary operators.

Another quantity we will be using in the next sections is the *relative entropy*, which is a strictly non-negative quantity defined as:

$$S(\hat{\rho}||\hat{\sigma}) = \mathrm{Tr}\{\hat{\rho}\ln\hat{\rho}\} - \mathrm{Tr}\{\hat{\rho}\ln\hat{\sigma}\}. \tag{4.4}$$

This quantity somehow measures the distance between two quantum states, though mathematically speaking it is not a distance. Nonetheless it is zero if and only if $\hat{\rho} = \hat{\sigma}$, just as a distance, while it is infinite when the kernel of $\hat{\sigma}$ has a non-null intersection with the support of $\hat{\rho}$, as in this case it is impossible to distinguish the two states. An important property of the relative entropy that will be used is the contractivity under the action of a CPT map Φ:

$$S(\hat{\rho}||\hat{\sigma}) \geq S(\Phi(\hat{\rho})||\Phi(\hat{\sigma})). \tag{4.5}$$

We conclude the section with the definition of the last entropic functional we will encounter, the quantum mutual information between to quantum systems A and B:

$$I_{A:B} = S(\hat{\rho}_A) + S(\hat{\rho}_B) - S(\hat{\rho}_{AB}). \tag{4.6}$$

The mutual information is always non-negative, reaching its minimum value when the joint state of the $A + B$ system is a tensor product.

4.2. Irreversibility quantification

We want to consider a quantum system A in contact with a thermal bath B at temperature T. We choose different symbols with respect to the other chapters in order to avoid confusion between the quantum system and the entropy $S(\cdots)$.

Assuming that during its interaction with B, system A undergoes an entropy variation ΔS_A, exchanging an amount of heat ΔQ_A with the bath, then from purely thermodynamical considerations it is possible to write the Clausius formulation of the second principle of thermodynamics:

$$\Delta S_A \geq \beta \Delta Q_A, \tag{4.7}$$

where $\beta = 1/k_B T$ is the inverse temperature of the bath, k_B being the Boltzmann constant. The formulation of the second principle given in Eq. (4.7) provides an *intrinsic* lower bound on the local entropy production. When using the word "intrinsic" we want to highlight that the inequality in Eq. (4.7) involves quantities referring to system A only. On the other hand it is possible to derive, from information-theoretical considerations, another formulation of the second principle which reads:

$$\Delta S_A \geq -\Delta S_B. \tag{4.8}$$

In opposition with the Clausius formulation, we define this bound as *extrinsic*, as it involves quantities depending on both A and B.

Since these two bounds put a limit on the entropy variation of A, they provide a characterization of the irreversibility of the thermalization process. As we are going to see in the next sections, these two bounds are not completely independent, though no ordering between them can be established. Both expressions can be derived by modeling our system with the Hamiltonian $\hat{H} = \hat{H}_A + \hat{H}_B + \hat{H}_{\text{int}}$, where $\hat{H}_A$ and $\hat{H}_B$ are the free Hamiltonians of system and bath respectively, while $\hat{H}_{\text{int}}$ describes the interaction between the two systems. Further assuming no initial correlations between A and B, we can write the initial $A + B$ state as:

$$\hat{\rho}_{AB}(0) = \hat{\rho}_A(0) \otimes \hat{\eta}_B^{(\beta)}, \tag{4.9}$$

where $\hat{\rho}_A(0)$ is the initial state of A and $\hat{\eta}_B^{(\beta)}$ indicates the Gibbs state at temperature β

of the bath, which is worth:

$$\hat{\eta}_B^{(\beta)} = \frac{e^{-\beta \hat{H}_B}}{\mathrm{Tr}_B \left\{ e^{-\beta \hat{H}_B} \right\}}. \tag{4.10}$$

With this hypothesis, we are sure that the dynamics is Markovian, so that we can describe the evolution of A through the set of CPT maps $\{\Phi_t\}_{t\geq 0}$ defining the mapping:

$$\hat{\rho}_A(0) \to \hat{\rho}_A(t) = \Phi_t[\hat{\rho}_A(0)] := \mathrm{Tr}_B \left\{ \hat{\rho}_{AB}(t) \right\}, \tag{4.11}$$

where, according to Chap. 2, we have:

$$\hat{\rho}_{AB}(t) = e^{-\frac{i}{\hbar}\hat{H}t} \left(\hat{\rho}_A(0) \otimes \hat{\eta}_B^{(\beta)} \right) e^{\frac{i}{\hbar}\hat{H}t}, \tag{4.12}$$

since the $A + B$ system is a closed system. With these expressions in mind, we can say that the bath B induces thermalization on A, by this meaning that the mapping $\{\Phi_t\}_{t\geq 0}$ leads A to an equilibrium configuration where A has transitioned to a thermal state, i.e. $\hat{\rho}_A = \hat{\eta}_A^{(\beta)}$, irrespectively of the initial state $\hat{\rho}_A(0)$. Whether the equilibrium configuration is reached for some finite time t or in the infinite time limit $t \to \infty$, this has no importance in the derivation of the inequalities in Eqs.(4.7, 4.8). What is of interest to us is the fact that no external work is performed on the system, so that the local energy variation of A can be safely identified with the heat exchanged with the thermal bath B:

$$\Delta Q_A = \mathrm{Tr} \left\{ \hat{H}_A (\hat{\rho}_A(t) - \hat{\rho}_A(0)) \right\}. \tag{4.13}$$

Moreover, since $A + B$ is a closed system, total energy conservation must hold, so that:

$$\mathrm{Tr} \left\{ \hat{H} (\hat{\rho}_{AB}(t) - \hat{\rho}_{AB}(0)) \right\} = 0 \Rightarrow \Delta Q_A = -\Delta Q_B - \Delta E_{\mathrm{int}}, \tag{4.14}$$

where

$$\Delta Q_B = \mathrm{Tr} \left\{ \hat{H}_B (\hat{\rho}_B(t) - \hat{\rho}_B(0)) \right\}, \tag{4.15}$$

$$\Delta E_{\mathrm{int}} = \mathrm{Tr} \left\{ \hat{H}_{\mathrm{int}} (\hat{\rho}_{AB}(t) - \hat{\rho}_{AB}(0)) \right\}. \tag{4.16}$$

While ΔQ_B can be immediately and clearly identified with the heat absorbed by the bath in the thermalization process, ΔE_{int} does not allow for such a clear interpretation: it is

the energy of the joint system due to the interaction between A and B. In most works, and we make no exception, it is neglected either because the interaction is assumed to be small, meaning that E_{int} is negligible, or because an excitations exchange Hamiltonian is used, so that $\Delta E_{\text{int}} = 0$ by definition. In both cases one is allowed to write $\Delta Q_A = -\Delta Q_B$.

All of this being said and done, Eq. (4.7) can be derived by identifying the lhs as:

$$\Delta S_A = S(\hat{\rho}_A(t)) - S(\hat{\rho}_A(0)), \tag{4.17}$$

so that we can write:

$$\Delta S_A - \beta \Delta Q_A = S(\hat{\rho}_A(0)||\hat{\eta}_A^{(\beta)}) - S(\hat{\rho}_A(t)||\hat{\eta}_A^{(\beta)}). \tag{4.18}$$

At this point we can simply exploit the contractivity of the relative entropy under CPT evolution to conclude that the expression above is non-negative, so that Eq. (4.7) holds. Given our setting, at least in the infinite time limit, the thermal state $\hat{\eta}_A^{(\beta)}$ can be assumed to be invariant with respect to the action of the CPT map Φ_t. Exploiting then the monotonicity property of the relative entropy under CPT maps, Eq. (4.7) follows.

The inequality in Eq. (4.8), on the other hand, is simply derived by considering the subadditivity of the entropy and its invariance under unitary transformations, which imply:

$$S(\hat{\rho}_A(t)) + S(\hat{\rho}_B(t)) \geq S(\hat{\rho}_{AB}(t)) = S(\hat{\rho}_{AB}(0)) = S(\hat{\rho_A(0)}) + S(\hat{\rho}_B(0)), \tag{4.19}$$

from which Eq. (4.8) follows. The same equation can also be derived equivalently using the quantum mutual information via:

$$I_{A:B}(0) = 0 \leq I_{A:B}(t) = S(\hat{\rho}_A(t)) + S(\hat{\rho}_B(t)) - S(\hat{\rho}_{AB}(t)), \tag{4.20}$$

which will turn out to be useful in the next sections.

As we anticipated, the two inequalities under examination are not independent, but rather the difference between their rhs can be computed following the derivation in [Reeb and Wolf 2014], finding[1]:

$$\beta \Delta Q_A + \Delta S_B = -S(\hat{\rho}_B(t)||\hat{\eta}_B^{(\beta)}) - \beta E_{\text{int}}. \tag{4.21}$$

[1] Actually in [Reeb and Wolf 2014] the identity $\beta \Delta Q_B = -\Delta S_A + I_{A:B}(t) + S(\hat{\rho}_B(t)||\hat{\eta}_B^{(\beta)})$ is derived, which reduces to the one in the main text upon considering Eq. (4.20).

In general, rhs of Eq. (4.21) has no definite sign, as E_{int} can be either positive or negative depending on the specific characteristics of the system. Anyway, whenever $E_{\text{int}} = 0$ for any of the reasons already exposed, from the positivity of the relative entropy we can deduce that the extrinsic bound in Eq. (4.8) is tighter than the intrinsic one in Eq. (4.7).

Before proceeding and illustrate the collisional model describing the thermalization process, we want to remember that for the case the CPT maps $\{\Phi_t\}$ are time-homogeneous and Markovian, i.e. they possess a dynamical semigroup structure, the dynamics can be described in terms of a Markovian generator in GKSL form: when this is the case, the intrinsic inequality in Eq. (4.7) can be extended to its differential form. This amounts to defining both a differential entropy variation and a differential heat variation as:

$$\partial S_A(t) = S(\hat{\rho}_A(t+dt)) - S(\hat{\rho}_A(t)), \tag{4.22}$$

$$\partial Q_A(t) = \text{Tr}\left\{\hat{H}_A(\hat{\rho}_A(t+dt) - \hat{\rho}_A(t))\right\}, \tag{4.23}$$

so that the Clausius inequality becomes:

$$\partial S_A(t) \geq \beta \partial Q_A(t). \tag{4.24}$$

While this formulation supersedes the discrete one in Eq. (4.7), which can now be derived by integrating Eq. (4.24) itself, a similar operation cannot be done with the extrinsic inequality in Eq. (4.8): as shown in Sec. 2.2.3, the GKSL form of the Markovian generator is derived under the assumption that system-environment correlations are negligible, this feature hindering the possibility of a differential version of the bound in Eq. (4.8). This last observation is the reason we rely on a collisional model in order to study and compare the two inequalities, as shown in the next section.

4.3. Collisional model and thermalization

The collisional model we are going to use in this section differs in more than one aspect from the ones used in Chap. 2 to derive the Markovian master equation and in Chap. 3 to describe cascade networks. Let us show this step by step deriving the model.

Once again we depict the bath as a collection of ancillas $\{b_1, b_2, \dots\}$, each described by a free Hamiltonian $\hat{H}_{b_n}$, all in the same reference thermal Gibbs state $\hat{\eta}_{b_n}^{(\beta)}$. The first difference with the others collisional models seen up to now, is that in order to study the

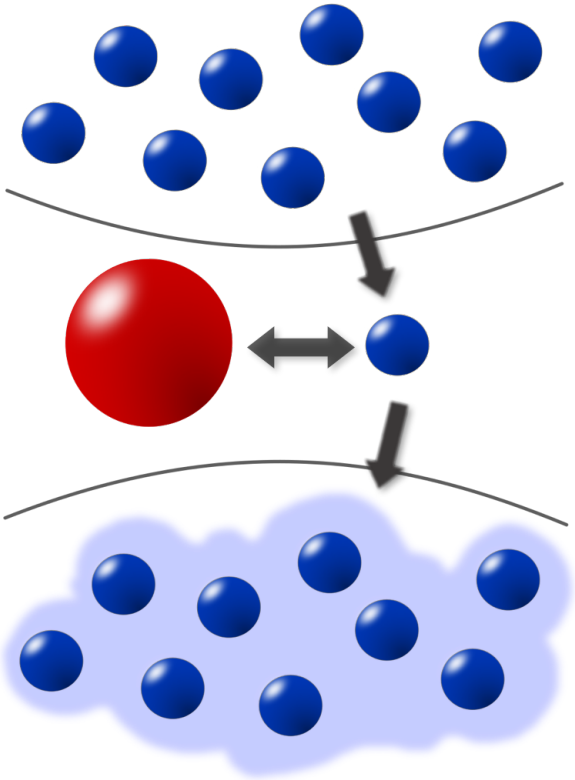

Figure 4.1.: Pictorial representation of the thermalization process in the collisional model framework: one has the system A in its initial state undergoing sequential collisions with ancillas all in the same thermal reference state. This causes system A to homogenize with B, i.e. it thermalizes to temperature T if B is a thermal bath.

bounds in Eqs.(4.7, 4.8), we will be interested not only on the reduced state of $\hat{\rho}_A$, but also in the reduced state of the bath $\hat{\rho}_B$ and in the joint state $\hat{\rho}_{AB}$ of the two systems. The joint state is given, as we already saw, by an equation of the form:

$$\hat{\rho}_{AB}(n) = \mathcal{U}_n \circ \cdots \circ \mathcal{U}_2 \circ \mathcal{U}_1 \left(\hat{\rho}_A(0) \bigotimes_{i=1}^{n} \hat{\eta}_{b_i}^{(\beta)} \right), \tag{4.25}$$

where $\mathcal{U}_i(\cdots) = \hat{U}_i(\cdots)\hat{U}_i^\dagger$ is the superoperator describing the interaction between A and the i-th ancilla. The reduced state of A can then be computed accordingly in the standard way via:

$$\hat{\rho}_A(n) = \mathrm{Tr}_{b_n}\left\{ \mathcal{U}_i(\hat{\rho}_A(n-1) \otimes \hat{\eta}_{b_n}^{(\beta)}) \right\} = \Phi(\hat{\rho}_A(n-1)), \tag{4.26}$$

where the Markovian character of the evolution has been understood, and in the last

equality we have explicitly written the evolution in terms of the stroboscopic dynamical map Φ. It also clear from this that the state of A is equivalently written as $\hat{\rho}_A(n) = \Phi^n(\hat{\rho}_A(0))$.

In a perfectly symmetrical way, we can compute also the environmental state as:

$$\hat{\rho}_B(n) = \mathrm{Tr}_A\left\{\hat{\rho}_{AB}(n)\right\} = \mathrm{Tr}_A\left\{\mathcal{U}_n \circ \cdots \circ \mathcal{U}_2 \circ \mathcal{U}_1 \left(\hat{\rho}_A(0) \bigotimes_{i=1}^{n} \hat{\eta}_{b_i}^{(\beta)}\right)\right\}. \tag{4.27}$$

Now, in order to ensure the thermalization for large enough n, we follow the receipt in [Bäumer et al. 2019; Campbell et al. 2018; Diòsi, Feldmann, and Kosloff 2006; Lorenzo, McCloskey, et al. 2015; Pezzutto, Paternostro, and Omar 2016; Scarani et al. 2002], which consists of assuming the ancillas to be isomorphic with A, so that it makes sense to choose the interaction Hamiltonian $\hat{H}_{\mathrm{int}}$ to be a partial SWAP generator, i.e. to be such that the unitary operator $\hat{U}_n$ can be written as:

$$\hat{U}_n = \exp\left[i\theta\hat{S}_n\right] = \cos(\theta)\hat{\mathbb{I}}_n + i\sin(\theta)\hat{S}_n, \tag{4.28}$$

where we indicate with $\theta \in]-\pi, \pi]$ a parameter gauging the strength of the swap interaction between A and an ancilla, the equivalent of what we previously indicated as $g\,\delta t$, and with $\hat{S}_n$ the swap operator acting on A and b_n. The swap operator is self-adjoint, i.e. $\hat{S}_n = \hat{S}_n^\dagger = \hat{S}_n^{-1}$, and it acts on a joint state of two isomorphic quantum systems as:

$$\hat{S}_n \left|\psi\right\rangle_A \otimes \left|\phi\right\rangle_{b_n} = \left|\phi\right\rangle_A \otimes \left|\psi\right\rangle_{b_n}. \tag{4.29}$$

We note that the action of the swap operator ensures thermalization, i.e.

$$\lim_{n\to\infty} \hat{\rho}_A(n) = \hat{\eta}_A^{(\beta)}, \tag{4.30}$$

and that with this choice the unitary operator $\hat{U}_i$ in Eq. (4.28) commutes with the sum of the free Hamiltonians $\hat{H}_A + \sum_i \hat{H}_{b_i}$, so that within this model we can state $E_{\mathrm{int}} = 0$, this implying that we can safely state $\Delta Q_A(n) = -\Delta Q_B(n)$, where we define:

$$\Delta Q_X(n) = \mathrm{Tr}\left\{\hat{H}_X(\hat{\rho}_X(n) - \hat{\rho}_X(0))\right\} \quad X = A, B. \tag{4.31}$$

Moreover, as shown in App. B.1, one can verify that the inequalities in Eqs.(4.7, 4.8)

still hold in the form:

$$\Delta S_A(n) \geq \beta \Delta Q_A(n), \tag{4.32}$$

$$\Delta S_A(n) \geq -\Delta S_B(n), \tag{4.33}$$

where $\Delta S_X(n)$ stands for the entropy difference between the zeroth and the n-th step of the process, namely:

$$\Delta S_X(n) = S(\hat{\rho}_X(n)) - S(\hat{\rho}_X(0)), \quad X = A, B. \tag{4.34}$$

At this point it is worth highlighting that computing ΔS_B with the environmental state at the n-th step as in Eq. (4.27) is in general a heavy task from the computational point of view, as one is required to diagonalize the full density matrix $\hat{\rho}_B(n)$ in order to keep track of the internal correlations of the environment due to the common interaction of the ancillas $b_1, b_2, \dots$ with A.

A different path consist instead in neglecting such correlations, following for instance [Campbell et al. 2018], obtaining a local version of the extrinsic bound as:

$$\Delta S_A(n) \geq \Delta S_B^{(\mathrm{loc})}(n), \tag{4.35}$$

which is weaker than the one in Eq. (4.8), as shown in App. B.1. Furthermore, since $E_{\mathrm{int}} = 0$, we still can use Eq. (4.21), so that we can derive the ordering:

$$\Delta S_A(n) \geq -\Delta S_B(n) \geq -\Delta S_B^{(\mathrm{loc})}(n) \geq \beta \Delta Q_A(n). \tag{4.36}$$

As proved numerically in the following, we effectively observe that the gap between $\Delta S_A(n)$ and $\Delta S_B(n)$ goes to zero asymptotically, so that the extrinsic bound in Eq. (4.8) turns out to be optimal. This result can be recast in a more informative shape considering that the mutual information $I_{A:B}$ can be expressed in terms of entropies relative to A and B via:

$$I_{A:B}(n) = S(\hat{\rho}_A(n)) + S(\hat{\rho}_B(n)) - S(\hat{\rho}_{AB}(n)), \tag{4.37}$$

so that saying that the gap between $\Delta S_A(n)$ and $-\Delta S_B(n)$ closes asymptotically amounts

to:

$$\lim_{n\to\infty} I_{A:B}(n) = 0. \tag{4.38}$$

The statement implied by Eq. (4.38) is far stronger than the one implied by Eq. (4.30): while the latter only implies that the joint state of A and B is locally thermal on A, the former also implies the explicit factorization of this joint state in the asymptotic limit, i.e.

$$\lim_{n\to\infty} \hat{\rho}_{AB}(n) = \hat{\eta}_A^{(\beta)} \otimes \hat{\Lambda}_B. \tag{4.39}$$

This result will be proved analytically for the strong collision regime ($|\theta| \geq \tan^{-1} 2$) in Sec. 4.4. A sort of analytical proof can be given also for the weak coupling regime, but under slightly different hypothesis. On the other hand, in the remaining of this section we will provide some numerical evidence for Eq. (4.39) in the weak coupling regime, assuming A and the b_i to be qubits.

We assume system A to have Hamiltonian:

$$\hat{H}_A = \frac{1}{2}\hat{\sigma}_A^{(3)}, \tag{4.40}$$

where $\hat{\sigma}^{(3)}$ is the diagonal Pauli operator and we measure the energy in units of $\hbar\omega = 1$. We also model the ancillas as two level systems with Hamiltonian $\hat{H}_{b_i} = \frac{1}{2}\hat{\sigma}_{b_i}^{(3)}$, so that A and the ancillas are isomorphic and the swap operator has a clear operational meaning.

To describe the state of A we exploit the Bloch representation of a qubit state, which consists in expressing the density matrix as:

$$\hat{\rho}_A(n) = \frac{\hat{\mathbb{I}}_A + \vec{r}(n)\cdot\vec{\sigma}_A}{2}, \tag{4.41}$$

where $\vec{r}^{\,(n)}$ is a three dimensional vector with $|\vec{r}(n)| \leq 1$ and $\vec{\sigma}_A = (\hat{\sigma}_A^{(1)}, \hat{\sigma}_A^{(2)}, \hat{\sigma}_A^{(3)})$. This representation allows for very simple expressions for the entropy and the mean energy of A:

$$S(\hat{\rho}_A(n)) = H_2\left(\frac{1+|\vec{r}(n)|}{2}\right), \tag{4.42}$$

$$E_A(n) = \mathrm{Tr}\left\{\hat{H}_A\hat{\rho}_A(n)\right\} = \frac{r_3(n)}{2}, \tag{4.43}$$

where $H_2(x) = -x\ln x-(1-x)\ln(1-x)$ is the Shannon binary entropy. From Eq. (4.42) we can immediately write:

$$\Delta S_A(n) = H_2\left(\frac{1+|\vec{r}(n)|}{2}\right) - H_2\left(\frac{1+|\vec{r}(0)|}{2}\right), \tag{4.44}$$

$$\Delta Q_A(n) = \frac{r_3(n)-r_3(0)}{2}. \tag{4.45}$$

Once we have expressed all the quantities of interest in terms of the vector $\vec{r}(n)$, we are interested in writing a master equation for this vector. Indeed it is easy to see that applying the partial swap transformation in Eq. (4.28) we have:

$$\begin{aligned}\hat{\rho}_{AB}(n) &= \hat{U}_n(\hat{\rho}A(n-1)\otimes\hat{\eta}_{b_n}^{(\beta)})\hat{U}_n^\dagger \\ &= \sin^2(\theta)\hat{\eta}_A^{(\beta)}\otimes\hat{\rho}_{b_n}(n-1)+\cos^2(\theta)\hat{\rho}_A(n-1)\otimes\hat{\eta}_{b_n}^{(\beta)} \\ &\quad -i\sin(\theta)\cos(\theta)\left[\hat{S}_n,\hat{\rho}_A(n-1)\otimes\hat{\eta}_{b_n}^{(\beta)}\right],\end{aligned} \tag{4.46}$$

so that tracing away the ancilla b_n we get:

$$\hat{\rho}_A(n) = \mathrm{Tr}\left\{\hat{\rho}_{AB}(n)\right\} = \sin^2(\theta)\hat{\eta}_A^{(\beta)} + \cos^2(\theta)\hat{\rho}_A(n-1). \tag{4.47}$$

From the last equation one can immediately deduce the following master equation:

$$\vec{r}(n) = \sin^2(\theta)\vec{s} + \cos^2(\theta)\vec{r}(n-1), \tag{4.48}$$

where $\vec{s}$ is the vector associated to $\hat{\eta}_A^{(\beta)}$ in the Bloch sphere, and has the very simple form:

$$\vec{s} = (0,0,s(\beta)) \qquad s(\beta) = -\tanh(\beta/2). \tag{4.49}$$

Iterating Eq. (4.48), we can formally integrate it, obtaining:

$$\vec{r}(n) = \cos^{2n}(\theta)\vec{r}(0) + (1-\cos^{2n}(\theta))\vec{s} \tag{4.50}$$

$$= \vec{s} + \cos^{2n}(\theta)\Delta\vec{r}(0), \tag{4.51}$$

where the symbol $\Delta\vec{r}(0) = \vec{r}(0) - \vec{s}$ stands for the difference between the Bloch vector of the input state of A and the Bloch vector associated to the thermal state $\hat{\eta}^{(\beta)}$. From the expression in Eq. (4.50) one is able to compute the modulus and the third component

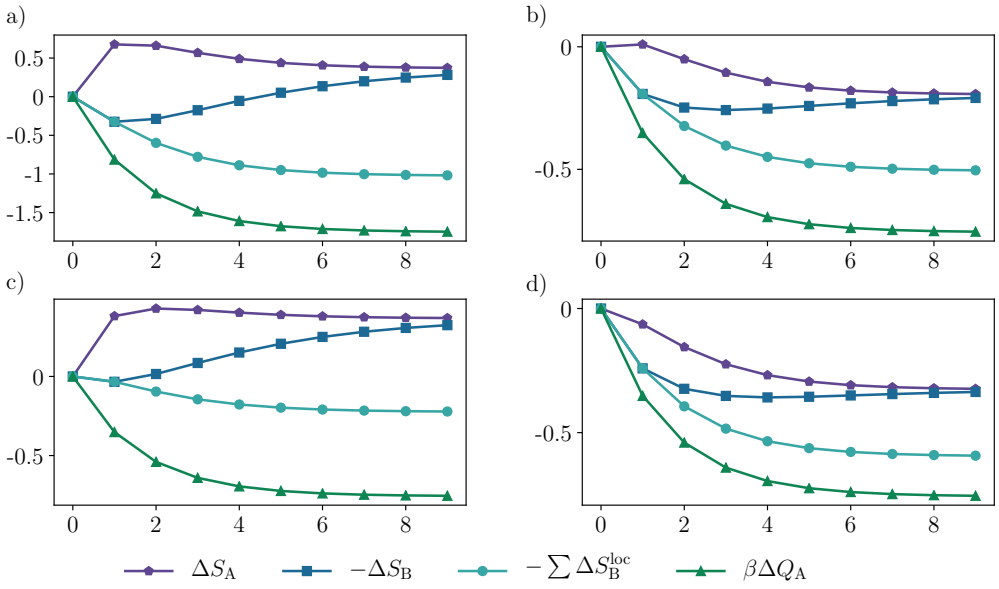

Figure 4.2.: Plot of the quantities involved in the bounds in Eq. (4.36) using the collisional model for a qubit. The plots show the behavior of this quantities for the first steps of the evolution, starting from different initial states of A. In particular we have $\vec{r}(0) = (0,0,1), (1/2,0,0), (1,0,0), (0,0,)$ in panels (a), (b), (c) and (d) respectively. As it is immediately seen the plotted quantities fulfill the ordering in Eq. (4.36). Moreover, as n increases the quantity $-\Delta S_B$ approaches ΔS_A, confirming that the extrinsic bound is optimal.

of $\vec{r}(n)$ as:

$$|\vec{r}(n)| = \sqrt{s(\beta)^2 + \cos^{4n}(\theta)|\Delta\vec{r}(0)|^2 + \cos^{2n}(\theta)s(\beta)\Delta r_3(0)}, \tag{4.52}$$

$$r_3(n) - r_3(0) = \left[\cos^{2n}(\theta) - 1\right]\Delta r_3(0). \tag{4.53}$$

We can follow the same reasoning to get analogous expressions for the output state of the ancillas after their interaction with A, obtaining:

$$\vec{s}(n) = \sin^2(\theta)\vec{r}(n-1) + \cos^2(\theta)\vec{s} = \vec{s} + \sin^2(\theta)\cos^{2(n-1)}(\theta)\Delta\vec{r}(0), \tag{4.54}$$

$$|\vec{s}(n)| = \sqrt{s(\beta)^2 + \sin^4(\theta)\cos^{4(n-1)}(\theta)|\Delta\vec{r}(0)|^2 + \sin^2(\theta)\cos^{2(n-1)}(\theta)s(\beta)\Delta r_3(0)}. \tag{4.55}$$

The last expression in particular can be used to compute the local entropy variation of the bath defined in App. B.1. In Fig. 4.2 we show some results obtained from this

model for different initial states of A. In particular the quantities ΔS_A, $-\beta\Delta Q_A$ and $-\sum \Delta S_B^{(loc)}$ have been plotted using the formulas derived above, while the computation of $-\Delta S_B$ requires the diagonalization of the full density matrix of the environmental state. As one can observe from the plot, independently from the initial state of A, the ordering between the bound that we stated in Eq. (4.36) is always fulfilled. Furthermore, we observe that ΔS_A always approaches $-\Delta S_B$ as n increases, suggesting that the bound in Eq. (4.8) is optimal.

4.4. Decay of correlations

In this section we want to demonstrate the factorization property conjectured in Eq. (4.39). We start noticing that Eq. (4.39) is trivially fulfilled if the initial state of A is already the thermal one. In facts in this case we have the initial joint state:

$$\hat{\rho}_{AB}(0) = \hat{\eta}_A^{(\beta)} \bigotimes_i \hat{\eta}_{b_i}^{(\beta)} \Rightarrow \hat{\rho}_{AB}(n) = \hat{\eta}_A^{(\beta)} \bigotimes_i \hat{\eta}_{b_i}^{(\beta)}, \tag{4.56}$$

since the state $\hat{\eta}^{(\beta)} \otimes \hat{\eta}^{(\beta)}$ is invariant under the action of the swap operator $\hat{S}$, so that the action of the unitary operator in Eq. (4.28) becomes trivial. The factorization property is also fulfilled trivially for an arbitrary initial state of A when the thermal state of the bath is the zero temperature one, i.e. $\beta \to \infty$ and the ground state of A is non-degenerate: in this case the Gibbs thermal state $\hat{\eta}_{b_i}^{(\beta)}$ corresponds to the pure state $|0\rangle_{b_i}$, so that:

$$\lim_{n\to\infty} \hat{\rho}_A(n) = |0_A\rangle\langle 0_A|\,, \tag{4.57}$$

which can be fulfilled only if the joint state of A and B approaches a state of the form $|0_A\rangle\langle 0_A| \otimes \hat{\Lambda}_B$.

Given these specific cases, we want to demonstrate Eq. (4.39) analytically. In order to reach the goal we consider a generic initial state of A, $\hat{\rho}_A(0) \neq \hat{\eta}_A^{(\beta)}$ and a finite temperature β of the thermal bath. We start our proof from the recursive equation for the joint state of A and B:

$$\hat{\rho}_{AB}(n) = \mathcal{U}_n(\hat{\rho}_{AB}(n-1)), \tag{4.58}$$

and write the joint state $\hat{\rho}_{AB}(n)$ as the sum of two contributions:

$$\hat{\rho}_{AB}(n) = \hat{R}_{AB}(n) + \hat{T}_{AB}(n). \tag{4.59}$$

The first term $\hat{R}_{AB}(n)$ contains all the contributions where the state of A is the thermal state factorized from the one of B, $\hat{T}_{AB}(n)$ containing all the other contributions. For the initial state we have clearly $\hat{R}_{AB}(0) = 0$ and $\hat{T}_{AB}(0) = \hat{\rho}_{AB}(0)$. Exploiting the properties of the swap operator, it is then possible to write two distinct recursive equations for $\hat{R}_{AB}(n)$ and $\hat{T}_{AB}(n)$ respectively. Since, as we already said, the state $\hat{\eta}^{(\beta)} \otimes \hat{\eta}^{(\beta)}$ is invariant under the action of the swap operator, we get immediately:

$$\mathcal{U}_{n+1}\left(\hat{R}_{AB}(n)\right) = \hat{R}_{AB}(n). \tag{4.60}$$

As a consequence $\hat{R}_{AB}(n+1)$ differs from $\hat{R}_{AB}(n)$ only via the contributions coming from the action of the swap on $\hat{T}_{AB}(n)$, so that we have:

$$\begin{aligned} \hat{R}_{AB}(n+1) &= \hat{R}_{AB}(n) + \sin^2(\theta)\hat{S}_{n+1}\hat{T}_{AB}(n)\hat{S}_{n+1}, & (4.61)\\ \hat{T}_{AB}(n+1) &= \cos^2(\theta)\hat{T}_{AB}(n) + i\sin(\theta)\cos(\theta)\Big[\hat{S}_{n+1}, \hat{T}_{AB}(n)\Big]. & (4.62) \end{aligned}$$

At this point, in order to demonstrate the factorization property, we only need to show that the norm of $\hat{T}_{AB}(n)$ goes to zero as n increases. From Eq. (4.62) and the subadditivity of the norm we get:

$$\begin{aligned} \left\|\hat{T}_{AB}(n+1)\right\| &\leq |\cos^2(\theta)| \left\|\hat{T}_{AB}(n)\right\| + |\sin(\theta)\cos(\theta)| \left\|\left[\hat{S}_{n+1}, \hat{T}_{AB}(n)\right]\right\| & (4.63)\\ &\leq \left(|\cos^2(\theta)| + 2|\sin(\theta)\cos(\theta)|\right) \left\|\hat{T}_{AB}(n)\right\|, & (4.64) \end{aligned}$$

where in the second line, thanks to the unitarity of $\hat{S}_n$, we used $\left\|\hat{S}_{n+1}\hat{T}_{AB}(n)\right\| = \left\|\hat{T}_{AB}(n)\right\|$. Iterating Eq. (4.63) we easily arrive to:

$$\left\|\hat{T}_{AB}(n+1)\right\| \leq \left(|\cos^2(\theta)| + 2|\sin(\theta)\cos(\theta)|\right)^{n+1} \|\hat{\rho}_{AB}(0)\|. \tag{4.65}$$

The proof is finally completed for the strong coupling regime by noticing that for $|\theta| > \tan^{-1}(2)$ the quantity in parenthesis is smaller than one, from which it follows:

$$\lim_{n\to\infty} \|T_{AB}(n)\| = 0, \tag{4.66}$$

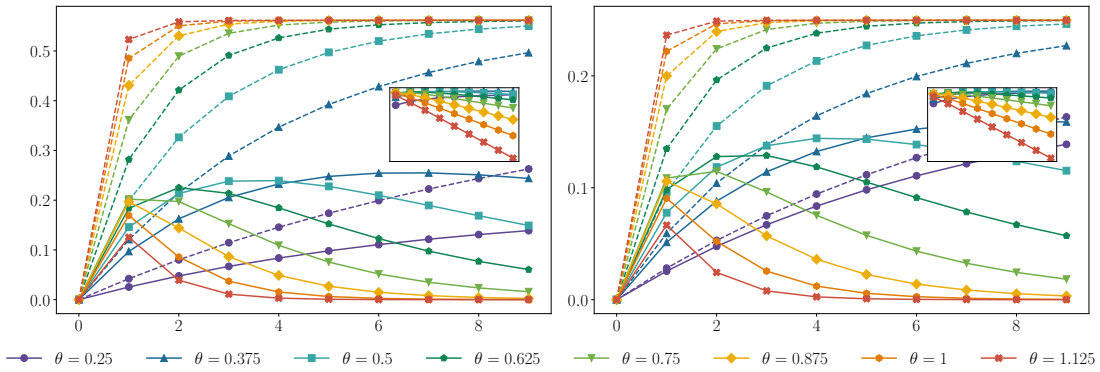

Figure 4.3.: Numerical evaluation of the bounds in Eqs.(4.7, 4.8) using the collisional model for a qubit. The dashed lines represent the quantity $\Delta S_A(n) - \beta \Delta Q_A(n)$ as a function of n for different values of θ, the swapping parameter: one can observe that this quantity grows monotonically with n, reaching an asymptotic value, as it is to be expected from Eq. (4.18). The solid lines show instead the quantity $\Delta S_A(n) + \Delta S_B(n)$, which is immediately seen to be non-monotonic and to become asymptotically zero as n increases, thus confirming the asymptotic factorization prediction. In the inset we inserted the same plots in logarithmic scale. The numerical values have been evaluated starting from an initial state of A described by the vector $\vec{r}(0) = (1/2, 0, 0)$, while the temperature of the bath correspond to $\beta = 1$ and $\beta = 0.5$ in left and right panel respectively.

which allows us to identify $\hat{\rho}_{AB}(n)$ with $\hat{R}_{AB}(n)$ for n large enough, thus proving our claim.

As for the weak coupling regime, we were able to give an analytical proof of the property only by slightly changing our hypotheses, as shown in App. B.2. On the other hand, as it can be observed from Fig. 4.3, we were able to collect numerical evidence that the factorization property holds also for the weak coupling regime under the same hypotheses used to prove the strong coupling regime. In facts the plots show how the mutual information between A and B goes to zero asymptotically for different coupling strengths, all below the threshold of $\tan^{-1} 2$.

CHAPTER 5

Interlude

This brief chapter is meant to be a sort of second introduction for the following two chapters. In fact, while in previous chapters we dealt with the study of open quantum systems, focusing in particular on collisional models, the next two chapters have a more practical spirit. In facts in Chap. 6 we will present a class of potential profiles that give rise to a special class of states which we dub "stretchable", in analogy with analogous phenomena in optics. In Chap. 7 we will instead see how a particle moving in a potential that varies in space can acquire a geometric phase which depends only on how the potential varies, and not on the velocity of the particle.

Both the problems are better understood if thought in the context of condensed matter physics, specifically in the context of semiconductors and band engineering: in facts, since the seminal work by Esaki and Tsu [Esaki and Tsu 1970], the field of band engineering in semiconductor has developed enormously [Capasso 1986; Franciosi and Walle 1996; Wolfe, Stillman, and Holonyak 1989; Yu, McCaldin, and McGill 1992], allowing for high-precision material engineering in order to achieve new effects, such as the negative differential resistance [Beltram, Capasso, Hutchinson, et al. 1989; Beltram, Capasso, Sivco, et al. 1990; Capasso and Kiehl 1985] and resonant tunneling [L. L. Chang, Esaki, and Tsu 1974; Luryi 1985], and to be able to build new conductors [Mimura et al. 1980], such as superlattice structures [L. Canali et al. 1996; Carpena, Gasparian, and Ortuño 1999; Esaki and L. L. Chang 1974; Helm 1995; Stęślicka et al. 2002] and 2-dimensional electron gases (2DEG) [Heiblum, Mendez, and Stern 1984; Stern and Das Sarma 1984].

Such precision is possible thanks to innovative techniques, such as the Molecular-Beam Epitaxy [Madhukar 1990; Orton and Foxon 2015] or Metal-Organic Chemical Vapor Deposition [Dauelsberg et al. 2005], where a semiconductor is built one layer of atoms after another. Thanks to these technologies it is possible nowadays to build electronic systems of any dimensionality, from quantum dots [Beenakker 1991; Hanson et al. 2007; Petta et al. 2005; Reimann and Manninen 2002; Wiel et al. 2002] to quantum wires [Harrison and Valavanis 2016; Hurt 2000; Nazarov and Blanter 2009] and electron waveguides [Alamo et al. 1998; McLennan et al. 1991; Timp 1992].

Given the importance of this branch of physics, before proceeding with the next chapters, we want to briefly review some basic concepts of the field, starting from the Bloch theorem and the band structure of solids in Sec. 5.1 before introducing the effective mass approximation in Sec. 5.2 and electron waveguiding in 2DEG in Sec. 5.3.

5.1. Bloch theorem and band structure

To understand the way actual solids are modeled and described, it is useful to start from a 1D situation, where some difficulties due to higher dimensionality are absent, this allowing us to focus on the main concepts. It must be however remembered that not all the properties of 1D systems can be straightforwardly extended to 2D or 3D systems, so that caution is required.

As solids are made out of a regular array of atoms, the simplest way to describe a solid is to start from the Schrödinger equation describing the motion of electrons in the array of atoms:

$$-\frac{\hbar^2}{2m}\frac{d^2\psi(x)}{dx^2} + \hat{V}(x)\psi(x) = E\psi(x) \tag{5.1}$$

where we assume the potential $V(x)$ to be periodic. A periodic potential is characterized by its period a, so that it holds:

$$\hat{V}(x) = \hat{V}(x + ma) \quad \forall m \in \mathbb{Z}. \tag{5.2}$$

An important property of a periodic potential is that its Fourier transform includes only plane waves with wavenumbers $h_n = n\frac{2\pi}{a}$, so that:

$$\hat{V}(x) = \sum_{n=-\infty}^{+\infty} V_n e^{ih_n x}. \tag{5.3}$$

In the following we want to see the implications for the eigenenergies and eigenstates of the Hamiltonian when the potential fulfills Eq. (5.3). In order to do so, we first note that for the special case $V(x) = 0$, the eigenfunctions of the Hamiltonian are the plane waves:

$$W_k(x) = \frac{1}{\sqrt{L}} e^{ikx} \tag{5.4}$$

where L is the length of the array under examination and the wavenumbers k are real, so that the energy eigenvalues are $E(k) = \frac{\hbar^2 k^2}{2m}$. The important point here is that the plane waves $W_k(x)$ form an orthonormal set, and thus can be used as an expansion set.

We further note that applying the operator $\hat{H} = \frac{\hat{p}_x^2}{2m} + \hat{V}(x)$ to a plane wave $W_k(x)$ we obtain a plane wave belonging to the subset $\mathbb{S}_k = \{W_k(x), W_{k+h_1}(x), W_{k-h_1}(x), \cdots\}$ of plane waves with wavenumbers $k + \hat{h}_n$. Also, the set $\mathbb{S}_k$ is closed with respect to the application of $\hat{H}$ to any of its elements, as it can be directly verified using Eq. (5.3): this implies that diagonalizing $\hat{H}$ within any $\mathbb{S}_k$ provides a valid set of eigenfunctions of $\hat{H}$ which we dub $\psi_k(x)$.

Moreover it is evident that two sets $\mathbb{S}_k$ and $\mathbb{S}_{k'}$ are different if and only if k and k' do not differ by an integer multiple of $2\pi/a$. One then defines the *Brillouin zone* as the fundamental region in k-space limited by $[-\pi/a, \pi/a]$.

All of this being said and done, we have that a generic wave function $\psi_k(x)$ can be expanded in terms of plane waves belonging to the set $\mathbb{S}_k$ as:

$$\psi_k(x) = \sum_n c_n(k) \frac{1}{\sqrt{L}} e^{i(k+h_n)x} \tag{5.5}$$

where we have that:

$$u_k(x) = \sum_n c_n(k) \frac{1}{\sqrt{L}} e^{ih_n x} = \sum_n c_n(k) \frac{1}{\sqrt{L}} e^{in(\frac{2\pi}{a})x} \tag{5.6}$$

is a periodic function with the same period a of the potential $\hat{V}(x)$. This is essentially the content of the *Bloch theorem*: any physically acceptable solution of the Schrödinger equation in presence of a periodic potential can be expressed in the form of a traveling wave modulated by a periodic function with the same periodicity of the potential:

$$\psi_k(x) = e^{ikx} u_k(x) \tag{5.7}$$

A first necessary remark is that up to now we are considering the Schrödinger equation in the interval $[-\infty, +\infty]$: from the physical point of view this is equivalent to considering the region $[0, L = Na]$, N being the total number of atoms in the chain, as N is in fact very large (already of the order 10^8 for $L = 1$ cm). The reason why one usually considers a large but finite region is that this allows one to count the states and distribute the electrons in the *energy bands*, a concept we are going to explore in a few lines. In order for the physics not to be influenced by the choice of a finite region, one usually considers periodic boundary conditions to solve the problem given by a periodic crystal, which amounts to require:

$$\psi(x + Na) = \psi(x) \tag{5.8}$$

As $\psi(x)$ must also be a Bloch function of wavenumber k, periodic boundary conditions restrict the allowed values of k to the ones fulfilling:

$$e^{ikNa} = 1 \Rightarrow k = \frac{2\pi}{Na} n, \quad n \in \mathbb{Z}. \tag{5.9}$$

Thus, as $L = Na$ becomes large, k must be considered as a discrete, though dense, variable.

As anticipated, the Bloch theorem also entails the fact that the energy spectrum of a periodic potential is made out of allowed regions, separated by gaps, called *energy bands*. To better understand this, we consider the instructive and paradigmatic example of the Kronig-Penney model: in this model one assumes the periodic potential $V(x)$ to be composed of quantum wells of width w separated by potential barriers of width b and height V_0, so that the period of the potential is $a = w + b$.

Within the unit cell in the region $[-w\, b]$ we can write the solution to the associated Schrödinger equation for $0 < E < V_0$ as the union of the solution in the region $[-w, 0]$, where $\hat{V}(x) = 0$, and the solution in the region $[0, b]$, where $\hat{V}(x) = V_0$, so that we have:

$$\psi(x) = \begin{cases} \psi_{\text{well}}(x) = Ae^{iqx} + Be^{-iqx} & \text{for } -w \leq x \leq 0 \\ \psi_{\text{bar}}(x) = Ce^{\beta x} + De^{-\beta x} & \text{for } 0 \leq x \leq b, \end{cases} \tag{5.10}$$

where $q = \sqrt{2mE/\hbar^2}$ and $\beta = \sqrt{2m(V_0 - E)/\hbar^2}$. The constants A, B, C, D must be found with the usual method of imposing the continuity of $\psi(x)$ and its first derivative at the point $x = 0$, and by imposing the boundary conditions required by the Bloch

theorem, namely:

$$\psi_{\text{bar}}(b) = e^{ika}\psi_{\text{well}}(-w) \tag{5.11}$$

$$\frac{d\psi_{\text{bar}}(x)}{dx}\Big|_{x=b} = e^{ika}\frac{\psi_{\text{well}}(x)}{dx}\Big|_{x=-w}. \tag{5.12}$$

This leads to a system of four equations in four unknown variables. As known from elementary algebra, a homogeneous system of n equations in n variables has a non-trivial solution if and only if the determinant of the coefficients matrix is zero. A direct computation of the determinant for the Kronig-Penney model leads to the equation:

$$\frac{\beta^2 - q^2}{2q\beta}\sinh(\beta b)\sin(qw) + \cosh(\beta b)\cos(qw) = \cos(ka). \tag{5.13}$$

This *compatibility equation* can be solved graphically, i.e. via numerical methods, as shown in Fig. 5.1, leading to the individuation of allowed energy regions, the already cited energy bands. In the standard approach, which can be found in any standard textbook on solid state physics, one usually consider the further simplification obtained by considering the width b of the barriers to go to zero while at the same time the height V_0 goes to infinity, keeping constant the product $V_0\, b$. Under this hypothesis the compatibility equation becomes:

$$P\frac{\sin(qa)}{qa} + \cos(qa) = \cos(ka) \tag{5.14}$$

where $P = mV_0ba/\hbar^2$ is a dimensionless parameter proportional to $V_0\, b$. $P = 0$ correspond to a free electron situation, whereas in the limit $P \to \infty$ one would recover the energy levels of the infinite well.

We saw how electrons moving in periodic potentials have their energy distributed in bands separated by energy gaps. However we assumed a perfect regular crystal, thus neglecting the presence of impurities and the vibrations of the lattice. In order to add this effects in the description of electrons in solid state systems, other approximations and methods are more convenient, such as the effective mass approximation we are going to review in the next section.

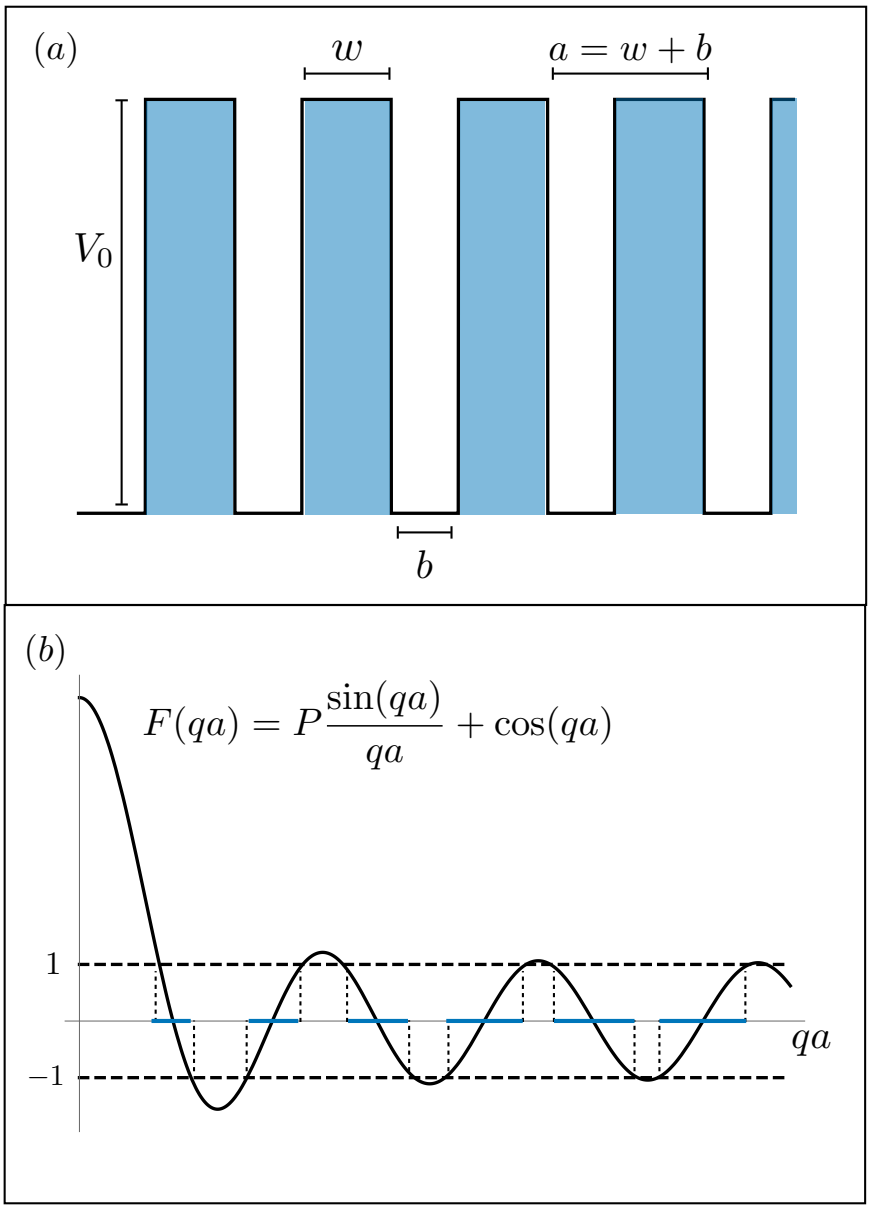

Figure 5.1.: The Kronig-Penney model. In panel (a) a sketch of the periodic potential assumed in the Kronig-Penney model is shown. In panel (b) we plotted of the lhs of Eq. (5.14) as a function of qa, where the constant P has been set equal to $3\pi/2$. When $|F(qa)| < 1$ the compatibility equation is satisfied, individuating the allowed values of qa and thus the allowed energies. This leads to the formation of energy bands, which have been highlighted in blue.

5.2. The effective mass approximation

In Sec. 5.1 we discussed the band structure of solids starting from the Schrödinger equation of an electron moving in a periodic potential. While it is true that a perfect lattice gives rise to a periodic potential, actual lattices contain impurities, so that the actual potential is almost periodic, but not quite. Also the vibrational motion of the atoms in the lattice gives rise to a deviation from a perfectly periodic potential. Moreover a voltage bias could be applied, so that also a drift potential would be present. In formulas we could write the actual potential, in three dimensions, as the sum of three distinct contributions:

$$\hat{V}(\vec{r}) = \hat{V}_L(\vec{r}) + \hat{V}_S(\vec{r}) + \hat{V}_E(\vec{r}), \tag{5.15}$$

where $V_L(\vec{r})$ is the periodic potential generated by the lattice in absence of impurities, $V_S(\vec{r})$ accounts for the random fluctuations due to vibrations and impurities and $V_E(\vec{r})$ is due to the applied bias. In order to find the electronic eigenfunctions we should thus solve the Schrödinger equation:

$$\frac{\partial}{\partial t}\psi(\vec{r},t) = \hat{H}\psi(\vec{r},t) + (V_S(\vec{r}) + V_E(\vec{r}))\,\psi(\vec{r},t), \tag{5.16}$$

$$\hat{H} = -\frac{\hbar^2}{2m}\nabla^2 + \hat{V}_L(\vec{r}). \tag{5.17}$$

Solving this equation is a very hard task. However it turns out that, under appropriate conditions, it is possible to use the *single band effective mass equation*:

$$\frac{\partial}{\partial t}\Psi(\vec{r},t) = E_\nu(-i\vec{\nabla})\Psi(\vec{r},t) + \hat{U}(\vec{r})\Psi(\vec{r},t), \tag{5.18}$$

$$\hat{U}(\vec{r}) = \hat{V}_S(\vec{r}) + V_E(\vec{r}), \tag{5.19}$$

where $\Psi(\vec{r},t)$ is known as the *envelope function* and $E_\nu(-i\vec{\nabla})$ is the dispersion relation of the band where the substitution $\vec{k} \to -i\vec{\nabla}$ has been performed. An important condition in order for the single band effective mass equation to be valid is that $\hat{U}(\vec{r})$ should not introduce relevant inter-band interactions, or, in other words, inter-band interactions should be negligible.

In order to demonstrate Eq. (5.18) we start from the Bloch theorem in Sec. 5.1, which

states that the eigenfunctions in presence of a periodic potential can be written as:

$$\psi_{\nu,\vec{k}}(\vec{r}) = u_{\nu,\vec{k}}(\vec{r})\frac{e^{i\vec{k}\cdot\vec{r}}}{\sqrt{\Omega}}, \tag{5.20}$$

where ν is the band index, $\vec{k}$ is the wavevector and Ω is the normalization volume. The periodic functions $\left|\nu,\vec{k}\right\rangle = \psi_{\nu,\vec{k}}(\vec{r})$ are orthogonal in both indexes, i.e.:

$$\left\langle \nu',\vec{k}\,'\middle|\nu,\vec{k}\right\rangle = \delta_{\nu,\nu'}\delta_{\vec{k},\vec{k}\,'}, \tag{5.21}$$

so that for $\vec{k}\,' = \vec{k}$ we have:

$$\left\langle \nu',\vec{k}\middle|\nu,\vec{k}\right\rangle = \int d^3r\, \Psi^*_{\nu',\vec{k}}(\vec{r})\Psi_{\nu,\vec{k}}(\vec{r}) = \int \frac{d^3r}{\Omega} u^*_{\nu',\vec{k}}(\vec{r})u_{\nu,\vec{k}}(\vec{r}) = \delta_{\nu,\nu'}, \tag{5.22}$$

which implies:

$$\int d^3r\, u^*_{\nu,\vec{k}}(\vec{r})u_{\nu,\vec{k}}(\vec{r}) = \Omega\delta_{\nu,\nu'}. \tag{5.23}$$

In order to see under which conditions Eq. (5.18) can be used, we expand the wave function in Eq. (5.16) in the $\left|\nu,\vec{k}\right\rangle$ basis:

$$\psi(\vec{r},t) = \sum_{\nu',\vec{k}'} c_{\nu',\vec{k}\,'}(t)\psi_{\nu',\vec{k}\,'}(\vec{r}) = \sum_{\nu',\vec{k}'} c_{\nu',\vec{k}\,'}(t)\left|\nu',\vec{k}\,'\right\rangle. \tag{5.24}$$

Inserting Eq. (5.24) in Eq. (5.16) and applying on the left $\left\langle \nu,\vec{k}\right|$ we obtain:

$$i\hbar\frac{d}{dt}c_{\nu,\vec{k}}(t) = \sum_{\nu',\vec{k}'}\left\langle \nu,\vec{k}\right|\hat{H} + \hat{U}(\vec{r})\left|\nu',\vec{k}\,'\right\rangle c_{\nu',\vec{k}\,'}(t). \tag{5.25}$$

Upon considering that the $\left|\nu',\vec{k}\,'\right\rangle$ are eigenfunctions of $\hat{H}$:

$$\left\langle \nu,\vec{k}\right|\hat{H}\left|\nu',\vec{k}\,'\right\rangle = E_{\nu'}(\vec{k}\,')\left\langle \nu,\vec{k}\middle|\nu',\vec{k}\,'\right\rangle = E_\nu(\vec{k})\delta_{\nu,\nu'}\delta_{\vec{k},\vec{k}\,'}, \tag{5.26}$$

we finally arrive to:

$$i\hbar\frac{d}{dt}c_{\nu,\vec{k}}(t) = E_\nu(\vec{k})c_{\nu,\vec{k}}(t) + \sum_{\nu',\vec{k}'}\left\langle \nu,\vec{k}\right|\hat{U}(\vec{r})\left|\nu',\vec{k}\,'\right\rangle c_{\nu',\vec{k}\,'}(t), \tag{5.27}$$

where the matrix elements $\left\langle \nu, \vec{k} \right| \hat{U}(\vec{r}) \left| \nu', \vec{k}' \right\rangle$ are worth:

$$\left\langle \nu, \vec{k} \right| \hat{U}(\vec{r}) \left| \nu', \vec{k}' \right\rangle = \int \frac{d^3r}{\Omega} u^*_{\nu,\vec{k}}(\vec{r}) u_{\nu',\vec{k}'}(\vec{r}) e^{i(\vec{k}'-\vec{k})\cdot\vec{r}} \hat{U}(\vec{r}). \tag{5.28}$$

We now go back to Eq. (5.18) and expand the envelope function in terms of the orthonormal base of plane waves $\left|\vec{k}\right\rangle = e^{i\vec{k}\cdot\vec{r}}/\sqrt{\Omega}$:

$$\Psi(\vec{r}, t) = \sum_{\vec{k}'} c_{\vec{k}'}(t) \left|\vec{k}'\right\rangle = \sum_{\vec{k}'} c_{\vec{k}'}(t) \frac{e^{i\vec{k}'\cdot\vec{r}}}{\Omega}. \tag{5.29}$$

Inserting this into Eq. (5.18) and multiplying on the left by $\left\langle \vec{k} \right|$ we get:

$$i\hbar \frac{d}{dt} c_{\vec{k}}(t) = \sum_{\vec{k}'} \left\langle \vec{k} \right| \hat{H} + \hat{U}(\vec{r}) \left| \vec{k}' \right\rangle c_{\vec{k}'}(t). \tag{5.30}$$

As the effect of a spatial derivative $\vec{\nabla}$ on $\left|\vec{k}\right\rangle$ is only to drop a factor $i\vec{k}$ from the exponential, Eq. (5.30) can be rewritten as:

$$i\hbar \frac{d}{dt} c_{\vec{k}}(t) = \sum_{\vec{k}'} \left\langle \vec{k} \right| E_\nu(-i\vec{\nabla}) + \hat{U}(\vec{r}) \left| \vec{k}' \right\rangle c_{\vec{k}'}(t), \tag{5.31}$$

where, as already anticipated, $E_\nu(-i\vec{\nabla})$ is the dispersion relation of the ν-th band where $\vec{k}$ has been substituted by $-i\vec{\nabla}$. From the orthogonality relation of the $\left|\vec{k}\right\rangle$, we can immediately derive the identity:

$$\left\langle \vec{k} \right| E_\nu(-i\vec{\nabla}) \left| \vec{k}' \right\rangle = E_\nu(\vec{k}) \delta_{\vec{k},\vec{k}'}, \tag{5.32}$$

thanks to which we are allowed to write:

$$i\hbar \frac{d}{dt} c_{\vec{k}}(t) = E_\nu(\vec{k}) c_{\vec{k}}(t) + \sum_{\vec{k}'} \left\langle \vec{k} \right| \hat{U}(\vec{r}) \left| \vec{k}' \right\rangle c_{\vec{k}'}(t), \tag{5.33}$$

where the matrix elements $\left\langle \vec{k} \right| \hat{U}(\vec{r}) \left| \vec{k}' \right\rangle$ can be written explicitly as:

$$\left\langle \vec{k} \right| \hat{U}(\vec{r}) \left| \vec{k}' \right\rangle = \int \frac{d^3r}{\Omega} e^{i(\vec{k}'-\vec{k})\cdot\vec{r}} \hat{U}(\vec{r}). \tag{5.34}$$

At this point we compare Eq. (5.27) with Eq. (5.34), noticing that the two differential equations are equivalent if it holds:

$$\left\langle \nu, \vec{k} \right| \hat{U}(\vec{r}) \left| \nu', \vec{k}\,' \right\rangle = \delta_{\nu,\nu'} \left\langle \vec{k} \right| \hat{U}(\vec{r}) \left| \vec{k}\,' \right\rangle . \tag{5.35}$$

This is basically the condition we anticipated at the beginning of the section: for the single band effective mass equation to be valid, the matrix elements of the potential $\hat{U}(\vec{R})$ between states from different bands should be negligible. We can be more precise on this by considering the following integral over a unit cell of the lattice:

$$\int d^3r u^*_{\nu,\vec{k}}(\vec{r}) u_{\nu',\vec{k}'}(\vec{r}) e^{i(\vec{k}'-\vec{k})\cdot\vec{r}} \hat{U}(\vec{r}) = e^{i(\vec{k}'-\vec{k})\cdot\vec{r}_n} \hat{U}(\vec{r}_n) \int d^3r\, u^*_{\nu,\vec{k}}(\vec{r}) u_{\nu',\vec{k}'}(\vec{r}) \tag{5.36}$$

$$e^{i(\vec{k}'-\vec{k})\cdot\vec{r}_n} \hat{U}(\vec{r}_n) \delta_{\nu,\nu'} \frac{\Omega}{N}, \tag{5.37}$$

where $\vec{r}_n$ is the position of the center of the unit cell and N is the number of unit cells in the lattice. In writing Eq. (5.36) we have made two assumptions: first we assumed the potential $\hat{U}(\vec{r})$ to be slowly varying, so that we can consider it constant over a unit cell, thus allowing us to bring it out of the integral; secondly we have assumed that:

$$\int d^3r\, u^*_{\nu,\vec{k}}(\vec{r}) u_{\nu',\vec{k}'}(\vec{r}) \simeq \int d^3r\, u^*_{\nu,\vec{k}}(\vec{r}) u_{\nu',\vec{k}}(\vec{r}) = \delta_{\nu,\nu'} \frac{\Omega}{N}, \tag{5.38}$$

that is, we assumed the periodic functions $u_{\nu,\vec{k}}(\vec{r})$ not to vary much with $\vec{k}$. Within these assumptions it is also possible to write a relation between the real electronic wavefunction and the envelope function via:

$$\psi(\vec{r},t) = \sum_{\vec{k}} c_{\nu,\vec{k}}(t) \frac{e^{i\vec{k}\cdot\vec{r}}}{\sqrt{\Omega}} u_{\nu,\vec{k}}(\vec{r}) = u_{\nu,\vec{k}}(\vec{r}) \sum_{\vec{k}} c_{\nu,\vec{k}}(t) \frac{e^{i\vec{k}\cdot\vec{r}}}{\sqrt{\Omega}} = u_{\nu,\vec{k}}(\vec{r}) \Psi(\vec{r},t). \tag{5.39}$$

So one can see from Eq. (5.39) that the real electronic wave function is the product of a microscopic periodic function and the envelope function. So what one practically does using Eq. (5.18) is to ignore the microscopic periodic part of the wavefunction, focusing on the envelope function, which describes the electrons on a somehow course-grained scale. This is possible given the assumptions we made are valid, namely that the potential is slowly varying and that the microscopic periodic functions $u_{\nu,\vec{k}}(\vec{r})$ do not change much with $\vec{k}$. The single band effective mass equation is widely used to describe electrons in the conduction band, while as anticipated it breaks down when

dealing with the valence band, for which the multi-band effective mass equation must be used [Datta 1989]. Nonetheless Eq. (5.18) has also been used to describe some kinds of heterojunctions where the gap between the two materials is not too large as to involve the valence band. All in all the single band effective mass equation is a precious tool which will be used in the next section to describe electrons in the conduction band of 2DEGs and electron waveguides.

5.3. 2DEG and electron waveguiding

As anticipated at the beginning of this chapter, it is possible nowadays to build semiconductors one layer of atoms after another: this entails the possibility of building *heterojunctions*, i.e. semiconductors made out by the junction of two different materials with similar crystalline structure, like for instance GaAs and AlGaAS.

An exhaustive discussion over heterojunctions would take us quite a long time, and it would be beyond the scope of the present chapter. What is important to highlight here is that, by inserting donor impurities in the AlGaAS (n-AlGaAS) it is possible to have free charge carriers, this leading to a rise of the Fermi level of the material. When joined with an undoped semiconductor such as GaAs, due to the mismatch of the Fermi levels and energy gap between valence and conduction bands in the two materials, this causes the free electron to move from the n-AlGaAs to the interface between the two materials, thus giving rise to a 2-dimensional electron gas (2DEG).

This is all that concerns us about heterojunctions for the scopes of this chapter, and we suggest the interested reader to check the large amount of literature available on the subject [Bastard 1988; Capasso 1990].

2DEGs are characterized by a high carrier concentration, typically one order of magnitude higher than in bulk semiconductors, and high mobility, which can be even two orders of magnitude higher than in bulk semiconductors, depending also on other factors such as temperature and magnetic field.

The motion of electrons in the conduction band can be described through the single band effective mass equation in Eq. (5.18). Allowing for the presence of a magnetic field, this equation can be rewritten in a time-independent form as:

$$\left[E_c + \frac{(i\hbar\vec{\nabla} + e\vec{A})^2}{2m^*}\hat{U}(\vec{r})\right]\Psi(\vec{r}) = E\Psi(\vec{r}), \tag{5.40}$$

where E_c is the energy at the bottom of the conduction band and $\vec{A}$ is the vector potential accounting for the magnetic field. For the case of a 2DEG, there will be some confining potential $\hat{U}(z)$ along the z axis, limiting the motion of the electrons in the $x-y$ plane. Assuming for the moment a zero magnetic field, the envelope function will have the form:

$$\Psi(\vec{r}) = \phi_n(z)e^{ik_x x}e^{ik_y y}, \tag{5.41}$$

with a dispersion relation of the form:

$$E = E_c + \epsilon_n + \frac{\hbar^2}{2m^*}\left(k_x^2 + k_y^2\right), \tag{5.42}$$

where $\phi_n(z)$ are eigenfunctions of the n-th subband along the z direction, and ϵ_n are the corresponding eigenenergies. In the low temperature regime only the lowest of these subbands will be occupied, so that the motion of the electrons along z can be ignored as a matter of fact. We can thus rewrite the effective mass equation in two dimensions as:

$$\left[E_s + \frac{(i\hbar\vec{\nabla} + e\vec{A})^2}{2m^*} + \hat{U}(x,y)\right]\Psi(x,y) = E\Psi(x,y), \tag{5.43}$$

where $E_s = E_c + \epsilon_1$. This equation allows for a simple treatment and understanding of the motion of conduction electrons in 2DEGs, leading to the concept of *magneto-electric subbands* and electron waveguiding.

Consider a conductor which is uniform along the x direction and is characterized by some confining potential $\hat{U}(y)$ along the y direction. The effective mass equation can then be written as:

$$\left[E_s + \frac{(i\hbar\vec{\nabla} + e\vec{A})^2}{2m^*} + \hat{U}(y)\right]\Psi(x,y) = E\Psi(x,y). \tag{5.44}$$

If we also assume the magnetic field to be constant and directed along z, which can be described through the vector potential

$$\vec{A} = -By\,\hat{x} \Rightarrow A_x = -By,\ A_y = 0, \tag{5.45}$$

the equation can be further rewritten as:

$$\left[E_s + \frac{(p_x + eBy)^2}{2m^*} + \frac{p_y^2}{2m^*} + \hat{U}(y)\right]\Psi(x,y) = E\Psi(x,y), \tag{5.46}$$

where

$$p_x = -i\hbar\frac{\partial}{\partial x}, \quad p_y = -i\hbar\frac{\partial}{\partial y}. \tag{5.47}$$

The solutions to Eq. (5.46) are easily seen to be of the form:

$$\Psi(x,y) = \frac{1}{\sqrt{L}}e^{ik_x x}\chi(y), \tag{5.48}$$

where L is the normalization length and $\chi(y)$ satisfies:

$$\left[E_s + \frac{(\hbar k_x + eBy)^2}{2m^*} + \frac{p_y^2}{2m^*} + \hat{U}(y)\right]\chi(y) = E\chi(y). \tag{5.49}$$

Equation (5.49), as a matter of fact, is a one-dimensional Schrödinger equation giving rise to a set of discrete levels described by functions $(\chi_1(y), \chi_2(y), \cdots)$. So, as it can be seen from Eq. (5.48), the envelope function for the electrons in the conduction band of a 2DEG is made out of plane waves along the x direction, describing the fact that electrons are propagating along that direction, multiplied by a transverse eigenfunction given by the solution of Eq. (5.49), thus dividing the electrons into subbands, which are analogous to the transverse modes of electromagnetic waveguides. The form of the functions $\chi_1(y), \chi_2(y), \cdots$ depends on both the magnetic field and the confining potential, so that by engineering the latter it is possible to obtain traveling waves with an almost arbitrary transverse profile: it is with this in mind that the following chapters were originally conceived. Specifically, in absence of magnetic field, the transverse profile of the wave will depend only on the confining potential $\hat{U}(y)$, which can be chosen in order to obtain a desired profile.

CHAPTER 6

Stretchable states

The huge increase in our ability to build materials with specific desired property has led in recent years to a growing attention towards photonic metamaterials with *near-zero parameters* [Liberal and Engheta 2017; Niu et al. 2018]: by this one means media where the relative permittivity or the relative permeability, or both, are almost zero. This interest is readily explained looking at the Helmholtz equation for electro-magnetic waves propagating in a medium:

$$\nabla^2 \boldsymbol{E} = v_{\text{ph}} \frac{\partial^2}{\partial t^2} \boldsymbol{E} = \mu\epsilon\omega^2 \boldsymbol{E}, \tag{6.1}$$

where $\boldsymbol{E}$ is the electric field and $v_{\text{ph}} = 1/\sqrt{\epsilon\mu}$ is the phase velocity, with ϵ being the permittivity of the medium and μ its permeability. From Eq. (6.1) one can immediately see that as either ϵ or μ becomes zero, then the phase velocity goes to infinity [Reshef et al. 2017]: this has profound consequences on the wave propagation [Alù et al. 2007; Nguyen, L. Chen, and Halterman 2010; M. Silveirinha and Engheta 2006; Ziolkowski 2004], as an infinite phase velocity implies the decoupling of the electrical and magnetic components of the wave, and thus an effective decoupling of the spatial and temporal field variations.

Thanks to this in a metamaterial one can have, for instance, a wave whose frequency and wavelength are independent, so that one can have large frequency and large wavelength at the same time: the increase of the wavelength without affecting the frequency

corresponds to a "stretching" of the wave. This kind of effects has deep technological implications, from which the great interest in such materials arises, as it allows for tunneling in distorted channels [Edwards, Alù, M. G. Silveirinha, et al. 2009; Edwards, Alù, Young, et al. 2008; M. Silveirinha and Engheta 2006], radiation pattern tailoring [Alù et al. 2007; Pacheco-Peña et al. 2014], boosted non-linear effects [Argyropoulos, P.-Y. Chen, et al. 2012; Argyropoulos, D'Aguanno, and Alù 2014; Sokhoyan and Atwater 2013; Suchowski et al. 2013] and cloaking [Pendry, Schurig, and Smith 2006; Schurig et al. 2006], just to cite some.

On the other side, as reviewed in the previous chapter, also the field of band engineering in semiconductor has reached a level where we can build materials within the atomic layer precision [D. E. Chang et al. 2018]: this possibility, together with the analogies between photon and electrons [Datta 1995], has lead some researchers to investigate how the discoveries made in the field of photonic metamaterials [Song and Gabor 2018] can be exported to the field of semiconductor physics.

It is in this spirit that some pioneering works have started the field of quantum metamaterials, leading to matter waves cloaking [Liao et al. 2013; Zhang et al. 2008], subwavelength focusing [Cheianov, Fal'ko, and Altshuler 2007; M. G. Silveirinha and Engheta 2013] and spintronics applications [Chesi and Coish 2015], inspiring also the project of new devices, such as superconducting structures [Castellanos-Beltran et al. 2008; Zheludev 2010], faster circuits and optical devices [M. G. Silveirinha and Engheta 2012, 2014].

In this chapter we are going to show how, thanks to the electron-photon analogy, it is possible to build media, dubbed quantum metamaterials, where matter waves behave with similar effects to the ones observed in photonic metamaterials. It is in this context that the following sections take steps: by following a reverse engineering approach, in Sec. 6.1 we are going to give sufficient and necessary conditions on a potential profile for it to sustain stable configurations of stretched wave functions, i.e. wave functions that are flat in a region of the potential. We will then see in Sec. 6.2 how this potential profiles can be applied when dealing with more than one spatial dimension, for instance in 2D materials. After establishing these conditions we will give some examples building stretching profiles starting from the well-known infinite well potential in Sec. 6.3, deriving both the expression of the wave function and the energy eigenvalues corresponding to such profiles, seeing how they differ from the corresponding potential without stretching.

6.1. Stretching potentials in 1D systems

The starting point of our analysis is the electron-photon analogy. In facts matter waves are described by the Schrödinger equation:

$$\nabla^2\psi_E(x) = -\frac{2m}{\hbar^2}\left(E - V(\vec{x})\right)\psi_E(x). \tag{6.2}$$

Comparing Eq. (6.2) with Eq. (6.1), we recognize that the $-\frac{2m}{\hbar^2}(E - V(\vec{x}))$ term is the matter waves counterpart of the $\epsilon\mu\omega^2$ term of the Helmholtz equation. Thus we see that in a quantum metamaterial the equivalent of the condition of having ϵ or μ near-zero is to have $E - V(\vec{x}) = 0$. Reversing the perspective, Eq. (6.2) can be used to identify the spatial properties a potential $V(\vec{x})$ must have in order to obtain a target wave-function $\psi_{\text{tar}}(\vec{x})$ which is energetically stable, in formulas:

$$V(\vec{x}) - E = \frac{\hbar^2}{2m}\frac{\nabla^2\psi_{\text{tar}}(\vec{x})}{\psi_{\text{tar}}(\vec{x})}. \tag{6.3}$$

This equation allows us to easily write down a condition for the wave-function $\psi_{\text{tar}}(\vec{x})$ to have a constant value in some spatial region $\mathcal{R}$. Specifically it is clear that a necessary condition for a stretched wave-function is to have a constant potential in the region of interest, i.e.:

$$\psi_{\text{tar}}(\vec{x}) = \text{const.} \Rightarrow V(\vec{x}) = \text{const.} \qquad \forall\vec{x} \in \mathcal{R}. \tag{6.4}$$

Starting from this necessary condition, it is not so simple to find a sufficient condition for the stretching. In facts, even a constant potential does not guarantee the stretching of the wave-function, as one must consider also the matching of the boundary conditions for the wave function.

Our method to solve this problem consist in creating a new potential profile starting from a given original one, which we call *seeding potential*, so that we are able to define energetically stable stretched state starting from the original non stretched ones. We are now going to show this method for the simple but paradigmatic case of a particle trapped in a 1D potential, which allows for an analytical treatment of the problem. In a 1D setting the Schrödinger equation becomes:

$$\partial_x^2\psi_E(x) = -\frac{2m}{\hbar^2}(E - V(x))\psi_E(x), \tag{6.5}$$

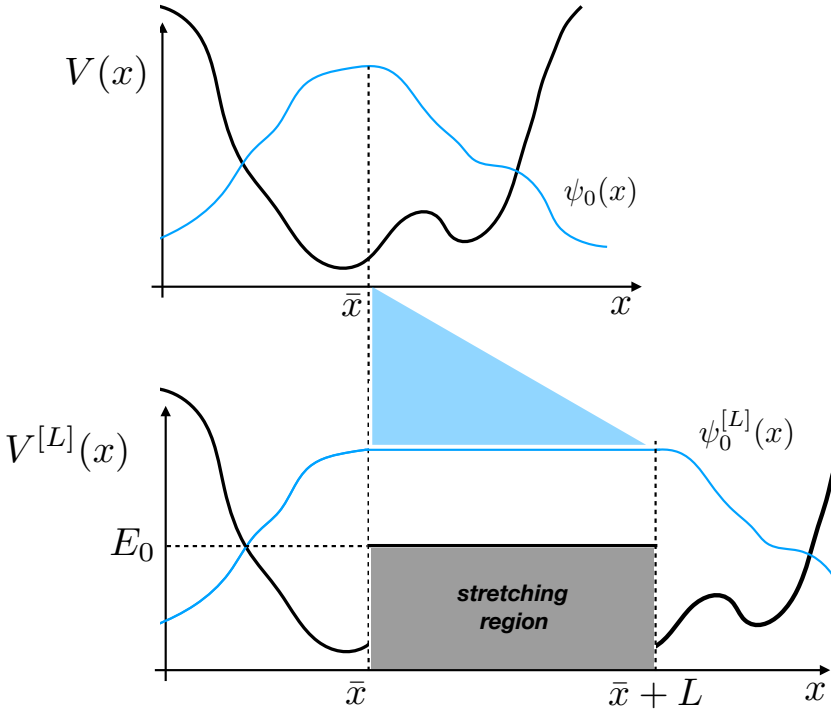

Figure 6.1.: A sketch of the stretching procedure. In the upper panel we show the original potential profile $V(x)$, or seeding potential (black line), and the associated wave function $\psi_0(x)$(blue line) with eigenenergy E_0. In the lower panel we show instead a modified version of the potential $V^{[L]}(x)$ where we performed a cut in correspondence of the stationary point of $\bar{x}$ of $\psi_0(x)$, inserting a constant profile with energy E_0 connecting the two regions. This new potential supports a stretched wave function $\psi_0^{[L](x)}$ whose energy is still E_0, but is flat in the region $[\bar{x}, \bar{x}+L]$.

where $V(x)$ is some arbitrary seeding potential. As it can be found in any quantum mechanics textbook [Sakurai and Napolitano 2017], Eq. (6.5) admits an orthonormal set of bound-state eigenfunctions $\{\psi_n(x), E_n\}$ where the E_n are the associated eigenenergies which we assume to be ordered in increasing order with respect to n. Another known fact is that the n-th eigenfunction $\psi_n(x)$ has n nodes, and thus at least $n+1$ stationary points. Let us indicate with $\bar{x}$ the only stationary point of the ground state wave-function, for which it holds:

$$\partial_x \psi_0(\bar{x}) = 0. \tag{6.6}$$

We then consider a modified version of the seeding potential, shown in Fig. 6.1, where we cut it at point $\bar{x}$, separating the two halves with a spatial distance L. In the region

$[\bar{x}, \bar{x}+L]$ we insert a constant potential of value E_0, the energy of the original ground state wave-function, obtaining the new potential:

$$V^{[L]}(x) = \begin{cases} V(x) & \text{for } x \leq \bar{x}, \\ E_0 & \text{for } \bar{x} < x < \bar{x}+L, \\ V(x-L) & \text{for } x \geq \bar{x}+L. \end{cases} \tag{6.7}$$

The crucial observation is that the new Schrödinger equation:

$$\partial_x^2 \psi_E(x) = -\frac{2m}{\hbar^2}(E - V^{[L]}(x))\psi_E(x), \tag{6.8}$$

still admits E_0 as eigenvalue for any choice of L. Moreover it is simple to find a solution $\psi^{[L]}_{E=E_0}(x)$ for Eq. (6.8): in facts in the region $x < \bar{x}$ we can take $\psi^{[L]}_{E=E_0}(x) = \psi_0(x)$, as well as in the region $x \geq \bar{x}+L$ we can take $\psi^{[L]}_{E=E_0}(x) = \psi_0(x-L)$. Being left with the central region, we notice that this region admits solutions with energy E_0 once we choose $\psi^{[L]}_{E=E_0}(x)$ to be constant and equal to $\psi_0(\bar{x})$ in order to match the boundary conditions.

Resuming, starting from a seeding potential $V(x)$ we have defined an entire family of stretching potential depending on the parameter L:

$$\mathcal{F}^{[L]}(V) = \{V^{[L]}(x);\ L \geq 0\}, \tag{6.9}$$

whose elements admit as ground state the stretched wave-function

$$\psi_0^{[L]}(x) = \begin{cases} \psi_0(x) & \text{for } x \leq \bar{x}, \\ \psi_0(\bar{x}) & \text{for } \bar{x} < x < \bar{x}+L, \\ \psi_0(x-L) & \text{for } x \geq \bar{x}+L, \end{cases} \tag{6.10}$$

which has still E_0 as associated eigenvalue. As by construction the wave functions $\psi_0^{[L]}(x)$ have no nodes, we are assured that they still represent the ground-state of the stretched potential. As for the other energy levels of the seeding potential, none of the observation above applies. We can instead say that, in general, the other levels will not correspond to the stretched version of their original counterpart, as it would be impossible to match the boundary conditions. Moreover, even their energy eigenvalues will be different from the original ones: as the new potential $V^{[L]}(x)$ will be in general shallower than the seeding one, one can expect the energy gaps between different levels to reduce:

$$E_{n+1} - E_n \geq E^{[L]}_{n+1} - E^{[L]}_n, \tag{6.11}$$

vanishing in the limit of $L \to \infty$.

The procedure we just described can be applied also when the ground state wave function has more than one stationary point $\{\bar{x}_1, \bar{x}_2, \dots\}$. In this case it is possible to define a vector $\vec{L} = (L_1, L_2, \dots)$ to identify the family of potentials:

$$\mathcal{F}^{[\vec{L}]}(V) = \{V^{[\vec{L}]}(x); \vec{L} = (L_1, L_2, \dots)\}, \tag{6.12}$$

characterized by the positive independent parameters $L_1, L_2, \dots$ each inducing a different modification on $V(x)$. If for instance the wave function $\psi_0(x)$ have j stationary points, we can obtain the new potential $V^{[\vec{L}]}(x)$ by cutting $V(x)$ into $j+1$ parts in correspondence of the stationary points $\bar{x}_j$ and inserting constant potential regions of length L_j and height E_0 to sew the different regions. The corresponding ground state $\psi_0^{[L]}(x)$ can then be found along the same line above, using the former solution $\psi_0(x)$ in the regions corresponding to the seeding potential and connecting them with constant lines of values $\psi_0(\bar{x}_1), \psi_0(\bar{x}_2), \dots$ in order to match the proper boundary conditions. For the same zero-node argument, we re also ensured that $\psi_0^{[L]}(x)$ represents the ground-state configuration in the new potential.

This very construction can be further generalized to the excited states of the seeding potential, as illustrated in Fig. 6.2: considering an excited state wave function $\psi_n(x)$, it is sufficient to consider its stationary points and perform the cuts on the seeding potential $V(x)$ in correspondence of these points. The only difference with the previous case will be in the height of the constant potentials connecting the regions of the original seeding potential, which will be the energy E_n of the state considered and not the ground state energy E_0. Moreover, when stretching the n-th excited state, we are ensured that its stretched counterpart will still be the n-th level, because of the node counting argument already illustrated. As for the other energy levels, because of the same reasons illustrated for the ground state, the ones above E_n get compressed as L increases:

$$E_{n'+1}^{[L']} - E_{n'}^{[L']} \leq E_{n'+1}^{[L]} - E_{n'}^{[L]} \quad \text{for } n' \geq n,\ L' \geq L. \tag{6.13}$$

As for the states with energy below E_n, their behavior will typically be richer than the one observed for the states above the stretched one, and in general no forecast can be done on it. However, we anticipate, explaining it better in Sec. 6.3, that in general the levels below the stretched one will form multiplexes of almost degenerate states.

We conclude this section by showing that, at least in 1D, the construction we presented exhaust the problem. In facts considering a potential $W(x)$ admitting a stretched state

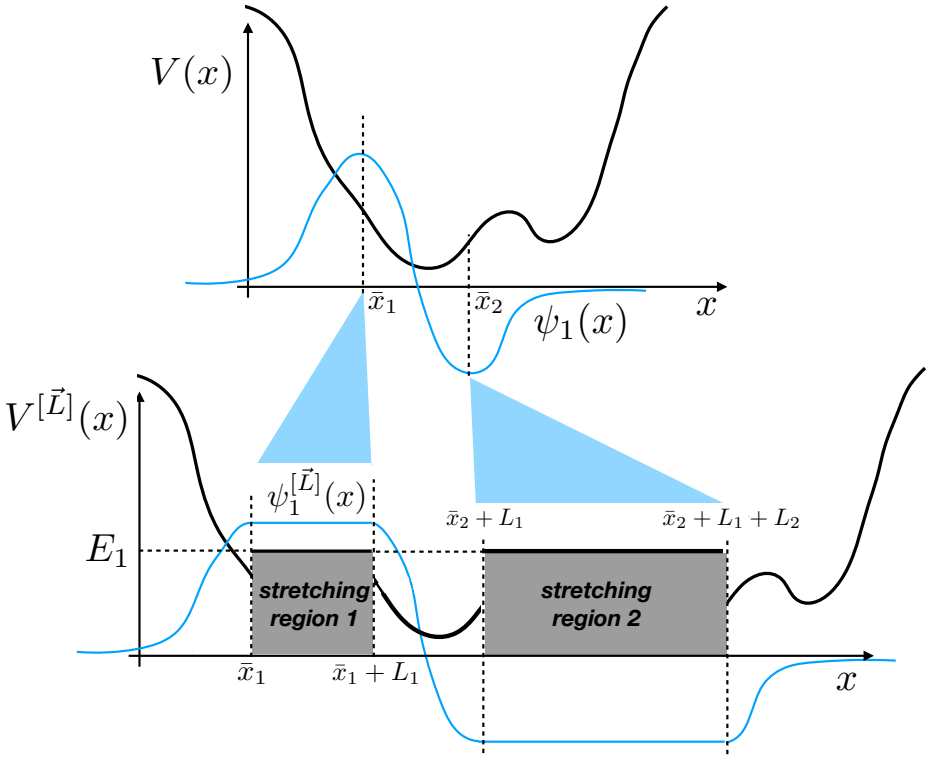

Figure 6.2.: Pictorial representation of a potential with two stretching region. In the upper panel the seeding potential $V(x)$ is shown (black line) together with the wave function $\psi_1(x)$ which present two stationary points. In the lower panel one can see the modified version of the potential $V^{[\vec{L}]}(x)$ where there are two cuts in correspondence of the two stationary points $\bar{x}_1$ and $\bar{x}_2$ where two constant profiles of energy E_1 have been inserted. The corresponding wave function presents, accordingly, two stretched region of length L_1 and L_2 respectively.

$\psi_E(x)$ as eigenvector with associated energy E, we can show that $W(x)$ must stem from a seeding potential which has a non stretched eigenstate with energy E. In practice we are saying that a potential $W(x)$ admits a stretched eigenstate if and only if it belongs to a family $\mathcal{F}^{[L]}(V)$. We already proved with our construction that if $W(x)$ belongs to $\mathcal{F}^{[L]}(V)$, then it admits a stretched eigenstate. The reversed implication can be proved by reversing the construction previously shown.

We consider, for simplicity but without loss of generality, a potential $W(x)$ which admits a stretched ground state with energy E. As the generalization to multiple stretching regions is straightforward, we also assume this ground state to have only one stretching

region $\mathcal{I} = [\bar{x}, \bar{x} + L]$ for which:

$$\psi_E(x) = \text{const.} \Rightarrow W(x) = \text{const.} \quad \forall x \in \mathcal{I}. \tag{6.14}$$

We then take $L' < L$ and define the potential $W^{[L']}(x)$, which is identical to $W(x)$ for $x \leq \bar{x} + L - L'$, while for $x > \bar{x} + L - L'$ it amounts to the shifted version of $W(x)$, $W(x + L')$:

$$W^{[L']}(x) = \begin{cases} W(x) & \text{for } x \leq \bar{x} + L - L', \\ W(x + L') & \text{for } x > \bar{x} + L - L'. \end{cases} \tag{6.15}$$

Reversing the construction of the stretched state, one sees immediately that the potential $W^{[L']}(x)$ admits the following eigenvector with energy E:

$$\psi_E^{[L']}(x) = \begin{cases} \psi_E(x) & \text{for } x \leq \bar{x} + L - L' \\ \psi_E(x + L') & \text{for } x > \bar{x} + L - L' \end{cases}, \tag{6.16}$$

where one can see that the boundary conditions are automatically matched, as $\psi_E(x + L')$ and $W^{[L']}(x + L')$ are constant in the region $]\bar{x} + L - L', \bar{x} + L] \subseteq \mathcal{I}$. For all $L' < L$, $\psi_E^{[L']}(x)$ is a stretched state, while as $L' = L$ this is not true anymore, since $W^{[L]}(x)$ becomes a seeding potential with eigenfunction $\psi_E^{[L]}(x)$, which by construction admits a stationary point in $\bar{x}$ and no stretching. Finally, taking $V(x) = W^{[L]}(x)$ we can write $W(x) = V^{[L]}(x)$, thus proving that $W(x)$ belongs to $\mathcal{F}^{[L]}(W^{[L]}(x))$, completing our discussion.

6.2. Stretching in higher spatial dimensions

A natural path to follow after investigating 1D stretching potentials, is to check wether the 1D construction can be extended to higher dimensionality. A very simple generalization is obtained for instance when dealing with seeding potentials exhibiting an explicit separation of the spatial coordinates:

$$V(\vec{x}) = \sum_j V_j(x_j), \tag{6.17}$$

where x_j is the j-th element of $\vec{x}$. In this case the eigensolutions can be written in the form:

$$\psi_E(\vec{x}) = \prod_j \psi_{E_j}^{(j)}(x_j) \quad E = \sum_j E_j, \tag{6.18}$$

where all the $\psi_{E_j}^{(j)}(x_j)$ satisfy:

$$\partial_{x_j}^2 \psi_{E_j}^{(j)}(x_j) = -\frac{2m}{\hbar^2}(E_j - V_j(x_j))\psi_{E_j}^{(j)}(x_j). \tag{6.19}$$

It is clear that in this specific case we can treat each spatial dimension separately, following the same procedure illustrated for 1D potentials. An example of this is given in App. C.1.

Unlucky, extending the stretched construction in more than one dimension beyond the simple case just shown is a more demanding task. In facts the interplay between the various spatial coordinates in the seeding potential does not allow us to separate the spatial coordinates acting on only one of them without interfering with the others. On the other hand it is possible to give a solution to this problem for potentials where the interplay between the different spatial coordinates is small. In order to illustrate this concept, we focus on a 2D geometry: we consider a particle A moving in the (x, y) plane under the action of seeding potential which is translationally invariant with respect to the y coordinate, which amounts to say $V(x, y) = V(x)$, from which it follows the Schrödinger equation:

$$(\partial_x^2 + \partial_y^2)\psi_E(x, y) = -\frac{2m}{\hbar^2}(E - V(x))\psi_E(x, y). \tag{6.20}$$

The solutions to this equation can be readily written as:

$$\psi_E(x, y) = e^{iky}\psi_n(x), \quad E = E_n + \frac{\hbar^2 k^2}{2m}, \tag{6.21}$$

where $\psi_n(x)$ is the n-th eigenstate with eigenvalue E_n of the 1D problem defined by $V(x)$. We then proceed taking, for simplicity, the case $n = 0$, so that $\psi_0(x)$ is the ground state of $V(x)$ with energy E_0, and we consider the new Schrödinger equation:

$$(\partial_x^2 + \partial_y^2)\psi_E(x, y) = -\frac{2m}{\hbar^2}(E - V^{[L(y)]}(x))\psi_E(x, y), \tag{6.22}$$

where with $V^{[L(y)]}$ we mean a stretched version of the seeding potential $V(x)$ where the stretching length depends on the y coordinate. We focus now on the case where the $L(y)$ varies only on a limited interval $y \in \mathcal{I} = [y_{\text{in}}, y_{\text{fin}}]$, while for $y < y_{\text{in}}$ or $y > y_{\text{fin}}$ we assume the stretching length to be constant with values $L_{\text{in}} = L(y_{\text{in}})$ and $L_{\text{fin}} = L(y_{\text{fin}})$ respectively.

A very simple instance allowing for an analytical solution is given when $L(y)$ is constant and $L_{\text{in}} = L_{\text{fin}}$, where we can write the ansatz:

$$\psi_E(x,y) = e^{iky}\psi_n^{[L]}(x), \quad E = E_n^{[L]} + \frac{\hbar^2 k^2}{2m}, \tag{6.23}$$

where $\psi_n^{[L]}(x)$ and $E_n^{[L]}$ are eigensolutions of the 1D problem defined by the potential $V^{[L]}(x)$. Taking for instance $n = 0$, what we get is a wave-function that is uniformly stretched along the x direction for any given y:

$$\psi_E(x,y) = e^{iky}\psi_0^{[L]}(x), \quad E = E_0 + \frac{\hbar^2 k^2}{2m}. \tag{6.24}$$

This is nothing but a specific instance of the situation described in Eq. (6.17). This is however only a very simple exception, since as soon as $L(y)$ is not constant the potential acquires an y dependence. A useful way to tackle the problem is to consider the ansatz:

$$\psi_E(x,y) = e^{iky}\tilde{\psi}(x,y), \tag{6.25}$$

where, apart from the phase factor, we allow for a residual dependence on y in $\psi(x,y)$. Inserting this ansatz in the Schrödinger equation associated to the problem we get:

$$\partial_x^2\tilde{\psi}(x,y) = -\frac{2m}{\hbar^2}[E - V^{[L(y)]}(x)]\tilde{\psi}(x,y) + \Delta(x,y), \tag{6.26}$$

$$\Delta(x,y) = -\partial_y^2\tilde{\psi}(x,y) - 2ik\partial_y\tilde{\psi}(x,y). \tag{6.27}$$

Now, the point to note is that Eq (6.26) is identical to Eq. (6.8) apart from the $\Delta(x,y)$ contribution. Thus, as long as we can neglect this term, we can use the solution in Eq. (6.10) to approximate $\tilde{\psi}(x,y)$, obtaining:

$$\psi_E(x,y) \simeq e^{iky}\psi_0^{[L(y)]}(x), \quad E = E_0 + \frac{\hbar^2 k^2}{2m}. \tag{6.28}$$

Intuitively we can imagine that this solution will be valid, i.e. $\Delta(x,y)$ will be negligible, as long as the function $L(y)$ varies slowly. For the ansatz choice in Eq. (6.28), the extra

term becomes:

$$\Delta(x,y)\Big|_{\psi_0^{[L(y)]}(x)} = \tag{6.29}$$
$$-\Theta(x'-x)\left[\partial_{x'}\psi_0(x')L''(y) + \left(2ik\partial_{x'}\psi_0(x') + \partial_{x'}^2\psi_0(x')L'(y)\right)L'(y)\right]_{x'=x-L(y)},$$

where $L'(y)$ and $L''(y)$ are the first and second derivative of $L(y)$ respectively. It is immediate to see that in the limit where $L(y)$ is almost constant, the rhs of the last equation gets suppressed. We can be more quantitative on this respect by computing the ℓ^2 norm [Nielsen and Chuang 2010] of $\Delta(x,y)$:

$$\begin{aligned}
\|\Delta(x,y)\|^2 &= \int_{-\infty}^{\infty} dx\,|\Delta(x,y)|^2 = \int_{\bar{x}}^{\infty} dx\left|\partial_x\psi_0(x)\left(L''(y)+2ikL'(y)\right)+\partial_x^2\psi_0(x)\left(L'(y)\right)^2\right|^2 \\
&\leq \int_{-\infty}^{\infty} dx\left|\partial_x\psi_0(x)\left(L''(y)+2ikL'(y)\right)+\partial_x^2\psi_0(x)\left(L'(y)\right)^2\right|^2 \\
&\leq |L''(y)+2ikL'(y)|\int_{-\infty}^{\infty} dx\,|\partial_x\psi_0(x)|^2 + |L'(y)|^4\int_{-\infty}^{\infty} dx\left|\partial_x^2\psi_0(x)\right|^2 \\
&+ 2\,|L'(y)|^2\,|L''(y)+2ikL'(y)|\sqrt{\int_{-\infty}^{\infty} dx\,|\partial_x\psi_0(x)|^2\int_{-\infty}^{\infty} dx\,|\partial_x^2\psi_0(x)|^2} \\
&= \left(|L''(y)+2ikL'(y)|\sqrt{\int_{-\infty}^{\infty} dx\,|\partial_x\psi_0(x)|^2} + |L'(y)|^2\sqrt{\int_{-\infty}^{\infty} dx\,|\partial_x^2\psi_0(x)|^2}\right)^2 \\
&= \left(|L''(y)+2ikL'(y)|\,\frac{\sqrt{\langle\hat{p}_x^2\rangle_0}}{\hbar} + |L'(y)|^2\,\frac{\sqrt{\langle\hat{p}_x^4\rangle_0}}{\hbar^2}\right)^2,
\end{aligned} \tag{6.30}$$

where to keep notation simple we indicate with $\langle\cdots\rangle_0$ the expectation value with respect to $\psi_0(x)$ and $\hat{p}_x^2$ is the transverse kinetic energy. Our next goal is to compute the ℓ^2 norm of the function $f(x,y) = -\frac{2m}{\hbar^2}[E - V^{[L(y)]}(x)]\psi_0^{[L(y)]}(x)$:

$$\begin{aligned}
\|f(x,y)\|^2 &= \int_{-\infty}^{\infty} dx\,|f(x,y)|^2 = \int_{-\infty}^{\infty} dx\left|\partial_x^2\psi_0^{[L(y)]}(x)\right|^2 \\
&= \int_{-\infty}^{\bar{x}} dx\left|\partial_x^2\psi_0(x)\right|^2 + \int_{\bar{x}+L}^{\infty} dx\left|\partial_x^2\psi_0(x-L)\right|^2 \\
&= \int_{-\infty}^{\infty} dx\left|\partial_x^2\psi_0(x)\right|^2 = \frac{\langle\hat{p}_x^4\rangle_0}{\hbar^4}.
\end{aligned} \tag{6.31}$$

Finally, comparing the final expression of Eq. (6.31) with the final expression in

Eq. (6.30), we can state that as long as the inequality

$$\frac{\langle \hat{p}_x^4 \rangle_0}{\langle \hat{p}_x^2 \rangle_0 \hbar^2} \gg \frac{|L''(y)|^2 + 4k^2 |L'(y)|^2}{(1 - |L'(y)|^2)^2} \tag{6.32}$$

holds, we are sure that also

$$\|f(x,y)\| \gg \|\Delta(x,y)\| \tag{6.33}$$

is valid, thus showing that the $\Delta(x,y)$ contribution is negligible when integrating over a not too large interval.

With this we have concluded our treatment of stretching in higher dimensions, showing how the problem is not trivial, but instead requires many considerations in order to get a meaningful approximate solution. In the next section we are going to return to the analytically treatable 1D situation, illustrating practically through some examples the effect of stretching a potential on the wave functions and their energy eigenvalues.

6.3. Stretching the infinite well

In this section we want to show through some examples how the presence of a stretched state influences the system, in particular the shape of the wave function and its associated energy eigenvalue, both for the stretched state and the others.

In order to be practical, we consider as seeding potential an infinite well of width a:

$$V(x) = \begin{cases} 0 & \text{for } |x| < a/2 \\ +\infty & \text{otherwise} \end{cases}, \tag{6.34}$$

whose eigenfunctions are well known to be:

$$\psi_n(x) = \sqrt{2}a \begin{cases} \cos\left(\frac{\pi(n+1)x}{a}\right) & \text{for } n \geq 0 \text{ even}, \\ \sin\left(\frac{\pi(n+1)x}{a}\right) & \text{for } n \geq 1 \text{ odd}, \end{cases} \tag{6.35}$$

with associated energy eigenvalues:

$$E_n = \frac{\pi^2 (n+1)^2 \hbar^2}{2ma^2}. \tag{6.36}$$

As first instance of stretching potential, we want to build a potential profile that

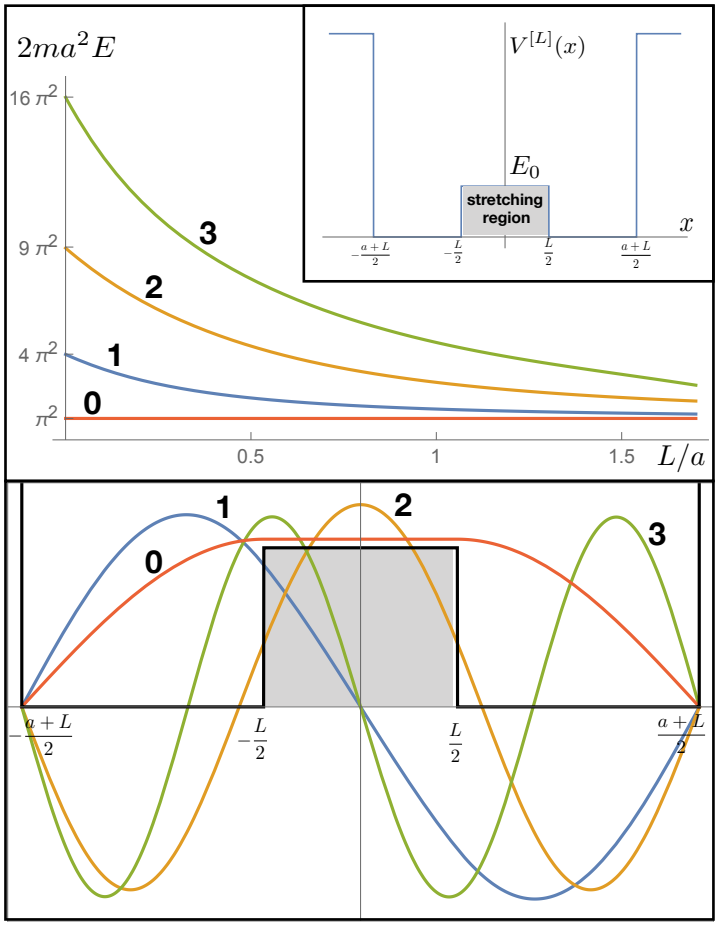

Figure 6.3.: Wave functions and energy levels for ground state stretching. Upper panel: the inset shows a sketch of the potential profile under examination, which gives rise to a stretched ground state, while in the panel the energy of the first four levels is plotted as a function of the stretching length L. As one can notice, as L increases the energy of the ground state is unaffected, as it is the energy of the stretched state, while the higher energy levels get compressed, as it would be expected in a continuum limit. Lower panel: plot of the wave functions of the first four energy levels of the infinite well modified in order to sustain a stretched ground state for the specific ratio $L/a = 0.4$. It is possible to notice how the ground state wave function is flat in correspondence of the barrier, while all the other wave functions retain their oscillatory behavior.

supports a stretched ground state. From the expression of $\psi_0(x)$ in Eq. (6.35) we immediately verify that it has only one extremal point at the center of the well. Hence, we perform a cut at this point, inserting a potential barrier of length L and height E_0, obtaining the potential shown in the inset of Fig. 6.3. The new problem defined by the

stretching potential can be solved analytically with no difficulties.

As we are stretching the ground state, we are sure that the first allowed solution is $E = E_0 = \frac{\pi^2\hbar^2}{2ma^2}$, with associated wave function as in Eq. (6.10). As for the excited states, their energy and eigenfunctions can be found with the standard method [Griffiths and Schroeter 2018] of solving the Schrödinger equation in each region of the potential and imposing the continuity of the wave function and its first derivative. We define:

$$\bar{k} = \sqrt{\frac{2m(E - E_0)}{\hbar^2}}, \quad k = \sqrt{\frac{2mE}{\hbar^2}}, \tag{6.37}$$

getting the two following quantization conditions:

$$k \cot\left(\frac{ak}{2}\right) = \bar{k} \tan\frac{\bar{k}L}{2}, \tag{6.38}$$

$$k \cot\left(\frac{ak}{2}\right) = -\bar{k} \cot\left(\frac{\bar{k}L}{2}\right). \tag{6.39}$$

for even and odd states respectively. The solutions to this two equations are plot in the upper panel of Fig. 6.3 of a function of the stretching length L: as one can see the energy of the ground state is not influenced by the stretching, while the other energy levels get compressed, as anticipated in Sec. 6.1. This is due to the fact that as L becomes large, the system becomes more and more similar to free space, and hence the energy levels approach the continuum. On the other hand, as L approaches zero we recover the energies of the infinite well, as expected.

As for the wave functions, plotted in the lower panel of Fig. 6.3, we can observe that in the region corresponding to the barrier the ground state wave-function is flat, as we wanted it to be, while the other wave functions still keep an oscillatory nature.

Another possibility to examine is to stretch an excited state of the infinite well. Considering for instance an excited state wave function $\psi_n(x)$, with n even, we can verify that it has a stationary point in $x = 0$, just as the ground state. Thus, in order to stretch such state, we can use the same potential shown in the inset of Fig. 6.3, but setting the height of the barrier equal to E_n. Making this choice, by virtue of what has been said in Sec. 6.1, $E = E_n$ is a proper eigenvalue of the problem irrespectively of the stretching length L. For $E > E_n$, one can easily find that the quantization conditions are the same of the previous instance, as in Eqs.(6.38, 6.39). However, now the model admits also eigenvalues for $E < E_n$. These energies can be found via the following two

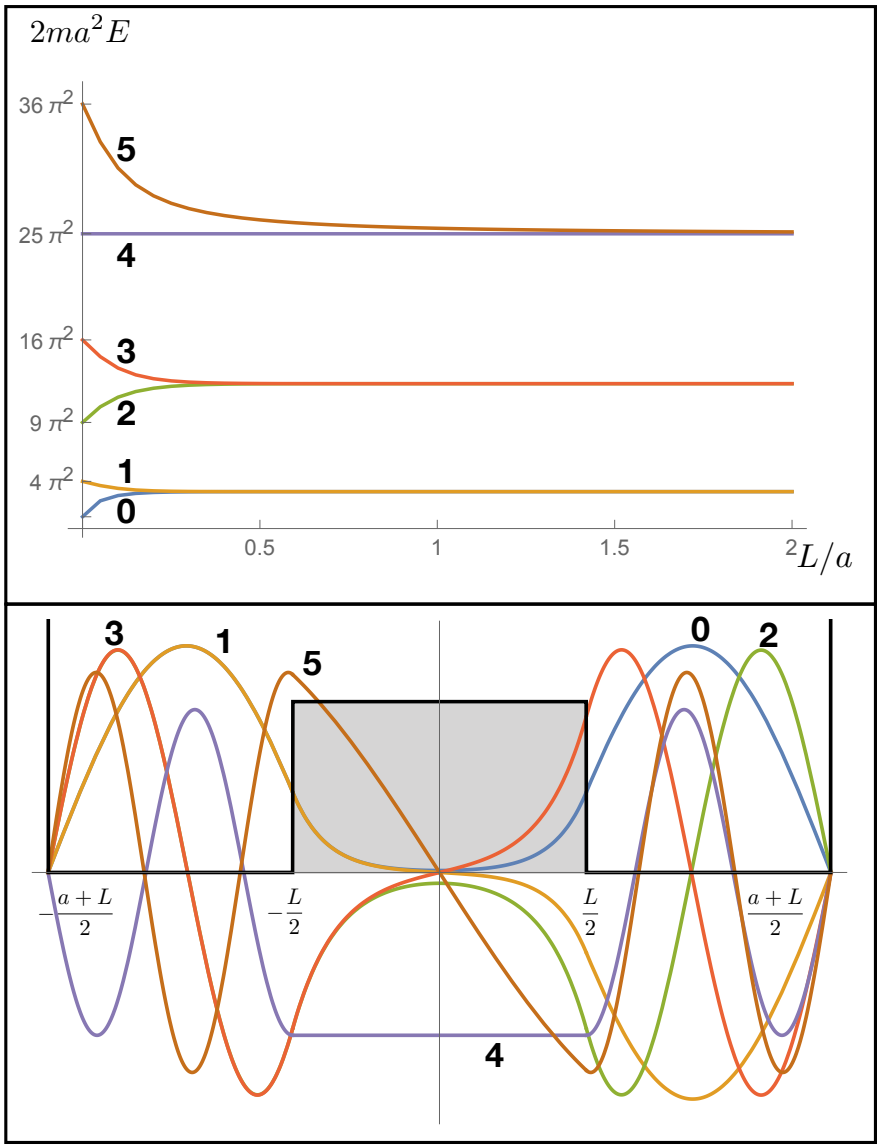

Figure 6.4.: Upper panel: plot of the first six energy levels for the case where the height of the barrier equals the energy E_4 of the fifth energy level. As one can observe, the states with higher energy than E_4 behave as in the case of ground state stretching, while the levels below E_4 form a doublets structure. Lower panel: plot of the wave functions for the first six levels for the specific ratio $a/L = 0.6$. From here it is possible to observe that the doublets in the upper panel correspond to states with opposite symmetry.

quantization conditions:

$$-k\cot\left(\frac{ak}{2}\right) = \gamma\tanh\left(\frac{\gamma L}{2}\right), \tag{6.40}$$

$$-k\cot\left(\frac{ak}{2}\right) = \gamma\coth\left(\frac{\gamma L}{2}\right), \tag{6.41}$$

for even and odd states respectively, where $\gamma = \sqrt{2m(E_n - E)/\hbar^2}$. We note that these two quantization conditions become exactly the same in the limit $L \gg a$, and thus we expect them to lead to a doublet structure in the lower part of the spectrum. This fact has a simple physical interpretation: we can look at the system as the union of two distinct identical wells separated by a potential barrier, that interact via tunnel effect. As L becomes large, the tunnel coupling becomes weaker and thus the two wells start behaving as independent, giving rise to the doublets structure. While these predictions are confirmed in the upper panel of Fig. 6.4, we notice that the same argument can also be applied to the stretched state and the next higher level, i.e. $n = 4, 5$: as L becomes large the energy E_5 approaches E_4, and thus its wave function becomes essentially linear in the stretching interval, as for small argument $\sin(x) \simeq x$.

The last instance we want to analyze is one where we deal with multi-parameter stretching, that is, a situation where there is more than one stretching region. To this aim we consider the stretching of the first excited level of the infinite well $\psi_1(x) = \sqrt{\frac{2}{a}} \sin\left(\frac{2\pi}{a}\right)$, which possesses two extremal points located at $\bar{x}_\pm = \pm\frac{a}{4}$. Accordingly we want to look at the potential profile:

$$V(x) = \begin{cases} \infty & \text{for } x < -\frac{a}{2} - L_1 \\ 0 & \text{for } \frac{a}{2} - L_1 \leq x \leq -\frac{a}{4} - L_1 \\ E_1 & \text{for } -\frac{a}{4} - L_1 \leq x \leq -\frac{a}{4} \\ 0 & \text{for } -\frac{a}{4} \leq x \leq \frac{a}{4} \\ E_1 & \text{for } \frac{a}{4} \leq x \leq \frac{a}{4} + L_2 \\ 0 & \text{for } \frac{a}{4} + L_2 \leq x \leq \frac{a}{2} + L_2 \\ \infty & \text{for } x > \frac{a}{2} + L_2 \end{cases} \tag{6.42}$$

where $E_1 = \frac{4\pi^2\hbar^2}{2ma^2}$ and L_1, L_2 are the stretching parameters, as shown in the bottom panel of Fig. 6.5. The spectrum can be easily computed also in this case. We have of course the solution $E = E_1$, which does not depend on the stretching parameters, while

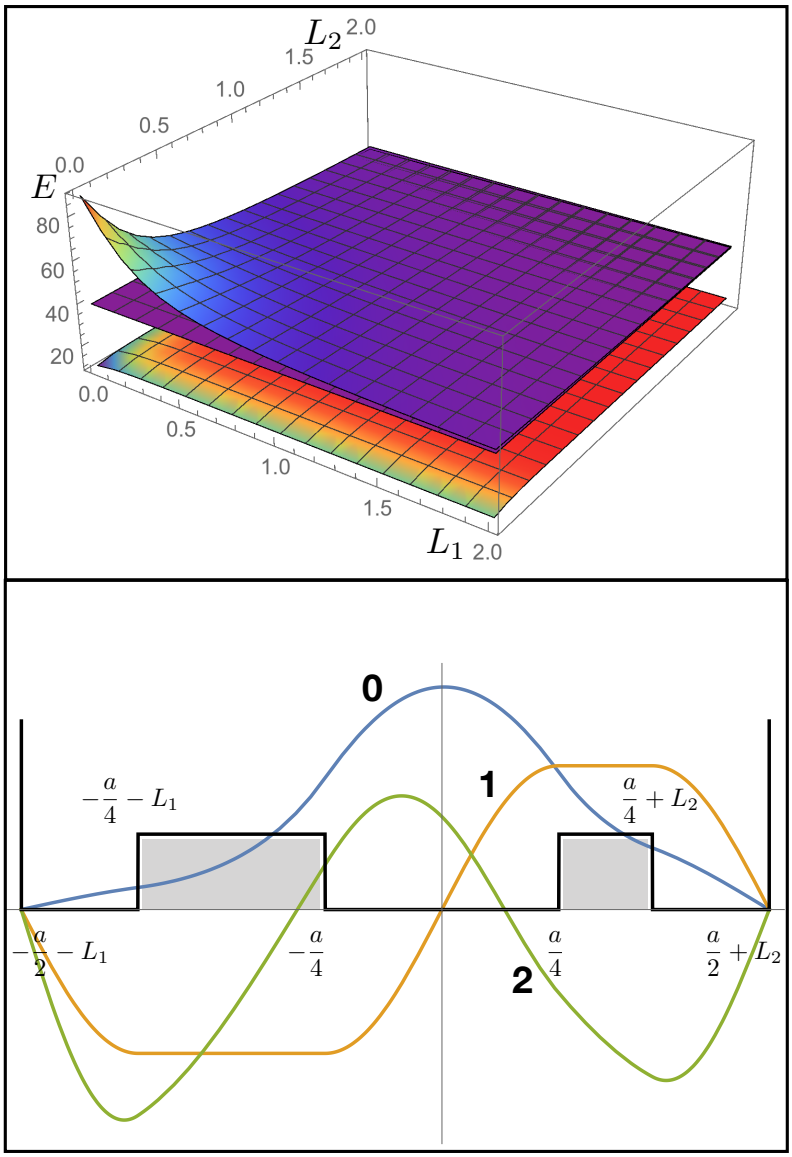

Figure 6.5.: Upper panel: plot of the first three energy levels for the infinite well with two stretching regions, as a function of L_1 and L_2. While the energy of the second level stays constant, the upper levels get compressed. Lower panel: plot of the wave functions of the first three levels for $L_1/a = 0.4$ and $L_2/a = 0.2$.

for $E < E_1$ we have the quantization condition:

$$\frac{1}{4k^2\gamma^2\cos\left(k(\frac{a}{2}+L_1)\right)}\Bigg\{-2\sinh(\gamma(L_1+L_2))k\gamma\left((k^2+\gamma^2)\cos\left(\frac{ak}{2}\right)+(k^2-\gamma^2)\cos(ak)\right)$$
$$+\sinh(\gamma L_1)\sinh(\gamma L_2)\sin(ak)(k^2-\gamma^2)^2+2\sinh(\gamma L_2)\sinh(\gamma L_1)\sin\left(\frac{ak}{2}\right)(k^4-\gamma^4)$$
$$-4k^2\gamma^2\cosh(\gamma L_2)\cosh(\gamma L_1)\sin(ak)\Bigg\}=0, \tag{6.43}$$

where now $\gamma = \sqrt{\frac{2m(E_1-E)}{\hbar^2}}$ and $\bar{k} = \sqrt{\frac{2m(E-E_1)}{\hbar^2}}$. For $E > E_1$ we have instead the condition:

$$\frac{1}{8k^2\bar{k}^2\cos\big(k(\frac{a}{2}+L_1)\big)}\Bigg\{-(k^2-\bar{k}^2)^2\cos\big(\bar{k}(L_2-L_1)\big)\sin(ak)$$
$$+(k^4+6k^2\bar{k}^2+\bar{k}^4)\cos\big(\bar{k}(L_1+L_2)\big)\sin(ak)-4(k^4-\bar{k}^4)\sin\left(\frac{ak}{2}\right)\sin\big(\bar{k}L_1\big)\sin\big(\bar{k}L_2\big)$$
$$+4k\bar{k}\sin\big(\bar{k}(L_1+L_2)\big)\left[(k^2-\bar{k}^2)\cos\left(\frac{ak}{2}\right)+(k^2+\bar{k}^2)\cos(ak)\right]\Bigg\}=0. \tag{6.44}$$

In Fig. 6.5 both the first three energy levels and the corresponding wave functions are plotted. As one can see the ground state energy quickly reaches an asymptotic value as L_1 and L_2 increases, while the energy of the first excited level stays constant. Concerning the other levels, as the stretching parameters grow they go towards the asymptotic value E_1: this in once again to be expected, since as in the other instances we examined increasing the stretching parameters implies approaching the free particle limit.

All the concepts exposed in this section can be adapted also to the case where the seeding potential is a harmonic oscillator, as reported in App. C.

CHAPTER 7

Geometric phases

The growing importance of quantum engineering has been fostered by the need for new more efficient circuits and transistors, and also by the creation of the first prototypes of quantum computers. Having this in mind, it becomes clear that coherence manipulation becomes of great importance in present technological challenges, as coherence is considered to be at the origin of quantum supremacy.

One possibility in this direction is to exploit the so called *Berry phase* [Wilczek and Shapere 1989]. When the Hamiltonian of a quantum system changes, the state of the system acquires a phase: though this effect was known before the work by Berry, his key insight was to recognize that for a cyclic change of the Hamiltonian this phase becomes gauge independent, and thus a measurable and meaningful quantity.

This effect is nowadays exploited by some approaches to quantum information processing [A. Ekert et al. 2000; Faoro, Siewert, and Fazio 2003; Sjöqvist, Azimi Mousolou, and C. M. Canali 2016; Zanardi and Rasetti 1999] and quantum state manipulation [De Chiara and Palma 2003; Duan, Cirac, and Zoller 2001; Vepsäläinen, Danilin, and Paraoanu 2018; Zhu and Wang 2002], where target states are obtained by applying a, possibly unitary, transformation implemented through a cyclic driving of the Hamiltonian, either adiabatically [Wilczek and Shapere 1989] or non-adiabatically [Aharonov and Anandan 1987], and even in dissipative processes [A. Carollo and Palma 2006; A. Carollo, Santos, and Vedral 2006]. The resulting operations are usually referred to as *holonomies*, and have also been proved experimentally [Hansom et al. 2014; Leek et al.

2007; Yale et al. 2016; Zhou et al. 2017]. Another very important feature of these operations is their resiliency to local fluctuations [Berger et al. 2013; Snizhko, Egger, and Gefen 2019; Yale et al. 2016], due to the geometrical character of the phenomenon.

What we propose here is to extend this approach to Hamiltonian that vary in space, and not in time: as we saw in Chap. 5, present day techniques for nanofabrication allow for the creation of very arbitrary and sharp potential profiles. By allowing the confining potential of a traveling wave to change adiabatically, we will show how it is possible to attach a phase to the state of the system. The adiabatic assumption is not strictly necessary to implement an holonomy, but it allows one to invoke a partial decoupling of fast and slow degrees of freedom [Aldinger, Böhm, and Loewe 1991; Mead 1992; Novičenko, Ruseckas, and Anisimovas 2019], see also Sec. 6.2.

In Sec. 7.1 we will briefly review the standard derivation of the adiabatic Berry's phase, seeing how a time dependent Hamiltonian can give rise to a geometric phase when it varies along a closed path in parameters space. Then in Sec. 7.2 we will show how also in the case of a coordinate dependent Hamiltonian it is possible to attach a geometric phase to a quantum state. Finally in Sec. 7.3 we will give some examples of coordinate-dependent Hamiltonian where a geometric phase is attached to a quantum state.

7.1. Standard Berry phase

In the standard approach to the Berry phase, one typically considers a Hamiltonian $\hat{H}(\vec{R}(t))$ which depends upon a set of time dependent parameters described by the vector $\vec{R}(t) = (R_1(t), R_2(t), \cdots)$. A necessary assumption in order to stay in the adiabatic regime is that the spectrum of $\hat{H}(\vec{R}(t))$ has always a finite gap between the ground state and the rest of the spectrum for all the considered values of $\vec{R}(t)$.

We then let the vector $\vec{R}(t)$ change slowly (i.e. adiabatically) in time such that:

$$\frac{\hbar}{T} << \Delta_{\min} \tag{7.1}$$

where T is the time necessary for the transformation and $\Delta_{\min}$ is the minimum energy gap between the ground state and the first excited state. When Eq. (7.1) holds we are ensured that as $\hat{H}(\vec{R})$ varies, the system remains always in the instantaneous ground

state $\left|\phi^{(0)}_{\vec{R}(t)}\right\rangle$. At this point we consider the instantaneous set of eigenvectors of $\hat{H}(\vec{R}(t))$:

$$\hat{H}(\vec{R}(t))\left|\phi^{(j)}_{\vec{R}(t)}\right\rangle = \epsilon^{(j)}_{\vec{R}(t)}\left|\phi^{(j)}_{\vec{R}(t)}\right\rangle, \tag{7.2}$$

thanks to which the solution to the time dependent Schödinger equation

$$i\hbar\frac{\partial}{\partial t}\left|\psi(t)\right\rangle = \hat{H}(\vec{R}(t))\left|\psi(t)\right\rangle \tag{7.3}$$

can be written as:

$$\left|\psi(t)\right\rangle = e^{i\gamma(t)}e^{-\frac{i}{\hbar}\int_0^t dt'\epsilon^{(0)}_{\vec{R}(t)}}\left|\phi^{(0)}_{\vec{R}(t)}\right\rangle + \sum_{j\neq 0} a_j(t)\left|\phi^{(j)}_{\vec{R}(t)}\right\rangle. \tag{7.4}$$

If the adiabatic approximation in Eq. (7.1) holds, this allows us to neglect the sum on the rhs of Eq. (7.4). Focusing hence on the ground state contribution, we see that it has two phases attached to it: one is the dynamical phase given by free evolution of the system, while $\gamma(t)$ is known as the Berry phase.

In order to find the value of this phase, one requires the state to fulfill the time dependent Schrödinger equation. Evaluating the lhs of Eq. (7.3) we get:

$$i\hbar\frac{\partial}{\partial t}\left|\psi(t)\right\rangle = \left[-\hbar\dot{\gamma}(t) + \epsilon^{(0)}_{\vec{R}(t)}\right]\left|\psi(t)\right\rangle + i\hbar e^{i\gamma(t)}e^{-\frac{i}{\hbar}\int_0^t dt'\epsilon^{(0)}_{\vec{R}(t)}}\dot{\vec{R}}(t)\cdot\frac{d}{d\vec{R}}\left|\phi^{(0)}_{\vec{R}(t)}\right\rangle, \tag{7.5}$$

where dotted quantities indicate time derivatives and the sum over the excited states has been neglected. Evaluating the rhs of Eq. (7.3) we get instead:

$$\hat{H}(\vec{R}(t))\left|\psi(t)\right\rangle = \epsilon^{(0)}_{\vec{R}(t)}\left|\psi(t)\right\rangle, \tag{7.6}$$

where once again we neglect the excited states contribution. At this point we can use the completeness relation and the adiabatic approximation to write:

$$\frac{d}{d\vec{R}}\left|\phi^{(0)}_{\vec{R}(t)}\right\rangle = \sum_j \left|\phi^{(j)}_{\vec{R}(t)}\right\rangle\left\langle\phi^{(j)}_{\vec{R}(t)}\right|\frac{d}{d\vec{R}}\left|\phi^{(0)}_{\vec{R}(t)}\right\rangle \simeq \left\langle\phi^{(0)}_{\vec{R}(t)}\right|\frac{d}{d\vec{R}}\left|\phi^{(0)}_{\vec{R}(t)}\right\rangle\left|\phi^{(0)}_{\vec{R}(t)}\right\rangle, \tag{7.7}$$

which substituted in Eq. (7.5) leads to:

$$i\hbar\frac{\partial}{\partial t}\left|\psi(t)\right\rangle = \left[-\hbar\dot{\gamma}(t) + i\hbar\dot{\vec{R}}(t)\left\langle\phi^{(0)}_{\vec{R}(t)}\right|\frac{d}{d\vec{R}}\left|\phi^{(0)}_{\vec{R}(t)}\right\rangle + \epsilon^{(0)}_{\vec{R}(t)}\right]\left|\psi(t)\right\rangle. \tag{7.8}$$

At this point we note that Eq. (7.8) and Eq. (7.6) are equal if:

$$\dot{\gamma}(t) = i\dot{\vec{R}}(t) \left\langle \phi^{(0)}_{\vec{R}(t)} \right| \frac{d}{d\vec{R}} \left| \phi^{(0)}_{\vec{R}(t)} \right\rangle , \tag{7.9}$$

where the normalization condition $\left\langle \phi^{(0)}_{\vec{R}(t)} \middle| \phi^{(0)}_{\vec{R}(t)} \right\rangle = 1$ ensures the reality of $\gamma(t)$.

At this point it should be noted that one is always free to choose the phase attached to the basis states for each value of $\vec{R}$, so that $\gamma(t)$ would result to be somehow gauge dependent: the key point observed by Berry is that if we let the vector $\vec{R}$ vary along a closed path Γ in parameters space, i.e. if:

$$\vec{R}(0) = \vec{R}(T), \tag{7.10}$$

then $\gamma(t)$ is not gauge dependent anymore, becoming a geometric quantity:

$$\gamma_{\text{Berry}} = \int_0^T \dot{\gamma}(t)dt' = i \oint_\Gamma d\vec{R} \left\langle \phi^{(0)}_{\vec{R}} \right| \frac{d}{d\vec{R}} \left| \phi^{(0)}_{\vec{R}} \right\rangle . \tag{7.11}$$

The Berry phase is said to be a geometric quantity because it does not depend on the velocity with which the transformation happen, but only on the path covered in parameters' space. The Berry phase is also gauge independent, in analogy with what happens in electrodynamics, where the line integral of the vector potential along a closed path is a gauge independent quantity. Following this analogy one can define the *Berry connection* $\vec{\mathcal{A}}$ as:

$$\vec{\mathcal{A}} = i \left\langle \phi^{(0)}_{\vec{R}} \right| \frac{d}{d\vec{R}} \left| \phi^{(0)}_{\vec{R}} \right\rangle \tag{7.12}$$

so that the Berry phase in Eq. (7.11) can be rewritten as

$$\gamma_{\text{Berry}} = \oint_\Gamma d\vec{R} \cdot \vec{\mathcal{A}}. \tag{7.13}$$

We conclude this section by noting that the Berry connection is a gauge dependent quantity, and thus it is not an observable quantity. However it is possible to define a gauge independent, and hence observable, quantity starting from the Berry connection, the so called *Berry curvature*:

$$\Omega = \Omega_{ij} = \frac{\partial}{\partial R_i}\mathcal{A}_j - \frac{\partial}{\partial R_j}\mathcal{A}_i. \tag{7.14}$$

Using the Berry curvature and applying the Stokes theorem, it is possible to write the Berry phase in the alternative, and sometimes simpler to treat, form:

$$\gamma_{Berry} = \int_{S(\Gamma)} d\vec{S} \cdot \Omega \tag{7.15}$$

where $S(\Gamma)$ is the surface enclosed in the loop Γ.

Having reviewed the Berry phase mechanism we are now ready to see how to obtain geometric phases with coordinate dependent Hamiltonians.

7.2. Spatial Berry phase

In order to show our result, let us consider a non relativistic particle A of mass m propagating in the xy-plane in a potential landscape $\hat{V}(\hat{x}, \hat{y})$ like the one shown in Fig. 7.1, which confines the particle along the x direction, while letting it propagate along y. Thus the particle has Hamiltonian:

$$\hat{H} = \frac{\hat{p}_x^2}{2m} + \frac{\hat{p}_y^2}{2m} + \hat{V}(\hat{x}, \hat{y}). \tag{7.16}$$

As shown pictorially in Fig. 7.1, we are considering a situation where the particle A enters the potential landscape with energy E, this corresponding to an input state that far away from the scattering region has the form of a plane wave propagating with impulse $p_0 > 0$, hence setting the largest energy scale in the system, as $E_{\text{kin}} = p_0^2/(2m) \simeq E$.

What we want to do now is to look for solutions of the time independent Schrödinger equation compatible with the boundary conditions. In order to achieve the goal we move to a representation with respect to the y coordinate, i.e. we multiply both sides of the Schrödinger equation by the bra $\langle y|$, obtaining:

$$\langle y| \hat{H} |\psi_E\rangle = \langle y| E |\psi_E\rangle \Rightarrow -\frac{\hbar^2}{2m}\frac{\partial^2}{\partial y^2} |\psi_E(y)\rangle + \hat{h}_y(\hat{x}) |\psi_E(y)\rangle = E |\psi_E(y)\rangle , \tag{7.17}$$

where we have defined $|\psi_E(y)\rangle = \langle y|\psi_E\rangle$ as the transverse wave vector component for assigned longitudinal position. The self-adjoint operator

$$\hat{h}_y(\hat{x}) = \frac{\hat{p}_x^2}{2m} + \hat{V}_y(\hat{x}), \tag{7.18}$$

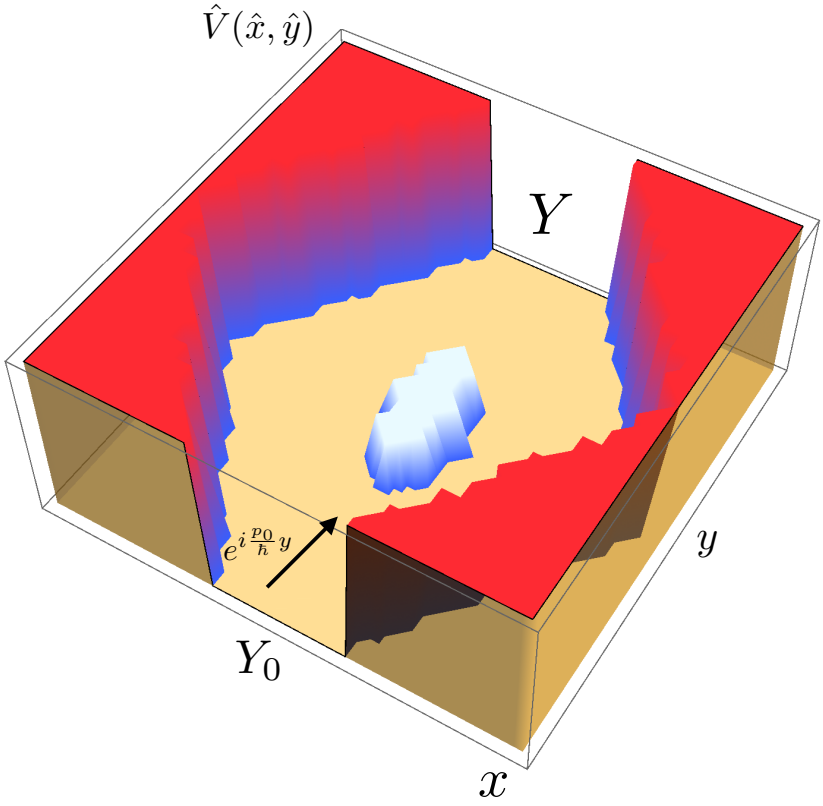

Figure 7.1.: Pictorial representation of the system under examination: a particle A is moving in the potential landscape described by the operator $\hat{V}(\hat{x},\hat{y})$ with a certain energy E.

with $\hat{V}_y(\hat{x}) = \hat{V}(\hat{x}, y)$, is obtained by replacing the operator $\hat{y}$ with its eigenvalue y.

In analogy with the previous section, we assume the dependence upon y of $\hat{V}_y(\hat{x})$ to be mediated by a set of control parameters $R_y^{(i)}$, described collectively by the vector $\vec{R}_y = (R_y^{(1)}, R_y^{(2)}, \cdots)$, so that we can write:

$$\hat{V}_y(\hat{x}) = V_0(\hat{x}; \vec{R}_y). \tag{7.19}$$

We further assume that the operator $\hat{h}_y(\hat{x})$, via the potential $\hat{V}_y(\hat{x})$, induces confinement along x, so that for each assigned y we can identify a discrete set of eigenvectors $\{\left|\phi_y^{(\ell)}\right\rangle; \ell = 0, 1, 2, \cdots\}$ with associated eigenvalues $E_y^{(\ell)} = \frac{\hbar^2}{2m}\epsilon_y^{(\ell)}$, i.e.:

$$\hat{h}_y(\hat{x}) \left|\phi_y^{(\ell)}\right\rangle = E_y^{(\ell)} \left|\phi_y^{(\ell)}\right\rangle \tag{7.20}$$

We can then expand the state $|\psi_E(y)\rangle$ in the instantaneous eigenbasis as

$$|\psi_E(y)\rangle = \sum_\ell C_y^{(\ell)} \left|\phi_y^{(\ell)}\right\rangle, \quad C_y^{(\ell)} \in \mathbb{C}, \tag{7.21}$$

so that we can write:

$$\begin{aligned}\left\langle\phi_y^{(\ell)}\right| \frac{\partial^2}{\partial y^2} |\psi_E(y)\rangle &= \frac{\partial^2}{\partial y^2} C_y^{(\ell)} + \sum_{\ell'} 2\frac{\partial}{\partial y} C_y^{(\ell')} \left\langle\phi_y^{(\ell)}\right| \frac{\partial}{\partial y} \left|\phi_y^{(\ell')}\right\rangle + \sum_{\ell'} C_y^{(\ell')} \left\langle\phi_y^{(\ell)}\right| \frac{\partial^2}{\partial y^2} \left|\phi_y^{(\ell')}\right\rangle \\ &= \frac{\partial^2}{\partial y^2} C_y^{(\ell)} + \sum_{\ell'} \left(2[K_y]_{\ell\ell'} \frac{\partial}{\partial_y} C_y^{(\ell')} + [\Gamma_y]_{\ell\ell'} C_y^{(\ell')} \right). \end{aligned} \tag{7.22}$$

Here we have defined the two matrices of elements:

$$[K_y]_{\ell\ell'} = \left\langle\phi_y^{(\ell)}\right| \frac{\partial}{\partial y} \left|\phi_y^{(\ell')}\right\rangle, \qquad [\Gamma_y]_{\ell\ell'} = \left\langle\phi_y^{(\ell)}\right| \frac{\partial^2}{\partial y^2} \left|\phi_y^{(\ell')}\right\rangle. \tag{7.23}$$

We anticipate here, and demonstrate in App. D.1, that the matrix K_y is anti-Hermitean, having only real elements and its diagonal terms being null.

Inserting the expression in Eq. (7.22) in Eq. (7.17), we can get a set of coupled differential equations for the coefficients $C_y^{(\ell)}$:

$$\frac{\partial^2}{\partial y^2} C_y^{(\ell)} + \sum_{\ell'} \left(2[K_y]_{\ell\ell'} \frac{\partial}{\partial y} C_y^{(\ell')} + [\Gamma_y]_{\ell\ell'} C_y^{(\ell')} \right) + \frac{2m}{\hbar^2}(E - E_y^{(\ell)}) C_y^{(\ell)} = 0. \tag{7.24}$$

Defining the column vector $\vec{C}_y = (C_y^{(1)}, C_y^{(2)}, \cdots)$ and introducing the rescaled energy $\epsilon = \frac{2m}{\hbar^2} E$, we can recast this system of differential equations in vectorial form as:

$$\frac{\partial^2}{\partial y^2} \vec{C}_y + 2K_y \frac{\partial}{\partial y} \vec{C}_y + (\Gamma_y + \epsilon - \Omega_y) \vec{C}_y = 0, \tag{7.25}$$

where we introduced the diagonal matrix:

$$[\Omega_y]_{\ell\ell'} = \frac{2m}{\hbar^2} E_y^{(\ell)} \delta_{\ell\ell'} = \epsilon_y^{(\ell)} \delta_{\ell\ell'}. \tag{7.26}$$

As shown in App. D.1, it holds:

$$[K_y^2]_{\ell\ell'} = -\left(\frac{\partial}{\partial_y} \left\langle\phi_y^{(\ell)}\right| \right) \frac{\partial}{\partial_y} \left|\phi_y^{(\ell)}\right\rangle, \tag{7.27}$$

and we notice that:

$$[\Gamma_y - \frac{\partial}{\partial y}K_y]_{\ell\ell'} = \left\langle \phi_y^{(\ell)} \right| \frac{\partial^2}{\partial y^2} \left| \phi_y^{(\ell')} \right\rangle - \frac{\partial}{\partial y}\left(\left\langle \phi_y^{(\ell)} \right| \frac{\partial}{\partial y} \left| \phi_y^{(\ell')} \right\rangle \right) \tag{7.28}$$

$$= -\left(\frac{\partial}{\partial_y} \left\langle \phi_y^{(\ell)} \right| \right) \frac{\partial}{\partial_y} \left| \phi_y^{(\ell)} \right\rangle = [K_y^2]_{\ell\ell'}, \tag{7.29}$$

which allows us to finally rewrite Eq. (7.25) in the form:

$$\left(\frac{\partial}{\partial y} + K_y \right)^2 \vec{C}_y + (\epsilon - \Omega_y)\, \vec{C}_y = 0 \tag{7.30}$$

The presence of the term K_y in Eq. (7.30) is analogous to a coupling to a non Abelian vector potential, and hence it can be gauged away via an appropriate transformation. This transformation is the unitary map given by:

$$\mathcal{U}_{Y_0 \to y} = P \exp\left[-\int_{Y_0}^{y} dy' K_{y'} \right], \tag{7.31}$$

where P indicates a path ordered integral and Y_0 is the coordinate of the beginning of the scattering region. Applying this transformation, i.e. defining the vector $\tilde{\vec{C}}_y = \mathcal{U}^\dagger_{Y_0 \to y} \vec{C}_y$, we can write:

$$\frac{\partial^2}{\partial y^2}\tilde{\vec{C}}_y + (\epsilon - \tilde{\Omega}_y)\tilde{\vec{C}}_y = 0, \tag{7.32}$$

with $\tilde{\Omega}_y = \mathcal{U}^\dagger_{Y_0 \to y} \Omega_y \mathcal{U}_{Y_0 \to y}$. When ϵ, and thus the kinetic energy, is the largest energy scale in the system, Eq. (7.32) admits solutions of the form:

$$\tilde{\vec{C}}_y = \mathcal{W}_y^{(+)} \vec{A} + \mathcal{W}_y^{(-)} \vec{B}, \tag{7.33}$$

where $\vec{A}$ and $\vec{B}$ are determined by the boundary conditions of the problem and the matrices $\mathcal{W}^{(\pm)}$ describe the propagation of the particle in the $\pm y$ direction. Moreover, when ϵ is so large that the gaps in Ω_y are negligible, an approximate solution is given by $\mathcal{W}_y^{(\pm)} = e^{\pm i\sqrt{\epsilon}(y - Y_0)}$, which explicitly depends upon the integration length and thus its effect on the state is just an irrelevant global phase.

At this point we want to consider the case where the scattering region starts at Y_0 and ends at some Y. We then assume $\vec{B} = 0$ and $\vec{A} = \vec{C}_{Y_0}$, that is, we assume a situation where the particle propagates only in one direction with no back-scattering contributions, which can always be achieved for large enough values of the kinetic energy. Given the

initial condition $\vec{C}_{Y_0}$, we can write the evolved vector at the coordinate Y as:

$$\vec{C}_Y = \mathcal{U}_{Y_0 \to Y} \mathcal{W}_Y^{(+)} \vec{C}_{Y_0}. \tag{7.34}$$

What we want to show now is that the operator $\mathcal{U}_{Y_0 \to Y}$ is an holonomy that attaches a geometric non Abelian phase to the particle state. To see this we first notice that the dependence on y of the eigenvectors $\left|\phi_y^{(\ell)}\right\rangle$ is mediated by the control parameters $\vec{R}_y$, so that we can rewrite the matrix elements of K_y as:

$$K_y = \vec{K}(\vec{R}_y) \cdot \frac{\partial}{\partial y} \vec{R}_y, \quad [\vec{K}(\vec{R}_y)]_{\ell\ell'} = \left\langle \phi_y^{(\ell)} \right| \frac{d}{d\vec{R}} \left| \phi_y^{(\ell')} \right\rangle. \tag{7.35}$$

The matrix $\vec{K}(\vec{R}_y)$ defines a connection analogous to the one we saw in Eq. (7.12) for the standard Berry phase. If now we assume that the trajectory $\mathcal{R} = \{\vec{R}_y\}_{y \in [Y_0, Y]}$ in parameters space followed by $\vec{R}_y$ is closed, which is equivalent to requiring $\vec{R}_{Y_0} = \vec{R}_Y$, it is possible to use Eq. (7.35) to rewrite $\mathcal{U}_{Y_0 \to Y}$ as:

$$\mathcal{U}_{Y_0 \to Y} = \mathcal{U}(\mathcal{R}) = P \exp\left[- \oint_{\mathcal{R}} d\vec{R} \cdot \vec{K}(\vec{R}) \right], \tag{7.36}$$

where the path ordering is formally defined as:

$$P \exp\left[- \oint_{\mathcal{R}} d\vec{R} \cdot \vec{K}(\vec{R}) \right] = \sum_{n=0}^{+\infty} (-1)^n \int_{\vec{R}_{Y_0}}^{\vec{R}_Y} d\vec{r}_1 \cdot \vec{K}(\vec{r}_1) \int_{\vec{R}_{Y_0}}^{\vec{r}_1} d\vec{r}_2 \cdot \vec{K}(\vec{r}_2) \cdots \int_{\vec{R}_{Y_0}}^{\vec{r}_{n-1}} d\vec{r}_n \cdot \vec{K}(\vec{r}_n), \tag{7.37}$$

where for a given $j = 0, 1, \cdots n-1$, the vector $\vec{r}_j = \vec{R}_{y_j}$ is the element of the curve $\mathcal{R}$ assumed by the parameters vector $\vec{R}_y$ at the point $y = y_j$, the points $y_1, y_2, \cdots y_n$ being coordinate values in the interval $[Y_0, Y[$ ordered according to $y_j \geq y_{j+1}$.

Now, the point is that the path ordered integral does not depend anymore on the speed of the longitudinal variation of the potential, or, in other words, $\frac{\partial \vec{R}}{\partial y}$ does not appear in Eq. (7.36), a feature that makes manifest the geometric nature of the phase shift induced by $\mathcal{U}(\mathcal{R})$.

Note also that, at glance with the previous section, the phase shift generated by the holonomy in Eq. (7.36) is of non Abelian nature [Wilczek and Zee 1984], as it mixes different energy levels of the system.

Moreover it is possible to invoke the non Abelian version of the Stokes theorem [Halpern 1979] to further rewrite $\mathcal{U}(\mathcal{R})$ in terms of the curvature tensor $\mathcal{F}_{ij}(\vec{R})$ obtained from

$\vec{K}(\vec{R})$. The latter can be written as:

$$\mathcal{F}_{ij}(\vec{R}) = i\frac{\partial K^{(j)}}{\partial R^{(i)}} - i\frac{\partial K^{(i)}}{\partial R^{(j)}} + i\Big[K^{(i)}(\vec{R}), K^{(j)}(\vec{R})\Big], \tag{7.38}$$

so that the operator $\mathcal{U}(\mathcal{R})$ becomes:

$$\mathcal{U}(\mathcal{R}) = \mathcal{P}\exp\left[\frac{i}{2}\int_{\mathcal{S}}\mathcal{F}_{ij}(\vec{R})dR^{(i)}\wedge dR^{(j)}\right], \tag{7.39}$$

where $\mathcal{P}$ indicates the surface ordered product and $\mathcal{S}$ is any regular surface in parameters space which can be bounded by $\mathcal{R}$. While Eq. (7.39) is quite evocative, it is actually not much informative, as the surface ordered product is typically quite demanding from a computational perspective.

7.2.1. The case of two dimensional models

When the dynamics of the system can be reduced to an Hilbert space spanned by only two eigenstates $\left|\phi_y^{(0)}\right\rangle, \left|\phi_y^{(1)}\right\rangle$ of the transverse Hamiltonian $\hat{h}_y(\hat{x})$, a great simplification occurs to all the formalism we exposed in the previous section. Such a situation can be reached, for instance, when the energy gap $\Delta_y = \epsilon_y^{(1)} - \epsilon_y^{(0)}$ is the smallest among all the energy gaps, i.e.:

$$\Delta_y << |\epsilon_y^{(\ell)} - \epsilon_y^{(\ell')}|, \quad \forall \ell \neq \ell',\ \forall y. \tag{7.40}$$

When this assumption is fulfilled we can write the matrix Ω_y as:

$$\Omega_y = \omega_y\hat{\mathbb{I}} - \Delta_y\frac{\hat{\sigma}_3}{2}, \tag{7.41}$$

where $\mathbb{I}$ is the 2×2 identity matrix, $\hat{\sigma}_3$ is the diagonal Pauli matrix and $\omega_y = \frac{(\epsilon_y^{(0)}+\epsilon_y^{(1)})}{2}$. Moreover, the matrix K_y reduces to a 2×2 matrix as well, becoming:

$$K_y = i\lambda_y\hat{\sigma}_2 \tag{7.42}$$

where $\hat{\sigma}_2$ is the imaginary Pauli matrix and $\lambda_y = \lambda_y^* = \left\langle\phi_y^{(0)}\right|\frac{\partial}{\partial y}\left|\phi_y^{(1)}\right\rangle$. This feature leads to a great simplification, as now the auto-commutator becomes trivial:

$$[K_y, K_{y'}] = 0, \quad \forall y, y'. \tag{7.43}$$

From Eq. (7.43) it follows that the operator $\mathcal{U}_{Y_0\to y}$ reduces to an $SU(2)$ rotation:

$$\mathcal{U}_{Y_0\to y} = \exp\left[-i\alpha_y\hat{\sigma}_2\right] = \cos\alpha_y\mathbb{I} - i\sin\alpha_y\hat{\sigma}_2 \tag{7.44}$$

where $\alpha_y = \int_{Y_0}^{y} dy'\lambda(y')$. For the case of our interest where $y = Y$, the expression further simplifies to:

$$\mathcal{U}(\mathcal{R}) = e^{i\alpha\hat{\sigma}_2}, \tag{7.45}$$

where

$$\alpha = \oint_{\mathcal{R}} d\vec{R}\cdot\vec{\lambda}(\vec{R}) = \int_{\mathcal{S}} d\vec{S}\cdot(\vec{\nabla}_{\vec{R}}\wedge\vec{\lambda}(\vec{R})), \tag{7.46}$$

with $\vec{\lambda}(\vec{R}) = \left\langle\phi_y^{(0)}\right| \frac{\partial}{\partial\vec{R}} \left|\phi_y^{(1)}\right\rangle$. All of this implies the possibility of rewriting Eq. (7.32) as:

$$\frac{\partial^2}{\partial y^2}\tilde{\vec{C}}_y + \left[(\epsilon-\omega_y)\,\hat{\mathbb{I}} + \Delta_y\frac{\tilde{\hat{\sigma}}_3}{2}\right]\tilde{\vec{C}}_y = 0, \tag{7.47}$$

with $\tilde{\hat{\sigma}}_3 = e^{i\alpha_y\hat{\sigma}_2}\hat{\sigma}_3 e^{-i\alpha_y\hat{\sigma}_2}$. At this point, assuming once again ϵ to be the largest energy scale in the problem, which in this case amounts to requiring $\epsilon >> |\omega_y|, |\Delta_y|$, it is possible to exploit the Wentzel-Kramers-Brillouin (WKB) approximation [Messiah 1999] to obtain the solution $\mathcal{W}_Y^{(\pm)} \simeq e^{\pm i\int_{Y_0}^{Y}\sqrt{\epsilon-\omega_{y'}}dy'}\hat{\mathbb{I}}$, which still represents an irrelevant global phase, and can thus be neglected.

Accordingly we can describe the effect of $\mathcal{U}_{Y_0\to Y}$ as a qubit gate: given an input state of the form $|\psi_E(Y_0)\rangle = a\left|\phi_{Y_0}^{(0)}\right\rangle + b\left|\phi_{Y_0}^{(1)}\right\rangle$, with $a, b\in\mathbb{C}$, it will result in an output at the end of the scattering region of the form:

$$\begin{aligned}\mathcal{U}_{Y_0\to Y}\,|\psi_E(Y_0)\rangle &= |\psi_E(Y)\rangle \\ &\simeq e^{+i\int_{Y_0}^{Y}\sqrt{\epsilon-\omega_{y'}}dy'}\left[(a\cos\alpha - b\sin\alpha)\left|\phi_{Y_0}^{(0)}\right\rangle + (b\cos\alpha + a\sin\alpha)\left|\phi_{Y_0}^{(1)}\right\rangle\right].\end{aligned} \tag{7.48}$$

This concludes our demonstration, while in the next section we provide some examples of the theory we exposed in this section.

7.3. Examples

In this section we want to examine a potential profile where the system Hilbert space is effectively two fold, in order to exploit the simplification exposed in Sec. 7.2.1. To this aim we consider a potential profile like the one shown in the inset of Fig. 7.2, which reads:

$$\hat{V}_{\vec{R}}(\hat{x}) = \begin{cases} 0 & \text{for } 0 \leq x \leq \frac{a}{2} \\ V_0 = \frac{9\pi^2\hbar^2}{2ma^2} & \text{for } \frac{a}{2} \leq x \leq \frac{a}{2} + L \\ 0 & \text{for } \frac{a}{2} + L \leq x \leq a + L + w \\ +\infty & \text{otherwise} \end{cases}, \tag{7.49}$$

which resembles the stretched construction we met in Chap. 6. Here a is the width of the original well and L is the width of the barrier. We also introduce the parameter w which describes the amount we increase the well width, as in what follows we will only want to increase such width from the right side (i.e. in a non-symmetrical way).

The eigenfunctions of the potential in Eq. (7.49) are readily written as:

$$\phi_{\vec{R}}(x) = \begin{cases} \sin(kx) & \text{for } 0 \leq x \leq \frac{a}{2} \\ Ae^{-\gamma x} + Be^{\gamma x} & \text{for } \frac{a}{2} \leq x \leq \frac{a}{2} + L \\ C\sin(kx) + D\cos(kx) & \text{for } \frac{a}{2} + L \leq x \leq a + L + w \end{cases}. \tag{7.50}$$

Imposing the usual boundary conditions we can compute the coefficients A, B, C, D via:

$$\sin\left(k\frac{a}{2}\right) = Ae^{-\gamma\frac{a}{2}} + Be^{\gamma\frac{a}{2}} \tag{7.51}$$

$$k\cos\left(k\frac{a}{2}\right) = \gamma\left(-Ae^{-\gamma\frac{a}{2}} + Be^{\gamma\frac{a}{2}}\right) \tag{7.52}$$

$$Ae^{-\gamma\left(\frac{a}{2}+L\right)} + Be^{\gamma\left(\frac{a}{2}+L\right)} = C\sin\left(k(\frac{a}{2}+L)\right) + D\cos\left(k(\frac{a}{2}+L)\right) \tag{7.53}$$

$$\gamma\left(-Ae^{-\gamma\left(\frac{a}{2}+L\right)} + Be^{\gamma\left(\frac{a}{2}+L\right)}\right) = k\left(C\cos\left(k(\frac{a}{2}+L)\right) - D\sin\left(k(\frac{a}{2}+L)\right)\right) \tag{7.54}$$

where we have defined

$$k = \sqrt{\frac{2mE}{\hbar^2}}, \qquad \gamma = \sqrt{\frac{2m(V_0 - E)}{\hbar^2}}. \tag{7.55}$$

The energies can be found solving the equation:

$$C \sin\left(k(a + L + w)\right) + D \cos\left(k(a + L + w)\right) = 0, \tag{7.56}$$

whose solutions for the first three energy levels are plotted in Fig. 7.2.

From Fig. 7.2 we notice that, at least in the region of small L and w, the energy gap between the first two levels and the third is very large. Furthermore, the energy gap between the first two levels becomes small in the same region, so that the matrix elements $[K_y]_{\ell\ell'}$ become negligible for $\ell, \ell' > 2$. This allows us to treat the system effectively as two fold, as confirmed from the plot in Fig. 7.3.

Moreover, we can show that only the variation of L contributes to the phase, while varying w gives no effects. To show this we start by writing a regularized version of the potential in Eq. (7.49) as a sum of Heavyside step functions:

$$\begin{aligned} V_{\vec{R}}^{(\kappa)}(x) \;=\; & V_0 \Big[\Theta(x - \frac{a}{2}) - \Theta(\frac{a}{2} + L - x) \\ & \kappa f(x)\Theta(-x) + \kappa f(x - a - L - w)\Theta(x - a - L - w)\Big], \end{aligned} \tag{7.57}$$

where $k >> 1$ is a regularization parameter that will be sent to infinity to recover $V_{\vec{R}}(x)$ and $f(x)$ is any regular function that nullifies in $x = 0$ and is strictly positive everywhere else.

From Eq. (7.57) we can write:

$$\frac{\partial}{\partial L} V_{\vec{R}}^{(\kappa)}(x) = -V_0 \delta(\frac{a}{2} + L - x) - \kappa V_0 f(x - a - L - w)\delta(x - a - L - w), \tag{7.58}$$

$$\frac{\partial}{\partial w} V_{\vec{R}}^{(\kappa)}(x) = -\kappa V_0 f(x - a - L - w)\delta(x - a - L - w), \tag{7.59}$$

so that we are able to write, for any finite κ:

$$\left\langle \phi_{\vec{R}}^{(\ell,\kappa)} \right| \frac{\partial}{\partial L} V_{\vec{R}}^{(\kappa)}(x) \left| \phi_{\vec{R}}^{(\ell,\kappa)} \right\rangle = -V_0 \phi_{\vec{R}}^{*(\ell,\kappa)}(\frac{a}{2} + L)\phi_{\vec{R}}^{(\ell',\kappa)}(\frac{a}{2} + L) \tag{7.60}$$

$$\left\langle \phi_{\vec{R}}^{(\ell,\kappa)} \right| \frac{\partial}{\partial w} V_{\vec{R}}^{(\kappa)}(x) \left| \phi_{\vec{R}}^{(\ell',\kappa)} \right\rangle = 0, \tag{7.61}$$

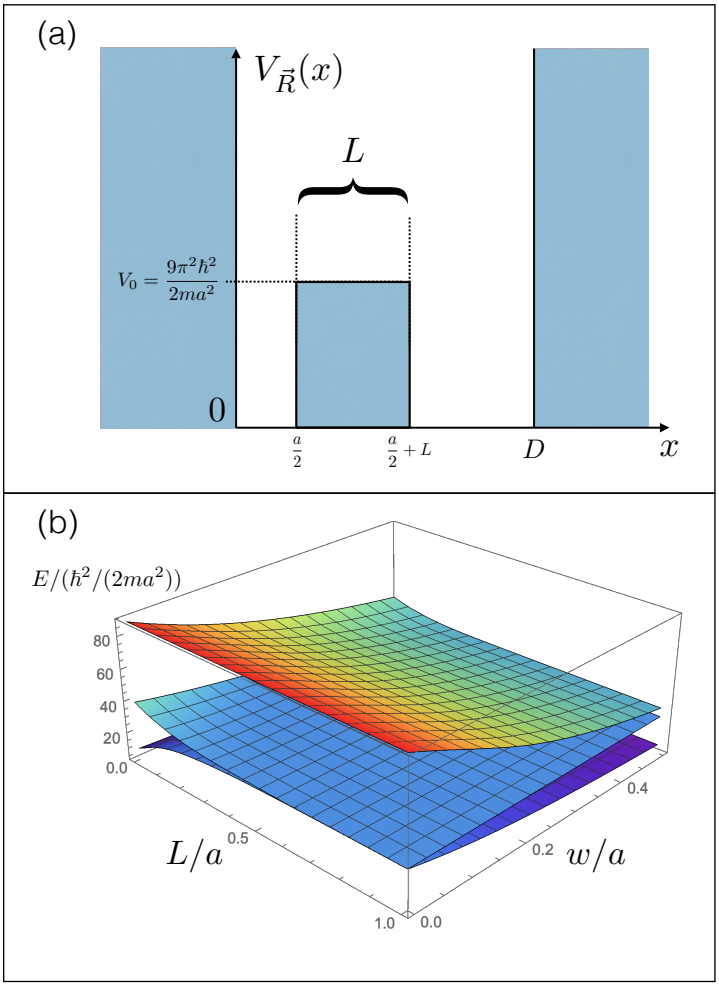

Figure 7.2.: Panel (a): Sketch of the potential in Eq. (7.49): we have an infinite well of variable width $D = a + L + w$ with a potential barrier of length L and height $V_0 = \frac{9\pi^2\hbar^2}{2ma^2}$ inside. Panel (b): Energies of the first three levels of the potential in Eq. (7.49) as functions of L and w. It can be noticed that the energy decrease as w increases, just as expected from a well with larger width. On the other hand we will have to pay attention whenever $w = 0$, as in this case, for sufficiently large values of L the energies of the first two levels might become equal. Inset: sketch of the potential profile under examination.

where with $\left|\phi_{\vec{R}}^{(\ell,\kappa)}\right\rangle$ we mean the ℓ-th energy eigenvector of the Hamiltonian associated with the regularized potential $V_{\vec{R}}^{(\kappa)}(x)$. Finally in the limit $\kappa \to +\infty$ we have:

$$\left\langle \phi_{\vec{R}}^{(\ell)} \right| \frac{\partial}{\partial L} V_{\vec{R}}(x) \left| \phi_{\vec{R}}^{(\ell')} \right\rangle = -V_0 \phi_{\vec{R}}^{*(\ell)}(\frac{a}{2}+L)\phi_{\vec{R}}^{(\ell')}(\frac{a}{2}+L), \tag{7.62}$$

$$\left\langle \phi_{\vec{R}}^{(\ell)} \right| \frac{\partial}{\partial w} V_{\vec{R}}(x) \left| \phi_{\vec{R}}^{(\ell')} \right\rangle = 0. \tag{7.63}$$

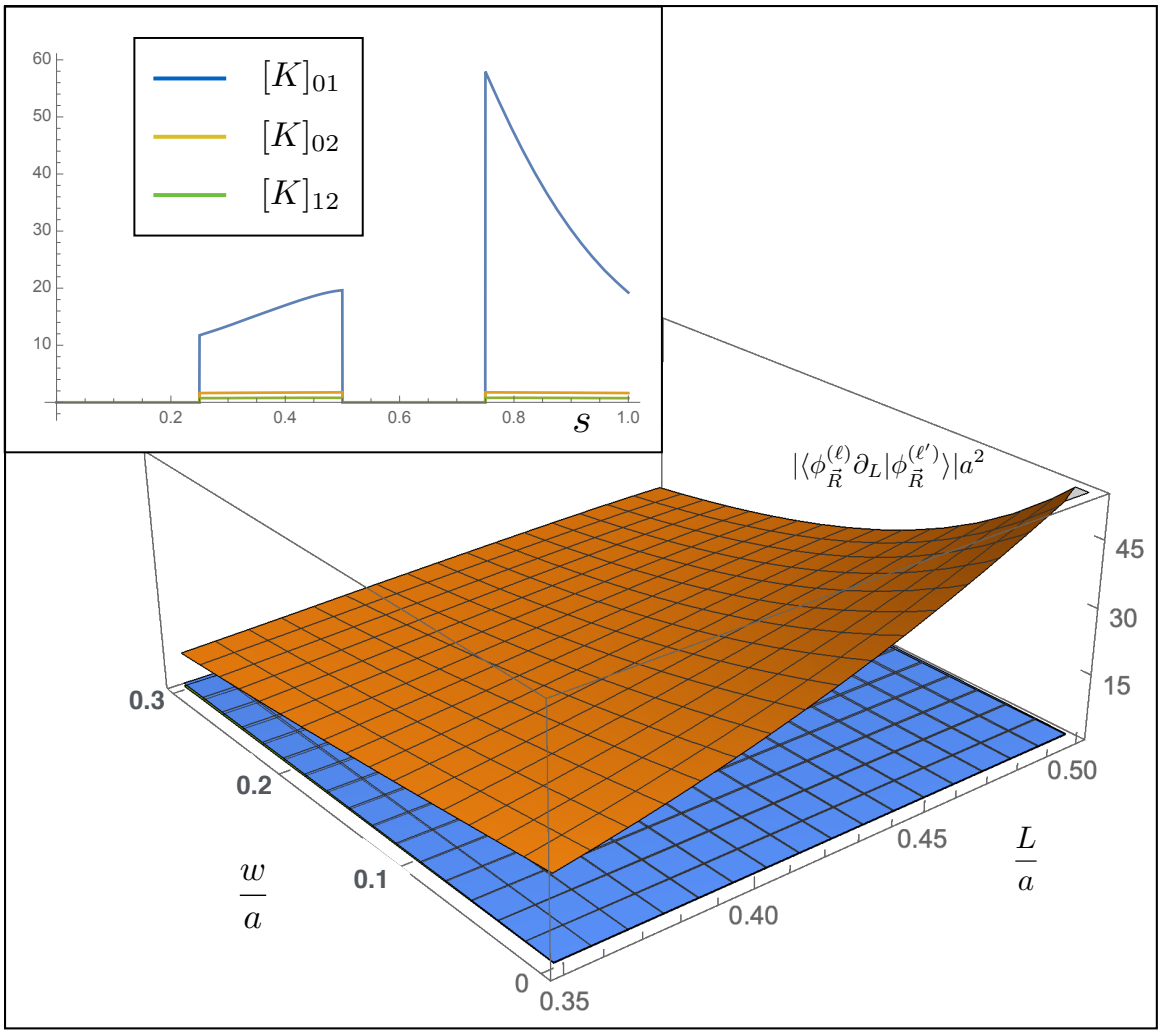

Figure 7.3.: Panel (a): Plot of the quantities $|\left\langle\phi^{(\ell)}_{\vec{R}}\right|\frac{\partial}{\partial L}\left|\phi^{(\ell')}_{\vec{R}}\right\rangle|a^2$ for the couples $(\ell,\ell')=(0,1),(1,2),(0,2)$. We can observe how, in the region used to compute the phase in shown in Fig. 7.4, $|\left\langle\phi^{(0)}_{\vec{R}}\right|\frac{\partial}{\partial L}\left|\phi^{(1)}_{\vec{R}}\right\rangle|a^2$ is far larger than the same quantity evaluated for the other two indices couples. Panel (b): Plot of the matrix elements $[K]_{\ell\ell'}$ along one of the paths used to plot the phase in Fig. 7.4. The path is parametrized as $\mathcal{R}(s)$ with $s\in[0,1]$. As one can observe the matrix element $[K]_{01}$ is always far larger than the other two, thus confirming our working hypotheses.

Inserting Eqs.(7.62, 7.63) into Eq. (D.86) in App. D we finally get:

$$\begin{aligned}\left\langle\phi^{(0)}_{\vec{R}}\right|\frac{\partial}{\partial L}\left|\phi^{(1)}_{\vec{R}}\right\rangle &= \frac{\left\langle\phi^{(0)}_{\vec{R}}\right|\frac{\partial}{\partial L}\hat{V}_{\vec{R}}(x)\left|\phi^{(1)}_{\vec{R}}\right\rangle}{E^{(1)}_{\vec{R}}-E^{(0)}_{\vec{R}}}\\ &= -\frac{V_0}{E^{(1)}_{\vec{R}}-E^{(0)}_{\vec{R}}}\phi^{*(0)}_{\vec{R}}\left(\frac{a}{2}+L\right)\phi^{(1)}_{\vec{R}}\left(\frac{a}{2}+L\right).\end{aligned} \tag{7.64}$$

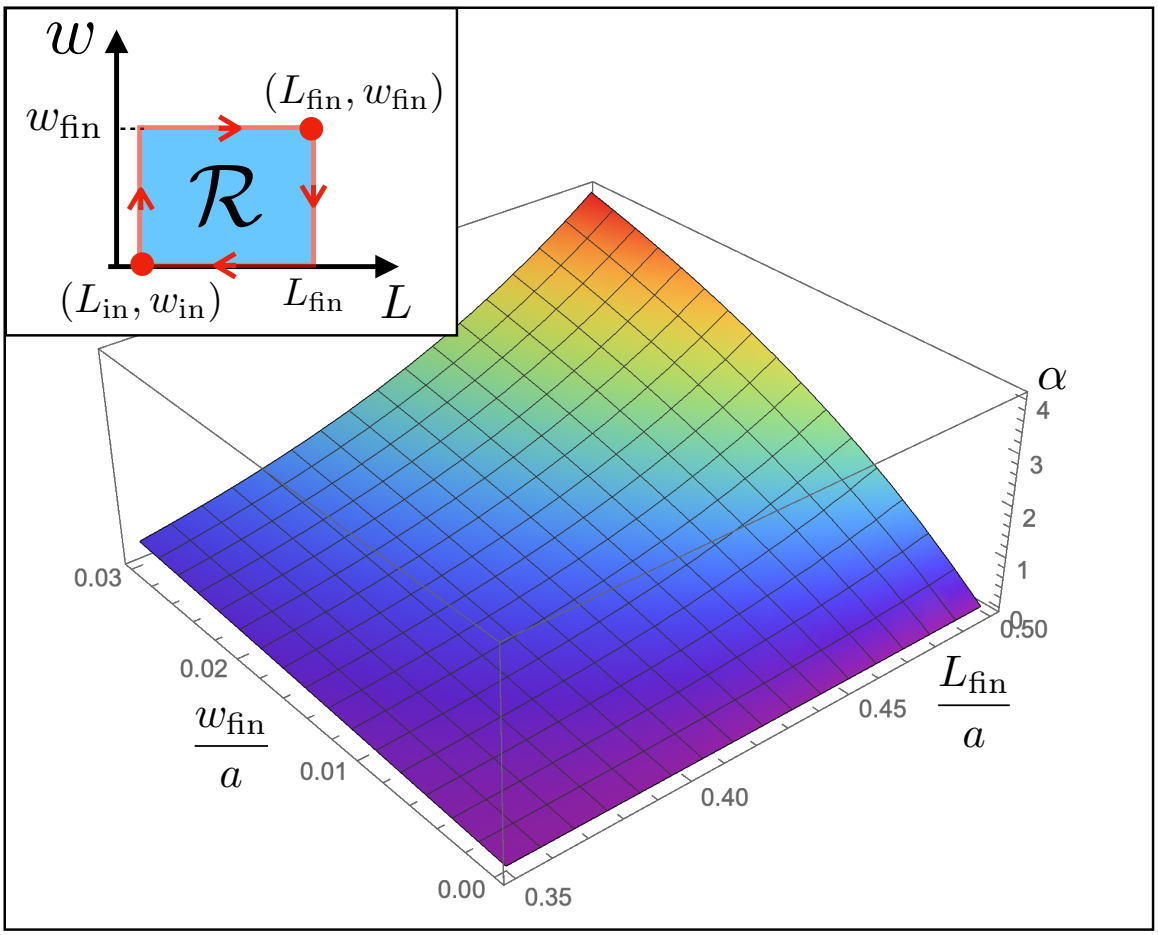

Figure 7.4.: Plot of the geometric phase obtained following the paths shown in the inset: we choose as initial point in parameters space $\vec{R}_{\text{int}} = (0.35a, 0)$, plotting the geometric phase α as a function of L_{fin} and w_{fin}. Inset: sketch of the paths followed in parameters space.

Equation (7.64) implies that the computation of the geometric phase α is greatly simplified, as we will only need to compute two integrals. We choose the integration paths shown in the inset of Fig. 7.4: we start from an initial point in parameters space $\vec{R}_{\text{in}} = (L_{\text{in}}, w_{\text{in}})$, and then we increase w up to a final value w_{fin}, before increasing L up to its final value L_{fin}. We then move back to the initial point $\vec{R}_{\text{in}}$, so that the geometric phase can be computed as:

$$\alpha = V_0 \left[\int_{L_{\text{in}}}^{L_{\text{fin}}} dL \, \frac{\phi^{*(0)}_{\vec{R}} \left(\frac{a}{2} + L\right) \phi^{(1)}_{\vec{R}} \left(\frac{a}{2} + L\right)}{E^{(1)}_{\vec{R}} - E^{(0)}_{\vec{R}}} \Bigg|_{w_{\text{fin}}} + \int_{L_{\text{fin}}}^{L_{\text{in}}} dL \, \frac{\phi^{*(0)}_{\vec{R}} \left(\frac{a}{2} + L\right) \phi^{(1)}_{\vec{R}} \left(\frac{a}{2} + L\right)}{E^{(1)}_{\vec{R}} - E^{(0)}_{\vec{R}}} \Bigg|_{w_{\text{in}}} \right] . \tag{7.65}$$

Exploiting Eq. (7.65) we obtain the plot shown in Fig. 7.4: we notice that it is possible to obtain, by appropriately choosing the path in parameter space, a wide range of values of the phase α, by only exploring the small parameters region. This fully shows how it is possible to attach a geometric phase by letting the Hamiltonian of the system vary in space, other than in time.

CHAPTER 8

Conclusions

We are now moving towards the conclusion of this thesis. During the exposition we went through many different topics in quantum engineering, ranging from open quantum system dynamics to potential engineering for state control and manipulation.

Collisional models are now quickly spreading as an effective tool to describe quantum dynamics in very different scenarios, from thermodynamics to quantum metrology. In Chap. 3 we showed how the elasticity given by collisional models in setting the causal structure of the interaction between different quantum systems allowed us to derive in a simple fashion the master equation describing the dynamics of a quantum cascade network. As the field of network study, both classical [R. Albert and Barabási 2002; Barrat, Barthélemy, and Vespignani 2008] and quantum [Chiribella, D'Ariano, and Perinotti 2009; Nikolopoulos and Jex 2013], is nowadays rapidly expanding, it would be interesting to check whether collisional models, and more in general the theory of open system dynamics, can give further contributions in the field, from the modeling of socio-technical systems [Antal, Redner, and Sood 2006; Castellano, Marsili, and Vespignani 2000] and infrastructure networks [Barrat, Barthélemy, et al. 2004], such as environmental networks [Montoya, Pimm, and Solé 2006; Pimm 2002], telecommunications networks [R. Albert, Jeong, and Barabási 1999, 2000], scientific networks [Newman 2001a,b; Redner 2005], to the exploitation of quantum networks for state engineering [Pichler and Zoller 2016; Ramos et al. 2014; Ringel, Pletyukhov, and Gritsev 2014; Söllner et al. 2015] and quantum computation [Pichler, Choi, et al. 2017; Zheng, Gauthier, and Baranger 2013].

On the other hand in Chap. 4 we exploited another important feature of collisional models, namely the easiness in keeping track of the environmental degrees of freedom, in order to study a simple, yet fundamental thermodynamical process, the thermalization of a quantum system interacting with a thermal bath. By keeping track of the environmental state, we were able to compute the thermodynamic functionals needed at each step of the thermalization process, getting greater insight on the resulting final state of the process. Also in this case it must be said that the possibility of studying the environmental state has been a scarcely exploited feature of collisional models up to know, mostly because of the large memory required to describe the state as the time steps increase. Nonetheless this might represent an interesting topic to investigate, maybe exploiting some computational techniques from the field of many-body physics [Silvi et al. 2013; Verstraete, Garcia-Ripoll, and Cirac 2004; Vidal 2004].

Besides open quantum system theory, also potential engineering has been treated in this thesis. Specifically, after introducing the band engineering paradigm and the concept of confining potential and subbands in electron waveguides in Chap 5, we have shown how to arbitrary create potential profiles giving rise to what we dubbed *stretchable states*. This class of states, in analogy to what happens to an electromagnetic wave in an ϵ-near-zero metamaterial, has its wave profile stretched, i.e. the wave function of the particle has a flat region. While it is not easy to think to a specific outlook to this work, it must be noted that the field of quantum metamaterials is still expanding, and as such it will be interesting to further explore the analogies between electromagnetic waves in photonic metamaterials [Cai and Shalaev 2009; Caloz 2005] and matter waves in quantum metamaterials [Rakhmanov et al. 2008].

Finally in Chap. 7 we have shown how it is possible to attach a Berry phase to a quantum state by spatially varying the potential landscape dictating the particle dynamics. Though the mathematics behind this phenomenon was already known and exploited in different contexts [Grosso and Parravicini 2000], it was never highlighted the possibility of imprinting a geometric phase on a quantum state. While we developed our theory for a two dimensional potential landscape, the result can be straightforwardly generalized to a three dimensional situation, where however the phenomenology would be richer, due to the greater freedom in choosing the basis and the gauge. It is also worth highlighting that much work has been done on the relation between holonomies and networks [Bascone et al. 2019; Lahtinen et al. 2008] and critical behavior [Pachos and A. C. Carollo 2006; Plastina, Liberti, and A. Carollo 2006]. Moreover it would be interesting to see how shortcuts to adiabaticity techniques [Guéry-Odelin et al. 2019; Menchon-Enrich et

al. 2016; Vepsäläinen, Danilin, and Paraoanu 2018] might help in relaxing the hypothesis under which the theory has been developed, possibly leading to a simpler experimental feasibility.

Appendices

A. Appendix to Chap. 3

A.1. Positivity of the matrix $\Omega_{jj'}$

In this section we demonstrate the non-negativity of the matrix $\Omega_{jj'}$ defined in Sec. 3.2, remembering that j stands for the joint index (ℓ, k, m) and the elements of $\Omega_{jj'}$ are the coefficients $D^{(\ell,\ell')}_{mm'(kk')}$ defined in Eq. (3.73), which amounts to show that for any vector $\vec{q}$ of complex elements q_j, it holds:

$$\vec{q}\,\Omega\,\vec{q}^{\,\dagger} = \sum_{jj'} q_j \Omega_{jj'} q^*_{j'} \geq 0. \tag{A.1}$$

Starting from the definition of the coefficients in Eqs.(3.54, 3.56, 3.57) and exploiting Eq. (3.61) we get:

$$\begin{aligned} 2\vec{q}\,\Omega\,\vec{q}^{\,\dagger} &= \sum_m q_{(\ell,k,m)} q^*_{(\ell',k',m)} \gamma^{(\ell,\ell')}_{m(kk')} + \sum_{m'>m} \left[q_{(\ell,k,m)} q^*_{(\ell',k',m')} \zeta^{(\ell,\ell')}_{mm'(kk')} \right] \\ &= \sum_m \mathrm{Tr}_{\mathcal{E}_n} \left\{ \hat{Q}^{(m)\dagger}_{\mathcal{E}_n} \hat{Q}^{(m)}_{\mathcal{E}_n} \mathcal{M}^{(m-1\leftarrow 1)}_{\mathcal{E}_n}(\hat{\eta}_{\mathcal{E}_n}) \right\} \\ &+ \sum_{m'>m} \left[\mathrm{Tr}_{\mathcal{E}_n} \left\{ \hat{Q}^{(m')\dagger}_{\mathcal{E}_n} \mathcal{M}^{(m'-1\leftarrow m)}_{\mathcal{E}_n} \left(\hat{Q}^{(m)}_{\mathcal{E}_n} \mathcal{M}^{(m-1\leftarrow 1)}_{\mathcal{E}_n}(\hat{\eta}_{\mathcal{E}_n}) \right) \right\} + h.c. \right], \end{aligned} \tag{A.2}$$

where we are using the summation over repeated indices convention and we have defined for easiness of notation:

$$\hat{Q}^{(m)}_{\mathcal{E}_n} = \sum_{\ell,k} q_{(\ell,k,m)} \hat{B}^{(\ell,m)}_{E^{(k)}_n}. \tag{A.3}$$

We now invoke the Stinespring representation to write the CPT maps in the expression as:

$$\mathcal{M}^{(m)}_{\mathcal{E}_n}(\cdots) = \mathrm{Tr}_{\mathcal{A}} \left\{ \mathcal{V}^{(m)}_{\mathcal{E}_n,\mathcal{A}}(\cdots \otimes |0\rangle\langle 0|_{\mathcal{A}}) \right\}, \tag{A.4}$$

$$\mathcal{V}^{(m)}_{\mathcal{E}_n,\mathcal{A}} = \hat{V}^{(m)}_{\mathcal{E}_n,\mathcal{A}}(\cdots)\hat{V}^{(m)\dagger}_{\mathcal{E}_n,\mathcal{A}}, \tag{A.5}$$

where $|0\rangle_{\mathcal{A}}$ is some reference state of an ancillary system $\mathcal{A}$ and $\hat{V}^{(m)}_{\mathcal{E}_n,\mathcal{A}}$ is a unitary

transformation coupling $\mathcal{A}$ and $\mathcal{E}_n$. Thanks to Eq. (A.4) we can write:

$$\mathcal{M}_{\mathcal{E}_n}^{(m'\leftarrow m)} = \mathrm{Tr}_{\mathcal{A}}\left\{\mathcal{V}_{\mathcal{E}_n,\mathcal{A}}^{(m'\leftarrow m)}(\cdots\otimes|0_{\mathcal{A}}\rangle\langle 0_{\mathcal{A}}|)\right\}, \tag{A.6}$$

$$\mathcal{V}_{\mathcal{E}_n,\mathcal{A}}^{(m'\leftarrow m)}(\cdots) = \hat{V}_{\mathcal{E}_n,\mathcal{A}}^{(m'\leftarrow m)}(\cdots)\hat{V}_{\mathcal{E}_n,\mathcal{A}}^{(m'\leftarrow m)\dagger}, \tag{A.7}$$

$$\hat{V}_{\mathcal{E}_n,\mathcal{A}}^{(m'\leftarrow m)} = \hat{V}_{\mathcal{E}_n,\mathcal{A}}^{(m')}\hat{V}_{\mathcal{E}_n,\mathcal{A}}^{(m'-1)}\cdots\hat{V}_{\mathcal{E}_n,\mathcal{A}}^{(m)}. \tag{A.8}$$

Inserting these expressions in Eq. (A.2) we get:

$$2\vec{q}\,\Omega\,\vec{q}^{\,\dagger} = \sum_m \mathrm{Tr}_{\mathcal{E}_n,\mathcal{A}}\left\{\hat{Q}_{\mathcal{E}_n}^{(m)\dagger}\hat{Q}_{\mathcal{E}_n}^{(m)}\mathcal{V}_{\mathcal{E}_n,\mathcal{A}}^{(m-1\leftarrow 1)}(\hat{\eta}_{\mathcal{E}_n}\otimes|0_{\mathcal{A}}\rangle\langle 0_{\mathcal{A}}|)\right\} \tag{A.9}$$

$$+\sum_{m'>m}\left[\mathrm{Tr}_{\mathcal{E}_n,\mathcal{A}}\left\{\hat{Q}_{\mathcal{E}_n}^{(m')\dagger}\mathcal{V}_{\mathcal{E}_n,\mathcal{A}}^{(m'-1\leftarrow m)}\left(\hat{Q}_{\mathcal{E}_n}^{(m)}\mathcal{V}_{\mathcal{E}_n,\mathcal{A}}^{(m-1\leftarrow 1)}(\hat{\eta}_{\mathcal{E}_n}\otimes|0_{\mathcal{A}}\rangle\langle 0_{\mathcal{A}}|)\right)\right\}+h.c.\right]$$

$$=\sum_m \mathrm{Tr}_{\mathcal{E}_n,\mathcal{A}}\left\{\tilde{\mathcal{V}}_{\mathcal{E}_n,\mathcal{A}}^{(m-1\leftarrow 1)}\left(\hat{Q}_{\mathcal{E}_n}^{(m)\dagger}\hat{Q}_{\mathcal{E}_n}^{(m)}\right)(\hat{\eta}_{\mathcal{E}_n}\otimes|0_{\mathcal{A}}\rangle\langle 0_{\mathcal{A}}|)\right\} \tag{A.10}$$

$$+\sum_{m'>m}\left[\mathrm{Tr}_{\mathcal{E}_n,\mathcal{A}}\left\{\tilde{\mathcal{V}}_{\mathcal{E}_n,\mathcal{A}}^{(m-1\leftarrow 1)}\left(\tilde{\mathcal{V}}_{\mathcal{E}_n,\mathcal{A}}^{(m'-1\leftarrow m)}\left(\hat{Q}_{\mathcal{E}_n}^{(m')\dagger}\right)\hat{Q}_{\mathcal{E}_n}^{(m)}\right)(\hat{\eta}_{\mathcal{E}_n}\otimes|0_{\mathcal{A}}\rangle\langle 0_{\mathcal{A}}|)\right\}+h.c.\right].$$

At this point we observe that:

$$\tilde{\mathcal{V}}_{\mathcal{E}_n}^{(m-1\leftarrow 1)}\left(\hat{Q}_{\mathcal{E}_n}^{(m)\dagger}\hat{Q}_{\mathcal{E}_n}^{(m)}\right) =$$

$$\tilde{\mathcal{V}}_{\mathcal{E}_n}^{(m-1\leftarrow 1)}(\hat{Q}_{\mathcal{E}_n}^{(m)\dagger})\tilde{\mathcal{V}}_{\mathcal{E}_n}^{(m-1\leftarrow 1)}(\hat{Q}_{\mathcal{E}_n}^{(m)}) = \hat{T}_{\mathcal{E}_n,\mathcal{A}}^{(m)\dagger}\hat{T}_{\mathcal{E}_n,\mathcal{A}}^{(m)}, \tag{A.11}$$

$$\tilde{\mathcal{V}}_{\mathcal{E}_n,\mathcal{A}}^{(m-1\leftarrow 1)}\left(\tilde{\mathcal{V}}_{\mathcal{E}_n,\mathcal{A}}^{(m'-1\leftarrow m)}\left(\hat{Q}_{\mathcal{E}_n}^{(m')\dagger}\right)\hat{Q}_{\mathcal{E}_n}^{(m)}\right) =$$

$$\tilde{\mathcal{V}}_{\mathcal{E}_n}^{(m'-1\leftarrow 1)}(\hat{Q}_{\mathcal{E}_n}^{(m')\dagger})\tilde{\mathcal{V}}_{\mathcal{E}_n}^{(m-1\leftarrow 1)}(\hat{Q}_{\mathcal{E}_n}^{(m)}) = \hat{T}_{\mathcal{E}_n,\mathcal{A}}^{(m')\dagger}\hat{T}_{\mathcal{E}_n,\mathcal{A}}^{(m)}, \tag{A.12}$$

where we have introduced the operators:

$$\hat{T}_{\mathcal{E}_n,\mathcal{A}}^{(m)} = \tilde{\mathcal{V}}_{\mathcal{E}_n,\mathcal{A}}^{(m-1\leftarrow 1)}(\hat{Q}_{\mathcal{E}_n}^{(m)}). \tag{A.13}$$

Inserting Eqs.(A.11, A.12) into Eq. (A.10) and rearranging the terms, we finally prove the thesis:

$$2\,\vec{q}\Omega\,\vec{q}^{\,\dagger} = \sum_{m,m'=1}^{M}\mathrm{Tr}_{\mathcal{E}_n,\mathcal{A}}\left\{\hat{T}_{\mathcal{E}_n,\mathcal{A}}^{(m')\dagger}\hat{T}_{\mathcal{E}_n,\mathcal{A}}^{(m)}(\hat{\eta}_{\mathcal{E}_n}\otimes|0_{\mathcal{A}}\rangle\langle 0_{\mathcal{A}}|)\right\}. \tag{A.14}$$

A.2. Calculations from Sec. 3.3.2

In this section we report the calculations for the master equation in Sec. 3.3.2.

First of all we are interested in the expressions for the CPT maps $\mathcal{M}_{\mathcal{E}_n}^{(m)}$ acting on the ancillas. As it can be seen from Fig. 3.6, the map $\mathcal{M}_{\mathcal{E}_n}^{(1)}$ acting after the interaction of the ancillas with the first node Q_1 but before their interaction with Q_2, is associated with beam splitter BS_1. Complementary, we have the map $\mathcal{M}_{\mathcal{E}_n}^{(2)}$ acting after the interaction with node Q_2 associated to the phase shift PS and the second beam splitter BS_2. We can then write:

$$\mathcal{M}_{\mathcal{E}_n}^{(1)}(\cdots) = \hat{V}_{BS_1}(\cdots)\hat{V}_{BS_1}^{\dagger}, \tag{A.15}$$

$$\mathcal{M}_{\mathcal{E}_n}^{(2)}(\cdots) = \hat{V}_{BS_2}\hat{V}_{PS}(\cdots)\hat{V}_{PS}^{\dagger}\hat{V}_{BS_2}^{\dagger}. \tag{A.16}$$

Once we have these expressions, it is very simple to see that the stability condition still holds for the same reasons exposed in Sec. 3.3.1. Moreover, we have already said that the coefficients $\gamma_{1(kk')}^{(\ell,\ell')}$ relative to the term $\mathcal{L}_1$ are identical to the ones computed in Sec. 3.3.1, together with the $\gamma_{3(kk')}^{(\ell,\ell')}$ associated to $\mathcal{L}_3$, and the coefficients $\zeta_{13(kk')}^{(\ell,\ell')}$, $\xi_{13(kk')}^{(\ell,\ell')}$ associated with $\mathcal{D}_{13}$, as they are identical to the coefficients for the $\mathcal{D}_{12}$ term in Sec. 3.3.1. We are then left with the computation of the coefficients relative to the terms $\mathcal{L}_2$, $\mathcal{D}_{12}$ and $\mathcal{D}_{23}$. As for the local term $\mathcal{L}_2$ we have:

$$\begin{aligned}
\gamma_{2(kk')}^{(1,1)} &= \left[\gamma_{2(kk')}^{(2,2)}\right]^* = \delta_{k,1}\delta_{k',1}\,\mathrm{Tr}_{\mathcal{E}_n}\left\{\hat{b}^2_{E_n^{(1)}}\mathcal{M}_{\mathcal{E}_n}^{(1)}(\hat{\eta}_{\mathcal{E}_n})\right\} = 0,\\
\gamma_{2(kk')}^{(1,2)} &= \delta_{k,1}\delta_{k',1}\,\mathrm{Tr}_{\mathcal{E}_n}\left\{\hat{b}^{\dagger}_{E_n^{(1)}}\hat{b}_{E_n^{(1)}}\mathcal{M}_{\mathcal{E}_n}^{(1)}(\hat{\eta}_{\mathcal{E}_n})\right\}\\
&= \delta_{k,1}\delta_{k',1}\,\mathrm{Tr}_{\mathcal{E}_n}\left\{\left(\sqrt{\epsilon_1}\hat{b}^{\dagger}_{E_n^{(1)}} + i\sqrt{1-\epsilon_1}\hat{b}^{\dagger}_{E_n^{(2)}}\right)\left(\sqrt{\epsilon_1}\hat{b}_{E_n^{(1)}} - i\sqrt{1-\epsilon_1}\hat{b}_{E_n^{(2)}}\right)\hat{\eta}_{\mathcal{E}_n}\right\}\\
&= \delta_{k,1}\delta_{k',1}\bar{N}_{12},\\
\gamma_{2(kk')}^{(2,1)} &= \delta_{k,1}\delta_{k',1}\,\mathrm{Tr}_{\mathcal{E}_n}\left\{\hat{b}_{E_n^{(1)}}\hat{b}^{\dagger}_{E_n^{(1)}}\mathcal{M}_{\mathcal{E}_n}^{(1)}(\hat{\eta}_{\mathcal{E}_n})\right\}\\
&= \delta_{k,1}\delta_{k',1}\,\mathrm{Tr}_{\mathcal{E}_n}\left\{\left(\sqrt{\epsilon_1}\hat{b}_{E_n^{(1)}} - i\sqrt{1-\epsilon_1}\hat{b}_{E_n^{(2)}}\right)\left(\sqrt{\epsilon_1}\hat{b}^{\dagger}_{E_n^{(1)}} + i\sqrt{1-\epsilon_1}\hat{b}^{\dagger}_{E_n^{(2)}}\right)\hat{\eta}_{\mathcal{E}_n}\right\}\\
&= \delta_{k,1}\delta_{k',1}(\bar{N}_{12}+1).
\end{aligned}$$

The coefficients for $\mathcal{D}_{12}$ are instead worth:

$$\begin{aligned}
\zeta^{(1,1)}_{12(kk')} &= \left[\xi^{(2,2)}_{12(kk')}\right]^* = \delta_{k,1}\delta_{k',1}\,\mathrm{Tr}_{\mathcal{E}_n}\left\{\hat{b}_{E_n^{(1)}}\mathcal{M}^{(1)}_{\mathcal{E}_n}\left(\hat{b}_{E_n^{(1)}}\hat{\eta}_{\mathcal{E}_n}\right)\right\} = 0,\\
\zeta^{(2,2)}_{12(kk')} &= \left[\xi^{(1,1)}_{12(kk')}\right]^* = \delta_{k,1}\delta_{k',1}\,\mathrm{Tr}_{\mathcal{E}_n}\left\{\hat{b}^\dagger_{E_n^{(1)}}\mathcal{M}^{(1)}_{\mathcal{E}_n}\left(\hat{b}^\dagger_{E_n^{(1)}}\hat{\eta}_{\mathcal{E}_n}\right)\right\} = 0,\\
\zeta^{(1,2)}_{12(kk')} &= \left[\xi^{(2,1)}_{12(kk')}\right]^* = \delta_{k,1}\delta_{k',1}\,\mathrm{Tr}_{\mathcal{E}_n}\left\{\hat{b}^\dagger_{E_n^{(1)}}\mathcal{M}^{(1)}_{\mathcal{E}_n}\left(\hat{b}_{E_n^{(1)}}\hat{\eta}_{\mathcal{E}_n}\right)\right\}\\
&= \delta_{k,1}\delta_{k',1}\,\mathrm{Tr}_{\mathcal{E}_n}\left\{\left(\sqrt{\epsilon_1}\hat{b}^\dagger_{E_n^{(1)}} + i\sqrt{1-\epsilon_1}\hat{b}^\dagger_{E_n^{(2)}}\right)\hat{b}_{E_n^{(1)}}\hat{\eta}_{\mathcal{E}_n}\right\} = \delta_{k,1}\delta_{k',1}\sqrt{\epsilon_1}N_1,\\
\zeta^{(2,1)}_{12(kk')} &= \left[\xi^{(1,2)}_{12(kk')}\right]^* = \delta_{k,1}\delta_{k',1}\,\mathrm{Tr}_{\mathcal{E}_n}\left\{\hat{b}_{E_n^{(1)}}\mathcal{M}^{(1)}_{\mathcal{E}_n}\left(\hat{b}^\dagger_{E_n^{(1)}}\hat{\eta}_{\mathcal{E}_n}\right)\right\}\\
&= \delta_{k,1}\delta_{k',1}\,\mathrm{Tr}_{\mathcal{E}_n}\left\{\left(\sqrt{\epsilon_1}\hat{b}_{E_n^{(1)}} - i\sqrt{1-\epsilon_1}\hat{b}_{E_n^{(2)}}\right)\hat{b}^\dagger_{E_n^{(1)}}\hat{\eta}_{\mathcal{E}_n}\right\} = \delta_{k,1}\delta_{k',1}\sqrt{\epsilon_1}(N_1+1).
\end{aligned}$$

Finally, the coefficients for $\mathcal{D}_{23}$ can be written as:

$$\begin{aligned}
\zeta^{(1,1)}_{23(kk')} &= \left[\xi^{(2,2)}_{23(kk')}\right]^* = \delta_{k,1}\delta_{k',1}\,\mathrm{Tr}_{\mathcal{E}_n}\left\{\hat{b}_{E_n^{(1)}}\mathcal{M}^{(2)}_{\mathcal{E}_n}\left(\hat{b}_{E_n^{(1)}}\mathcal{M}^{(1)}_{\mathcal{E}_n}(\hat{\eta}_{\mathcal{E}_n})\right)\right\} = 0,\\
\zeta^{(2,2)}_{23(kk')} &= \left[\xi^{(1,1)}_{23(kk')}\right]^* = \delta_{k,1}\delta_{k',1}\,\mathrm{Tr}_{\mathcal{E}_n}\left\{\hat{b}^\dagger_{E_n^{(1)}}\mathcal{M}^{(2)}_{\mathcal{E}_n}\left(\hat{b}^\dagger_{E_n^{(1)}}\mathcal{M}^{(1)}_{\mathcal{E}_n}(\hat{\eta}_{\mathcal{E}_n})\right)\right\} = 0,\\
\zeta^{(1,2)}_{23(kk')} &= \left[\xi^{(2,1)}_{23(kk')}\right]^* = \delta_{k,1}\delta_{k',1}\,\mathrm{Tr}_{\mathcal{E}_n}\left\{\hat{b}^\dagger_{E_n^{(1)}}\mathcal{M}^{(2)}_{\mathcal{E}_n}\left(\hat{b}_{E_n^{(1)}}\mathcal{M}^{(1)}_{\mathcal{E}_n}(\hat{\eta}_{\mathcal{E}_n})\right)\right\}\\
&= \delta_{k,1}\delta_{k',1}\,\mathrm{Tr}_{\mathcal{E}_n}\left\{\left(c^*(\varphi)\hat{b}^\dagger_{E_n^{(1)}} + is^*(\varphi)\hat{b}^\dagger_{E_n^{(2)}}\right)\left(\sqrt{\epsilon_1}\hat{b}_{E_n^{(1)}} - i\sqrt{1-\epsilon_1}\hat{b}_{E_n^{(2)}}\right)\hat{\eta}_{\mathcal{E}_n}\right\}\\
&= \delta_{k,1}\delta_{k',1}M^*_{12}(\varphi),\\
\zeta^{(2,1)}_{23(kk')} &= \left[\xi^{(1,2)}_{23(kk')}\right]^* = \delta_{k,1}\delta_{k',1}\,\mathrm{Tr}_{\mathcal{E}_n}\left\{\hat{b}_{E_n^{(1)}}\mathcal{M}^{(2)}_{\mathcal{E}_n}\left(\hat{b}^\dagger_{E_n^{(1)}}\mathcal{M}^{(1)}_{\mathcal{E}_n}(\hat{\eta}_{\mathcal{E}_n})\right)\right\}\\
&= \delta_{k,1}\delta_{k',1}\,\mathrm{Tr}_{\mathcal{E}_n}\left\{\left(c(\varphi)\hat{b}_{E_n^{(1)}} + is(\varphi)\hat{b}_{E_n^{(2)}}\right)\left(\sqrt{\epsilon_1}\hat{b}^\dagger_{E_n^{(1)}} + i\sqrt{1-\epsilon_1}\hat{b}^\dagger_{E_n^{(2)}}\right)\hat{\eta}_{\mathcal{E}_n}\right\}\\
&= \delta_{k,1}\delta_{k',1}\left(M_{12}(\varphi) + \lambda_{12}(\varphi)\right).
\end{aligned}$$

As for the GKSL form of the master equation, the matrix $D^{(\ell,\ell')}_{mm'(kk')}$ can be written as:

$$\left[\begin{array}{cc|cc|cc}
N_1 & 0 & \sqrt{\epsilon_1}N_1 & 0 & c^*(\varphi)N_1 & 0\\
0 & N_1+1 & 0 & \sqrt{\epsilon_1}(N_1+1) & 0 & c(\varphi)(N_1+1)\\
\hline
\sqrt{\epsilon_1}N_1 & 0 & \bar{N}_{12} & 0 & M^*_{12}(\varphi) & 0\\
0 & \sqrt{\epsilon_1}(N_1+1) & 0 & (\bar{N}_{12}+1) & 0 & M_{12}(\varphi)+\lambda(\varphi)\\
\hline
c(\varphi)N_1 & 0 & M_{12}(\varphi) & 0 & N_{12}(\varphi) & 0\\
0 & c^*(\varphi)(N_1+1) & 0 & M^*_{12}(\varphi)+\lambda^*(\varphi) & 0 & (N_{12}(\varphi)+1)
\end{array}\right].$$

Diagonalizing this matrix, one finds the following Hamiltonian contributions:

$$\hat{H}_{12} = -\frac{i}{2}\sqrt{\epsilon_1}\left(\hat{a}_1\hat{a}_2^\dagger - \hat{a}_1^\dagger\hat{a}_2\right), \tag{A.17}$$

$$\hat{H}_{23} = -\frac{i}{2}\left(\lambda^*(\varphi)\hat{a}_2\hat{a}_3^\dagger - \lambda(\varphi)\hat{a}_2^\dagger\hat{a}_3\right), \tag{A.18}$$

$$\hat{H}_{13} = -\frac{i}{2}\left(c^*(\varphi)\hat{a}_1\hat{a}_3^\dagger - c(\varphi)\hat{a}_1^\dagger\hat{a}_3\right). \tag{A.19}$$

A.3. Lindblad operators for the network of Sec. 3.4

The master equation for the network of Sec. 3.4 reported in Eq. (3.134) can be diagonalized following the receipt already shown in Sec. 3.2, obtaining the Lindblad operators in Eq. (A.3).

To achieve our goal we write the $2M \times 2M$ matrix $\Omega_{jj'}$ in a block representation:

$$\Omega = \begin{pmatrix} \Xi_{11} & \Xi_{12} & \cdots & \Xi_{1M} \\ \Xi_{21} & \Xi_{22} & \cdots & \Xi_{2M} \\ \cdots & \cdots & \cdots & \cdots \\ \Xi_{M1} & \Xi_{M2} & \cdots & \Xi_{MM} \end{pmatrix}, \tag{A.20}$$

where each $\Xi_{mm'}$ is a 2×2 diagonal block of the form:

$$\Xi_{mm'} = \begin{pmatrix} 0 & 0 \\ 0 & \zeta_{mm'} \end{pmatrix} \quad \forall m' > m, \tag{A.21}$$

$\zeta_{mm'}$ being the coefficients in Eq. (3.140). The κ_i in Eq. (3.138) are nothing but the eigenvalues of $\Omega_{jj'}$, while the Lindblad operators $\hat{L}_i$ in the same equation are obtained via:

$$\hat{\boldsymbol{L}} = W \begin{pmatrix} \hat{a}_1^\dagger \\ \hat{a}_1 \\ \hat{a}_2^\dagger \\ \hat{a}_2 \\ \vdots \\ \hat{a}_M^\dagger \\ \hat{a}_M \end{pmatrix}, \tag{A.22}$$

where W is the $2M \times 2M$ matrix diagonalizing $\Omega_{jj'}$, i.e. $\Omega = WDW^\dagger$, $D = \mathrm{diag}[\kappa_i]$

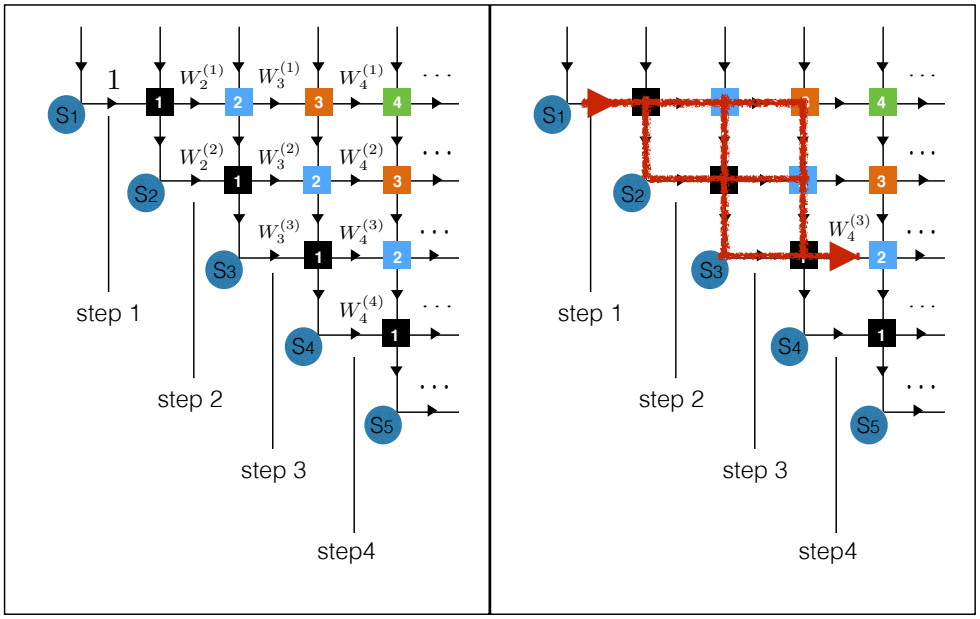

Figure A.1.: Schematic illustration of the amplitudes $W_k^{(\ell)}$ labelling the horizontal lines of the network. As made clear by the figure in left panel, these amplitudes are associated with the propagation of a signal from S_1 to the k-th horizontal step of the ℓ-th level of the network. To better exemplify this, in the right panel the paths contributing the definition of $W_4^{(3)}$ have been highlighted.

being the diagonal matrix whose elements are the eigenvalues of $\Omega_{jj'}$. For the case under consideration the construction above can be further simplified if we consider the we are dealing with environmental channels in the vacuum state. This is manifested in $\Omega_{jj'}$ by the fact that its odd column, as well as its odd rows, contain only zero elements, so that they can be safely removed, their corresponding eigenvalues being null. Upon this consideration, Ω becomes an $M \times M$ matrix and we can write the Lindblad operators as in Eq. (3.138).

A.4. Proof of Eq. (3.196)

Before proceeding in demonstrating Eq. (3.196), in order to obtain more compact expressions, it is useful to adopt a change of notation. In fact in our demonstration we will need to label the horizontal elements of the network: for ℓ and k integers we use $W_k^{(\ell)}$ to indicate the amplitude of the signal reaching the k-th horizontal step of the network at the ℓ-th level, as exemplified in Fig. A.1.

The various elements $W_k^{(\ell)}$ are connected through the action of the beam splitters in

the network, giving rise to linear relationships which we report for the first values of k:

$$
\begin{aligned}
&W_2^{(1)} = \sqrt{\tau_1} \quad W_2^{(2)} = -i\sqrt{1-\tau_1}e^{-i\varphi_1} \quad W_3^{(1)} = \sqrt{\tau_2}W_2^{(1)}, \\
&W_3^{(2)} = (-i\sqrt{1-\tau_1}e^{-i\varphi_1})(-i\sqrt{1-\tau_2}e^{-i\varphi_2})W_2^{(1)} + \sqrt{\tau_1}W_2^{(2)}, \\
&W_3^{(3)} = (\sqrt{\tau_1}e^{-i\varphi_1})(-i\sqrt{1-\tau_2}e^{-i\varphi_2})W_2^{(1)} + (-i\sqrt{1-\tau_1}e^{-i\varphi_1})W_2^{(2)}.
\end{aligned}
$$

Using this notation we have that $A^{(1)}_{k\leftarrow 1}$ corresponds to the element $W_k^{(k)}$, so that we have:

$$
\xi_k = A^{(1)}_{k+1\leftarrow 1} = W_{k+1}^{(k+1)}. \tag{A.23}
$$

Moreover we also have that for $\ell = 1$ and any k it holds:

$$
W_k^{(1)} = \sqrt{\tau_{k-1}\tau_{k-2}\cdots\tau_2\tau_1}, \tag{A.24}
$$

so that Eq. (3.196) can be equivalently written as:

$$
\tau_k = 1 - \left(\frac{1-|W_k^{(1)}|^2}{|W_k^{(1)}|^2}\right)\left(\frac{1-\tau_{k-1}}{\tau_{k-1}}\right). \tag{A.25}
$$

Now, let us assume that we want to nullify second-neighbor interactions, i.e. $\xi_2 = 0$. This is tantamount to nullify $W_3^{(3)}$:

$$
\begin{aligned}
&\sqrt{\tau_1}(-i\sqrt{1-\tau_2}e^{-i\varphi_2})W_2^{(1)} + (-i\sqrt{1-\tau_1})W_2^{(2)} = 0 \\
&\Rightarrow \varphi_2 = \varphi_1 + \frac{\pi}{2}, \quad \tau_2 = 1 - \left(\frac{1-|W_2^{(1)}|^2}{|W_2^{(1)}|^2}\right)\left(\frac{1-\tau_1}{\tau_1}\right).
\end{aligned} \tag{A.26}
$$

The solution for τ_2 in Eq. (A.26) shows the validity of Eq. (3.196) for $k = 2$. To proceed further we note that when we eliminate second-neighbor interactions, this implies that the signal from S_1 reaches the third level of the interferometer without interacting with S_3, thus producing the amplitudes $W_3^{(1)}$ and $W_3^{(2)}$. Though we already computed the explicit value of these amplitudes, actually we only need to note that probability conservation and $W_3^{(3)} = 0$ imply the complementarity of $W_3^{(1)}$ and $W_3^{(2)}$, leading to

$$
W_3^{(2)} = e^{-i\alpha_3}\sqrt{1-|W_3^{(1)}|^2}, \tag{A.27}
$$

α_3 being an irrelevant phase. At this point we pose ourselves the problem of eliminat-

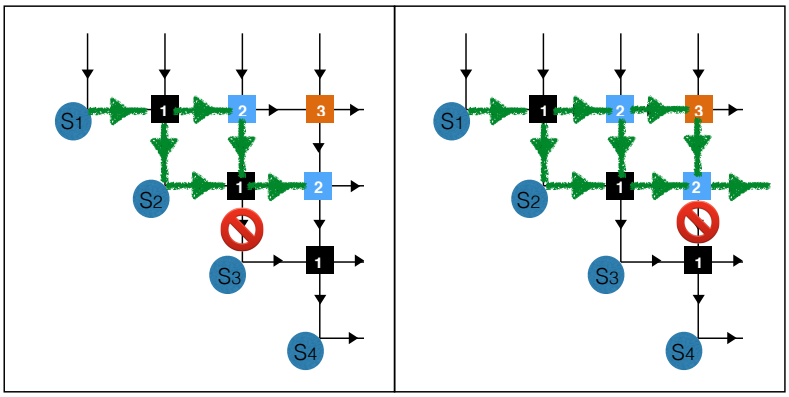

Figure A.2.: Left panel: sketch of the possible paths when nullifying ξ_2. As highlighted, the signal from S_1 (green) splits away in the first beam splitter following two paths that recombine themselves in the beam splitter with transmissivity τ_1 at the second level of the network. From there, if the relative phase has been tuned properly, the signal goes all in the horizontal output branch of the beam splitter, thus not interacting with S_3. Right panel: still a sketch of the possible paths the signal can follow, but for third-neighbor interactions. From this picture one can observe how the signal must remain confined in the first two level of the network in order to eliminate third-neighbor interactions.

ing third-neighbor interactions: in order to do this we must prevent the signal to reach the node S_4, i.e. we require $W_4^{(4)} = 0$. However we are faced with the problem that we already imposed the condition $W_3^{(3)} = 0$, so that there is no horizontal signal that can be used by the beam splitter of transmissivity τ_1 to interfere destructively with the one coming from above. From this we conclude that in order to reach our goal, the signal must be confined in the first two levels of the network (see right panel in Fig. A.2), leading to the condition:

$$\sqrt{\tau_2}(-i\sqrt{1-\tau_3}e^{-i\varphi_3})W_3^{(1)} + (-i\sqrt{1-\tau_2})W_3^{(2)} = 0. \tag{A.28}$$

Exploiting Eq. (A.27) we can solve the equation for φ_3 and τ_3, obtaining:

$$\varphi_3 = \alpha_3 + \pi \tag{A.29}$$

$$\tau_3 = 1 - \left(\frac{1-|W_3^{(1)}|^2}{|W_3^{(1)}|^2}\right)\left(\frac{1-\tau_2}{\tau_2}\right), \tag{A.30}$$

so that we proved Eq. (3.196) to be valid also for $k = 3$. In order to complete the demonstration we iterate the procedure we just performed, noting that having imposed

$\xi_2 = \xi_3 = 0$ implies that the signal must be confined in the first two levels, so that the fourth step of the network is populated only through the complementary terms $W_4^{(1)}$ and $W_4^{(2)}$ which must fulfill:

$$\sqrt{\tau_3}\left(-i\sqrt{1-\tau_4}e^{-i\varphi_4}\right)W_4^{(1)} + (-i\sqrt{1-\tau_3})W_4^{(2)} = 0, \tag{A.31}$$

leading to

$$\tau_4 = 1 - \left(\frac{1-|W_4^{(1)}|^2}{|W_4^{(1)}|^2}\right)\left(\frac{1-\tau_3}{\tau_3}\right), \tag{A.32}$$

so that Eq. (3.196) is proved by construction. Nonetheless this is not all: in the main text we anticipated that Eq. (3.196) is valid only when we choose $\tau_1 \in [3/4, 1]$. The necessity of a lower bound for τ_1 is readily seen if we consider the functional dependence of the other transmissivities on τ_1:

$$\tau_2(\tau_1) = 1 - \frac{(1-\tau_1)^2}{\tau_1^2}, \tag{A.33}$$

$$\tau_3(\tau_1) = 1 - \frac{(1-\tau_1)^3}{(2\tau_1-1)^2}, \tag{A.34}$$

$$\tau_4(\tau_1) = 1 - \frac{(1-\tau_4)^4}{(\tau_1^2+\tau_1-1)^2}. \tag{A.35}$$

Since $\tau_k \in [0,1]$ for any k, we see immediately that not all values of τ_1 are allowed. Considering for instance Eq. (A.33), we get instantly the condition $\tau_1 > 1/2$, while from the condition on τ_3 we get $\tau_1 > (\sqrt{5}-1)/2 \simeq 0.618$ and finally from Eq. (A.35) we have $\tau_1 > 2/3$. Before discussing why Eq. (3.196) is valid for any k given $\tau_1 \in [3/4, 1]$, we want to highlight that the condition $\tau_k \leq 1$ is easily shown to be true for any k, since it suffices to note that $1-\tau_{k+1}$ and $1-\tau_{k-1}$ must have the same sign, as can be seen by the formula:

$$1 - \tau_{k+1} = \left(\frac{1-\tau_{k-1}\tau_{k-2}\cdots\tau_1}{1-\tau_{k-1}\tau_{k-2}\cdots\tau_1-\tau_{k-1}}\right)^2(1-\tau_{k-1}), \tag{A.36}$$

which is obtained via a simple iteration of Eq. 3.196.

Going back to the problem of setting a lower bound on τ_1, we proceed as follows: consider $\bar{\tau}_1 \in [0,1]$ such that $\tau_k \geq 0$ for all k; then, for any $\bar{\bar{\tau}}_1 > \bar{\tau}_1$, it must still hold that all the other transmissivities are posiive, since for a given k the rhs of Eq. (3.196) is an

increasing function of the parameters τ_{k-1}, τ_{k-2}, ..., τ_1. We then notice that $\tau_1 = 3/4$ is a legitimate choice, since it yields:

$$\tau_k(\tau_1 = 3/4) = 1 - \frac{1}{(k+1)^2} = \frac{k(k-2)}{(k+1)^2}, \tag{A.37}$$

the last expression being easily obtained by induction. We finally justify $\tau_1 \geq 3/4$ as lower bound considering that a direct evaluation of the transmissivities up to $k = 10$ already shows numerically that $\tau_1 > 0.74$ at least.

B. Appendix to Chap. 4

B.1. Derivation of the inequalities in the collisional model

In Sec. 4.2 we derived the Clausius inequality in Eq. (4.7) by exploiting the contractivity of the relative entropy under CPT evolution. In order to generalize the inequality to the collisional setting one can follow the same procedure, comparing the relative entropies of $\hat{\rho}_A(n)$ and $\hat{\rho}_A(n-1)$ with the thermal state $\hat{\eta}_A^{(\beta)}$, obtaining:

$$\begin{aligned} dS_A(n) &\geq \beta dQ_A(n), \\ dS_A(n) = S(\hat{\rho}_A(n)) - S(\hat{\rho}_A(n-1)), &\qquad dQ_A(n) = \mathrm{Tr}\left\{\hat{H}_A(\hat{\rho}_A(n) - \hat{\rho}_A(n-1))\right\}. \end{aligned} \tag{B.38}$$

showing that the intrinsic inequality holds also when considering a discrete step evolution.

The extrinsic inequality is obtained by invoking the subadditivity of the entropy, obtaining:

$$\Delta S_A(n) \geq -\Delta S_B(n) = nS(\hat{\eta}_b^{(\beta)}) - S(\hat{\rho}_B(n)), \tag{B.39}$$

where $\hat{\rho}_B(n)$ is the full state of the environment at the n-th step of the evolution, including all possible correlations among the ancillas. Also in this case we can write an incremental version of the inequality:

$$dS_A(n) \geq -dS_{b_n} = S(\hat{\eta}_b) - S(\hat{\rho}_{b_n}), \tag{B.40}$$

where $\hat{\rho}_{b_n} = \mathrm{Tr}_A\{\hat{U}_n(\hat{\rho}_A(n) \otimes \hat{\eta}_{b_n}^{(\beta)})\hat{U}_n^\dagger\}$ is the output state of the ancilla after the collision with A. Eq. (B.40) defines a weaker inequality than the one in Eq. (4.8). In fact starting from the previous equation we can define the local entropy variation appearing in Eq. (4.36) as:

$$\Delta S_B^{(\mathrm{loc})}(n) = \sum_{k=1}^{n} S(\hat{\rho}_{b_k}) - nS(\hat{\eta}_b^{(\beta)}). \tag{B.41}$$

The inequality defined starting from Eq. (B.41) is immediately seen to be weaker than the extrinsic bound because of the entropy subadditivity, $\sum_k S(\hat{\rho}_{b_k}) \geq S(\hat{\rho}_B(n))$. This must come as no surprise, since computing the entropy variation of the environment as in Eq. (B.41) is tantamount to approximating the environmental state at the n-th step

of the evolution with $\bigotimes_n \hat{\rho}_{b_n}$, thus neglecting all the correlations among the ancillas.

Finally it is worth noticing that Eq. (4.21) can be rewritten in the collisional framework as:

$$\beta\Delta Q_A(n) + \Delta S_B(n) = -S(\hat{\rho}_B(n)||\hat{\rho}_B(0)) \Rightarrow -\Delta S_B(n) \geq \beta\Delta Q_A(n). \tag{B.42}$$

For the local entropy variation we can write similarly:

$$\beta dQ_A(n) + dS_{b_n} = -S(\hat{\rho}_{b_n}||\hat{\eta}_b^{(\beta)}) \Rightarrow -\Delta S_B^{(\mathrm{loc})}(n) \geq \beta\Delta Q_A(n). \tag{B.43}$$

B.2. Asymptotic factorization with full dephasing

The asymptotic factorization, as anticipated in the main text, can be proved also in the weak coupling regime with a little modification of the model. In particular we are able to prove the factorization by forcing A to undergo a full dephasing $\mathcal{D}_A$ every $k >> 1$ steps of the dynamical evolution. The action of the transformation $\mathcal{D}_A$ is to destroy the off-diagonal elements of the density matrix of A:

$$\mathcal{D}_A(|j_A\rangle\langle j'_A|) = \delta_{jj'}\,|j_A\rangle\langle j_A|\,. \tag{B.44}$$

Without loss of generality, we now proceed in demonstrating our claim assuming A to be a qubit. Moreover our proof does not depend upon the specific form of the unitary operator describing the dynamics, the only requirement being that the corresponding CPT map gives rise to thermalization and acts trivially on the thermal state.

We divide the ancillas into sets, $B_1, B_2 \cdots$, each one containing k ancillas. After A has interacted with all the ancillas in B_1 we are left with the joint state:

$$\hat{\rho}_{AB_1}(k) = \mathcal{U}_k \circ \cdots \circ \mathcal{U}_2\mathcal{U}_1 \left[\hat{\rho}_A(0) \bigotimes_{i=1}^{k} \hat{\eta}_{b_i}^{(\beta)}\right] = \sum_{j,j'} |j_a\rangle\langle j'_a|\,\hat{\Pi}_{B_1}^{(j,j')}(\hat{\rho}_A(0)), \tag{B.45}$$

where $\Pi_{B_1}^{(j,j')}(\hat{\rho}_A(0))$ are operators of B_1 depending linearly on the input state of A. Tracing away B_1 we are left with:

$$\hat{\rho}_A(k) = \sum_{j,j'} M_{jj'}^{(k)}(\hat{\rho}_A(0))\,|j_A\rangle\langle j'_A|\,, \tag{B.46}$$

$$M_{jj'}^{(k)}(\hat{\rho}_A(0)) = \mathrm{Tr}_{B_1}\left\{\hat{\Pi}_{B_1}^{(j,j')}(\hat{\rho}_A(0))\right\}. \tag{B.47}$$

As we assumed the whole dynamics to induce thermalization on A, for large enough k we are ensured that A is approaching the thermal state $\hat{\eta}_A^{(\beta)}$, which is diagonal in the $\{|j\rangle_A\}$ basis with eigenvalues $\eta_j^{(\beta)} = e^{-\beta\hbar E_j}/\mathcal{Z}(\beta)$, $\mathcal{Z}(\beta)$ being the partition function. According to this, for any $\epsilon < 1$, it exists k sufficiently large such that:

$$\left|M_{jj'}^{(k)}(\hat{\rho}_A(0)) - \eta_j^{(\beta)}\right| < \epsilon, \tag{B.48}$$

$$\left|M_{jj'}^{(k)}(\hat{\rho}_A(0))\right| < \epsilon \quad \forall j \neq j' \tag{B.49}$$

hold. At this point we use the assumption of being dealing with a qubit, so that applying the full dephasing to the state in Eq. (B.45) we find:

$$\mathcal{D}_A(\hat{\rho}_{AB}(k)) = |0_A\rangle\langle 0_A| \otimes \hat{\Pi}_{B_1}^{(0,0)}(\hat{\rho}_A(0)) + |1_A\rangle\langle 1_A| \otimes \hat{\Pi}_{B_1}^{(1,1)}(\hat{\rho}_A(0)). \tag{B.50}$$

If we now sum and subtract the term $\frac{\eta_0^{(\beta)}}{\eta_1^{(\beta)}}\hat{\Pi}_{B_1}^{(1,1)}(\hat{\rho}_A(0))$ we can recast the last equation as

$$\hat{\rho}_{AB}(k) = |0_A\rangle\langle 0_A| \otimes \hat{\Delta}_{B_1}^{(k)}(\hat{\rho}_A(0)) + \hat{\eta}_A^{(\beta)} \otimes \hat{\Xi}_{B_1}^{(k)}(\hat{\rho}_A(0)), \tag{B.51}$$

with:

$$\hat{\Xi}_{B_1}(\hat{\rho}_A(0)) = \frac{\hat{\Pi}_{B_1^{(1,1)}}}{\eta_1^{(\beta)}}, \tag{B.52}$$

$$\hat{\Delta}_{B_1}^{(k)}(\hat{\rho}_A(0)) = \hat{\Pi}_{B_1}^{(0,0)}(\hat{\rho}_A(0)) - \frac{\eta_0^{(\beta)}}{\eta_1^{(\beta)}}\hat{\Pi}_{B_1}^{(1,1)}(\hat{\rho}_A(0)). \tag{B.53}$$

Now we want to show that the trace norm $\|\hat{\Delta}_{B_1}^{(k)}(\hat{\rho}_A(0))\|$ can be forced to be strictly smaller than one for large enough k. This is readily done by summing and subtracting $\frac{M_{00}^{(k)}(\hat{\rho}_A(0))}{M_{11}^{(k)}(\hat{\rho}_A(0))}\hat{\Pi}_{B_1}^{(1,1)}(\hat{\rho}_A(0))$ to $\hat{\Delta}_{B_1}^{(k)}(\hat{\rho}_A(0))$ and applying the triangular inequality to get:

$$\left\|\hat{\Delta}_{B_1}^{(k)}(\hat{\rho}_A(0))\right\| \leq \alpha^{(k)} + \beta^{(k)}, \tag{B.54}$$

$$\alpha^{(k)} = M_{00}^{(k)}(\hat{\rho}_A(0))\left\|\frac{\hat{\Pi}_{B_1}^{(0,0)}(\hat{\rho}_A(0))}{M_{00}^{(k)}(\hat{\rho}_A(0))} - \frac{\hat{\Pi}_{B_1}^{(1,1)}(\hat{\rho}_A(0))}{M_{11}^{(k)}(\hat{\rho}_A(0))}\right\|, \tag{B.55}$$

$$\beta^{(k)} = \left|M_{00}^{(k)}(\hat{\rho}_A(0)) - \frac{\eta_0^{(\beta)}}{\eta_1^{(\beta)}}M_{11}^{(k)}(\hat{\rho}_A(0))\right|\left\|\frac{\hat{\Pi}_{B_1}^{(1,1)}(\hat{\rho}_A(0))}{M_{11}^{(k)}(\hat{\rho}_A(0))}\right\|. \tag{B.56}$$

The quantity $\alpha^{(k)}$can be shown to be smaller than one, for k large enough: in facts, for

large k, the state of A approaches the thermal state, so that $M_{00}^{(k)}(\hat{\rho}_A(0))$ approaches $\eta_0^{(\beta)}$, which is smaller than one for positive β. Moreover the trace norm in the expression of $\alpha^{(k)}$ is computed over the difference between two properly normalized density matrices, so that we are ensured it is smaller than one. On the other hand for $\beta^{(k)}$ we have that $\left| M_{00}^{(k)}(\hat{\rho}_A(0)) - \frac{\eta_0^{(\beta)}}{\eta_1^{(\beta)}} M_{11}^{(k)}(\hat{\rho}_A(0)) \right|$ goes to zero for large k, thanks to Eq. (B.48). Finally $\left\| \frac{\hat{\Pi}_{B_1}^{(1,1)}(\hat{\rho}_A(0))}{M_{11}^{(k)}(\hat{\rho}_A(0))} \right\| = 1$, being the trace norm of a normalized state.

After having verified that $\|\hat{\Delta}_{B_1}^{(k)}(\hat{\rho}_A(0))\| < 1$, we go back to Eq. (B.51) describing the state of $\rho_{AB}(k)$ after the dephasing operation: we notice that repeating the above operations with the second set of ancillas B_2, the part of the state proportional to $\hat{\eta}_A^{(\beta)}$ is left unchanged by the evolution, so that after the second dephasing operation we are left with:

$$|0_A\rangle\langle 0_A| \otimes \hat{\Delta}_{B_1}^{(k)}(\hat{\rho_A}(0)) \otimes \hat{\Delta}_{B_2}^{(k)}(|0_A\rangle\langle 0_A|) + \hat{\eta}_A^{(\beta)} \hat{\Xi}_{B_1 B_2}(\hat{\rho}_A(0)), \tag{B.57}$$

where $\hat{\Xi}_{B_1 B_2}(\hat{\rho}_A(0))$ is a proper operator of $B_1 B_2$. Iterating the procedure with the other sets of ancillas, after q iterations we find:

$$|0_A\rangle\langle 0_A| \otimes \hat{\Delta}_{B_1}^{(k)}(\hat{\rho}_A(0)) \otimes_{\ell=2}^{q} \hat{\Delta}_{B_\ell}^{(k)}(|0_A\rangle\langle 0_A|) \otimes \hat{\eta}_A^{(\beta)} \otimes \hat{\Xi}_{B_1 B_2 \ldots B_q}(\hat{\rho}_A(0)). \tag{B.58}$$

To conclude the demonstration we only need to compute the trace norm of the first term of the equation above, obtaining:

$$\left\| |0_A\rangle\langle 0_A| \otimes \hat{\Delta}_{B_1}^{(k)}(\hat{\rho}_A(0)) \otimes_{\ell=2}^{q} \hat{\Delta}_{B_\ell}^{(k)}(|0_A\rangle\langle 0_A|) \right\| = \left\| \hat{\Delta}_{B_1}^{(k)}(\hat{\rho}_A(0)) \right\| \left\| \hat{\Delta}_{B_\ell}^{(k)}(|0_A\rangle\langle 0_A|) \right\|^{q-1} \tag{B.59}$$

which is exponentially decreasing in q, thus proving that for large q the state of $A + B$ is equal to the second contribution of Eq. (B.58), thus demonstrating the factorization property.

C. Appendix to Chap. 6

C.1. 2D stretchable separable potential

In this section we want to show an example of a 2D separable potential where it is possible to stretch the wave function. In particular, we will show how to stretch the ground state wave function. Consider an infinite 2D square well, which can be written as:

$$V(x,y) = V_x(x) + V_y(y) \tag{C.60}$$

with

$$V_{x_j}(x_j) = \begin{cases} 0 & \text{for } 0 \leq x_j \leq a_{x_j}, \\ +\infty & \text{otherwise,} \end{cases} \tag{C.61}$$

where a_{x_j} is the width of the well along x_j.

This potential is manifestly separable, and thanks to the fact that the potential is infinite at the boundaries, also the boundary conditions are separable. We want to consider the stretching of the ground state, which can be written as:

$$\psi_0(x,y) = \psi_0^{(x)}(x)\psi_0^{(y)}(y), \tag{C.62}$$

where

$$\psi_0^{(x_j)}(x_j) = \sqrt{\frac{2}{a_{x_j}}} \sin\left(\frac{\pi}{a_{x_j}} x_j\right), \tag{C.63}$$

whose associated eigenenergies are $E_0^{(x_j)} = \frac{\hbar^2\pi^2}{2ma_{x_j}^2}$, so that $E_0 = E_0^{(x)} + E_0^{(y)}$. From these expressions one immediately sees that the wave function $\psi_0(x,y)$ has zero gradient at the point $(\frac{a_x}{2}, \frac{a_y}{2})$: we hence insert a potential box of height $E_0^{(x)}$ and width L_x at the point $x = a_x/2$, and similarly a box of height $E_0^{(y)}$ and width L_y at point $y = a_y/2$, obtaining the potential shown in the inset of Fig. C.3. This new potential ground state eigenfunction reads:

$$\psi_0^{[L_x,L_y]} = \psi_0^{(x)[L_x]}(x)\psi_0^{(y)[L_y]}(y), \tag{C.64}$$

where now $\psi_0^{(x_j)[L_{x_j}]}(x_j)$ is worth:

$$\psi_0^{(x_j)[L_{x_j}]}(x_j) = \frac{1}{\sqrt{N_{x_j}}} \begin{cases} \sin\left(\frac{\pi}{a_{x_j}} x_j\right) & \text{for } 0 \leq x_j \leq \frac{a_{x_j}}{2}, \\ 1 & \text{for } \frac{a_{x_j}}{2} \leq x_j \leq \frac{a_{x_j}}{2} + L_{x_j}, \\ \sin\left(\frac{\pi}{a_{x_j}}(x_j - L_{x_j})\right) & \text{for } \frac{a_{x_j}}{2} + L_{x_j} \leq x_j \leq a_{x_j} + L_{x_j}. \end{cases} \tag{C.65}$$

This leads to the ground state wave function plotted in Fig. C.3, where one has a central region where $\psi_0^{[L_x,L_y]}(x,y)$ is constant, and four regions where one of the components of the gradient is null. These four regions correspond to the blue and green regions of the inset of Fig. C.3, where only one the kinetic components is absorbed into potential energy.

C.2. Stretched states of the harmonic oscillator

Here we want to show how to build a stretching potential using the harmonic oscillator as seed. The harmonic oscillator $V(x) = \frac{m\omega^2}{2}x^2$ is known to have equally spaced eigenvalues $E_n = \hbar\omega(n + 1/2)$ for $n \geq 0$ and associated eigenfunctions:

$$\psi_n(x) = \frac{\left(\frac{m\omega}{\pi\hbar}\right)^{1/4}}{\sqrt{2^n n!}} H_n\left(\frac{m\omega}{\hbar}x\right) \exp\left[-\frac{m\omega x^2}{2\hbar}\right], \tag{C.66}$$

where $H_n(x)$ is the n-th Hermite polynomial. As for n even the corresponding wave function has a stationary point in $x = 0$, we can use the following stretching potential:

$$V(x)^{[L]} = \begin{cases} \frac{m\omega^2}{2}\left(x + \frac{L}{2}\right) & \text{for } x \leq -\frac{L}{2}, \\ E_n & \text{for } |x| < \frac{L}{2}, \\ \frac{m\omega^2}{2}\left(x - \frac{L}{2}\right) & \text{for } x \geq \frac{L}{2}. \end{cases} . \tag{C.67}$$

We now solve the problem using once again the standard method of solving the Schrödinger equation in each region and then imposing the appropriate boundary conditions. One has that the only square-integrable solution for the region $x \leq -\frac{L}{2}$ (respectively $x \geq \frac{L}{2}$) is the parabolic cylinder function $D_{\epsilon-\frac{1}{2}}(-\sqrt{2}\xi(x + \frac{L}{2}))$ (resp. $D_{\epsilon-\frac{1}{2}}(\sqrt{2}\xi(x - \frac{L}{2}))$), where $\epsilon = \frac{E}{\hbar\omega}$ and $\xi = \sqrt{\frac{m\omega}{\hbar}}$. Once the quantities $\epsilon_n = \frac{E_n}{\hbar\omega}$, $\gamma = \sqrt{\epsilon_n - \epsilon}$ and $\bar{k} = \sqrt{\epsilon - \epsilon_n}$ have been introduced, we can write the solutions for

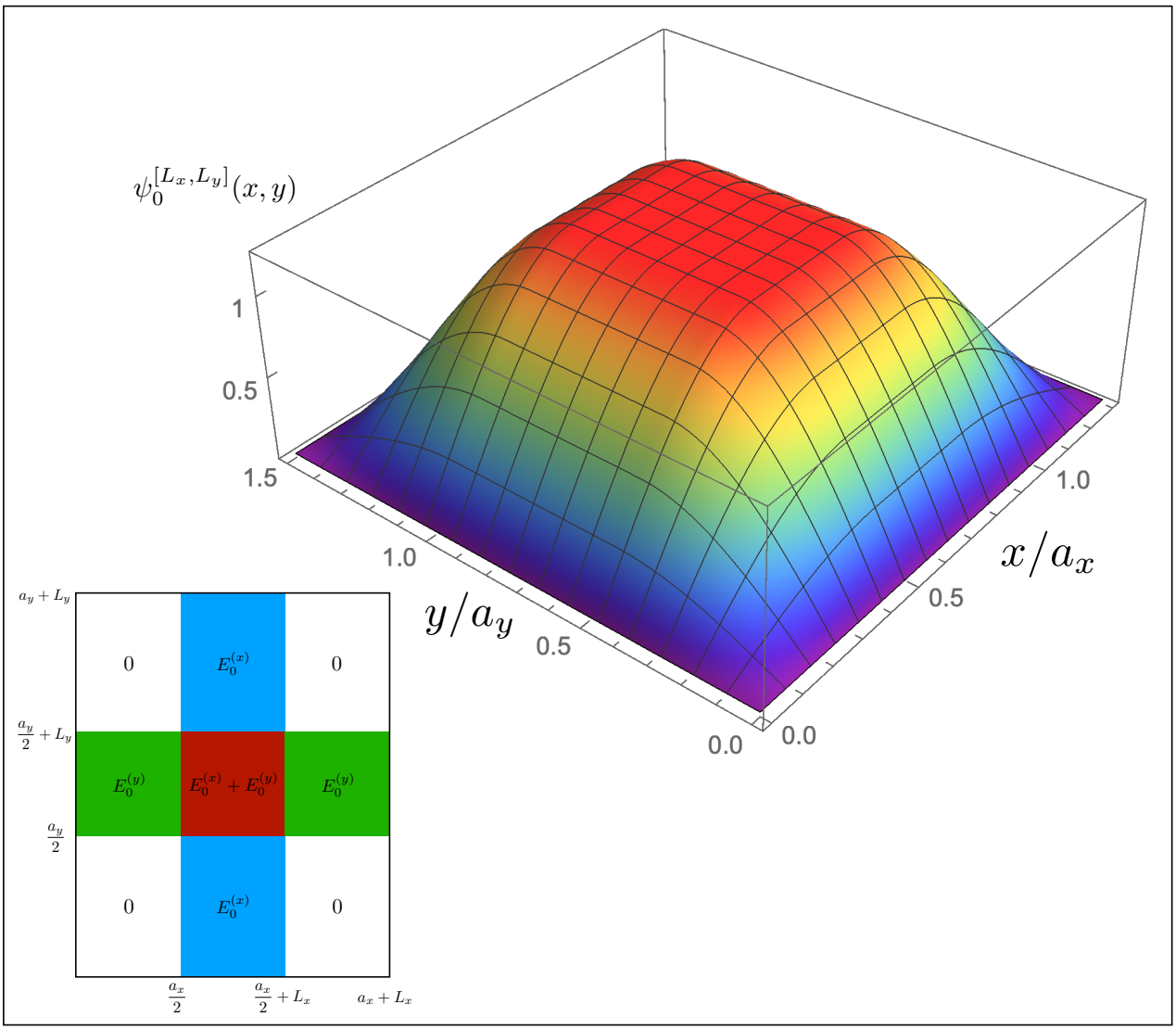

Figure C.3.: Inset: density plot of the stretching potential under examination. Figure: plot of the 2D stretched ground state $\psi_0^{[L_x,L_y]}(x,y)$ for $a_x = a_y = 1$, $L_x = 0.3a_x$ and $L_y = 0.5a_y$. One can observe the flat region at the center, in correspondence of the red region of the inset, where the wave function has a constant value. One can also observe four regions where only one component of the gradient nullifies, corresponding to the blue and green regions of the inset.

$E < E_n$, up to a normalization constant, as:

$$\psi_n(x) = \begin{cases} \frac{\cosh\left(\sqrt{2}\xi\gamma\frac{L}{2}\right)}{D_{\epsilon-\frac{1}{2}}(0)} D_{\epsilon-\frac{1}{2}}(-\sqrt{2}\xi(x+\frac{L}{2})) & \text{for } x \leq -\frac{L}{2}, \\ \cosh\left(\sqrt{2}\xi\gamma x\right) & \text{for } |x| < \frac{L}{2}, \\ \frac{\cosh\left(\sqrt{2}\xi\gamma\frac{L}{2}\right)}{D_{\epsilon-\frac{1}{2}}(0)} D_{\epsilon-\frac{1}{2}}(\sqrt{2}\xi(x-\frac{L}{2})) & \text{for } x \geq \frac{L}{2}, \end{cases} \tag{C.68}$$

for the even states, where ϵ_n is determined via:

$$\frac{D_{\epsilon+\frac{1}{2}}(0)}{D_{\epsilon-\frac{1}{2}}(0)} = -\gamma \tanh\left(\sqrt{2}\xi\gamma\frac{L}{2}\right). \tag{C.69}$$

As for the odd states we have instead:

$$\psi_n(x) = \begin{cases} -\frac{\sinh\left(\sqrt{2}\xi\gamma\frac{L}{2}\right)}{D_{\epsilon-\frac{1}{2}}(0)} D_{\epsilon-\frac{1}{2}}(-\sqrt{2}\xi(x+\frac{L}{2})) & \text{for } x \leq -\frac{L}{2}, \\ \sinh\left(\sqrt{2}\xi\gamma x\right) & \text{for } |x| < \frac{L}{2}, \\ \frac{\sinh\left(\sqrt{2}\xi\gamma\frac{L}{2}\right)}{D_{\epsilon-\frac{1}{2}}(0)} D_{\epsilon-\frac{1}{2}}(\sqrt{2}\xi(x-\frac{L}{2})) & \text{for } x \geq \frac{L}{2}, \end{cases} \tag{C.70}$$

where the quantization condition reads:

$$\frac{D_{\epsilon+\frac{1}{2}}(0)}{D_{\epsilon-\frac{1}{2}}(0)} = -\gamma \coth\left(\sqrt{2}\xi\gamma\frac{L}{2}\right). \tag{C.71}$$

After this we turn to the states with $E > E_n$. For the even states the wave-function can be written as:

$$\psi_n(x) = \begin{cases} \frac{\cos\left(\sqrt{2}\xi\bar{k}\frac{L}{2}\right)}{D_{\epsilon-\frac{1}{2}}(0)} D_{\epsilon-\frac{1}{2}}(-\sqrt{2}\xi(x+\frac{L}{2})) & \text{for } x \leq -\frac{L}{2}, \\ \cos\left(\sqrt{2}\xi\bar{k}x\right) & \text{for } |x| < \frac{L}{2}, \\ \frac{\cos\left(\sqrt{2}\xi\bar{k}\frac{L}{2}\right)}{D_{\epsilon-\frac{1}{2}}(0)} D_{\epsilon-\frac{1}{2}}(\sqrt{2}\xi(x-\frac{L}{2})) & \text{for } x \geq \frac{L}{2}, \end{cases} \tag{C.72}$$

while for the odd states one has

$$\psi_n(x) = \begin{cases} \frac{-\sin\left(\sqrt{2}\xi\bar{k}\frac{L}{2}\right)}{D_{\epsilon-\frac{1}{2}}(0)} D_{\epsilon-\frac{1}{2}}(-\sqrt{2}\xi(x+\frac{L}{2})) & \text{for } x \leq -\frac{L}{2}, \\ \sin\left(\sqrt{2}\xi\bar{k}x\right) & \text{for } |x| < \frac{L}{2}, \\ \frac{\sin\left(\sqrt{2}\xi\bar{k}\frac{L}{2}\right)}{D_{\epsilon-\frac{1}{2}}(0)} D_{\epsilon-\frac{1}{2}}(\sqrt{2}\xi(x-\frac{L}{2})) & \text{for } x \geq \frac{L}{2}, \end{cases} \tag{C.73}$$

where the two quantization conditions are:

$$\frac{D_{\epsilon+\frac{1}{2}}(0)}{D_{\epsilon-\frac{1}{2}}(0)} = \bar{k} \tan\left(\sqrt{2}\xi\gamma\frac{L}{2}\right), \tag{C.74}$$

$$\frac{D_{\epsilon+\frac{1}{2}}(0)}{D_{\epsilon-\frac{1}{2}}(0)} = -\bar{k} \cot\left(\sqrt{2}\xi\gamma\frac{L}{2}\right), \tag{C.75}$$

$$\tag{C.76}$$

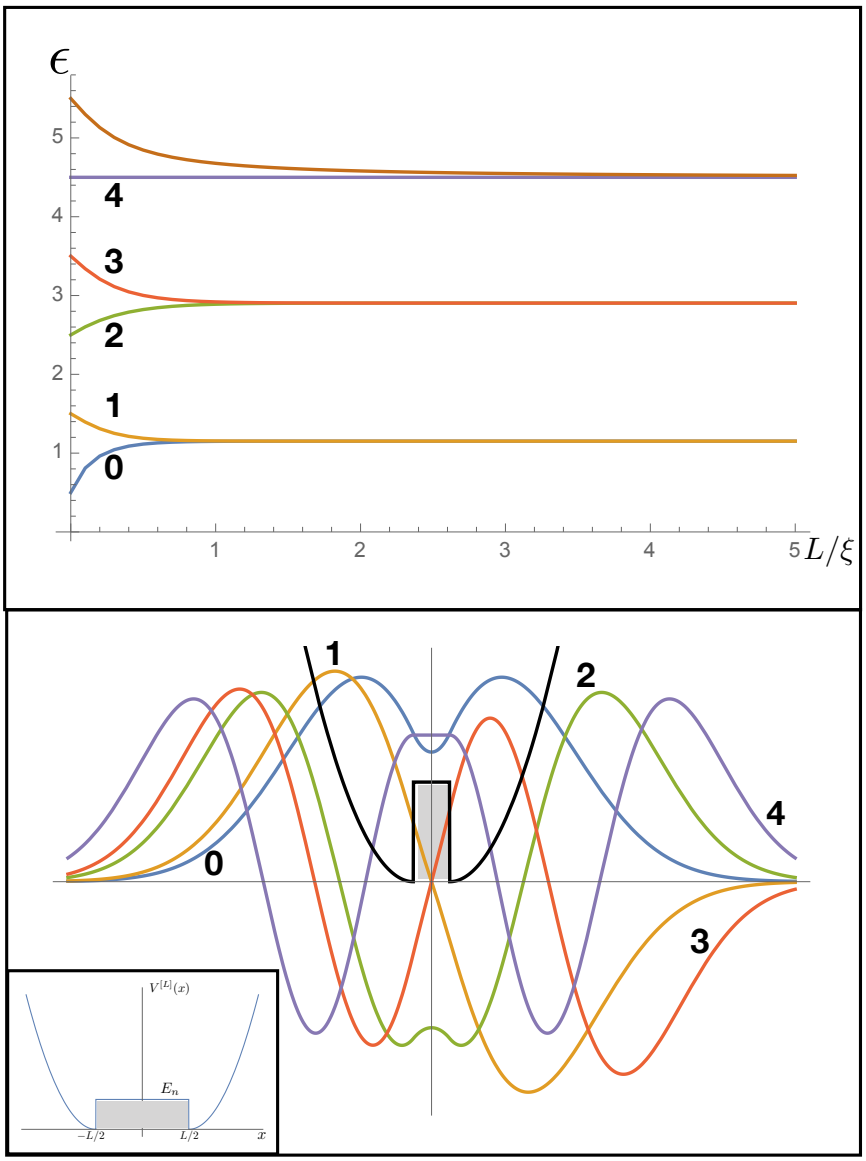

Figure C.4.: Upper panel: plot of the first six energy levels when we stretch the state $n = 4$. As L increases, just as for the infinite well, the levels with energy below E_4 form a doublet structure, while the levels above E_4 get compressed. Lower panel: plot of the wave functions of the first six levels for the specific choice $L/\xi = 0.4$. Inset: a sketch of the potential under examination.

for even and odd states respectively.

We first note that for $E = E_n$, both Eqs.(C.69, C.74) are fulfilled, and substituting this value into Eq. (C.68) one obtains the stretched version of $\psi_n(x)$. As in the case of the infinite well, we note that the two quantization conditions in Eqs.(C.69, C.71)

become identical in the limit of large L, giving rise to a doublet structure shown in Fig. C.4 for the case the barrier height is E_4. Finally, also in this case as L becomes large the system approach the free particle limit, so that the states with energy above E_n get energetically compressed.

D. Appendix to Chap. 7

D.1. Properties of the matrix K_y

In this section we derive some properties of the matrix K_y, whose elements are defined as:

$$[K_y]_{\ell\ell'} = \left\langle \phi_y^{(\ell)} \right| \frac{\partial}{\partial y} \left| \phi_y^{(\ell')} \right\rangle . \tag{D.77}$$

In order to do so, we start from the orthonormality relation between the eigenstates of the transverse Hamiltonian $\hat{h}_y(\hat{x})$:

$$\left\langle \phi_y^{(\ell)} \middle| \phi_y^{(\ell')} \right\rangle = \delta_{\ell\ell'}, \tag{D.78}$$

which derived with respect to y on both sides yelds:

$$[K_y]_{\ell\ell'} = \left\langle \phi_y^{(\ell)} \right| \frac{\partial}{\partial y} \left| \phi_y^{(\ell')} \right\rangle = - \left(\frac{\partial}{\partial y} \left\langle \phi_y^{(\ell)} \right| \right) \left| \phi_y^{(\ell')} \right\rangle = -[K_y]^*_{\ell'\ell}, \tag{D.79}$$

from which it follows the anti-hermiticity property $K_y = -K_y^\dagger$.

We also notice that, since the $\{ \left| \phi_y^{(\ell)} \right\rangle ; \ell = 0, 1, 2, \cdots \}$ form a complete basis, we have:

$$\begin{aligned}
[K_y^\dagger K_y]_{\ell\ell'} &= \sum_{\ell''} [K_y^\dagger]_{\ell\ell''} [K_y]_{\ell''\ell'} = \sum_{\ell''} [K_y]^*_{\ell''\ell} [K_y]_{\ell''\ell'} \\
&= \sum_{\ell''} \left\langle \phi_y^{(\ell'')} \right| \frac{\partial}{\partial y} \left| \phi_y^{(\ell)} \right\rangle^* \left\langle \phi_y^{(\ell'')} \right| \frac{\partial}{\partial y} \left| \phi_y^{(\ell')} \right\rangle \\
&= \sum_{\ell''} \left(\frac{\partial}{\partial y} \left\langle \phi_y^{(\ell)} \right| \right) \left| \phi_y^{(\ell'')} \right\rangle \left\langle \phi_y^{(\ell'')} \right| \frac{\partial}{\partial y} \left| \phi_y^{(\ell')} \right\rangle \\
&= \left(\frac{\partial}{\partial y} \left\langle \phi_y^{(\ell)} \right| \right) \frac{\partial}{\partial y} \left| \phi_y^{(\ell')} \right\rangle .
\end{aligned} \tag{D.80}$$

We further observe that the matrix elements $[K_y]_{\ell\ell'}$ are all real. This observation, together with the anti-Hermitian property, implies that:

$$[K_y]_{\ell\ell} = 0, \quad \forall \ell. \tag{D.81}$$

The reality of the matrix elements follows from the observation that the wave functions in the x representation associated with the eigenstates of $\hat{h}_y(\hat{x})$, the $\phi_y^{(\ell)}(x) = \left\langle x \middle| \phi_y^{(\ell)} \right\rangle$,

can always be chosen to be real together with all their derivatives with respect to y, i.e.:

$$\phi_y^{(\ell)}(x) = \phi_y^{(\ell)*}(x), \quad \frac{\partial^k}{\partial y^k}\phi_y^{(\ell)}(x) = \left(\frac{\partial^k}{\partial y^k}\phi_y^{(\ell)}(x)\right)^*. \tag{D.82}$$

Exploiting this last property we have:

$$\begin{aligned}\left\langle \phi_{y'}^{(\ell')}\right| \frac{\partial}{\partial y} \left|\phi_y^{(\ell)}\right\rangle &= \int dx\ \phi_{y'}^{(\ell')*}(x)\frac{\partial}{\partial y}\phi_y^{(\ell)}(x) = \int dx\ \phi_{y'}^{(\ell)}(x)\left(\frac{\partial}{\partial y}\phi_y^{(\ell')}(x)\right)^* \\ &= \left(\frac{\partial}{\partial y}\left\langle \phi_y^{(\ell)}\right|\right)\left|\phi_{y'}^{(\ell')}\right\rangle = \left\langle \phi_{y'}^{(\ell')}\right| \frac{\partial}{\partial y}\left|\phi_y^{(\ell)}\right\rangle^*,\end{aligned} \tag{D.83}$$

from which, setting $y' = y$, Eq. (D.81) follows.

Finally we consider the identity:

$$\left\langle \phi_{y'}^{(\ell')}\right| \hat{h}_y(\hat{x}) \left|\phi_y^{(\ell)}\right\rangle = E_y^{(\ell)} \left\langle \phi_{y'}^{(\ell')}\middle|\phi_y^{(\ell)}\right\rangle. \tag{D.84}$$

Deriving both sides of the identity with respect to y and setting $y' = y$ we get:

$$\begin{aligned}&\left\langle \phi_y^{(\ell')}\right| \frac{\partial}{\partial y}\hat{h}_y(\hat{x}) \left|\phi_y^{(\ell)}\right\rangle + \left\langle \phi_y^{(\ell')}\right| \hat{h}_y(\hat{x})\frac{\partial}{\partial y} \left|\phi_y^{(\ell)}\right\rangle = E_y^{(\ell)} \left\langle \phi_y^{(\ell')}\right| \frac{\partial}{\partial y} \left|\phi_y^{(\ell)}\right\rangle \\ &\Rightarrow [K_y]_{\ell\ell'} = \left\langle \phi_y^{(\ell)}\right| \frac{\partial}{\partial y} \left|\phi_y^{(\ell')}\right\rangle = \frac{\left\langle \phi_y^{(\ell)}\right| \frac{\partial}{\partial y}\hat{h}_y(\hat{x}) \left|\phi_y^{(\ell')}\right\rangle}{E_y^{(\ell')} - E_y^{(\ell)}} \\ &\qquad = \frac{\left\langle \phi_y^{(\ell)}\right| \frac{\partial}{\partial y}\hat{V}_y(\hat{x}) \left|\phi_y^{(\ell')}\right\rangle}{E_y^{(\ell')} - E_y^{(\ell)}}.\end{aligned} \tag{D.85}$$

Equation (D.85) can be used to write the analogous expression for the elements $[\vec{K}(\vec{R})]_{\ell\ell'}$:

$$[\vec{K}(\vec{R})]_{\ell\ell'} = \frac{\left\langle \phi_{\vec{R}}^{(\ell)}\right| \frac{\partial}{\partial \vec{R}}\hat{V}_{\vec{R}}(\hat{x}) \left|\phi_{\vec{R}}^{(\ell')}\right\rangle}{E_{\vec{R}}^{(\ell')} - E_{\vec{R}}^{(\ell)}}, \tag{D.86}$$

where we highlighted the dependence of both the energies and the wave functions on the control parameters.

List of personal publications

The following works have been wrote and published during and supported by my PhD scholarship at Scuola Normale Superiore.

Cusumano, S., A. Mari, and V. Giovannetti (2017). "Interferometric quantum cascade systems". *Phys. Rev. A* 95 (5), 053838.

Cusumano, S., A. Mari, and V. Giovannetti (2018). "Interferometric modulation of quantum cascade interactions". *Phys. Rev. A* 97 (5), 053811.

Cusumano, S., V. Cavina, et al. (2018). "Entropy production and asymptotic factorization via thermalization: A collisional model approach". *Phys. Rev. A* 98 (3), 032119.

Cusumano, S., A. D. Pasquale, et al. (2019). "Stretching potential engineering". *Journal of Physics A: Mathematical and Theoretical*.

Cusumano, S., A. De Pasquale, and V. Giovannetti (2019). "Geometric phase through spatial potential engineering". *arXiv e-prints*, arXiv:1911.05842. Submitted to *Phys. Rev. Lett.*

Bibliography

Aharonov, Y. and J. Anandan (1987). "Phase change during a cyclic quantum evolution". *Phys. Rev. Lett.* 58 (16), 1593–1596.

Alamo, J. del et al. (1998). "Electron waveguide devices". *Superlattices and Microstructures* 23, 121–137.

Albert, R. and A.-L. Barabási (2002). "Statistical mechanics of complex networks". *Rev. Mod. Phys.* 74 (1), 47–97.

Albert, R., H. Jeong, and A.-L. Barabási (1999). "Diameter of the World-Wide Web". *Nature* 401, 130–131.

Albert, R., H. Jeong, and A.-L. Barabási (2000). "Error and attack tolerance of complex networks". *Nature* 406, 378–382.

Albert, V. V. and L. Jiang (2014). "Symmetries and conserved quantities in Lindblad master equations". *Phys. Rev. A* 89 (2), 022118.

Aldinger, R. R., A. Böhm, and M. Loewe (1991). "Non-Abelian Berry phase in a quantum mechanical environment". *Foundations of Physics Letters* 4, 217–234.

Alicki, R. (2002). "Invitation to Quantum Dynamical Semigroups". In: *Dynamics of Dissipation*. Ed. by P. Garbaczewski and R. Olkiewicz. Berlin, Heidelberg: Springer Berlin Heidelberg, 239–264.

Alicki, R. and K. Lendi (1987). *Quantum Dynamical Semigroups and Applications*. Springer-Verlag Berlin Heidelberg.

Alicki, R. and R. Kosloff (2018). "Introduction to Quantum Thermodynamics: History and Prospects". In: *Thermodynamics in the Quantum Regime: Fundamental Aspects and New Directions*. Ed. by F. Binder et al. Cham: Springer International Publishing, 1–33.

Alipour, S. et al. (2016). "Correlations in quantum thermodynamics: Heat, work, and entropy production". *Scientific Reports* 6, 35568.

Altamirano, N. et al. (2017). "Unitarity, feedback, interactions—dynamics emergent from repeated measurements". *New Journal of Physics* 19, 013035.

Alù, A. et al. (2007). "Epsilon-near-zero metamaterials and electromagnetic sources: Tailoring the radiation phase pattern". *Phys. Rev. B* 75 (15), 155410.

Amato, G., H.-P. Breuer, and B. Vacchini (2019). "Microscopic modeling of general time-dependent quantum Markov processes". *Phys. Rev. A* 99 (3), 030102.

Andolina, G. M., D. Farina, et al. (2018). "Charger-mediated energy transfer in exactly solvable models for quantum batteries". *Phys. Rev. B* 98 (20), 205423.

Andolina, G. M., M. Keck, et al. (2019). "Extractable Work, the Role of Correlations, and Asymptotic Freedom in Quantum Batteries". *Phys. Rev. Lett.* 122 (4), 047702.

Antal, T., S. Redner, and V. Sood (2006). "Evolutionary Dynamics on Degree-Heterogeneous Graphs". *Phys. Rev. Lett.* 96 (18), 188104.

Arecchi, F. and R. Bonifacio (1965). "Theory of optical maser amplifiers". *IEEE Journal of Quantum Electronics* 1, 169–178.

Argyropoulos, C., P.-Y. Chen, et al. (2012). "Boosting optical nonlinearities in ϵ-near-zero plasmonic channels". *Phys. Rev. B* 85 (4), 045129.

Argyropoulos, C., G. D'Aguanno, and A. Alù (2014). "Giant second-harmonic generation efficiency and ideal phase matching with a double ϵ-near-zero cross-slit metamaterial". *Phys. Rev. B* 89 (23), 235401.

Aspect, A., J. Dalibard, and G. Roger (1982). "Experimental Test of Bell's Inequalities Using Time-Varying Analyzers". *Phys. Rev. Lett.* 49 (25), 1804–1807.

Aspect, A., P. Grangier, and G. Roger (1982). "Experimental Realization of Einstein-Podolsky-Rosen-Bohm Gedankenexperiment: A New Violation of Bell's Inequalities". *Phys. Rev. Lett.* 49 (2), 91–94.

Barenco, A. and A. K. Ekert (1995). "Dense Coding Based on Quantum Entanglement". *Journal of Modern Optics* 42, 1253–1259.

Barra, F. (2015). "The thermodynamic cost of driving quantum systems by their boundaries". *Scientific Reports* 5, 14873.

Barrat, A., M. Barthélemy, et al. (2004). "The architecture of complex weighted networks". *Proceedings of the National Academy of Sciences* 101, 3747–3752.

Barrat, A., M. Barthélemy, and A. Vespignani (2008). *Dynamical Processes on Complex Networks*. Cambridge University Press.

Bascone, F. et al. (2019). "Finite-temperature geometric properties of the Kitaev honeycomb model". *Phys. Rev. B* 99 (20), 205155.

Bastard, G. (1988). *Wave mechanics applied to semiconductor heterostructures*. Monographies de physique. Les Éditions de Physique.

Bäumer, E. et al. (2019). "Imperfect Thermalizations Allow for Optimal Thermodynamic Processes". *Quantum* 3, 153.

Beenakker, C. W. J. (1991). "Theory of Coulomb-blockade oscillations in the conductance of a quantum dot". *Phys. Rev. B* 44 (4), 1646–1656.

Bell, J. S. (1964). "On the Einstein Podolsky Rosen paradox". *Physics* 1, 195–200.

Beltram, F., F. Capasso, A. L. Hutchinson, et al. (1989). "Injection in a continuum miniband: Observation of negative transconductance in a superlattice-base transistor". *Applied Physics Letters* 55, 1534–1536.

Beltram, F., F. Capasso, D. L. Sivco, et al. (1990). "Scattering-controlled transmission resonances and negative differential conductance by field-induced localization in superlattices". *Phys. Rev. Lett.* 64 (26), 3167–3170.

Benenti, G. and G. M. Palma (2007). "Reversible and irreversible dynamics of a qubit interacting with a small environment". *Phys. Rev. A* 75 (5), 052110.

Bennett, C. H. and G. Brassard (2014). "Quantum cryptography: Public key distribution and coin tossing". *Theoretical Computer Science* 560. Theoretical Aspects of Quantum Cryptography – celebrating 30 years of BB84, 7–11.

Bennett, C. H., G. Brassard, et al. (1993). "Teleporting an unknown quantum state via dual classical and Einstein-Podolsky-Rosen channels". *Phys. Rev. Lett.* 70 (13), 1895–1899.

Bera, M. N. et al. (2017). "Generalized laws of thermodynamics in the presence of correlations". *Nature Communications* 8, 2180.

Berger, S. et al. (2013). "Exploring the effect of noise on the Berry phase". *Phys. Rev. A* 87 (6), 060303.

Binder, F. C. et al. (2015). "Quantacell: powerful charging of quantum batteries". *New Journal of Physics* 17, 75015.

Bloch, F. (1946). "Nuclear Induction". *Phys. Rev.* 70 (7-8), 460–474.

Bloch, F., W. W. Hansen, and M. Packard (1946). "The Nuclear Induction Experiment". *Phys. Rev.* 70 (7-8), 474–485.

Bohr, N. (1928). "The Quantum Postulate and the Recent Development of Atomic Theory". *Nature* 121, 580 EP -.

Breuer, H. P., K. Dietz, and M. Holthaus (1988). "Strong laser fields interacting with matter I". *Zeitschrift für Physik D Atoms, Molecules and Clusters* 10, 13–26.

Breuer, H. P. and F. Petruccione (2002). *The theory of open quantum systems*. Oxford University Press.

Breuer, H.-P. (2012). "Foundations and measures of quantum non-Markovianity". *Journal of Physics B: Atomic, Molecular and Optical Physics* 45, 154001.

Breuer, H.-P., E.-M. Laine, and J. Piilo (2009). "Measure for the Degree of Non-Markovian Behavior of Quantum Processes in Open Systems". *Phys. Rev. Lett.* 103 (21), 210401.

Breuer, H.-P., E.-M. Laine, J. Piilo, and B. Vacchini (2016). "Colloquium: Non-Markovian dynamics in open quantum systems". *Rev. Mod. Phys.* 88 (2), 021002.

Breuer, H.-P. and F. Petruccione (1997). "Dissipative quantum systems in strong laser fields: Stochastic wave-function method and Floquet theory". *Phys. Rev. A* 55 (4), 3101–3116.

Broglie, L. de (1924). "XXXV. A tentative theory of light quanta". *The London, Edinburgh, and Dublin Philosophical Magazine and Journal of Science* 47, 446–458.

Budini, A. A. (2018). "Quantum Non-Markovian Processes Break Conditional Past-Future Independence". *Phys. Rev. Lett.* 121 (24), 240401.

Cai, W. and V. Shalaev (2009). *Optical Metamaterials: Fundamentals and Applications*. Springer New York.

Caloz, C. (2005). *Electromagnetic Metamaterials: Transmission Line Theory and Microwave Applications: The Engineering Approach*. Vol. 15.

Campaioli, F. et al. (2017). "Enhancing the Charging Power of Quantum Batteries". *Phys. Rev. Lett.* 118 (15), 150601.

Campbell, S. et al. (2018). "System-environment correlations and Markovian embedding of quantum non-Markovian dynamics". *Phys. Rev. A* 98 (1), 012142.

Campisi, M. and R. Fazio (2016). "The power of a critical heat engine". *Nature Communications* 7, 11895.

Campisi, M. and J. Goold (2017). "Thermodynamics of quantum information scrambling". *Phys. Rev. E* 95 (6), 062127.

Canali, L. et al. (1996). "Stark-Cyclotron Resonance in a Semiconductor Superlattice". *Phys. Rev. Lett.* 76 (19), 3618–3621.

Cangemi, L. M. et al. (2018). "Beyond the Born-Markov approximation: Dissipative dynamics of a single qubit". *Phys. Rev. B* 98 (18), 184306.

Capasso, F. (1990). *Physics of quantum electron devices*. Springer series in electronics and photonics. Springer-Verlag.

Capasso, F. (1986). "Compositionally Graded Semiconductors and Their Device Applications". *Annual Review of Materials Science* 16, 263–291.

Capasso, F. and R. A. Kiehl (1985). "Resonant tunneling transistor with quantum well base and high-energy injection: A new negative differential resistance device". *Journal of Applied Physics* 58, 1366–1368.

Carmichael, H. J. (1993). "Quantum trajectory theory for cascaded open systems". *Phys. Rev. Lett.* 70 (15), 2273–2276.

Carollo, A. and G. M. Palma (2006). "Observable geometric phase induced by a cyclically evolving dissipative process". *Laser Physics* 16, 1595–1600.

Carollo, A., M. F. Santos, and V. Vedral (2006). "Coherent Quantum Evolution via Reservoir Driven Holonomies". *Phys. Rev. Lett.* 96 (2), 020403.

Carpena, P., V. Gasparian, and M. Ortuño (1999). "Number of bound states of a Kronig-Penney finite-periodic superlattice". *The European Physical Journal B - Condensed Matter and Complex Systems* 8, 635–641.

Caruso, F. et al. (2014). "Quantum channels and memory effects". *Rev. Mod. Phys.* 86 (4), 1203–1259.

Castellano, C., M. Marsili, and A. Vespignani (2000). "Nonequilibrium Phase Transition in a Model for Social Influence". *Phys. Rev. Lett.* 85 (16), 3536–3539.

Castellanos-Beltran, M. A. et al. (2008). "Amplification and squeezing of quantum noise with a tunable Josephson metamaterial". *Nature Physics* 4, 929.

Chang, D. E. et al. (2018). "Colloquium: Quantum matter built from nanoscopic lattices of atoms and photons". *Rev. Mod. Phys.* 90 (3), 031002.

Chang, L. L., L. Esaki, and R. Tsu (1974). "Resonant tunneling in semiconductor double barriers". *Applied Physics Letters* 24, 593–595.

Cheianov, V. V., V. Fal'ko, and B. L. Altshuler (2007). "The Focusing of Electron Flow and a Veselago Lens in Graphene p-n Junctions". *Science* 315, 1252–1255.

Chesi, S. and W. A. Coish (2015). "Theory of box-model hyperfine couplings and transport signatures of long-range nuclear-spin coherence in a quantum-dot spin valve". *Phys. Rev. B* 91 (24), 245306.

Chiara, G. D. et al. (2018). "Reconciliation of quantum local master equations with thermodynamics". *New Journal of Physics* 20, 113024.

Chiribella, G. and G. Adesso (2014). "Quantum Benchmarks for Pure Single-Mode Gaussian States". *Phys. Rev. Lett.* 112 (1), 010501.

Chiribella, G., G. M. D'Ariano, and P. Perinotti (2009). "Theoretical framework for quantum networks". *Phys. Rev. A* 80 (2), 022339.

Chruściński, D. (2014). "On Time-Local Generators of Quantum Evolution". *Open Systems & Information Dynamics* 21, 1440004.

Chruściński, D. and A. Kossakowski (2010). "Non-Markovian Quantum Dynamics: Local versus Nonlocal". *Phys. Rev. Lett.* 104 (7), 070406.

Ciccarello, F., G. M. Palma, and V. Giovannetti (2013). "Collision-model-based approach to non-Markovian quantum dynamics". *Phys. Rev. A* 87 (4), 040103.

Ciuti, C. and I. Carusotto (2006). "Input-output theory of cavities in the ultrastrong coupling regime: The case of time-independent cavity parameters". *Phys. Rev. A* 74 (3), 033811.

Clauser, J. F. et al. (1969). "Proposed Experiment to Test Local Hidden-Variable Theories". *Phys. Rev. Lett.* 23 (15), 880–884.

Combes, J., J. Kerckhoff, and M. Sarovar (2017). "The SLH framework for modeling quantum input-output networks". *Advances in Physics: X* 2, 784–888.

Cover, T. M. and J. A. Thomas (2006). *Elements of Information Theory (Wiley Series in Telecommunications and Signal Processing)*. New York, NY, USA: Wiley-Interscience.

Cusumano, S., V. Cavina, et al. (2018). "Entropy production and asymptotic factorization via thermalization: A collisional model approach". *Phys. Rev. A* 98 (3), 032119.

Cusumano, S., A. De Pasquale, and V. Giovannetti (2019). "Geometric phase through spatial potential engineering". *arXiv e-prints*, arXiv:1911.05842. Submitted to *Phys. Rev. Lett.*

Cusumano, S., A. Mari, and V. Giovannetti (2018). "Interferometric modulation of quantum cascade interactions". *Phys. Rev. A* 97 (5), 053811.

Cusumano, S., A. Mari, and V. Giovannetti (2017). "Interferometric quantum cascade systems". *Phys. Rev. A* 95 (5), 053838.

Cusumano, S., A. D. Pasquale, et al. (2019). "Stretching potential engineering". *Journal of Physics A: Mathematical and Theoretical*.

Daley, A. J. (2014). "Quantum trajectories and open many-body quantum systems". *Advances in Physics* 63, 77–149.

Dalibard, J., Y. Castin, and K. Mølmer (1992). "Wave-function approach to dissipative processes in quantum optics". *Phys. Rev. Lett.* 68 (5), 580–583.

Dann, R., A. Levy, and R. Kosloff (2018). "Time-dependent Markovian quantum master equation". *Phys. Rev. A* 98 (5), 052129.

Das, S. et al. (2018). "Photon scattering from a system of multilevel quantum emitters. II. Application to emitters coupled to a one-dimensional waveguide". *Phys. Rev. A* 97 (4), 043838.

Datta, S. (1989). *Quantum phenomena*. Modular Series on Solid State Devices, Vol 8. Addison-Wesley Longman, Incorporated.

Datta, S. (1995). *Electronic Transport in Mesoscopic Systems*. Cambridge Studies in Semiconductor Physics and Microelectronic Engineering. Cambridge University Press.

Dauelsberg, M. et al. (2005). "Chapter 4 - Technology of MOVPE Production Tools". In: *Optoelectronic Devices: III Nitrides*. Ed. by M. Razeghi and M. Henini. Oxford: Elsevier, 39–68.

Davies, E. B. (B. (1976). *Quantum theory of open systems*. English. Includes index. London ; New York : Academic Press.

De Chiara, G. and G. M. Palma (2003). "Berry Phase for a Spin 1/2 Particle in a Classical Fluctuating Field". *Phys. Rev. Lett.* 91 (9), 090404.

Deffner, S. and C. Jarzynski (2013). "Information Processing and the Second Law of Thermodynamics: An Inclusive, Hamiltonian Approach". *Phys. Rev. X* 3 (4), 041003.

Deutsch, D. (1985). "Quantum theory, the Church-Turing principle and the universal quantum computer". *Proceedings of the Royal Society of London. A. Mathematical and Physical Sciences* 400, 97–117.

Deutsch, D. and R. Jozsa (1992). "Rapid solution of problems by quantum computation". *Proceedings of the Royal Society of London. Series A: Mathematical and Physical Sciences* 439, 553–558.

Diòsi, L., T. Feldmann, and R. Kosloff (2006). "On the Exact Identity Between Thermodynamic and Informatic Entropies in a Unitary Model of Friction". *International Journal of Quantum Information* 04, 99–104.

Dirac, P. A. M. and N. H. D. Bohr (1927). "The quantum theory of the emission and absorption of radiation". *Proceedings of the Royal Society of London. Series A, Containing Papers of a Mathematical and Physical Character* 114, 243–265.

Duan, L.-M., J. I. Cirac, and P. Zoller (2001). "Geometric Manipulation of Trapped Ions for Quantum Computation". *Science* 292, 1695–1697.

Edwards, B., A. Alù, M. G. Silveirinha, et al. (2009). "Reflectionless sharp bends and corners in waveguides using epsilon-near-zero effects". *Journal of Applied Physics* 105, 044905.

Edwards, B., A. Alù, M. E. Young, et al. (2008). "Experimental Verification of Epsilon-Near-Zero Metamaterial Coupling and Energy Squeezing Using a Microwave Waveguide". *Phys. Rev. Lett.* 100 (3), 033903.

Einstein, A., B. Podolsky, and N. Rosen (1935). "Can Quantum-Mechanical Description of Physical Reality Be Considered Complete?" *Phys. Rev.* 47 (10), 777–780.

Ekert, A. K. (1991). "Quantum cryptography based on Bell's theorem". *Phys. Rev. Lett.* 67 (6), 661–663.

Ekert, A. et al. (2000). "Geometric quantum computation". *Journal of Modern Optics* 47, 2501–2513.

Elouard, C. et al. (2017). "Probing quantum fluctuation theorems in engineered reservoirs". *New Journal of Physics* 19, 103011.

Esaki, L. and L. L. Chang (1974). "New Transport Phenomenon in a Semiconductor "Superlattice"". *Phys. Rev. Lett.* 33 (8), 495–498.

Esaki, L. and R. Tsu (1970). "Superlattice and Negative Differential Conductivity in Semiconductors". *IBM Journal of Research and Development* 14, 61–65.

Faoro, L., J. Siewert, and R. Fazio (2003). "Non-Abelian Holonomies, Charge Pumping, and Quantum Computation with Josephson Junctions". *Phys. Rev. Lett.* 90 (2), 028301.

Farina, D. and V. Giovannetti (2019). "Open-quantum-system dynamics: Recovering positivity of the Redfield equation via the partial secular approximation". *Phys. Rev. A* 100 (1), 012107.

Ferialdi, L. (2016). "Exact Closed Master Equation for Gaussian Non-Markovian Dynamics". *Phys. Rev. Lett.* 116 (12), 120402.

Ferraro, D. et al. (2018). "High-Power Collective Charging of a Solid-State Quantum Battery". *Phys. Rev. Lett.* 120 (11), 117702.

Feynman, R. P. (1982). "Simulating physics with computers". *International Journal of Theoretical Physics* 21, 467–488.

Filippov, S. N. and D. Chruściński (2018). "Time deformations of master equations". *Phys. Rev. A* 98 (2), 022123.

Fischer, K. A. et al. (2018). "Scattering into one-dimensional waveguides from a coherently-driven quantum-optical system". *Quantum* 2, 69.

Franciosi, A. and C. G. V. de Walle (1996). "Heterojunction band offset engineering". *Surface Science Reports* 25, 1–140.

Gardiner, C. (2009). *Stochastic Methods: A Handbook for the Natural and Social Sciences*. Springer Series in Synergetics. Springer Berlin Heidelberg.

Gardiner, C. W. (1993). "Driving a quantum system with the output field from another driven quantum system". *Phys. Rev. Lett.* 70 (15), 2269–2272.

Gardiner, C. W. and M. J. Collett (1985). "Input and output in damped quantum systems: Quantum stochastic differential equations and the master equation". *Phys. Rev. A* 31 (6), 3761–3774.

Gardiner, C. W. and A. S. Parkins (1994). "Driving atoms with light of arbitrary statistics". *Phys. Rev. A* 50 (2), 1792–1806.

Gardiner, C. (2004). "Input and output in damped quantum systems III: formulation of damped systems driven by Fermion fields". *Optics Communications* 243. Ultra Cold Atoms and Degenerate Quantum Gases, 57–80.

Gardiner, C., C. Gardiner, and P. Zoller (2000). *Quantum Noise: A Handbook of Markovian and Non-Markovian Quantum Stochastic Methods with Applications to Quantum Optics*. Springer series in synergetics. Springer.

Gelbwaser-Klimovsky, D. and G. Kurizki (2015). "Quantum mechanically enhanced performance of simple heat machines". *Physica Scripta* T165, 014025.

Giovannetti, V. and G. M. Palma (2012a). "Master Equations for Correlated Quantum Channels". *Phys. Rev. Lett.* 108 (4), 040401.

Giovannetti, V., R. García-Patrón, et al. (2014). "Ultimate classical communication rates of quantum optical channels". *Nature Photonics* 8, 796.

Giovannetti, V., A. S. Holevo, and A. Mari (2015). "Majorization and additivity for multimode bosonic Gaussian channels". *Theoretical and Mathematical Physics* 182, 284–293.

Giovannetti, V. and G. M. Palma (2012b). "Master equation for cascade quantum channels: a collisional approach". *Journal of Physics B: Atomic, Molecular and Optical Physics* 45, 154003.

Goold, J. et al. (2016). "The role of quantum information in thermodynamics—a topical review". *Journal of Physics A: Mathematical and Theoretical* 49, 143001.

Gorini, V., A. Kossakowski, and E. C. G. Sudarshan (1976). "Completely positive dynamical semigroups of N-level systems". *Journal of Mathematical Physics* 17, 821–825.

Gough, J. E., R. Gohm, and M. Yanagisawa (2008). "Linear quantum feedback networks". *Phys. Rev. A* 78 (6), 062104.

Gough, J. and M. R. James (2009). "The Series Product and Its Application to Quantum Feedforward and Feedback Networks". *IEEE Transactions on Automatic Control* 54, 2530–2544.

Griffiths, D. J. and D. F. Schroeter (2018). *Introduction to Quantum Mechanics*. 3rd ed. Cambridge University Press.

Grimsmo, A. L. (2015). "Time-Delayed Quantum Feedback Control". *Phys. Rev. Lett.* 115 (6), 060402.

Grimsmo, A. L. et al. (2016). "Quantum Optics Theory of Electronic Noise in Coherent Conductors". *Phys. Rev. Lett.* 116 (4), 043602.

Grosso, G. and G. Parravicini (2000). *Solid State Physics*. Elsevier Science.

Grover, L. K. (1996). "A Fast Quantum Mechanical Algorithm for Database Search". In: *Proceedings of the Twenty-eighth Annual ACM Symposium on Theory of Computing*. STOC '96. Philadelphia, Pennsylvania, USA: ACM, 212–219.

Grover, L. K. (1997). "Quantum Mechanics Helps in Searching for a Needle in a Haystack". *Phys. Rev. Lett.* 79 (2), 325–328.

Guéry-Odelin, D. et al. (2019). *Shortcuts to adiabaticity: concepts, methods, and applications*. Tech. rep.

Halpern, M. B. (1979). "Field-strength and dual variable formulations of gauge theory". *Phys. Rev. D* 19 (2), 517–530.

Hansom, J. et al. (2014). "Environment-assisted quantum control of a solid-state spin via coherent dark states". *Nature Physics* 10, 725.

Hanson, R. et al. (2007). "Spins in few-electron quantum dots". *Rev. Mod. Phys.* 79 (4), 1217–1265.

Harrison, P. and A. Valavanis (2016). "Simple models of quantum wires and dots". In: *Quantum Wells, Wires and Dots*. John Wiley & Sons, Ltd. Chap. 8, 249–278.

Hatano, N. and G. Ordonez (2019). "Time-Reversal Symmetry and Arrow of Time in Quantum Mechanics of Open Systems". *Entropy* 21.

Hayashi, H., G. Kimura, and Y. Ota (2003). "Kraus representation in the presence of initial correlations". *Phys. Rev. A* 67 (6), 062109.

Heiblum, M., E. E. Mendez, and F. Stern (1984). "High mobility electron gas in selectively doped n:AlGaAs/GaAs heterojunctions". *Applied Physics Letters* 44, 1064–1066.

Heisenberg, W. (1927). "Über den anschaulichen Inhalt der quantentheoretischen Kinematik und Mechanik". *Zeitschrift für Physik* 43, 172–198.

Helm, M. (1995). "Infrared spectroscopy and transport of electrons in semiconductor superlattices". *Semiconductor Science and Technology* 10, 557–575.

Hewgill, A., A. Ferraro, and G. De Chiara (2018). "Quantum correlations and thermodynamic performances of two-qubit engines with local and common baths". *Phys. Rev. A* 98 (4), 042102.

Hofer, P. P. et al. (2017). "Markovian master equations for quantum thermal machines: local versus global approach". *New Journal of Physics* 19, 123037.

Holevo, A. S. and V. Giovannetti (2012). "Quantum channels and their entropic characteristics". *Reports on Progress in Physics* 75, 46001.

Horodecki, M., P. Horodecki, and R. Horodecki (1996). "Separability of mixed states: necessary and sufficient conditions". *Physics Letters A* 223, 1–8.

Horodecki, M. and J. Oppenheim (2013). "Fundamental limitations for quantum and nanoscale thermodynamics". *Nature Communications* 4, 2059.

Horodecki, R. et al. (2009). "Quantum entanglement". *Rev. Mod. Phys.* 81 (2), 865–942.

Hurt, N. E. (2000). "Quantum Wires and Devices". In: *Mathematical Physics of Quantum Wires and Devices: From Spectral Resonances to Anderson Localization*. Dordrecht: Springer Netherlands, 1–10.

Janßen, M. (2017). "On Generated Dynamics for Open Quantum Systems: Spectral Analysis of Effective Liouville". *arXiv e-prints*, arXiv:1707.09660.

Kiilerich, A. H. and K. Mølmer (2019). "Input-Output Theory with Quantum Pulses". *Phys. Rev. Lett.* 123 (12), 123604.

Kohler, S., T. Dittrich, and P. Hänggi (1997). "Floquet-Markovian description of the parametrically driven, dissipative harmonic quantum oscillator". *Phys. Rev. E* 55 (1), 300–313.

Kosloff, R. (2013). "Quantum Thermodynamics: A Dynamical Viewpoint". *Entropy* 15, 2100–2128.

Kosloff, R. and A. Levy (2014). "Quantum Heat Engines and Refrigerators: Continuous Devices". *Annual Review of Physical Chemistry* 65, 365–393.

Kraus, K. (1971). "General state changes in quantum theory". *Annals of Physics* 64, 311–335.

Kretschmann, D. and R. F. Werner (2004). "Tema con variazioni: quantum channel capacity". *New Journal of Physics* 6, 26.

Kretschmer, S., K. Luoma, and W. T. Strunz (2016). "Collision model for non-Markovian quantum dynamics". *Phys. Rev. A* 94 (1), 012106.

Kuhn, T. S. (1970). *The structure of scientific revolutions*. University of Chicago Press, xii, 210.

Lahtinen, V. et al. (2008). "Spectrum of the non-abelian phase in Kitaev's honeycomb lattice model". *Annals of Physics* 323, 2286–2310.

Leek, P. J. et al. (2007). "Observation of Berry's Phase in a Solid-State Qubit". *Science* 318, 1889–1892.

Lena, R. G., G. M. Palma, and G. De Chiara (2016). "Work fluctuations in bosonic Josephson junctions". *Phys. Rev. A* 93 (5), 053618.

Li, L., M. J. Hall, and H. M. Wiseman (2018). "Concepts of quantum non-Markovianity: A hierarchy". *Physics Reports* 759. Concepts of quantum non-Markovianity: A hierarchy, 1–51.

Liao, B. et al. (2013). "Isotropic and energy-selective electron cloaks on graphene". *Phys. Rev. B* 88 (15), 155432.

Liberal, I. and N. Engheta (2017). "Near-zero refractive index photonics". *Nature Photonics* 11, 149.

Lindblad, G. (1976). "On the generators of quantum dynamical semigroups". *Communications in Mathematical Physics* 48, 119–130.

Linden, N., S. Popescu, and P. Skrzypczyk (2010). "How Small Can Thermal Machines Be? The Smallest Possible Refrigerator". *Phys. Rev. Lett.* 105 (13), 130401.

Lorenzo, S., R. McCloskey, et al. (2015). "Landauer's Principle in Multipartite Open Quantum System Dynamics". *Phys. Rev. Lett.* 115 (12), 120403.

Lorenzo, S., F. Ciccarello, and G. M. Palma (2016). "Class of exact memory-kernel master equations". *Phys. Rev. A* 93 (5), 052111.

Lorenzo, S., F. Ciccarello, G. M. Palma, and B. Vacchini (2017). "Quantum Non-Markovian Piecewise Dynamics from Collision Models". *Open Systems & Information Dynamics* 24, 1740011.

Lorenzo, S., A. Farace, et al. (2015). "Heat flux and quantum correlations in dissipative cascaded systems". *Phys. Rev. A* 91 (2), 022121.

Luryi, S. (1985). "Frequency limit of double-barrier resonant-tunneling oscillators". *Applied Physics Letters* 47, 490–492.

Macchiavello, C. and G. M. Palma (2002). "Entanglement-enhanced information transmission over a quantum channel with correlated noise". *Phys. Rev. A* 65 (5), 050301.

Madhukar, A. (1990). "The Nature of Molecular Beam Epitaxy and Consequences for Quantum Microstructures". In: *Physics of Quantum Electron Devices*. Ed. by F. Capasso. Berlin, Heidelberg: Springer Berlin Heidelberg, 13–60.

Mahmoodian, S. et al. (2018). "Strongly Correlated Photon Transport in Waveguide Quantum Electrodynamics with Weakly Coupled Emitters". *Phys. Rev. Lett.* 121 (14), 143601.

Man, Z.-X., Y.-J. Xia, and R. Lo Franco (2018). "Temperature effects on quantum non-Markovianity via collision models". *Phys. Rev. A* 97 (6), 062104.

Man, Z.-X., Y.-J. Xia, and R. Lo Franco (2019). "Validity of the Landauer principle and quantum memory effects via collisional models". *Phys. Rev. A* 99 (4), 042106.

Manatuly, A. et al. (2019). "Collectively enhanced thermalization via multiqubit collisions". *Phys. Rev. E* 99 (4), 042145.

Manzano, G., F. Galve, et al. (2016). "Entropy production and thermodynamic power of the squeezed thermal reservoir". *Phys. Rev. E* 93 (5), 052120.

Manzano, G., J. M. Horowitz, and J. M. R. Parrondo (2018). "Quantum Fluctuation Theorems for Arbitrary Environments: Adiabatic and Nonadiabatic Entropy Production". *Phys. Rev. X* 8 (3), 031037.

Manzano, G., F. Plastina, and R. Zambrini (2018). "Optimal Work Extraction and Thermodynamics of Quantum Measurements and Correlations". *Phys. Rev. Lett.* 121 (12), 120602.

Mari, A., V. Giovannetti, and A. S. Holevo (2014). "Quantum state majorization at the output of bosonic Gaussian channels". *Nature Communications* 5, 3826.

Mascherpa, F. et al. (2019). "Optimized auxiliary oscillators for the simulation of general open quantum systems". *arXiv e-prints*, arXiv:1904.04822.

McCloskey, R. and M. Paternostro (2014). "Non-Markovianity and system-environment correlations in a microscopic collision model". *Phys. Rev. A* 89 (5), 052120.

McLennan, M. J. et al. (1991). "Dissipative Quantum Transport in Electron Waveguides". In: *Computational Electronics: Semiconductor Transport and Device Simulation*. Ed. by K. Hess, J. P. Leburton, and U. Ravaioli. Boston, MA: Springer US, 247–250.

Mead, C. A. (1992). "The geometric phase in molecular systems". *Rev. Mod. Phys.* 64 (1), 51–85.

Menchon-Enrich, R. et al. (2016). "Spatial adiabatic passage: a review of recent progress". *Reports on Progress in Physics* 79, 074401.

Messiah, A. (1999). *Quantum Mechanics*. Dover books on physics. Dover Publications.

Mimura, T. et al. (1980). "A New Field-Effect Transistor with Selectively Doped GaAs/n-AlxGa1-xAs Heterojunctions". *Japanese Journal of Applied Physics* 19, L225–L227.

Modi, K. (2012). "Operational approach to open dynamics and quantifying initial correlations". *Scientific Reports* 2, 581.

Montoya, J. M., S. L. Pimm, and R. V. Solé (2006). "Ecological networks and their fragility". *Nature* 442, 259–264.

Nakajima, S. (1958). "On Quantum Theory of Transport Phenomena: Steady Diffusion". *Progress of Theoretical Physics* 20, 948–959.

Nazarov, Y. V. and Y. M. Blanter (2009). *Quantum Transport: Introduction to Nanoscience*. Cambridge University Press.

Newman, M. E. J. (2001a). "Scientific collaboration networks. I. Network construction and fundamental results". *Phys. Rev. E* 64 (1), 016131.

Newman, M. E. J. (2001b). "Scientific collaboration networks. II. Shortest paths, weighted networks, and centrality". *Phys. Rev. E* 64 (1), 016132.

Nguyen, V. C., L. Chen, and K. Halterman (2010). "Total Transmission and Total Reflection by Zero Index Metamaterials with Defects". *Phys. Rev. Lett.* 105 (23), 233908.

Nielsen, M. A. and I. L. Chuang (2010). *Quantum Computation and Quantum Information: 10th Anniversary Edition*. Cambridge University Press.

Nikolopoulos, G. and I. Jex (2013). *Quantum State Transfer and Network Engineering*. Quantum Science and Technology. Springer Berlin Heidelberg.

Niu, X. et al. (2018). "Epsilon-Near-Zero Photonics: A New Platform for Integrated Devices". *Advanced Optical Materials* 6, 1701292.

Novičenko, V., J. Ruseckas, and E. Anisimovas (2019). "Quantum dynamics in potentials with fast spatial oscillations". *Phys. Rev. A* 99 (4), 043608.

Orton, J. and T. Foxon (2015). *Molecular Beam Epitaxy: A Short History*. OUP Oxford.

Pacheco-Peña, V. et al. (2014). "Mechanical 144 GHz beam steering with all-metallic epsilon-near-zero lens antenna". *Applied Physics Letters* 105, 243503.

Pachos, J. K. and A. C. Carollo (2006). "Geometric phases and criticality in spin systems". *Philosophical Transactions of the Royal Society A: Mathematical, Physical and Engineering Sciences* 364, 3463–3476.

Pellegrini, C. and F. Petruccione (2009). "Non-Markovian quantum repeated interactions and measurements". *Journal of Physics A: Mathematical and Theoretical* 42, 425304.

Pendry, J. B., D. Schurig, and D. R. Smith (2006). "Controlling Electromagnetic Fields". *Science* 312, 1780–1782.

Peres, A. (1996). "Separability Criterion for Density Matrices". *Phys. Rev. Lett.* 77 (8), 1413–1415.

Petta, J. R. et al. (2005). "Coherent Manipulation of Coupled Electron Spins in Semiconductor Quantum Dots". *Science* 309, 2180–2184.

Pezzutto, M., M. Paternostro, and Y. Omar (2016). "Implications of non-Markovian quantum dynamics for the Landauer bound". *New Journal of Physics* 18, 123018.

Pichler, H., S. Choi, et al. (2017). "Universal photonic quantum computation via time-delayed feedback". *Proceedings of the National Academy of Sciences* 114, 11362–11367.

Pichler, H. and P. Zoller (2016). "Photonic Circuits with Time Delays and Quantum Feedback". *Phys. Rev. Lett.* 116 (9), 093601.

Pimm, S. L. (2002). *Food Webs*. University of Chicago Press.

Pirandola, S. and S. Lloyd (2008). "Computable bounds for the discrimination of Gaussian states". *Phys. Rev. A* 78 (1), 012331.

Plastina, F., G. Liberti, and A. Carollo (2006). "Scaling of Berry's phase close to the Dicke quantum phase transition". *Europhysics Letters (EPL)* 76, 182–188.

Pollock, F. A. et al. (2018). "Non-Markovian quantum processes: Complete framework and efficient characterization". *Phys. Rev. A* 97 (1), 012127.

Prigogine, I. (1962). *Non-equilibrium statistical mechanics*. Monographs in statistical physics and thermodynamics. Interscience Publishers.

Rakhmanov, A. L. et al. (2008). "Quantum metamaterials: Electromagnetic waves in a Josephson qubit line". *Phys. Rev. B* 77 (14), 144507.

Ramos, T. et al. (2014). "Quantum Spin Dimers from Chiral Dissipation in Cold-Atom Chains". *Phys. Rev. Lett.* 113 (23), 237203.

Rau, J. (1963). "Relaxation Phenomena in Spin and Harmonic Oscillator Systems". *Phys. Rev.* 129 (4), 1880–1888.

Redfield, A. G. (1957). "On the Theory of Relaxation Processes". *IBM Journal of Research and Development* 1, 19–31.

Redner, S. (2005). "Citation Statistics from 110 Years of Physical Review". *Physics Today* 58, 49–54.

Reeb, D. and M. M. Wolf (2014). "An improved Landauer principle with finite-size corrections". *New Journal of Physics* 16, 103011.

Reimann, S. M. and M. Manninen (2002). "Electronic structure of quantum dots". *Rev. Mod. Phys.* 74 (4), 1283–1342.

Reimer, V. et al. (2019). "Five approaches to exact open-system dynamics: Complete positivity, divisibility, and time-dependent observables". *The Journal of Chemical Physics* 151, 044101.

Reshef, O. et al. (2017). "Direct Observation of Phase-Free Propagation in a Silicon Waveguide". *ACS Photonics* 4, 2385–2389.

Ringbauer, M. et al. (2015). "Characterizing Quantum Dynamics with Initial System-Environment Correlations". *Phys. Rev. Lett.* 114 (9), 090402.

Ringel, M., M. Pletyukhov, and V. Gritsev (2014). "Topologically protected strongly correlated states of photons". *New Journal of Physics* 16, 113030.

Rivas, Á., S. F. Huelga, and M. B. Plenio (2014). "Quantum non-Markovianity: characterization, quantification and detection". *Reports on Progress in Physics* 77, 094001.

Rodrigues, F. L. S. et al. (2019). "Thermodynamics of Weakly Coherent Collisional Models". *Phys. Rev. Lett.* 123 (14), 140601.

Rodríguez-Rosario, C. A., K. Modi, and A. Aspuru-Guzik (2010). "Linear assignment maps for correlated system-environment states". *Phys. Rev. A* 81 (1), 012313.

Sakurai, J. J. and J. Napolitano (2017). *Modern Quantum Mechanics*. 2nd ed. Cambridge University Press.

Scarani, V. et al. (2002). "Thermalizing Quantum Machines: Dissipation and Entanglement". *Phys. Rev. Lett.* 88 (9), 097905.

Schmidt, P. C. (1981). "K. Blum: Density Matrix Theory and Applications. Plenum Press, New York und London 1981. 217 Seiten, Preis: $ 32.50". *Berichte der Bunsengesellschaft für physikalische Chemie* 87, 73–73.

Schollwöck, U. (2011). "The density-matrix renormalization group in the age of matrix product states". *Annals of Physics* 326. January 2011 Special Issue, 96–192.

Schrödinger, E. (1926). "Quantisierung als Eigenwertproblem". *Annalen der Physik* 384, 361–376.

Schurig, D. et al. (2006). "Metamaterial Electromagnetic Cloak at Microwave Frequencies". *Science* 314, 977–980.

Scully, M. and M. Zubairy (1997). *Quantum Optics*. Cambridge University Press.

Seah, S. et al. (2019). "Collisional quantum thermometry". *arXiv e-prints*, arXiv:1904.12551.

Shannon, C. E. (1948). "A mathematical theory of communication". *The Bell System Technical Journal* 27, 379–423.

Shor, P. W. (1994). "Algorithms for quantum computation: discrete logarithms and factoring". In: *Proceedings 35th Annual Symposium on Foundations of Computer Science*, 124–134.

Shor, P. W. (1997). "Polynomial-Time Algorithms for Prime Factorization and Discrete Logarithms on a Quantum Computer". *SIAM Journal on Computing* 26, 1484–1509.

Silveirinha, M. G. and N. Engheta (2014). "Giant nonlinearity in zero-gap semiconductor superlattices". *Phys. Rev. B* 89 (8), 085205.

Silveirinha, M. G. and N. Engheta (2013). "Spatial Delocalization and Perfect Tunneling of Matter Waves: Electron Perfect Lens". *Phys. Rev. Lett.* 110 (21), 213902.

Silveirinha, M. G. and N. Engheta (2012). "Transformation electronics: Tailoring the effective mass of electrons". *Phys. Rev. B* 86 (16), 161104.

Silveirinha, M. and N. Engheta (2006). "Tunneling of Electromagnetic Energy through Subwavelength Channels and Bends using ϵ-Near-Zero Materials". *Phys. Rev. Lett.* 97 (15), 157403.

Silvi, P. et al. (2013). "Matrix Product State Representation for Slater determinants and configuration interaction states". *International Journal of Modern Physics B* 27, 1345029.

Sjöqvist, E., V. Azimi Mousolou, and C. M. Canali (2016). "Conceptual aspects of geometric quantum computation". *Quantum Information Processing* 15, 3995–4011.

Smirne, A. et al. (2013). "Interaction-induced correlations and non-Markovianity of quantum dynamics". *Phys. Rev. A* 87 (5), 052129.

Snizhko, K., R. Egger, and Y. Gefen (2019). "Non-Abelian Berry phase for open quantum systems: Topological protection versus geometric dephasing". *Phys. Rev. B* 100 (8), 085303.

Sokhoyan, R. and H. A. Atwater (2013). "Quantum optical properties of a dipole emitter coupled to an ϵ-near-zero nanoscale waveguide". *Opt. Express* 21, 32279–32290.

Söllner, I. et al. (2015). "Deterministic photon–emitter coupling in chiral photonic circuits". *Nat Nano* 10, 775–778.

Song, J. C. W. and N. M. Gabor (2018). "Electron quantum metamaterials in van der Waals heterostructures". *Nature Nanotechnology* 13, 986–993.

Štelmachovič, P. and V. Bužek (2001). "Dynamics of open quantum systems initially entangled with environment: Beyond the Kraus representation". *Physical Review A* 64, 62106.

Stern, F. and S. Das Sarma (1984). "Electron energy levels in GaAs-$Ga_{1-x}Al_xAs$ heterojunctions". *Phys. Rev. B* 30 (2), 840–848.

Stęślicka, M. et al. (2002). "Localised electronic states in semiconductor superlattices". *Surface Science Reports* 47, 93–196.

Strasberg, P. et al. (2017). "Quantum and Information Thermodynamics: A Unifying Framework Based on Repeated Interactions". *Phys. Rev. X* 7 (2), 021003.

Strunz, W. T., L. Diósi, and N. Gisin (1999). "Open System Dynamics with Non-Markovian Quantum Trajectories". *Phys. Rev. Lett.* 82 (9), 1801–1805.

Suchowski, H. et al. (2013). "Phase Mismatch–Free Nonlinear Propagation in Optical Zero-Index Materials". *Science* 342, 1223–1226.

Tacchino, F. et al. (2018). "Steady State Entanglement beyond Thermal Limits". *Phys. Rev. Lett.* 120 (6), 063604.

Terhal, B. M. (2000). "Bell inequalities and the separability criterion". *Physics Letters A* 271, 319–326.

Timp, G. (1992). "Chapter 3: When Does a Wire Become an Electron Waveguide". In: ed. by M. Reed. Vol. 35. Semiconductors and Semimetals. Elsevier, 113–190.

Torres, J. M. (2014). "Closed-form solution of Lindblad master equations without gain". *Phys. Rev. A* 89 (5), 052133.

Usha Devi, A. R., A. K. Rajagopal, and Sudha (2011). "Open-system quantum dynamics with correlated initial states, not completely positive maps, and non-Markovianity". *Phys. Rev. A* 83 (2), 022109.

Vega, I. de and D. Alonso (2017). "Dynamics of non-Markovian open quantum systems". *Rev. Mod. Phys.* 89 (1), 015001.

Vepsäläinen, A., S. Danilin, and G. S. Paraoanu (2018). "Optimal superadiabatic population transfer and gates by dynamical phase corrections". *Quantum Science and Technology* 3, 024006.

Verstraete, F., J. J. Garcia-Ripoll, and J. I. Cirac (2004). "Matrix Product Density Operators: Simulation of Finite-Temperature and Dissipative Systems". *Phys. Rev. Lett.* 93 (20), 207204.

Verstraete, F. and J. I. Cirac (2004). "Renormalization algorithms for Quantum-Many Body Systems in two and higher dimensions".

Vidal, G. (2004). "Efficient Simulation of One-Dimensional Quantum Many-Body Systems". *Phys. Rev. Lett.* 93 (4), 040502.

Vinjanampathy, S. and J. Anders (2016). "Quantum thermodynamics". *Contemporary Physics* 57, 545–579.

von Neumann, J. (1932). *Mathematical Foundations of Quantum Mechanics*.

Werner, R. F. (1989). "Quantum states with Einstein-Podolsky-Rosen correlations admitting a hidden-variable model". *Phys. Rev. A* 40 (8), 4277–4281.

Wiel, W. G. van der et al. (2002). "Electron transport through double quantum dots". *Rev. Mod. Phys.* 75 (1), 1–22.

Wilczek, F. and A. Shapere (1989). *Geometric Phases in Physics*. World Scientific.

Wilczek, F. and A. Zee (1984). "Appearance of Gauge Structure in Simple Dynamical Systems". *Phys. Rev. Lett.* 52 (24), 2111–2114.

Wolfe, C. M., G. E. Stillman, and 1. Holonyak Nick (1989). *Physical properties of semiconductors*. Englewood Cliffs, N.J. : Prentice Hall.

Yale, C. G. et al. (2016). "Optical manipulation of the Berry phase in a solid-state spin qubit". *Nature Photonics* 10, 184.

Yu, E. T., J. O. McCaldin, and T. C. McGill (1992). "Band Offsets in Semiconductor Heterojunctions". In: vol. 46. Solid State Physics. Academic Press, 1–146.

Zanardi, P., J. Marshall, and L. Campos Venuti (2016). "Dissipative universal Lindbladian simulation". *Phys. Rev. A* 93 (2), 022312.

Zanardi, P. and M. Rasetti (1999). "Holonomic quantum computation". *Physics Letters A* 264, 94–99.

Zhang, S. et al. (2008). "Cloaking of Matter Waves". *Phys. Rev. Lett.* 100 (12), 123002.

Zheludev, N. I. (2010). "The Road Ahead for Metamaterials". *Science* 328, 582–583.

Zheng, H., D. J. Gauthier, and H. U. Baranger (2013). "Waveguide-QED-Based Photonic Quantum Computation". *Phys. Rev. Lett.* 111 (9), 090502.

Zhou, B. B. et al. (2017). "Holonomic Quantum Control by Coherent Optical Excitation in Diamond". *Phys. Rev. Lett.* 119 (14), 140503.

Zhu, S.-L. and Z. D. Wang (2002). "Implementation of Universal Quantum Gates Based on Nonadiabatic Geometric Phases". *Phys. Rev. Lett.* 89 (9), 097902.

Ziolkowski, R. W. (2004). "Propagation in and scattering from a matched metamaterial having a zero index of refraction". *Phys. Rev. E* 70 (4), 046608.

Zurek, W. H. (2003). "Decoherence, einselection, and the quantum origins of the classical". *Rev. Mod. Phys.* 75 (3), 715–775.

Zurek, W. H. (1993). "Preferred States, Predictability, Classicality and the Environment-Induced Decoherence". *Progress of Theoretical Physics* 89, 281–312.

Zurek, W. H. (2018). "Quantum theory of the classical: quantum jumps, Born's Rule and objective classical reality via quantum Darwinism". *Philosophical Transactions of the Royal Society A: Mathematical, Physical and Engineering Sciences* 376, 20180107.

Zwanzig, R. (1960). "Ensemble Method in the Theory of Irreversibility". *The Journal of Chemical Physics* 33, 1338–1341.